KINETIC AND MECHANISTIC INVESTIGATIONS OF POLYIMIDE FORMATION AND CHARACTERIZATION OF THEIR BLENDS WITH POLYBENZIMIDAZOLES

by

Young Jun Kim

Dissertation submitted to the Faculty of the Virginia Polytechnic Institute and State University in partial fulfillment of the requirements for the degree of

Doctor of Philosophy

in

Chemistry

Approved by

James E. McGrath, Chairman

J. G. Dillard

H. W. Gibson

J. S. Riffle

J. M. Tanko

March, 1992

Blacksburg, Virginia

KINETIC AND MECHANISTIC INVESTIGATIONS OF POLYIMIDE FORMATION AND CHARACTERIZATION OF THEIR BLENDS WITH POLYBENZIMIDAZOLES

by

Young Jun Kim

James E. McGrath, Committee Chairperson

Department of Chemistry

(ABSTRACT)

This dissertation describes kinetic and mechanistic studies of high performance polyimide formation, synthesis and characterization of fully cyclized, molecular weight and end group controlled polyimides, and investigations of high performance polymer blends based upon polyimides and polybenzimidazole.

Imidization kinetics were successfully followed by the quantitative non-aqueous titration of the amic acid functional groups as a function of reaction conditions. The homogeneous solution imidization processes were described by auto-acid catalyzed second order kinetics. The effects of heteroatom bridging groups in the diamines and dianhydrides on reaction rates have been investigated and a possible reaction mechanism for the solution imidization processes has been proposed.

Detailed mechanistic investigations of the thermal solution imidization of polyamic acids were performed. A small amount of hydrolysis and possibly some unimolecular decomposition of amide bonds in the polyamic acid during thermal solution imidization processes were observed via combination of NMR and intrinsic viscosity measurements. However, complete "recombination" of the degraded polymer chains and their further cycloimidization could be achieved under proper imidization conditions. Potential side reactions involving intermolecular imide formation reaction were also investigated using a well characterized polyimide and also a model imide. For polyimide systems containing benzophenone tetracarboxylic acid dianhydride (BTDA), direct evidence for network formation involving imine crosslinking, was observed by high field ^{1}H-NMR spectroscopy. The gel formation was a strong function of reaction conditions, occurring under extremely dry reaction conditions and being favored at moderate reaction temperatures.

Various polyimide homo- and copolymers with controlled molecular weight and end groups were synthesized by the classic two step method and their thermal properties and solution viscosities were evaluated. Further, miscibility behavior of high performance polymer blends based upon polyimide (PI) and polybenzimidazole (PBI) was investigated. Several miscible PI/PBI blend material systems were

identified, some of which showed a lower critical solution temperature (LCST), which was consistent with earlier observations. It was found that miscibility was a strong function of polarity and possible specific interactions with the polyimide components. Thus, miscibility was possible over a wide composition range with polyimides containing polar groups such as ketones, sulfones and ethers. However, immiscible blends were obtained when these polar polyimide components were replaced by non-polar groups such as the hexafluoroisopropylidene linkages.

ACKNOWLEDGEMENTS

I would like to express wholehearted gratitude to my committee chair and advisor, Dr. James E. McGrath, for his guidance, encouragement, patience and strong support while pursuing this research. Without his patience and scholarly guidance, I surely would not have succeeded. I would also like to extend my deepest gratitude to other committee members, Dr. J. G. Dillard, Dr. H. W. Gibson, Dr. J. S. Riffle and Dr. J. M. Tanko for serving on my committee and for helpful discussions and suggestions.

I sincerely say "thank-you" to Dr. H. M. Bell for discussion on NMR data and to Mr. Tom Glass and Dr. John Hellgeth for their technical assistance with NMR and FTIR spectroscopy, respectively.

My sincere thanks go to my former and present colleagues in the "JEM's Polymer Group", especially to Dr. Milos Netopilik, Dr. Eric Moyer, Dr. Jim Senger, Dr. Carrington Smith, Susan Smith, Tom Moy, Sang Pak, Martin Rogers and Heather Woodard for their discussion, support and friendship. Special thanks also go to Greg Lyle for technical discussions and assistance with experiments.

To my parents, father in-law and mother in-law much love and gratitude are given for their love, sacrifice and support.

Finally, I am indebted to my wife, Eun Kyoung, who above all supported me in this endeavor and showed patience and never-ending love. I also sincerely say "I love you, Eun Kyoung".

Dedicated to the memory of my grandmother, Suk Hee Jeung, for her great love and sacrifice

to my wife, Eun Kyoung, and to my daughters, Ee Yeon and Ee Ji for their love

TABLE OF CONTENTS

LIST OF FIGURES

LIST OF TABLES

CHAPTER 1

INTRODUCTION

Aromatic polyimides are one of the most important classes of high performance polymers. Due to their excellent electrical, thermal, and high temperature mechanical properties, aromatic polyimides have found many applications as high temperature insulators and dielectrics, coatings, adhesives, and matrices for high performance composites. One of the most highly developed synthetic routes for these important materials is the classical two step method, the first step being the synthesis of polyamic acids from the reaction of diamines and dianhydrides and the latter step being subsequent thermal imidization of the polyamic acids. The conversion of a polyamic acid to the polyimide is most commonly accomplished by thermal treatment of the polyamic acid in the solid state. The polyamic acid has usually been considered to be completely imidized; however, there have been some questions on this point and it is probably dependent on the heating cycle (77,78). Thus, a final cure temperature above the glass transition temperature of the fully imidized material is needed to allow the adequate chain mobility required for a high degree of imidization. Alternatively, a polyamic acid could also be cyclized in solution at relatively mild reaction temperatures, for instance 160~180°C. Most of the aromatic polyimides

produced by the thermal solid phase imidization process often show insolubility, infusibility, and thus poor processability (1-3). These undesirable properties that limit wider applications of polyimides are due to their chain rigidity as well as poorly defined molecular architectures such as uncontrolled molecular weight and end groups and possibly some crosslinks formed during high temperature solid phase "curing" processes.

Solution imidization techniques together with molecular weight and end group control have been employed to overcome these problems (125-127). As a result, polyimides with improved solubility and processability have been successfully synthesized without sacrificing their many desirable properties. However, the reaction kinetics and mechanisms of thermal imidization processes, particularly a solid phase imidization process, are reported to be very complicated (79,149-155). Even though a first order kinetic equation has been almost exclusively used to treat imidization kinetic data, the rate law of imidization process is not well-established and kinetics of solid phase heterogeneous imidizations are observed to be affected by many factors such as amount of solvent, film thickness and heating rate. Moreover, possibilities of curing reactions other than cycloimidization were reported (111-124,133-141). These include degradation of the polyamic acid,

intermolecular imide link formation, and network formation via possible free radical intermediates at high temperatures such as 350°C. Promising results on the synthesis of polyimides which had improved solubility and processability and the very complicated imidization processes described in the literature emphasized the need for more detailed kinetic and mechanistic studies of the formation of these very important materials.

The main focus of this research was, therefore, to increase fundamental understanding of kinetic and mechanistic aspects of the imide formation reaction which is essential to the synthesis of high performance polyimides with well-defined polymer parameters such as topology, molecular weights and molecular weight distributions. Even though, from the synthetic viewpoint, the first step of polyimide synthesis, eg. synthesis of polyamic acid is as important as the subsequent cycloimidization step, it is reasonably well understood and the latter step of the polyimide formation was extensively investigated in this research. To shed important light on the kinetics and mechanism of thermal imidization processes, spectroscopic methods such as two dimensional ^{1}H-^{1}H NMR spectroscopy, FTIR spectroscopy, and mass spectroscopy, quantitative non-aqueous potentiometric titration and solution viscosity measurements were employed.

Additional efforts were also directed towards the synthesis and characterization of polyimides with controlled molecular weight and end groups employing the solution imidization technique. Thus, various homo- and copolyimides were synthesized from the reaction of aromatic diamines and aromatic dianhydrides employing the solution imidization technique. Phthalic anhydride was used to control molecular weight as well as to generate non-reactive end groups. These concepts of molecular weight control and non-reactive end groups were expected to be critical to increase in solubility and processability. Thermal properties and solution viscosities were examined. Miscibility behavior of various polyimides melt blended with high performance material, polybenzimidazole (PBI), were also explored using thermogravimetric analysis (TGA), differential scanning calorimetry (DSC), and Fourier transform infrared spectroscopy (FTIR).

In the forthcoming chapter, CHAPTER 2 LITERATURE REVIEW, detailed kinetic and mechanistic aspects of polyamic acid and the polyimide formation are discussed. CHAPTER 2 also provides an extensive discussion of thermodynamic aspects of equilibrium phase behavior, with particular emphasis on polybenzimidazole-polyimide blends. CHAPTER 3 discusses the experimental methods, both synthetic and analytical, used in this research. A discussion of the

experimental results is presented in CHAPTER 4, followed by conclusions, suggested future studies, appendix, and references.

CHAPTER 2

LITERATURE REWIEW

2.1. Synthesis of polyimides

Condensation or step-growth polyimides were discovered by Bogert and Renshaw in 1908 (4) and made practical by Edwards and Robinson (5). They are usually derived from dianhydride or dianhydride derivatives and diamines. Polyimides are characterized by presence of the phthalimide structure in the polymer backbone.

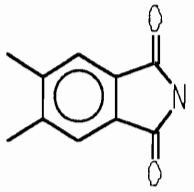

Due to their excellent electrical, thermal, thermo-oxidative, and high temperature mechanical properties polyimides have been used extensively as high temperature insulators and dielectrics, coatings, adhesives, and matrices for high performance composites (1-3,6-11). "Condensation" polyimides may be prepared from a number of reactant pairs (12). Among those are dianhydride/diamine (13,14), diester-diacid/diamine (5,15), diester-diacid dichloride/diamine (5), bis(diethylamide)-diacid/diamine (16), and dianhydride/diisocyanate (17,18). Edwards and Robinson prepared polyimides by a salt method (5) or a refined salt method (19) from diamine/tetra acid or

diamine/diacid-diester. These methods were limited to polyimides with melting points sufficiently low that they remained molten under conditions of polymerization. The most versatile synthetic method, a two-step method, was disclosed in the 1960s (20,21). This method involves synthesis of a soluble precursor, a polyamic acid, which is then subsequently converted to the polyimide through thermal (22) or chemical (23,24) cyclodehydration. The polyamic acid is prepared by reaction of a dianhydride and a diamine at ambient temperatures in polar solvents such as N-methyl pyrrolidone (NMP), N,N-dimethyl acetamide (DMAc) and N,N-dimethylformamide (DMF) as illustrated in Figure 2.1.1.

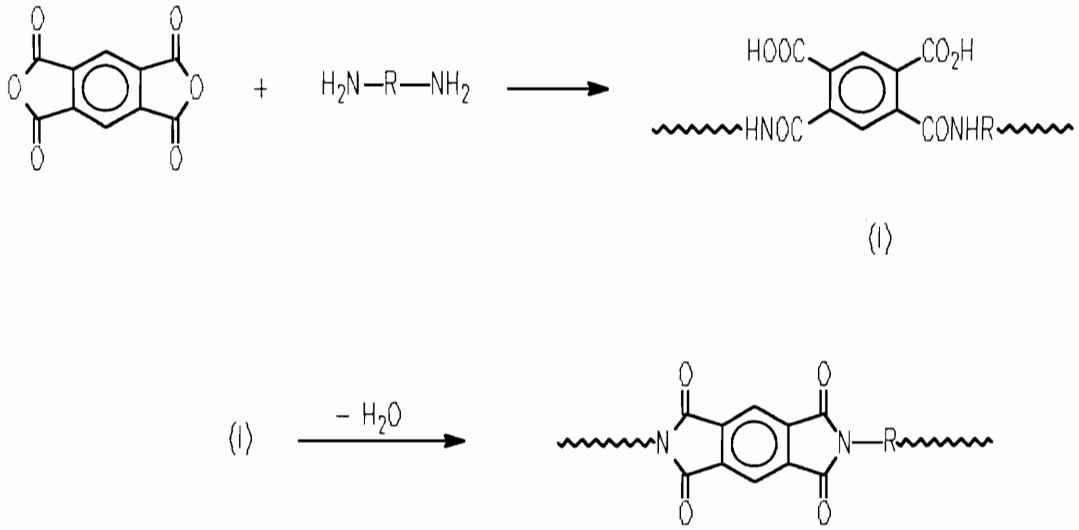

Figure 2.1.1. Polyimide synthesis via polycondensation of a dianhydride and a diamine.

In the following paragraphs synthetic aspects and solution properties of polyamic acids will be reviewed.

2.1.1. Mechanistic and kinetic features of polyamic acid formation reactions

One of the most important mechanistic features of the polyamic acid formation is that the reactants and the product are in equilibrium (25,26). Some important features of the equilibrium were observed. According to Ardashnikov et al. (26) the equilibrium constants depend on solvent properties and amine basicity. Thus, the equilibrium constants increased with increasing aromatic amine and solvent basicity. The forward reaction is spontaneous and exothermic if the reactants are properly solvated. (14,26). The magnitude of the heat of the reaction depends on the solvent basicity. Solvation is usually achieved by carrying out the reaction in a highly polar aprotic solvent such as dimethyl sulfoxide (DMSO), dimethylformamide (DMF), dimethylacetamide (DMAc), or N-methyl pyrrolidone (NMP). Due to the exothermic reaction, the equilibrium is shifted to the left and the product molecular weight is lowered when the reaction temperature is increased (27). In a basic aprotic solvent, however, the equilibrium already lies so far to the right at ambient temperature that the molecular weight increase upon cooling is usually not detectable. Kamzolkina et al.(28) carried out the reaction of phthalic anhydride and aniline as a model reaction of polyamic acid formation to investigate the temperature dependence of the

equilibrium constant. At a low temperature a large equilibrium constant was detected. From these findings they concluded that the strong temperature dependence of the equilibrium constant is critical to the high molecular weight polyamic acid synthesis.

The molecular weights of polyamic acids were dependent upon reaction conditions such as reaction temperature (12,14,29), monomer addition order (12,30) and monomer concentration (30). As discussed earlier, some of the behavior could be explained in terms of the monomers/polyamic acid equilibrium feature. In fact, a slight stoichiometric excess of dianhydride was used to enhance the molecular weight (12,30). For example, R. A. Dine-Hart and W. W. Wright (30) investigated a number of solution imidization methods which were classified according to the monomer addition order and heterogeneity (in solution or as a solid). The viscosities of the polyamic acid solutions were very dependent on the mixing technique, the highest values being obtained when PMDA was added as a solid. Maximum viscosities were obtained with PMDA in 0.4～0.5% excess of the equivalent amount. These observations were explained in terms of competitive aminolysis and hydrolysis reactions for the PMDA. The crucial difference between the heterogeneous and homogeneous mixing methods was that in the former case aminolysis and

hydrolysis reactions are in competition, whereas in the latter situation hydrolysis may occur freely before aminolysis is initiated. Similar reasons were used to explain the dependence of molecular weight on the concentration of monomers (30). If the amount of solvent is reduced the amount of solvent impurities that interfere with the build-up in molecular weight would be also reduced. However, Volksen and Cotts (31) proposed other mechanisms for the high molecular weight polyamic acid formation in the heterogeneous mixing method. They studied the synthesis of polyamic acid from PMDA and ODA in NMP. Polyamic acid solutions between 10~25 wt. % total solid contents were prepared under highly controlled conditions. Contrary to literature data (30), they found that the monomer addition sequence had no effect on the ultimate molecular weight of the polyamic acid solution when total solid contents were less than 10%. This might have been due to the rigorous exclusion of moisture from the polymerization system. When total solids were increased up to 25%, polymerization time to achieve a completely homogeneous system increased and the initial solution viscosity was abnormally high and then equilibrated to a lower value. The observation of higher molecular weights for the heterogeneous and high solid cases was reasoned by high local dianhydride concentrations and diffusional effects arising from heterogeneity. Namely, the

tendency of PMDA to form a 1:1 type charge transfer complex (32,33) with the diamine might account for high molecular weight polymer formation in spite of a non-equilibrium stoichiometry. Furthermore, the heterogeneous nature of the polymerization could be controlled by diffusional effects, yielding a "pseudo-interfacial polymerization" with similar results on the overall weight average molecular weight.

While the kinetics of the polyamic acid synthesis have been studied extensively (34-46), a great deal of discrepancy is found in the literature regarding the kinetic law that is followed. Experimental data on kinetics of polycondensation of diamines and dianhydrides can be generally treated as second-order reversible reactions (47). However, taking into account the great magnitude of the equilibrium constants of acylation reactions (26), it is also possible to calculate the rate constants according to an equation for second-order irreversible reaction(44). Many workers also proposed autocatalytic kinetics (48-51). Autocatalysis results when a product of the reaction, in this case the carboxylic acid, is a catalyst for the reaction. Kaas (51) has clearly showed that the amic acid formation from the reaction of phthalic anhydride and 4,4'-oxydianiline or aniline in tetrahydrofuran follows autocatalytic reversible kinetics. It was also found that both acid and base had significant effects on the

polymerization system. Thus, pyridine shifted the equilibrium to higher degrees of conversion affording higher molecular weights, while the opposite effect was obtained with acetic acid.

The rate of acylation reaction was a strong function of monomer structures (52-54). The reactivity of the dianhydride towards acylation reactions was directly correlated with the electron affinity (Ea) of the dianhydride, which increases with enhancement of the electron acceptor character of the dianhydride. The acceptor properties of molecules can be expressed in terms of characteristics of their electronic structures. In the course of chemical bond formation in the acylation reaction, the interaction between the highest occupied molecular orbital (HOMO) of the amine with the lowest unoccupied molecular orbital (LUMO) of the anhydride is of paramount importance since they are the closest in energies. Molecular orbital calculations showed the close correlation between the energy of the lowest unoccupied molecular orbital of dianhydrides and electron affinity. On the other hand the effect of substituents in the nucleophile (amine) was described by the well known Hammett equation (55), log k=log k_0 + $\rho\sigma$. A study has been carried out to estimate the reaction rates of dianhydrides of pyromellitic (PMDA) and 3,3',4,4'-benzophenonetetracarboxylic (BTDA) acids with

substituted anilines $H_2N-C_6H_4-X$ (X=m-NO_2, p-Br, H, p-OCH_3, p-CH_3) in various solvents N,N-dimethylacetamide (DMAc), N,N-dimethylformamide (DMF), and N-methyl pyrrolidone (NMP). The negative sign of the ρ constant demonstrated the acceleration of the reaction by electron donor substituents. Large absolute values of ρ also indicated high sensitivity of the reaction to structural changes in the amine molecule. The σ constant allowed the quantitative estimation of the effect of chemical structure of the diamine upon reactivity. For the amine components the reaction rate decreased with an increase in the electron-acceptor properties of the substituents. It was also found that the rate of amic acid formation increases on changing from the non-polar solvent to the polar solvent and that the presence of acids and water accelerates the reaction (56).

2.1.2. Properties of polyamic acid solutions

Many investigations of the various aspects of polyamic acid solution properties can be found in the literature (1-3). One of the conspicuous characteristic features of polyamic acid solutions is their molecular weight instability. Their solution stability is sensitive to temperature, concentration, and moisture (14,30). Concentrated polyamic acid solutions were more stable than dilute solutions (14). The mechanism of stability of

polyamic acid solutions has not been fully understood but has been considered to involve hydrolysis of amide bonds (57), unimolecular decomposition of the amic acid (58), chain length equilibration(63,64,66,222), and chemical (30,32) or physical (59,60) transformations such as imidization, isoimide formation, and gelation upon extended storage at low temperatures. The mechanism for the hydrolysis of phthalamic acids was first investigated thoroughly by Bender (61) in the late 1950s. The data showed that o-carboxyphthalamides exhibit a strong tendency to hydrolytic cleavage and they are considerably more unstable towards water than corresponding unsubstituted amides. The interpretation was that neighboring group catalysis is operative through reversible generation of cyclic anhydride and amine and the anhydride subsequently reacts with water to form o-phthalic acid as follows:

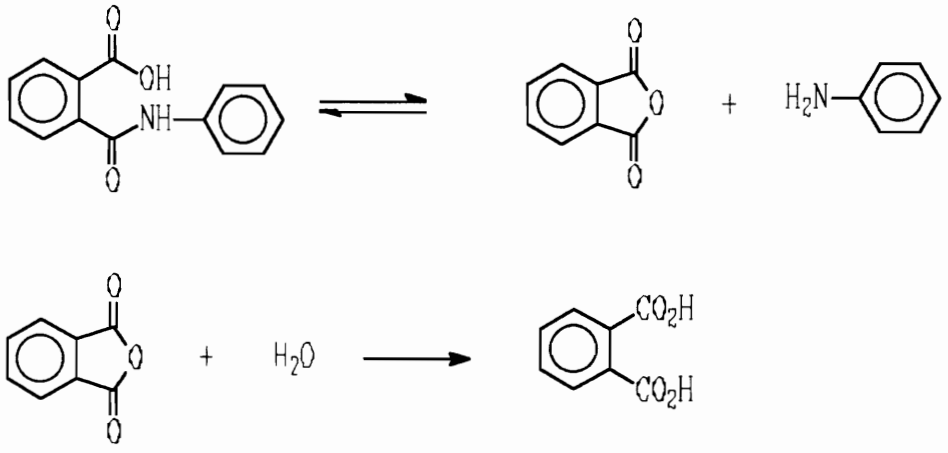

Many workers (12,14,32,62), observed a large viscosity drop in polyamic acid solutions and provided evidence that degradation was enhanced by the addition of water. It was concluded that hydrolysis was, therefore, occurring to some extent. However, Russian workers (58) proposed a unimolecular decomposition of polyamic acids and questioned Bender's interpretation (61).

Volksen (63) was first to report the decay of a skewed molecular weight distribution to a most probable one, as a result of a polyamic acid/anhydride-amine equilibrium. Walker (64) confirmed further the re-equilibration of the molecular weight distribution. Through high performance size exclusion chromatography (HPSEC) studies, it was shown that chain length equilibration was occurring in which the weight average molecular weight (<Mw>) decreased significantly, while the number average molecular weight (<Mn>) remained constant. Figure 2.1.2 shows <Mn> and <Mw> change as a function of reaction time during amic acid formation reaction of PMDA and 4,4'-ODA at 8° and 31°C in DMAc. The data clearly shows that <Mn> obtained at 31° and 8°C are the same at these two temperatures; however, <Mw> are maintained at their maximum value by keeping the temperature low, due to the inhibition of the interchange reaction leading to chain length equilibration. With light scattering and viscosity measurements Miwa and Numata (65) investigated the

properties of the polyamic acid solution derived from s-BPDA and p-PDA at 80°C in NMP. The data showed that the reduction of solution viscosity was also caused by a weight average molecular weight reduction.

Recently Kreuz (66) studied hydrolytic stability of several polyamic acids under similar conditions (at 30°C) in an attempt to relate polyamic acid structure to polyamic acid hydrolytic resistance. Since the previous studies showed that loss of <Mw> is strongly associated with chain equilibration, <Mw> or solution viscosity (which is strongly dependent upon <Mw>) were excluded as being the preferred measure of molecular weight. Dry polyamic acid solutions based on PMDA/4,4'-ODA (10% solids in DMAc) exhibited a loss from 4 to 15% of their number average molecular weight (<Mn>). Comparatively, the wet polymer solutions, composed of 10 polymer/10 water/80 wt. % DMAc, lost 46 to 52% of their corresponding <Mn> values. These hydrolysis data suggested that both polymers, in dry and wet solution states, degraded under time and temperature constraints of 7 to 12 days at 30°C to a very modest extent and the amount of chain scission induced through water alone was fairly small. Indeed, total hydrolysis of available amide bonds was only about one scission per chain. The rate of hydrolysis slowed considerably after only a minor percentage of amide linkages was cleaved and then leveled off. From these observations

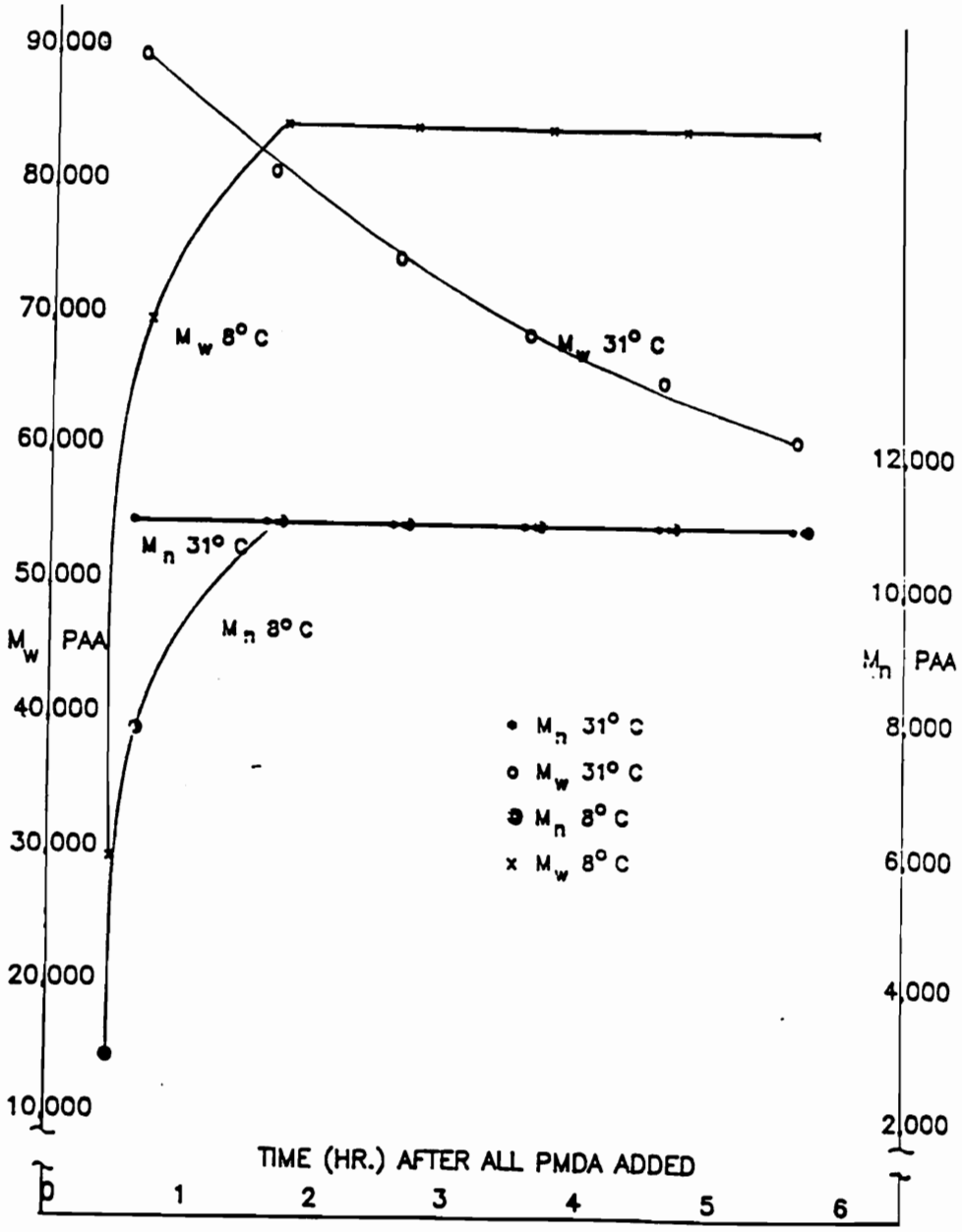

Figure 2.1.2. <Mn> and <Mw> at 31° and 8°C vs. time after all PMDA added. PMDA/ODA ratio=0.98 (64).

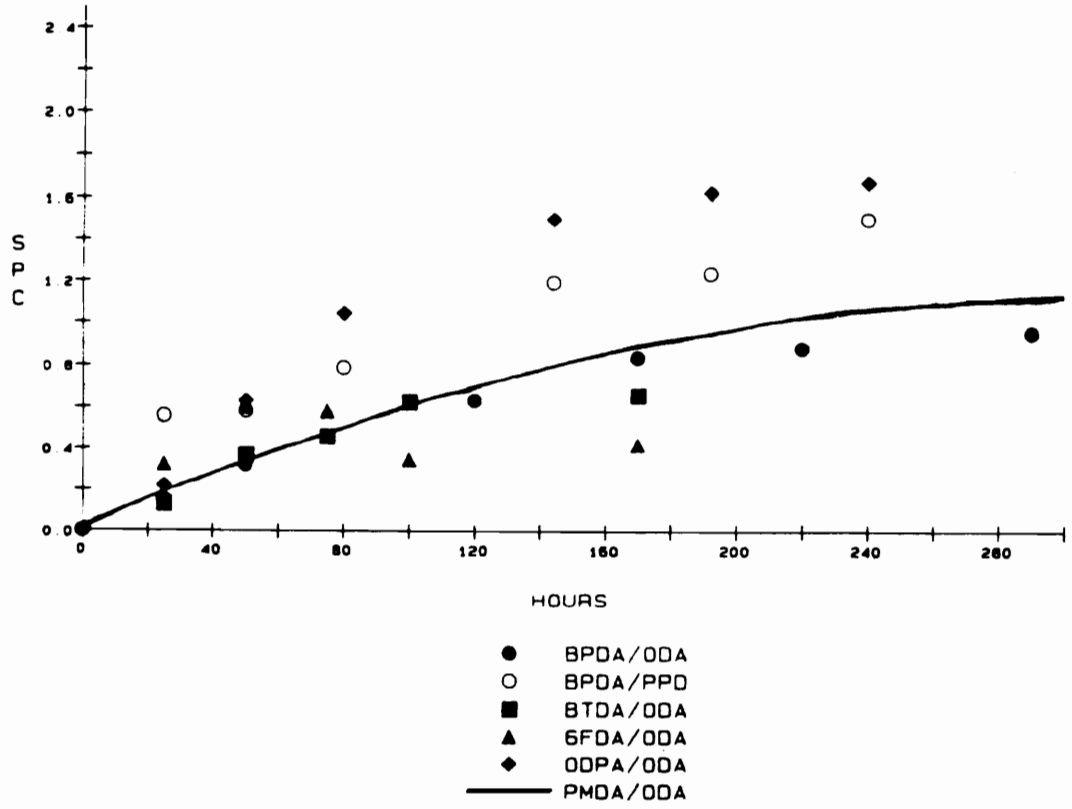

Figure 2.1.3. Scission per chain (SPC) during hydrolyses of polyamic acids based on several dianhydrides (66).

unspecified equilibrium reactions or the existence of hydrolytically unstable amide bonds were proposed. Various polyamic acid solutions experienced a small amount of hydrolysis, just about one scission per chain, occurring in a matter of 10 days at 30°C. The rates of chain length equilibration and hydrolysis were dependent upon chemical structures. However, a clear distinction betweenthe rates of hydrolysis as a function of chemical structures could not be made. A relevant figure regarding hydrolytic stabilities of various polyamic acid solutions is reproduced in Figure 2.1.3.

As mentioned earlier it was also found that polyamic acid solutions undergo chemical transformations such as imidization and isoimide formation upon extended storage (30). Although there is little tendency to cyclize to an imide at low temperatures, 20% imidization was detected in a 10% polyamic acid solution which was allowed to stand at 35°C for about 200 days (32). Some polyamic acid solutions showed gelation behavior (59). The nature of the junction points could be chemical networks or physical associations (60).

Besides the dynamic and unstable nature of polyamic acid solution properties, both dilute solution viscosity and light scattering measurements to determine molecular weight of polyamic acids have been complicated by the trace amount

of impurities in the solvent (67). Cotts (67) performed solution viscosity measurements on both dilute and concentrated solutions of PMDA/4,4'-ODA polyamic acid. Polyelectrolyte effects (12) were observed in dilute solutions prepared in NMP as received, without distillation. Dilute solution viscometry yielded viscosities increasing with dilution as shown in Figure 2.1.4. Addition of a small amount of water to a solution in distilled NMP resulted in a lower intrinsic viscosity, but no polyelectrolyte effect. Apparently, impurities in the NMP, such as amines, are basic enough to abstract a proton from the carboxylic acid groups, resulting in partially charged macromolecules. In a very dilute solution, the charges on different segments of the same molecule repel, greatly increasing the hydrodynamic size of the molecules, and thus their contribution to the viscosity. Light scattering in the as-received NMP also showed some unusual effects in very dilute solutions. The intensity of the scattered light from very dilute solutions was reduced. This unusual behavior was more pronounced for higher molecular weight polymers. Addition of LiBr(0.005N) to the solutions in NMP with decreased scattering caused the scattering to increase somewhat, although not to its expected value. The author presumed that the effect on the scattered light intensity was responsible for the non-random distribution of the scattering molecules produced by the

intermolecular forces. Addition of a salt, such as LiBr, provides a population of charges which act to screen the repulsive forces so that the molecules then behave as uncharged species. Measurements of both dilute solution viscosity and molecular weights by light scattering showed that the cured polyimides retain essentially the same molecular weight and molecular conformation as their precursor polyamic acids (67). As mentioned earlier addition of LiBr suppresses the polyelectrolyte effects; however; it reduces the solubility of polyamic acid and often causes precipitation. In 1981, Nefedov (68) reported the successful SEC (size exclusion chromatography) of a polyamic acid derived from 3,3',4,4'-diphenyloxide tetracarboxylic dianhydride and p-phenylene diamine. "Macro-porous glasses" and "Sephadex" columns were employed with a mobile phase of 0.03M LiBr/0.03M H_3PO_4/1 vol. % THF in DMF. Addition of H_3PO_4 markedly improved the solubility of the polyamic acid. Redistillation of solvent at reduced pressure from P_2O_5 provided a solvent which produced no polyelectrolyte effect thus avoiding the solubility problems accompanying the use of LiBr.

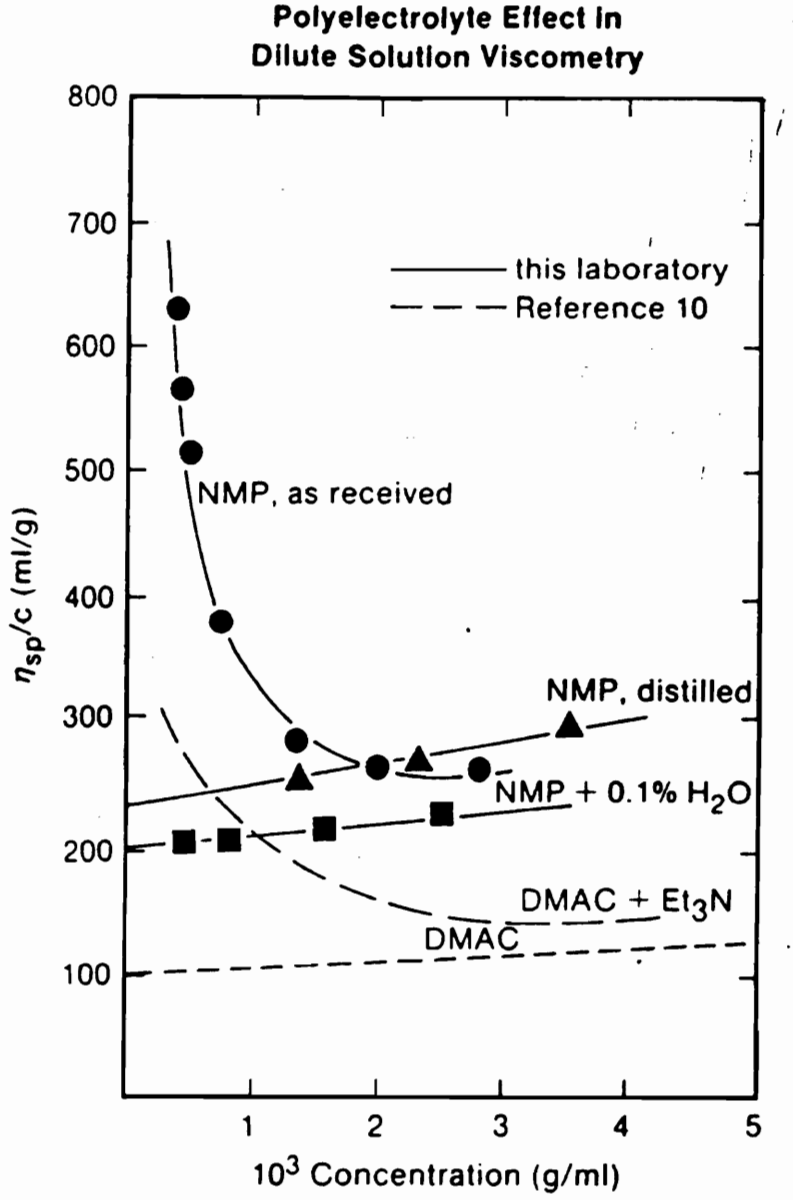

Figure 2.1.4. The reduced viscosity, η_{sp}/c as a function of concentration for PMDA/4,4'-ODA polyamic acid in as-received and distilled NMP, showing the polyelectrolyte effect obtained in the as-received solvent. Also shown are similar data obtained by Bower and Frost (12) in DMAc and DMAc with triethylamine added (67).

2.1.3. Thermal conversion of polyamic acid to polyimide

The conversion of a polyamic acid precursor to the polyimide is most commonly accomplished by the thermal treatment of the polyamic acid in the solid state. Various solid forms of polyamic acids such as film, fiber, and powder are usually prepared and then subjected to a specific heating cycle (69-71). A typical heating cycle is as follows:

1) one hour at 100°C
2) one hour at 200°C
3) one hour at 300°C

For complete conversion of the polyamic acid, temperatures above the Tg of the fully imidized material are needed to allow adequate chain mobility (72). However, there is always a question on the completeness of the imidization (73-76). For example, it was reported that complete imidization could not be obtained with the above mentioned heating cycle (77), however higher degrees of imidization, i.e. above 99%, were obtained by constant heating at 230~250°C for 10 minutes (78).

Various aspects of thermal imidization have been studied by numerous techniques such as FTIR spectroscopy (79-82), UV-vis absorption spectroscopy (83,84), fluorescence spectroscopy (85), ^{13}C-NMR spectroscopy (86-89), ^{1}H-NMR spectroscopy (88,90,91), ^{15}N-NMR spectroscopy

(92,93) and thermogravimetric analysis (94). Infrared spectroscopy has been most widely used to monitor the progress of imidization. The imide functional group is characterized by several absorptions near 1780 cm^{-1} (symmetrical C=O stretch), 1720 cm^{-1} (asymmetrical C=O stretch), 1380 cm^{-1} (C-N stretch), and 725 cm^{-1} (bending of C=O) (95,96). There is, however, little agreement on which of the various imide bands should be followed. The degree of imidization is usually determined by comparing the intensity of these bands in a treated sample to those in samples which are heated until no further changes in the band intensities can be detected (97-99). Thus, the degree of imidization, p, is given by following equation.

$$p = \frac{I(imide)/I(ref)}{I°(imide)/I°(ref)}$$

Where p, I(imide), and I(ref) are degree of imidization, absorbance or peak areas of imide peak and that of reference peak, respectively. I°(imide) and I°(ref) are intensities of imide peak and that of reference peak for a fully imidized standard sample. A sample heated at high temperature for a long time, for example 300°C for 30 minutes, is considered to be a fully imidized standard (95,96). Peaks whose intensity values are invariant throughout the imidization process are selected as reference peaks. For example, the

1012 and 1500 cm^{-1} frequencies (aromatic vibrations) are usually used as reference peaks. As the above equation implies, the accuracy of degree of imidization is dependent upon that of normalization factor, I°(imide)/I°(ref).

The 1720 cm^{-1} band is not generally used to follow imidization because it is strongly affected by the carbonyl absorbance from the acid moieties in the polyamic acid. Amide bands of polyamic acid, namely amide I, 1660 cm^{-1} (C=O stretch), amide II, 1550 cm^{-1} (CNH vibration) and a band at 3240~3320 cm^{-1} (NH stretch) are also employed less frequently. The imide bands near 1778, 1380, and 725 cm^{-1} are commonly used. However, in the later stages of imidization the bands near 1778 cm^{-1} and 725 cm^{-1} are insensitive to changes that could be detected by thermal techniques (100). Recently Pryde (101) has also found that the 1780 cm^{-1} band and the band near 725 cm^{-1} are affected by anhydride absorptions that appear when the polymer is heated. Clearly, this interference can result in significant errors in determining the degree of cyclization, particularly when the 1780 cm^{-1} band is used. A fourth imide band in the 1370 cm^{-1} region does not appear to suffer direct interference by any other peak. The imide absorptions measured in film samples can also be affected by anisotropy in the bulk imidized sample. It was also found that the average orientation of the imide groups changes as the cure

proceeds. However, the absorbance of the 1370 cm^{-1} region imide band showed little effect from anisotropy when normalized to the 1500 cm^{-1} internal standard.

Indeed, most of the kinetics of imidization processes reported in the literature have been studied by FTIR spectroscopy under isothermal conditions. Unfortunately, however, isothermal studies are often tedious and multiple samples are required at each time-temperature combination due to the additional curing that can occur during the heating and cooling cycle (102). A method for determining kinetic parameters from dynamic FTIR data was developed to overcome the problems mentioned above (103). Through the proper use of the dynamic FTIR technique (104,105) kinetic parameters such as activation energy and frequency factor could be obtained in a few hours. When performing the dynamic kinetic analysis, however, there are some effects which must be accounted for in order to correctly interpret the data. There is a temperature effect on the intensity of the 1780 cm^{-1} (imide) band that must be examined and a correction in the data must be made to relate the data to a constant temperature (106). Figure 2.1.5 shows the effect of temperature on the 1780 cm^{-1} band for polyimide systems. With these precautions the kinetic parameters may be calculated using the following equation.

$$\ln(-dC/dT) - \ln(C/m) = \ln(A) - Ea/RT$$

where m is the heating rate, C is one minus the concentration of the absorbing species (for example, 1780 cm-1 band area), R is the gas constant and T is the current temperature of the reaction.

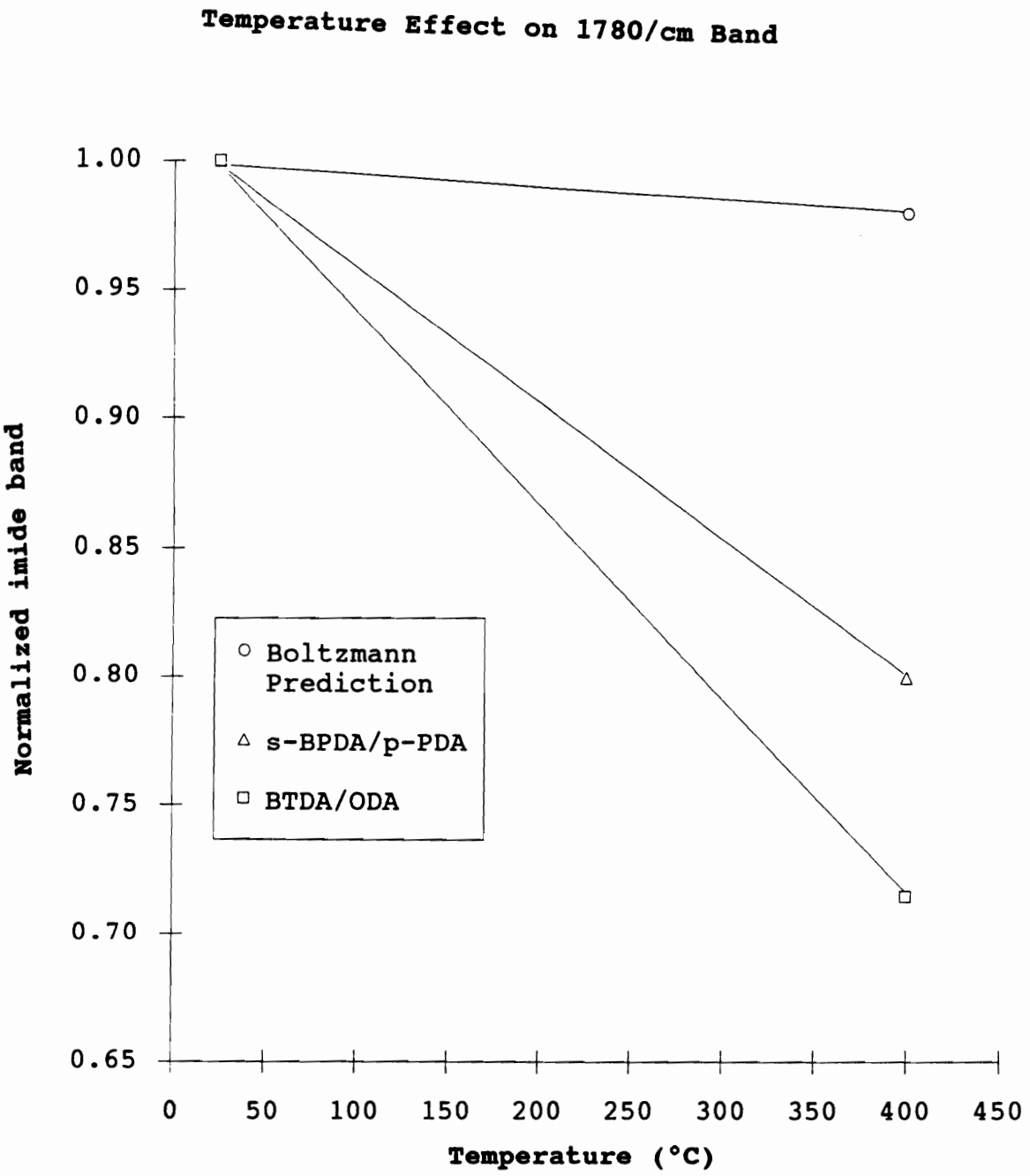

Figure 2.1.5. Plot showing the effect of temperature on the 1780 cm^{-1} band in two polyimides (107).

2.1.4. Mechanism of thermal imidization

The principal reaction of an o-carboxycarboxamide group upon heating is cycloimidization. However, because of the instability of polyamic acids, they undergo degradation reactions such as hydrolysis of amide bonds and chain scission/recombination during imidization processes. In addition to these reactions, a small amount of isoimide formation has also been reported and this can be very significant when catalysts are employed (108). Considering the equilibrium nature of the formation of polyamic acids, the reaction pathways of thermal imidization of polyamic acid can be represented by the following process under nearly anhydrous conditions (112).

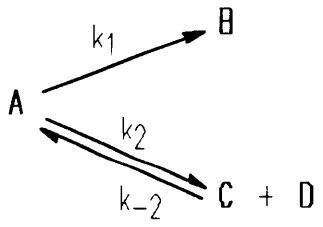

Here **A** is the concentration of o-carboxyl groups, **B** the concentration of imide groups and **C** and **D** are the concentrations of terminal anhydride and amine groups.

A hypothetical potential energy diagram for the above reaction pathway is shown in Figure 2.1.6 (109). As the temperature is increased, a small portion of the o-carboxycarboxamide groups revert to amine and anhydride or

acidic end groups. Some of the amic acid groups also undergo conversion to imides. The removal of the amic acid groups helps drive the equilibrium to the polyamic acid direction.

Kruez et al.(110) proposed a mechanism for thermal cycloimidization based upon the observation that tertiary amine salts of polyamic acid of PMDA/ODA cyclize about 10 times faster than free amic acid. These fast rates were due to very low entropies of activation. From these data it was speculated that the ionized form of the polyamic acid should be the preferred precursor to the activated complex. The reaction path for the imidization of amine salts of polyamic acid involving carboxylate ion is shown in Figure 2.1.7. Equilibration of the ortho carboxylate anion with amide hydrogen could afford an easy route to ring closure. They believed that the free polyamic acid also cyclizes by the same path, although "neutral" ring closure through undissociated acid is also possible.

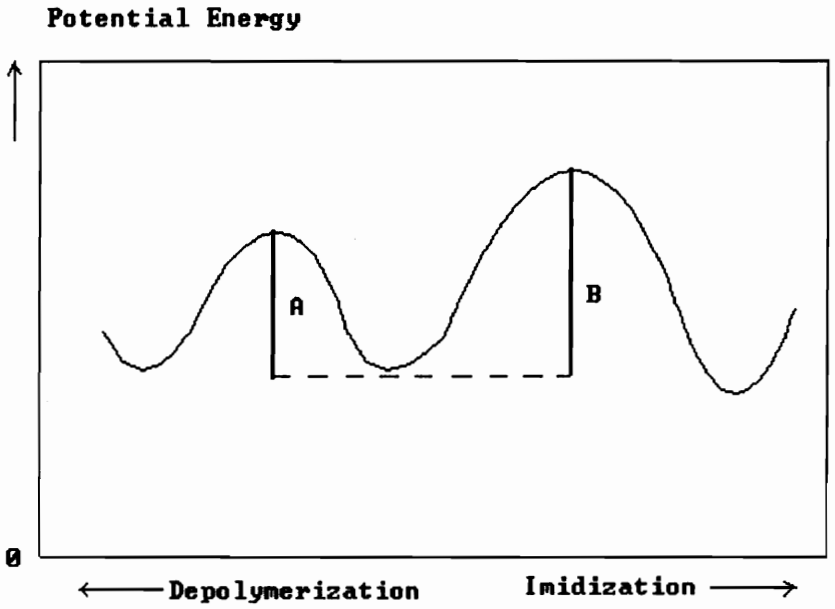

Figure 2.1.6. Hypothetical potential energy changes during thermal imidization: **A** and **B** are the activation energies for depolymerization and for imidization, respectively (109).

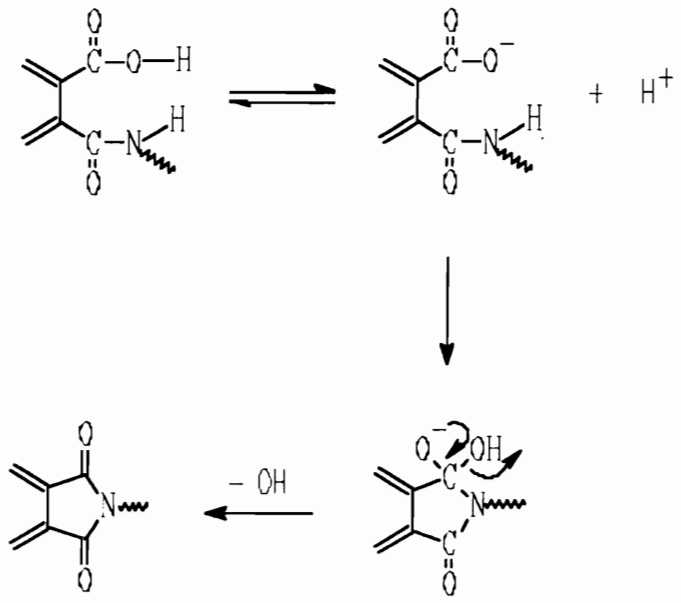

Figure 2.1.7. A possible reaction pathway for the imidization process (110).

2.1.4.1. Chain scission during the imidization process

Many researchers studying thermal imidization have observed that polyamic acids undergo an initial reduction in "molecular weight" or at least viscosity during imidization before possibly recombining to achieve their ultimate molecular weight as polyimides. This phenomenon was perhaps first observed by Dine-Hart and Wright in late 1960s (30). They noted that flexibility of solvent cast films was a strong function of the degree of cure and molecular weights. The pertinent figure is reproduced in Figure 2.1.8. As shown in Figure 2.1.8 medium molecular weight polyamic acid samples (η=0.2~1.0) which initially gave flexible films while plasticized by the casting solvent deteriorated to brittle films in the intermediate stage. Upon further curing at high temperatures, such as 300°C, the brittle films transformed into flexible ones. As mentioned earlier the possibility of chain cleavage during the thermal imidization process has been noted by numerous investigators (111-120,138). For example, Nechayev et al.(112) reported a decrease in <Mn> of the polyamic acids in the first few minutes of the reaction at 150°C from 17,000 to 2,500 during solution and solid phase imidization processes. Bell noted that a series of polyimides made from isomeric diamines were brittle after 5 hours at 175°C but flexible after one additional hour at 300°C. Spectroscopic evidence of chain

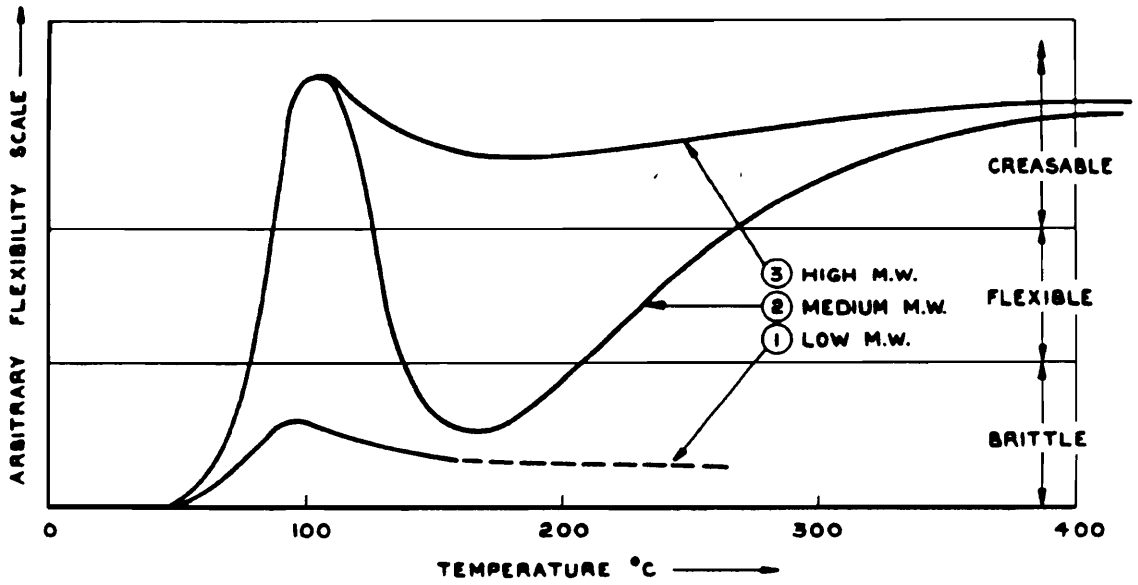

Figure 2.1.8. Effect of apparent molecular weight of polyamic acid on film-forming properties (30).

cleavage and resynthesis of polyamic acids can be found in the literature (115-120,138). Kamzolkina et al.(115) studied solid phase imidization of the polyamic acid derived from 3,3',4,4'-carboxydiphenyl-2,2-propane dianhydride and 9,9-bis(4-aminophenyl)fluorene. With the aid of UV/VIS spectroscopy they noted that number average molecular weight of the polymer decreased during solid phase imidization at 150°C, and "resynthesis" did not resume until the temperature was taken above 200°C. The concentration change of anhydride groups during thermal imidization processes was successfully followed by FTIR spectroscopy (116-118). Young and Chang (119) conducted the thermal imidization of a number of polyimide precursors by an in situ diffuse reflectance FTIR technique where infrared spectra were determined while the material was being heated. Infrared analysis of the thermally staged films revealed that the polyimide precursor developed an anhydride band around 1850 cm^{-1} during imidization which disappeared during final stages of cure. Recently more quantitative studies were conducted by Tsapovetskii et al.(138) who investigated the breakdown and resynthsis of polyamic acids in solid phase imidization process. They suggested that the initial development of anhydride end groups might be due to a change in the equilibrium of amine-anhydride/amic acid in the direction of breakdown to amine-anhydride, or to a rapid

restoration of hydrolyzed chain ends. They also observed that the absolute degree of polyamic acid breakdown varies between 1 and 6~8% according to chain structure. Thus, for a highly flexible chain polymer containing ester groups, the amount of anhydride formed does not exceed 1%. For rigid chain polymers, this value is much higher (8%) and semirigid polymers containing an -O- group are characterized by intermediate values. Young et al.(120) also investigated the thermal imidization process for soluble polyimide systems. A soluble polyamic acid film was converted a soluble polyimide by staging at 25°C intervals to 325°C and characterized at each interval by several analytical methods such as FTIR spectroscopy, thermogravimetric analysis (TGA), low angle laser light scattering (LALLS), and solution viscosity measurements. A plot of $[\eta]$ as a function of temperature is given in Figure 2.1.9. Viscosities of dissolved films decrease at initial stages of curing, reaching a minimum in the 150~200°C interval, and then increase upon prolonged curing above 200°C. FTIR spectra are shown in Figure 2.1.10. The anhydride carbonyl near 1856 cm^{-1} first appears at 150°C. Its intensity increases as temperature is increased with a maximum intensity at 150°C. The band then begins to decrease and almost disappears at 325°C. These FTIR spectra correlate well with the viscosity behaviors shown Figure 2.1.9.

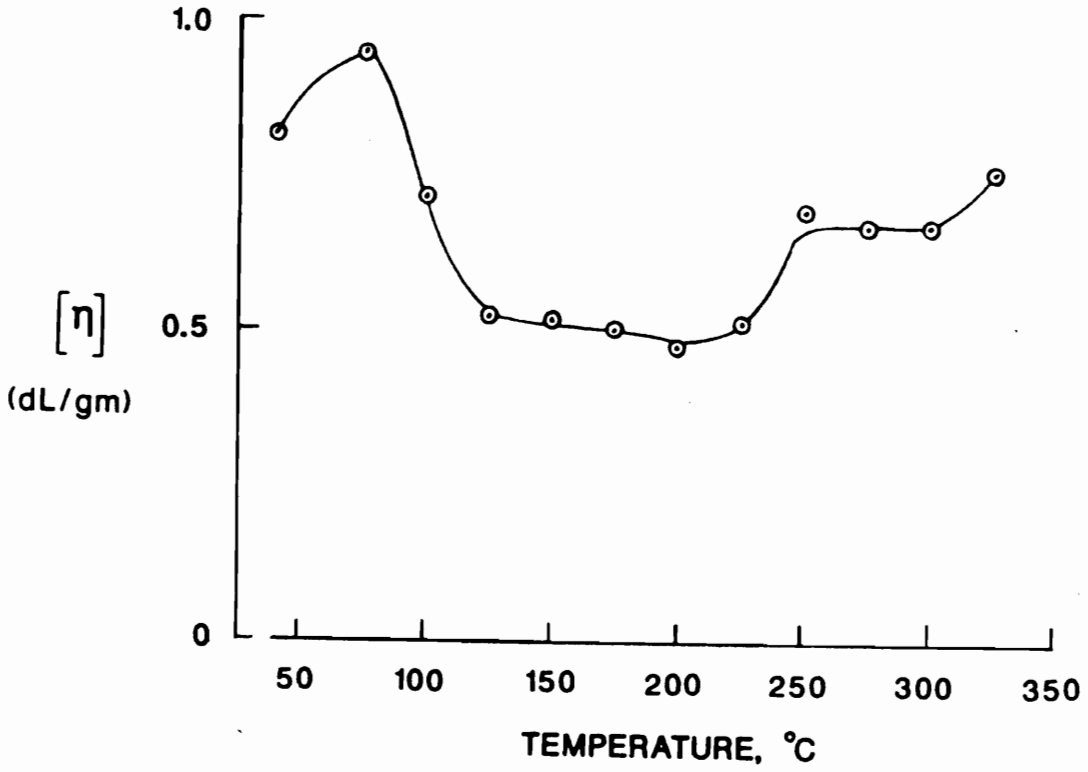

Figure 2.1.9. Intrinsic viscosity as a function of cure temperature for thermally staged films (120).

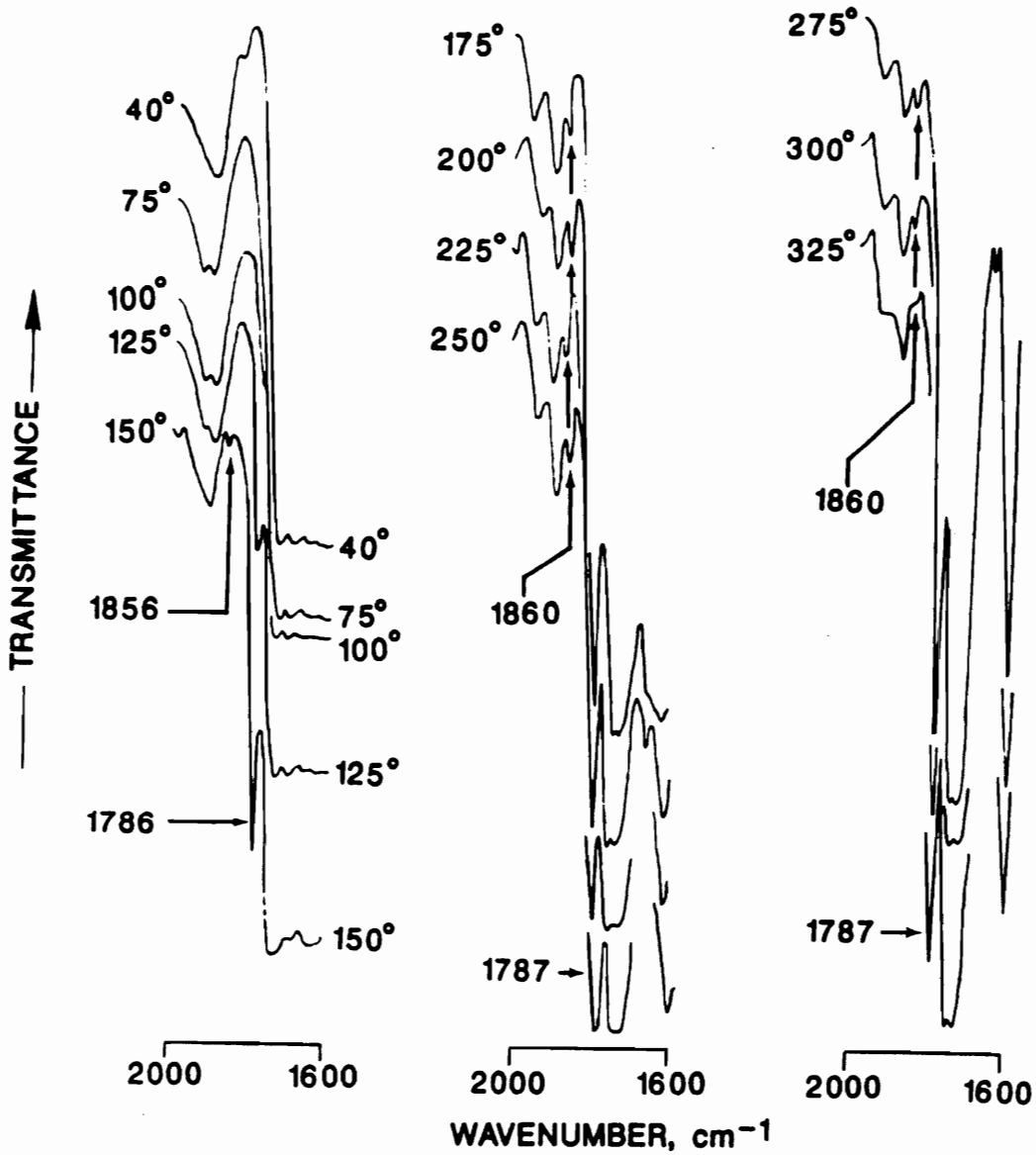

Figure 2.1.10. FTIR spectra of anhydride region of thermally staged films (120).

2.1.4.2. Crosslink formation

Crosslink formation has often been proposed because many polyimides show insolubility and infusibility and there is uncertainty over completeness of linear polyimidization by the thermal process (121-4,133-141).

In 1964, Hermans and Streef (121) proposed the idea of intra vs. intermolecular condensation during thermal imidization of solvent cast polyamic acid films. In 1986, Sacher (122) speculated on the intermolecular vs. intramolecular imide formation pathways during the PMDA/ODA polyamic acid curing process using steric and kinetic arguments. He concluded that thermal imidization proceeds through intermolecular imide link formation rather than cyclization due to a high ring strain, a delocalized nitrogen (amide nitrogen) lone pair, and steric inhibition at the carbonyl carbon. At sufficiently high temperatures, steric barriers are overcome and some intermolecularly formed imide links undergo cyclization.

Recently Snyder et al.(123,124) investigated thermal bulk imidization of PMDA/ODA polyamic acid. FTIR spectroscopy was utilized to identify the species actually formed during thermal bulk imidization of PMDA/ODA polyamic acid. An asymmetric imide carbonyl mode of the FTIR spectra of polyimides was investigated as a function of curing conditions. From FTIR data they concluded that curing of

polyamic acids at low temperatures (150~200°C) results in the formation of mixed products; principally ring closed imides and intermolecular imide links. It was also suggested that higher temperatures favors the formation of ring closed species relative to intermolecular links. From these data it could be speculated that intramolecular imidization is a thermodynamically controlled pathway and intermolecular imidization is a kinetically controlled pathway. However their data that support the intermolecular imide link formation mechanism seem to be somewhat unexpected because there are numerous examples of aromatic polyimides prepared by thermal imidization that are soluble in organic solvents or in strong acids (125-127). The unexpected conclusions might be drawn because C=O vibrational modes are very complicated by many factors such as dipole-dipole interaction (128) and Fermi resonance (129-132).

Heating at temperatures above 350°C for extended periods of time, however, resulted in crosslinking (133,134). Crosslinking at these temperatures would most likely proceed by a free radical mechanism. For example, Dine-Hart et al.(135,136) investigated the degradation of Kapton-H type polyimide by infrared analysis and hydrolyzing the degraded samples with hydrazine. They concluded that crosslinking occurs in the polyimide in the early stage of oxidative degradation when the weight loss is very small.

Jewell et al.(137) also suggested the possibility of crosslinking during degradation of polyimides. Tsapovetskii et al.(138) observed that polyimide films prepared from oligomer polyamic acid (average DP=5~10) with amine or anhydride end groups were very brittle when heated to 300°C. After heating to 400°C, the mechanical properties of these films greatly improved. When end groups in oligomer polyamic acid were blocked with phthalic anhydride, however, polyimide films remained very brittle with any heat treatment. These observations clearly suggested that reactive end groups (anhydride or amine group) play a significant role in the mechanical property improvement and thus in chain extension and crosslinking reactions. Data obtained from the analysis of the gaseous products liberated from oligomer polyimide films at high temperatures suggested the crosslinking mechanisms shown in Figure 2.1.11. Crosslink formation with an anhydride end group involves a biradical. When there are only amine end groups the crosslinking reaction may also take place by the biradical mechanism. Furthermore, crosslinking may be carried out by imide imine formation reaction at high temperatures (139).

Recently Koton et al.(140,141) investigated structural rearrangements that take place during thermal treatment of polyetherimides differing in the structure of the diamine component (Figure 2.1.12). It was observed that thermal

treatments led to the formation of a three-dimensional network. Thus, melt viscosities of polyetherimides increased upon heating at 350°C and finally went to infinity, implying network formation. Analysis of volatile materials using EPR and mass spectroscopy suggested that crosslinking proceeded by a two-stage free radical mechanism. The first stage proceeds through the formation of free radicals by decarboxylation of unreacted amic acid groups and by degradation of terminal anhydride groups with subsequent recombination of the radicals. In the second stage, the degradation of the main chains following random recombination of these fragments was observed. As a result of these reactions, flow and thus processability in these systems were changed dramatically upon exposure to high temperatures. The influence of chemical composition on the thermal degradative behavior was significant. Thus, it was observed that the bond C_6H_4-SO_2-C_6H_4 was the weakest link in SPEI-1, as evidenced by the evolution of SO_2 which set in at 320°C. The C_6H_4-O-C_6H_4 groups were somewhat stronger. Substantial decomposition of imide groups begins at 360°C, as demonstrated by the rapidly rising yield of CO_2 and CO. SPEI-2 which contains only oxyphenylene groups behaved similarly to SPEI-1, but SPEI-3 containing sulphur linkages raised resistance to heat-induced degradation.

Kuroda and Mita also observed thermally induced crosslink formation during thermal degradation of soluble polyimide (Mitsubishi PI2080) both in vacuum and in air (134). The FTIR study suggested that crosslinking occurs by recombination and addition to benzene rings of on-chain radicals formed in a chain reaction initiated by the cleavage of C_6H_4-$CH_2C_6H_4$ linkage.

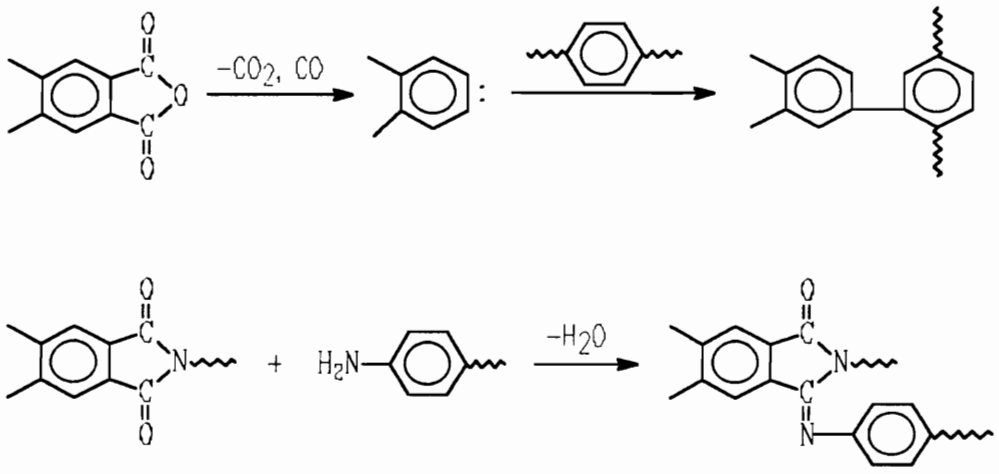

Figure 2.1.11. Proposed reaction scheme for crosslink formation with anhydride (138) and amine end groups (139).

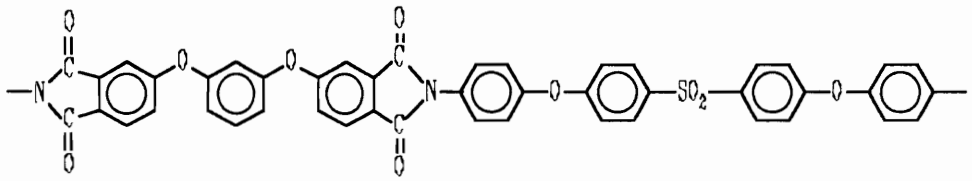

SPEI-1

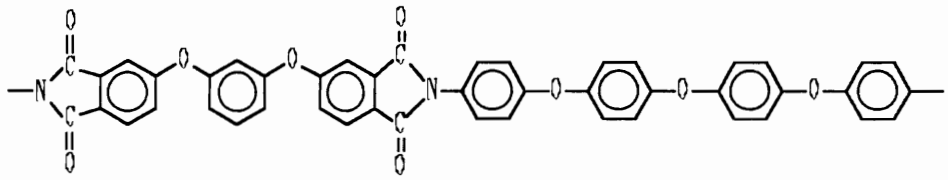

SPEI-2

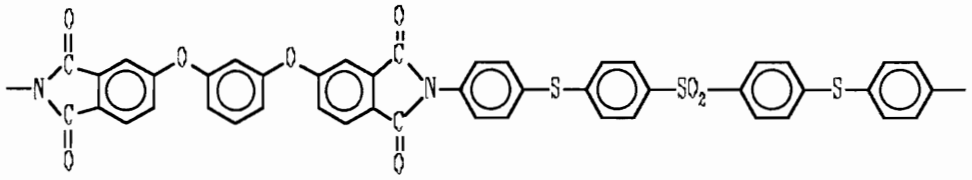

SPEI-3

Figure 2.1.12. Linear polyetherimides that were used for investigations of structural arrangements during thermal treatments (141)

2.1.5. Kinetics of thermal imidization

2.1.5.1. Rate law for the imidization of polyamic acids

Although two groups, -CONH- and -COOH, are involved in cycloimidization, the kinetic law that is followed during cycloimidization of polyamic acids has been considered as first order, because these groups belong to the same molecule, eg. an intramolecular cyclization (142). Due to this reason, the majority of imidization kinetic data have been analyzed using the first order kinetic equation: ln (1-p) = - kt, where p is degree of imidization, k is a rate constant, and t is reaction time (1−3).

However the problem concerning the reaction order of imidization of polyamic acid is not that simple. For example, Laius et al. obtained the reaction order of the imidization process which varies from 2.2 to 3.2 (143). Lavrov et al. (144) investigated imidization of model compound N-phenyl phthalamic acid, reaction product of aniline and phthalic anhydride, in various solvents such as DMAc (designated as DMAA), DMF, m-cresol, and diglyme. The solution imidization of the model amic acid in DMF at 145°C followed a second order kinetic equation. But the rate constant was not constant throughout the imidization process but was characterized by two distinct rate constants. At 40~60% conversion the rate constant reduced due to side reactions such as hydrolysis of amide bonds and reaction of

DMF with isophthalic acid (hydrolyzed product of phthalic anhydride). In addition, the rate of imidization of the model amic acid was influenced by the solvents, being decreased as the basicity of the solvent increased. This solvent effect on the reactivity suggested that autoprotonation of amic acid groups is suppressed when the basicity of the solvent is increased. There is additional evidence of acid catalysis on the rate of imidization. Lavrov et al. (171) observed that carboxylic acids accelerate ring formation of polyamic acids in the solid phase.

As discussed already polyamic acid undergoes side reactions during thermal imidization processes due to instability of polyamic acids. Many researchers, however, have not included the effects of such side reactions in the rate law for imidization kinetic investigations because it was considered that such side reactions occur to a small extent, therefore having practically no effect on the imidization kinetics. The equal reactivity assumption (145) has also been widely assumed for o-carboxycarboxamide groups although a polyamic acid has several microstructures in the polymer back bone, two or three depending on the monomers, and chemical environments of the functional groups change as imidization proceeds. Several works regarding these problems are found in the literature (84,146-148).

For example Eumi et al.(84) investigated thermal imidization of polyamic acid made from a conjugated diamine (p,p'-diaminoazobenzene, DAA) and a nonconjugated dianhydride (6FDA) in dilute solution and in solid state in the temperature range of 150~190°C. UV/VIS spectroscopy was the main tool used, but FTIR spectroscopy was also used for comparison with results from UV/VIS study. In this study, the azo functional group containing monomer was used to take advantage of the unique electronic states associated with each cure species and thus to magnify UV/VIS spectral shifts. Nonconjugated dianhydride was used to suppress the charge-transfer complex formation because charge transfer complexes might interfere in the UV/VIS spectra. In the 1% polyamic acid solution in NMP, dissociation and the first ring closure of polyamic acid proceeded faster than the second ring closure of polyamic acid/imide. This observation of reactivity difference was ascribed to the reduced basicity of the amide groups polyamic acid/imide compared to the analogous group in polyamic acid. However it is noteworthy to mention that the reactivity difference may not always be observed for other polyimide systems. In the above mentioned study that is a special case, involving the conjugate monomer p,p'-diaminoazobenzene, the imide group in the polyamic acid/imide exerts a direct influence on the electronic environment of amide nitrogen of the polyamic

acid/imide through resonance. They also found that the apparent rate constant in the solid phase imidization process was initially faster than in dilute solution and then leveled off. This observation was interpreted based upon the catalytic effect of the neighboring group of amic acid groups and vitrification.

2.1.5.2. Kinetic features of the imidization process

The solid phase thermal imidization process is a very complex physico-chemical process where imidization kinetics are influenced by many factors. For example, nominally dry polyamic acid contains quite a high portion of amide solvents (up to 25~30%) which is firmly retained by the polymer through specific interactions such as hydrogen bonding (12,30,97). During imidization of polyamic acids these associations are destroyed and the solvents are released (97). Thus, the physical and chemical properties of the polymers are continuously changed upon cyclization. Due to these complex characteristics of the imidization process, the rate of imidization has been reported to be dependent on many parameters such as the casting solvent (149-152), film thickness (79), imidization temperature(94,97,150-153,159), heating rate (154), and chemical structure (152,155).

The most typical feature of solid phase thermal cyclization is a sharp decrease in the rate of imidization

once a certain degree of imidization is achieved (143,97). Thus, the imidization process was characterized by an initial fast cyclization which changed into a second, slow cyclization process long before the reactive species are consumed (170). In most cases, the rate constant remains invariable only during the initial step of the reaction and then decreases continuously (52). Such a process is called kinetic interruption (170). There is no general consensus regarding the reasons for decrease in the imidization rate at the later stages of imidization process. The two step kinetic feature was rationalized in terms of non-equivalent kinetic states of polyamic acid (143), Tg increase during imidization process (94,143), which seems most appealing and "breakdown-resynthesis" of polyamic acid equilibrium.

For example, the "breakdown/resynthesis" of polyamic acids argument can be explained as follows. Polyamic acid degradation results in the formation of terminal anhydride and amino groups, and thus a definite fraction of the polyamic acid units is temporary excluded from the cyclization process, which in turn causes the slow down of cyclization. Bessonov et al.(52), however, concluded that the reason for slowdown of solid-phase cyclization cannot be accounted for by (or only by) degradation of amic acid units. Analyzing experimental data that had been reported previously: 1) no significant degradation of polyamic acid

was found during thermal solid phase imidization processes (156,157) and thus, the effect on the cyclization kinetics is insignificant; 2) although greater degradation was observed upon cyclization in solution imidization processes the latter could be treated by first order kinetics up to 70~80% (111), where as in solid phase cyclization, deviations from first order kinetics were already observed at 30~40% (158) imidization.

Other arguments (except the breakdown-resynthesis of polyamic acid) have considerable experimental support. For example, Kruez et al.(97) studied the rates of thermal cyclization of solvent cast polyamic acid films prepared from 4,4'-ODA and PMDA in the temperature range of 160° to 188°C. The rate of imidization was very slow below 150°C. Beyond this point, imidization increased rapidly with temperature and was characterized by an initial fast cyclization which changed into a second, slower cyclization process (Figure 2.1.13). Since the data did not allow an unequivocal determination of the order of the reaction, those data were interpreted in terms of rapid and slow first order processes with specific rate constants. Surprisingly, the activation energies for both the first and the second steps were nearly identical (≅105KJ/mol). However, the difference in the entropy of activation, -10 e.u. for the fast reaction and -24 e.u. for the slow, was significant and

indicative that control of the relative rates resides in the frequency factor. The authors suggested that the large entropy loss during the latter portion of imidization could be related to Tg increase with conversion and the possibility that the casting solvent (eg. DMAc) assists in favorable orientation for ring closure and its loss before complete conversion retards imidization rates. Furthermore, in contrast to imidization in polymeric systems, the model compounds, N-phenylphthalamic acid and N-p-methoxyphenyl-phthalamic acid, in DMAc at 150°C were observed to follow first order kinetics for greater than 75% of the total imidization.

More evidence that solvent aids the imidization process can be found in the literature (79,154,159). For example, Ginsgurg and Susko (79) investigated thermal imidization of solvent cast PMDA/ODA polyamic acid films of varying thickness. The technique employed for characterization of the polymer films was FTIR spectroscopy. As shown in Figure 2.1.14 it was demonstrated that the rate of imidization is dependent on film thickness. Thicker films cured to a greater extent of imidization than thinner films, because of their increased retention of entrapped solvent which permitted increased molecular chain motion (79).

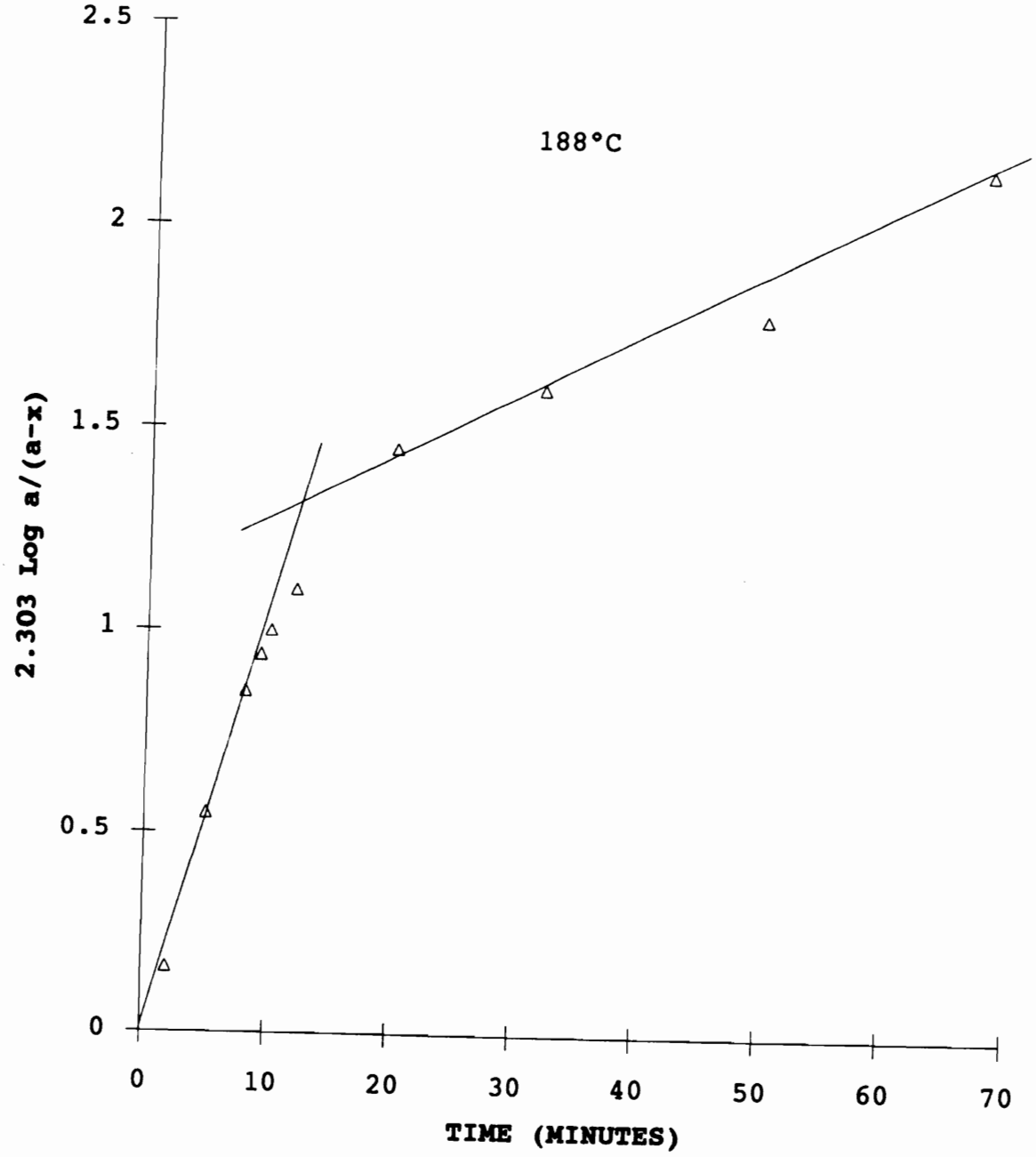

Figure 2.1.13. Logarithmic plot of conversion of polyamic acid (97).

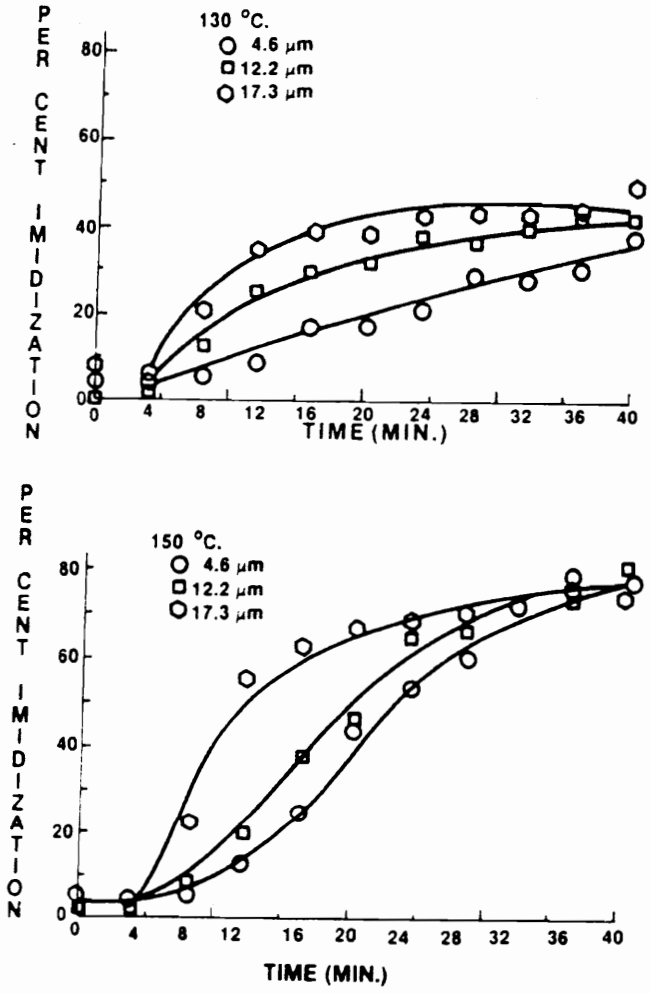

Figure 2.1.14. Per cent imidization versus time are shown at reaction temperature of 130°C and 150°C for three film thicknesses. Dynamic cure data was plotted to demonstrate the convergence of the degree of cure for films of varying thickness with time (79).

It was reported that polyamic acids interact with amide solvents such as DMAc and NMP through a hydrogen bond (160) and thus form strong hydrogen-bonded complexes with the solvents. For example, Kreuz et al. observed that after attaining constant weight at room temperature under reduced pressure, polyamic acid (PMDA/ODA) forms hydrogen bonded complexes with DMAc and the complexes contain one molecule of solvent (DMAc) per carboxy group (12,161). The hydrogen bonding interaction or complex formation tendency have been thought to significantly affect the thermal imidization process. Complex formation of polyamic acid and NMP and their effects on the imidization kinetics were thoroughly studied by Brekner and Feger (162,163). They reported that solvents such as N-methyl pyrrolidone (NMP) can form intimate complexes with amic acid model compounds from PMDA and aniline (Figure 2.1.15). The model diamic acid forms two complexes with NMP, both of which have characteristic stoichiometric ratios (1/4 and 1/2) and decomplexation temperatures as indicated by TGA analysis. They suggested that in the solid state these complexes have conformations held in place by hydrogen bonding. After full decomplexation hydrogen bonds still exist and hinder imidization. Only at temperatures high enough to break the hydrogen bonds can the highly reactive free groups react. The authors noted that the effects of complex formation on the imidization kinetics

are less pronounced in solution than in the solid state, because NMP exchange between solvent and complex takes place, and conformations change constantly. If a favored conformation is reached, imidization can occur. They also believed that the imidization process might be facilitated through solvent assistance during the proton transfer.

As mentioned earlier it has been shown that the stepwise behavior of imidization rates during thermal bulk imidization processes is related, to a large extent, to a Tg rise during an imidization process (94,143,164). As the imidization process continues, the polymer's Tg increases so that the polymer changes from a rubbery state to a glassy state. The decrease in the rate of cyclization is due to the decrease of molecular mobility in the glassy state, and segmental motion ceases (151). As a result, it is very difficult for the amic acid groups to attain suitable conformations for cyclization. For example, S. I. Numata et al. successfully followed thermal imidization processes by measuring the weight losses that occur during cyclodehydration (94). They also found that when polyamic acid films were heated isothermally the imidization reaction slowed down markedly after a given temperature was reached. The temperature at which the imidization reaction ended was around the glass transition temperature of the resulting polyimide. The observation that the abrupt decrease in rate

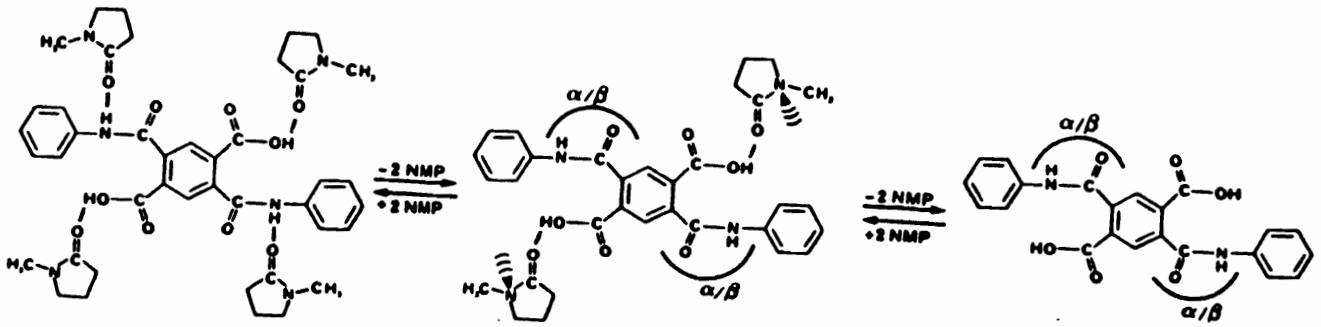

Figure 2.1.15. Complexation/decomplexation process: α/β indicates the possibility of two different molecular surroundings; ◄))) indicates the possibility of involvement in hydrogen bonding (162).

constants is ascribed to the decreased molecular mobility in the glass state was experimentally demonstrated by Korshak et al.(166). Tg and degree of imidization could be obtained because Tg corresponds very closely to the cure temperature at the maximum degree of imidization that can be achieved under a typical cure temperature. Using the experimentally determined relationship between Tg and degree of imidization they obtained viscosities of polymers as a function of temperature and degree of imidization from the important empirical correlation, Williams-Landel-Ferry (WLF) equation (166).

$$\log \eta(T,i) = 12 - \frac{17.44\ [T-Tg(i)]}{51.6 + [T-Tg(i)]}$$

Where $\eta(T,i)$ is the viscosity as a function of temperature and the degree of imidization and Tg(i) is the glass transition temperature of the cured material at the degree of imidization of i. When the calculated viscosity values were correlated with experimentally determined rate constants, it was found that rate constants were practically independent of the viscosity. Therefore they concluded that the rapid decrease in rate constants at the glass transition is not due to the dependence of rate constant on viscosity, but due to a large change in molecular mobility. Of course, these two parameters are often closely related.

Although the idea of the abrupt decrease in rate constants at glass transitions has been attested experimentally, even for other thermoset systems (167,168), the two step kinetic feature is not exclusively due to the Tg effect. Laius and Tsapovetsky (170) studied thermal imidization of polyamic acids of varying molecular weights under conditions such that molecular mobility and other characteristics of the environment remain practically constant during cyclization. Surprisingly under these conditions the rate of imidization did show a strong molecular weight dependence, being increased as the molecular weight decreased. These data suggested that the decrease in the rate of imidization was also caused by the polymeric nature of the polyamic acid. In such a case, the reduction of rate constant should be attributed to "kinetic non-equivalence" of various amic acid moieties, caused, for example, by differences in their conformations or in inter and intramolecular hydrogen bonding interactions. One typical example of the kinetic non-equivalence has been considered from the view point of possible conformational situations. Two of the possible planar conformations are shown in Figure 2.1.16. Conformation a) is more and conformation b) is less favorable for cyclization. The transition from a) into the state favorable for cyclization

is possible only when the motion of the CONH group in cooperative with the adjoining part of the polymer chain.

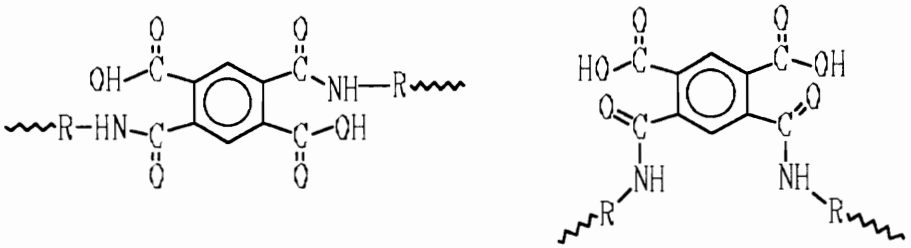

a b

Figure 2.1.16. Two possible planar conformations (169).

Laius et al.(170) proposed two models describing the cyclization of polyamic acids under both isothermal and non-stationary conditions. Cyclization was regarded as a two stage physico-chemical process in which both the molecular mobility of the polymer matrix and the physical state of interchain groups transformed into imide rings play an important role. According to this model cyclization of imidization process consists of the stage in which the amic acid groups change their physical state and the second stage, chemical transformation of amic acid groups into the imide ring. These models were used to explain the two-stage imidization process as follows. In the rubbery state (below Tg), molecular mobility is high and transitions between kinetically non-equivalent states are facilitated. Thus,

these transitions do not limit the rate of cyclization. The limiting factor is the rate of chemical transformation. Hence, the rate is high and the parameters of the process are weakly dependent on conversion and are close to those of the reaction occurring in solution. After the polymer passes from the rubbery to glassy state, the transitions between kinetically non-equivalent states become difficult and begin to limit the rate of imidization. The rate constant decreases sharply and becomes dependent on conversion. The amic acid groups are distributed according to reactivities and this distribution determines the further kinetics of the process.

2.1.4.3. Effects of chemical structure on reactivity

It was found that chemical structures exert a certain, although not quite clear, effect on the cyclization rate (111,171-175). For example, Laius et al. (175) investigated ring formation of PMDA based polyamic acids and model amic acids to investigate the effect of the structure of the diamine component on the rate of imidization.

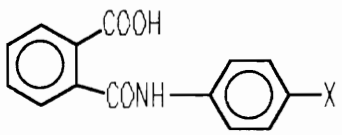

Where X=H, CH_3, OCH_3, OH, $N(CH_3)_2$, Br, NO_2.

The above model compounds shown below were imidized in a DMF solution at 145°C with initial concentration of 0.15 mole/l. After a given time interval samples were taken and the degree of imidization was determined by FTIR spectroscopy. It was found that the rate of imidization depends on the basicity of the initial amine, a deciding factor of which isthe electron acceptor or electron donor nature of substituent X. The rate is accelerated by an increase in electron donating nature of the substituent X: NO_2 (no cyclization)<<Br<H<CH_3<$O(CH_3)$<OH<$N(CH_3)_2$. The addition of a strong electron withdrawing group fully suppressed ring formation. A linear relationship was found between the logarithmic second order rate constant and the Hammett substituent constant (σ_H). A negative reaction constant (ρ), -0.84 reflected that the tendency to ring formation of the amidoacid is determined by nucleophilic character of the amide group. Solid phase imidization of PMDA based polyamic acids of varying diamine structures were also investigated. As shown in Table 2.1.1, the rate of imidization increased with an increase in the basicity of initial diamine, however; the linear logarithmic relationship between the rate constant and the value of pKa of the initial diamine was only maintained for a given series of polyamic acids, which were characterized by the presence of a bridge unit in the diamine residue: -NH-, -O-, -S-, $-CH_2$, and $-SO_2-$. The

rate constants of ring formation of PAA-I and PAA-II were considerably lower than the value that can be anticipated from the pKa values. From these findings it was suggested that polymer stiffness might play a role in the kinetics of imidization.

Lavrov et al.(171) also studied the thermal imidization of model amic acids and aromatic polyamic acids with different structures in the dianhydride components. It was shown that during ring formation of the model compounds in solution, addition of electron acceptor substituents to the anhydride component increased reactivity. At the same time, during ring formation of polyamic acids in the solid phase there was a tendency for an increase in the reactivity of amic acid units with an increase in electron donating properties of bridge units in the dianhydride components. The rate constant changes were relatively small.

Table 2.1. Second order rate constants of ring formation of polypyromellitamic acids with varying structures of the diamine residue (175)

Polyamic acid	Diamine residue	pKa of diamine	k, g/mole·sec
PAA-I	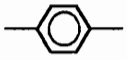	6.19	0.205
PAA-II	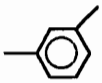	4.88	0.172
PAA-III	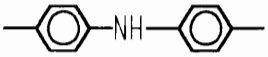	5.86	0.315
PAA-IV	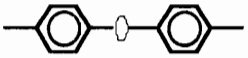	4.75	0.200
PAA-V	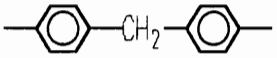	4.68	0.184
PAA-VI	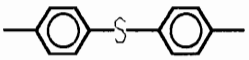	4.03	0.193
PAA-VII	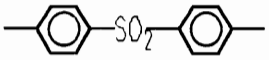	2.03	0.098
PAA-VIII	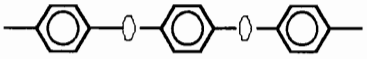	4.63	0.398

2.2. Polymer blends

Since the properties of a given homopolymer do not always meet an ever-expanding and seemingly endless number of industrial applications, modification of the physical and chemical properties has been required. Such modification of properties could be achieved through copolymerization or polymer blends by combining the properties of constituent polymers. Polymer blends, physical mixtures of structurally different homo- or copolymers, have attracted strong interest, since they are easily adapted to specific needs. Moreover, they provide material characteristics that may not be realized via a copolymerization approach (176-178). The equilibrium-phase behavior and polymer blends based upon polyimides are discussed here.

2.2.1. Thermodynamic aspects of equilibrium-phase behavior

Equilibrium-phase behavior of mixtures is governed by the free energy of mixing

$$\Delta G_{mix} = \Delta H_{mix} - T\Delta S_{mix} \qquad \text{Eq. 2.2.1}$$

and how this quantity, consisting of enthalpic (ΔH_{mix}) and entropic (ΔS_{mix}) parts, is affected by composition and temperature (170-182). For a system to be thermodynamically

stable, the Gibbs free energy of mixing (ΔG_{mix}) must be negative. This involves a balance between the enthalpy and entropy of mixing, and a boundary between stable and unstable states determined by the condition $\Delta G_{mix} = 0$. However, such a statement for thermodynamic stability, $\Delta G_{mix}<0$, is not a necessary and sufficient criterion. Indeed, mixtures can be and often are unstable at negative ΔG_{mix} (though not, of course, relative to the pure component), and can diminish ΔG_{mix} still further by separating into two phases. The stability of the system is, therefore, determined not only by a free energy of mixing, but also by the curvature of $\Delta G_{mix}(\varphi_2)$ where φ_2 is the volume fraction of the second component. For miscibility, the Gibbs free energy of mixing must be negative and satisfy the additional requirement

$$\left(\frac{\partial^2 \Delta G_{mix}}{\partial \varphi_i^2}\right)_{T,P} > 0 \qquad \text{Eq. 2.2.2}$$

which ensures stability against phase segregation (T=temperature and P=pressure). Figure 2.2.1 illustrates this situation for a strictly-binary mixture. At T_1, the above two conditions are fully satisfied, and miscible, single phase mixtures occur for all compositions at this temperature. The tangent line at any point on the curve of $\Delta G_{mix}/RT$ versus φ_2 gives us very important quantities. The intercepts of the tangent line at $\varphi_2=0$ ($\varphi_1=1$) and $\varphi_2=1$

correspond to $\Delta\mu_1/RT$ and $\Delta\mu_2/RT$, respectively, where $\Delta\mu_i=\mu_i-\mu_i°$, μ_i=chemical potential of the component i, and $\mu_i°$=chemical potential of the component i at the standard state. At T_2, Eq. 2.2.2 is not satisfied for all compositions. Thus, only mixtures with composition $\varphi_2<\varphi_2'$ and $\varphi_2>\varphi_2''$ are stable. Every other system with composition $\varphi_2'<\varphi_2<\varphi_2''$, at equilibrium, will separate into two phases with these compositions as this results in a total free energy falling on the dashed line (a common tangent line), which is lower than that of the homogeneous phase (solid line). The phases at compositions φ_2' and φ_2'' have the same chemical potential for both components as discussed above and thus they are in equilibrium. The border between the stable and unstable regions is called a binodal which is obtained by equating the chemical potentials of each component in both phases. The unstable region is further subdivided into a metastable and an unstable region and, in particular, the borders are called spinodals $\{(\partial^2\Delta G_{mix}/\partial\varphi_2^2)_{T,P}=0\}$. A metastable composition either forms a single phase if clean and relatively undisturbed or, at equilibrium, will separate into two phases (φ_2' and φ_2''). It is extremely difficult to observe metastable compositions before phase separation begins in mixtures of low molecular weight molecules (183), however, metastable compositions could remain as a single phase almost

indefinitely in very viscous polymer mixtures. The curve at T_c has been drawn in a manner satisfying the conditions of a critical point where two minima at concentrations of φ_2' and φ_2'', the maximum, and the two inflection points at $\varphi_{2,sp}'$ and $\varphi_{2,sp}''$ all merge into a common point. That is

$$\left(\frac{\partial^2 \Delta G_{mix}}{\partial \varphi_2^2}\right)_{T,P}=0, \text{ and } \left(\frac{\partial^3 \Delta G_{mix}}{\partial \varphi_2^3}\right)_{T,P}=0$$

In the phase diagram of T vs. φ_2 in Figure 2.2.1, $T_1>T_2$, and T_c is an upper critical solution temperature (UCST) above that complete mixing occurs. There are also systems that form one phase below a certain temperature, a lower critical solution temperature (LCST). The compositions demix above the LCST.

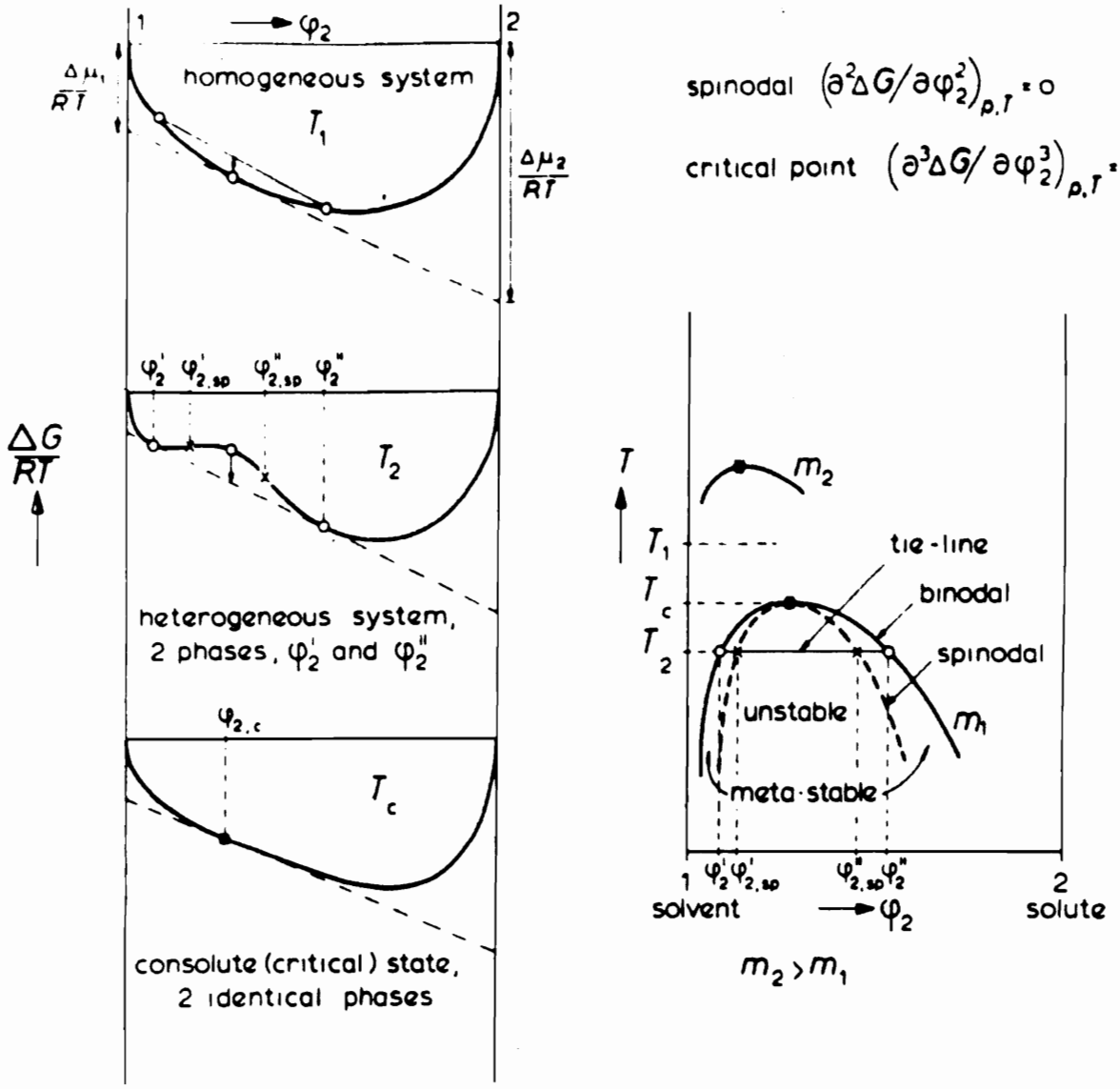

Figure 2.2.1. Gibbs free energy of mixing as a function of concentration in a binary liquid system showing partial miscibility (182).

2.2.2. Polyimide blends

Polymer blends of polyimides with polybenzimidazole (PBI) have received attention as means of developing polymeric matrix resins needed for advanced aerospace, fiber reinforced composite and adhesive applications. Commercially produced PBI possesses an unusually high glass transition temperature of 425°C and good high temperature mechanical properties, but it lacks true thermoplastic processibility and has poor long-term thermo-oxidative stability and high moisture regain (184,185). Polybenzimidazole was reported to be miscible with a wide range of polyimides (186-195). Among them are General Electric's Ultem 1000 (187-189,191,193), Ciba-Geigy's XU 218 (187-189), Dow Chemical Company's PI 2080 (187,188,192), Mitsui Toatsu Chemical's LaRC TPI (188), BTDA/3,3'-DDS based polyimides (190), and copolyimides containing hexafluoroisopropylidene moiety (194). In view of recent studies some modification of the earlier statements may be necessary. The chemical structures of PBI and the polyimides that were used in blend studies are shown in Figure 2.2.2. Blend miscibility was evidenced in the form of single Tg values, well-defined single tan δ relaxations intermediate to those of the component polymers, and the formation of clear films.

PBI/Ultem 1000, PBI/XU 218, and the PI 2080 blends were reported to undergo phase separation by heating above Tg's

Ultem 1000: General Electric, Tg=220°C

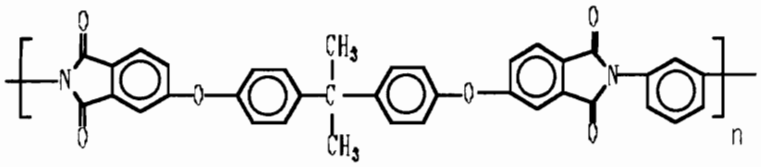

Ciba Geigy's XU 218: Tg=320°C

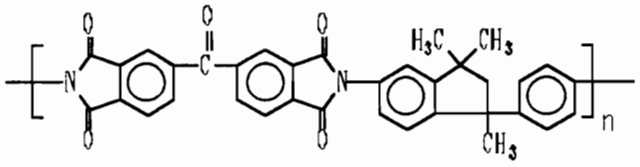

Dow 2080: Tg=310°C

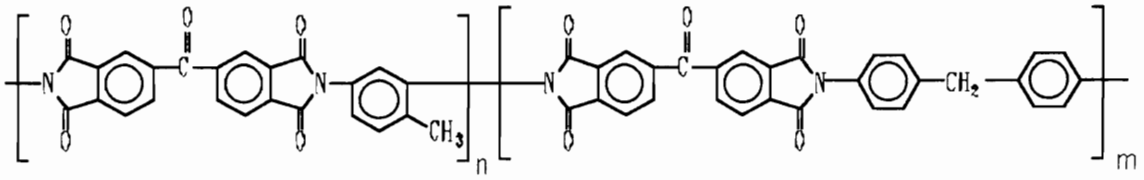

80 mole % 20 mole %

Mitsui Toatsu's LaRC TPI: Tg=267°C

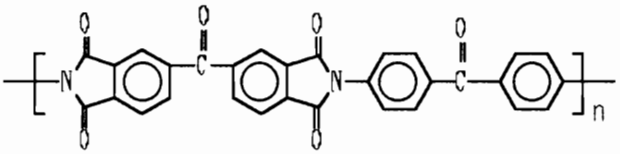

Hoechst Celenease PBI: Tg=425°C

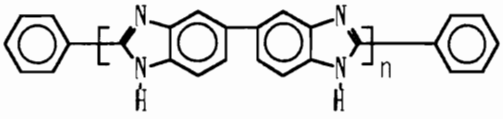

Figure 2.2.2. Chemical repeat unit structures of some commercial polyimides and PBI

and quenching (187). The equilibrium phase boundaries lie between room temperature and the glass transition temperatures and in the vicinity of 440 to 450°C for PBI/Ultem 1000 and for 50/50 wt. % PBI/XU 218 blends, respectively. For PBI/Ultem 1000 blends actual phase separation, however, did not occur above the phase boundary until Tg was reached because of the restricted mobility of the polymer chains in the glass state. To establish the approximate miscibility/immiscibility phase boundary for the PBI/Dow PI 2080 blends, an approach based on the temperature dependence of the infra-red spectral shift of the PBI N-H stretching band was used (192). The usual approach based on the analysis of the glass transitions of the system could not be used advantageously, due to the instability and gradual undetectability of the Tg values upon high temperature annealing. PBI/XU 218 blends subjected to the high temperature thermal conditioning (for example, 400°C) showed shifts in the tan δ peaks to higher temperatures and a decrease in the peak height. From these results thermally induced crosslinking was suggested (187).

FTIR spectroscopy was also used for studying the molecular interactions in PBI/Ultem 1000 blends (189,191). Information concerning the nature of the interactions, hydrogen bonding and their strengths were obtained by analyzing the N-H stretching region of PBI and carbonyl

stretching region of Ultem 1000. Because of the lack of the reliable correlations between peak shifts of N-H stretching bands in the blends and thermodynamic parameters for the specific donor-acceptor pair, the quantitative evaluation of the enthalpic content of the interaction was impossible. However the absolute value of the N-H band shift ($\sim$50 cm^{-1}), when compared with the corresponding shifts observed in other N-H containing systems, suggested the weak hydrogen bond nature in PBI/Ultem 1000 blends. FTIR spectroscopy was also used to investigate the temperature behavior of the PBI/Ultem 1000 blend. Recently Liang et al. studied thermal, dielectric, and mechanical relaxation measurements on the PBI/Ultem 1000 blends prepared by solution casting from DMAc and proposed that the observed miscibility is due to kinetically controlled metastable effects (193). Figure 2.2.3 shows DSC thermograms of a 60/40 wt. % PBI/Ultem 1000 prepared from solvent casting as a function of annealing temperatures. The most important feature of the thermograms is the appearance of an endotherm below the glass transition. With an increase of the annealing temperature, the endotherm peak temperature shifts toward Tg and finally overlaps the glass transition. The behavior was interpreted in terms of an enthalpy relaxation. Thus, the relatively large temperature difference between the Tg and the endotherm peak position at low annealing temperatures was

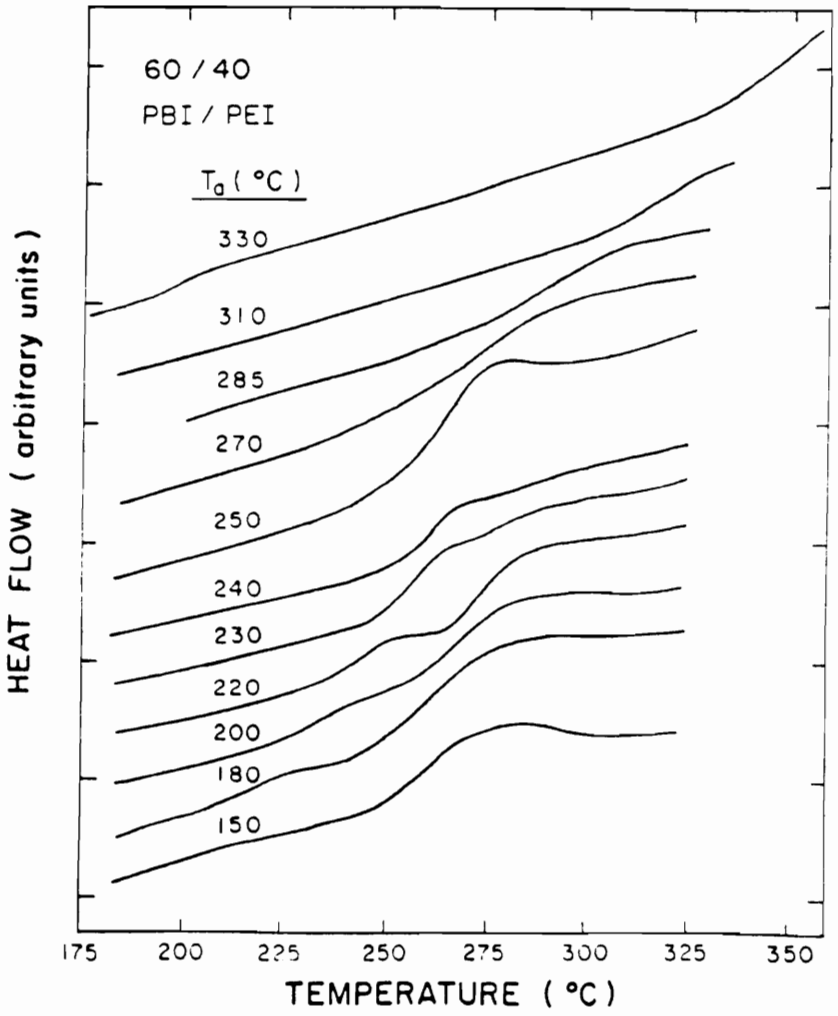

Figure 2.2.3. DSC traces of 60/40 wt. % PBI/Ultem 1000 blends annealed for 20 minutes at selected temperatures (193).

understood to be a consequence of the strained, nonequilibrium glassy structure formed during the casting process. Based upon the observed thermal and mechanical relaxation behavior it was concluded that the PBI/Ultem 1000 blend forms homogeneous dilute solutions in DMAc, and on the removal of the solvent, a non-equilibrium, single-phase structure remains. Thus, phase separation is prevented by kinetic factors (by low segmental mobility in the glassy state) but can and does occur above the glass transition, that is, as soon as the mobility is high enough.

Polymer blends of imides with imides have also received attention to produce a new advanced material whose properties meet the specific requirements needed for optimum performance in specialty applications (196-201). Yokota et al.(196) and Yoon et al.(197) reported their work on the "molecular composite" film comprizing a ductile matrix of a flexible polymer reinforced with a high strength, high modulus rigid-rod polymer. Due to the poor processability and poor solubility of many rigid aromatic polyimides, polymer blends were prepared by mixing polyamic acid solutions (196-200). Yokota et al.(196) investigated mechanical properties of imide/imide blends based upon a rigid imide, s-BPDA/p-PDA polyimide, and a ductile flexible coil polyimide, s-BPDA/4,4'-ODA as a function of drawing ratios, blend compositions, and "curing" conditions. Dynamic

mechanical thermal analysis and optical microscopy suggested that polyamic acid blends were experienced a randomization of the two homopolymers (198). This observation was, of course, consistent with the previous observation of an equilibrium between anhydride and amine components of the parent polyamic acids (202). Thus, miscibility behavior of imide/imide blends prepared via solution mixing of the corresponding polyamic acids, followed by a subsequent curing process was observed to depend not only on the interaction energy, χ, between two polymer segments but also on the degree of chemical randomization.

Chung et al.(201) studied miscibility behavior of hexafluoroisopropylidene containing polyimide blends. It was found that the strength of the molecular interaction resulting in miscibility was a function of monomer geometry as well as monomer rigidity. Thus, BTDA containing 6F polyimide blends had a higher tendency (small χ) for molecular packing than pairs containing ODPA since -CO- unit in BTDA causes less structure change from $-C(CF_3)_2-$ than -O- unit in ODPA. Moreover the polyimides with rigid dianhydrides, such as PMDA and s-BPDA, generally resulted in blends with greater calculated χ values. Nevertheless, the hexafluoro- isopropylidene group containing polyimide pairs were miscible with each other, if the dianhydride composition is the same in each pair.

CHAPTER 3

EXPERIMENTAL

3.1. Solvent purification

In order to obtain controlled, high molecular weight polymers carefully dried solvents were used. The solvents for synthetic reactions were distilled from drying agents such as phosphorus pentoxide(P_2O_5) and calcium hydride(CaH_2). Prior to vacuum distillation solvents were allowed to stir over drying agents for more than 12 hours under a nitrogen atmosphere, refluxed for an hour under vacuum, and then distilled. The distilled solvents were stored under nitrogen and were handled using syringe techniques to minimize moisture contact.

3.1.1. 1-Methyl-2-Pyrrolidinone (NMP)

Supplier:	Fisher Scientific
Molecular formula:	C_5H_9NO
Molecular weight, g/mol:	99.13
Boiling point, °C/mmHg:	205/760, 81~82/10
Melting point, °C:	-24
Density, g/cm^3:	1.033

Chemical structure:

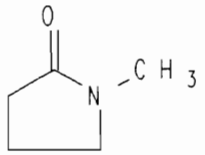

Purification procedure: NMP was purified by distillation under reduced pressure after drying over phosphorus pentoxide. The first fraction was discarded and a constant

boiling fraction was obtained as a colorless liquid and was stored in a flask sealed with a rubber septum.

3.1.2. 1-Cyclohexyl-2-pyrrolidinone (CHP)

Supplier: GAF Corporation
Molecular formula: $C_{10}H_{17}NO$
Molecular weight, g/mol: 167.25
Boiling point, °C/mmHg: 290/760, 154/7
Chemical structure:

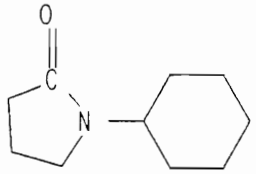

Purification procedure: CHP was purified by distillation under reduced pressure after drying over calcium hydride. The solvent was then distilled under reduced pressure generated by a mechanical vacuum pump. The constant boiling fraction was collected and stored in the sealed flask after nitrogen substitution.

3.1.3. 1,2-Dichlorobenzene (ODCB)

Supplier: Fisher Scientific
Molecular formula: $C_6H_4Cl_2$
Molecular weight, g/mol: 147.00
Boiling point, °C/mmHg: 179~180/760, 81~82/31
Melting point, °C: -18 ~ -15
Density, g/cm^3: 1.306
Chemical structure:

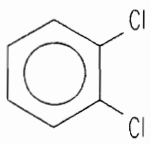

Purification procedure: ODCB was purified by distillation under reduced pressure after drying over calcium hydride. The solvent was then distilled under reduced pressure and the constant boiling middle fraction was collected in a round bottomed flask, sealed with a rubber septum, and stored under low nitrogen pressure.

3.1.4. Deuterated solvents

Chloroform-d (Aldrich, 99.8 atom % D), acetone-d_6 (Aldrich, 99.5 atom % D), and dimethyl sulfoxide-d_6 (Aldrich, 99.5 + atom % D) were used as received for NMR analysis.

3.2. Purification of amines

3.2.1. 1,4-Phenylene diamine(p-PDA)

Supplier:	Aldrich
Molecular formula:	C_6H_8N
Molecular weight,g/mol:	108.14
Boiling point, °C/mmHg:	267/760
Melting point, °C:	143~145

Chemical structure:

Purification procedure: p-PDA was purified by sublimation with the oil bath setting at 145°C under reduced pressure generated by a mechanical vacuum pump.

3.2.2. 1,3-Phenylene diamine(m-PDA)

Supplier: Aldrich
Molecular formula: C_6H_8N
Molecular weight, g/mol: 108.14
Boiling point, °C/mmHg: 282~284/760
Melting point, °C: 64~66
Chemical structure:

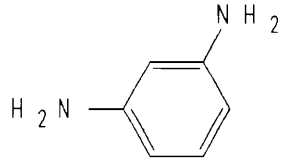

Purification procedure: m-PDA was purified by sublimation with the oil bath setting at 70°C under reduced pressure generated by a mechanical vacuum pump. m-PDA was very easily deactivated; for example, it was deactivated within few hours in the presence of light and air. Thus, m-PDA was collected in a brown colored bottle and stored in the desiccator under nitrogen.

3.2.3. 3,3'-Diaminodiphenyl sulfone (m-DDS)

Suppliers: Aldrich, Chriskev, Kennedy and Klim
Molecular formula: $C_{12}H_{12}N_2O_2S$
Molecular weight, g/mol: 248.30
Melting point, °C: 170~173
Chemical structure:

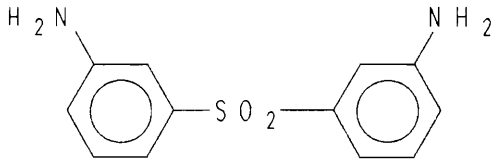

Purification procedure: The slight tan colored powder m-DDS was purified by recrystallization in deoxygenated methanol.

Thus, methanol in an erlenmeyer flask was deoxygenated by purging with nitrogen for 3~4 hours at ambient temperature, then heated to boiling. m-DDS was slowly added to the stirring deoxygenated methanol until a saturated solution was obtained. Then, the solution was cooled to room temperature and kept in the refrigerator for 24 hours. A very slightly tan crystalline powder was obtained after filtrating, washing with deoxygenated methanol, and drying at 100°C in a vacuum oven for at least 24 hours.

3.2.4. 4,4'-Diaminodiphenyl sulfone(p-DDS)

Suppliers: Aldrich, Chriskev, Kennedy and Klim
Molecular formula: $C_{12}H_{12}N_2O_2S$
Molecular weight, g/mol: 248.30
Melting point, °C: 175~177
Chemical structure:

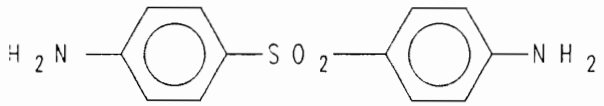

Purification procedure: p-DDS was purified by the similar procedure used for the purification of m-DDS.

3.2.5. 4,4'-Oxydianiline (4,4'-ODA)

Suppliers: Aldrich, Chriskev
Molecular formula: $C_{12}H_{12}N_2O$
Molecular weight, g/mol: 200.24
Boiling point, °C/mmHg: 190/0.1(Chriskev catalog)
Melting point, °C: 190~192
Chemical structure:

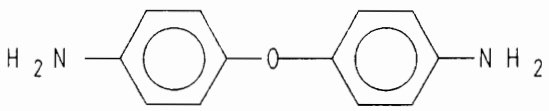

Purification procedure: High purity 4,4'-ODA(>99.5%, mp = 191.5°C, slightly tan crystalline powder) purchased from Chriskev Co. was used as received. Low purity grade monomer (97%, mp =190 ~ 192°C) purchased from Aldrich Chemical Co. was purified by either sublimation or recrystallization . When 4,4'-ODA needed to be sublimed a high vacuum was required since it slowly decomposed at sublimation temperature above the melting point of 4,4'-ODA, @193°C. The low purity 4,4'-ODA was also successfully purified following the experimental procedure of the Ishida, et. al.(203) as follows: a methanol solution of the original compound was prepared and the amine was converted to its hydrochloride salt. After filtrating of the solution through activated charcoal to remove unconverted quinones, the amine was regenerated as a precipitate by the addition of sodium hydroxide and subsequent washing and drying under vacuum.

3.2.6. 4,4'-isopropylidenedianiline (BIS-A)

Supplier: Air Products and Chemicals, Inc.
Molecular formula: $C_{15}H_{18}N_2$
Molecular weight, g/mol: 226.32
Melting point, °C: 132
Chemical structure:

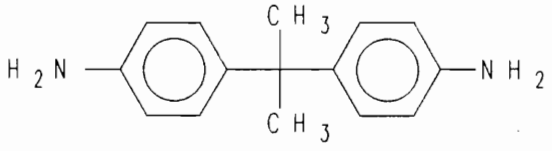

Purification procedure: High purity Bis-A was obtained from the supplier and it was used as received without further purification.

3.2.7. Aniline

Supplier:	Aldrich
Molecular formula:	C_6H_7N
Molecular weight, g/mol:	93.13
Boiling point, °C/mmHg:	184/760
Melting point, °C:	-6
Chemical structure:	

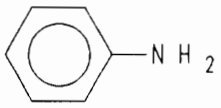

Purification procedure: Aniline was dried for at least 12 hours by stirring over calcium hydride and then distilled under reduced pressure. The constant boiling middle fraction was collected in a round bottomed flask, sealed with a rubber septum, and stored under nitrogen pressure. Aniline was used in the synthesis of model imides useful for imidization mechanism studies.

3.3. Purification of anhydrides

3.3.1. 3,3',4,4'-Benzophenone Tetracarboxylic Dianhydride (BTDA)

Supplier: Allco Chemical Co.
Molecular formula: $C_{17}H_6O_7$
Molecular weight, g/mol: 322.23
Melting point, °C: 225~226.5
Chemical structure:

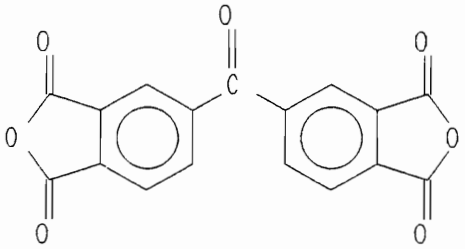

Purification procedure: Ultra-high purity BTDA was purchased as a white crystalline solid from Allco Chemical Co. and used after vacuum drying at 130°C for at least 12 hours. Low purity BTDA could be purified by recrystallization from acetic anhydride (204).

3.3.2. 3,4,3',4'-Biphenyl Tetracarboxylic Dianhydride (s-BPDA)

Supplier: Chriskev Chemical Co.
Molecular formula: $C_{16}H_6O_6$
Molecular weight, g/mol: 294.22
Melting point, °C: 300
Chemical structure:

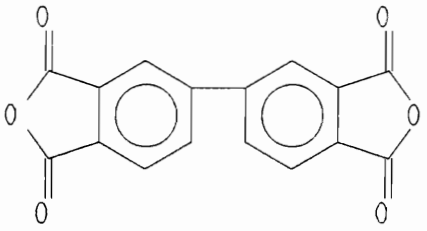

Purification procedure: High purity s-BPDA (a light gray free flowing powder, assays > 99.5%, ionic impurities (Na,

Fe) each < 2ppm) was purchased from the supplier and used after vacuum drying.

3.3.3. 4,4'-[Hexafluoroisopropylidene]-Bis[Phthalic Anhydride] (6FDA)

Supplier: Hoechst Celanese Corporation
Molecular formula: $C_{19}H_6F_6O_6$
Molecular weight, g/mol: 444.24
Melting point, °C: 247
Chemical structure:

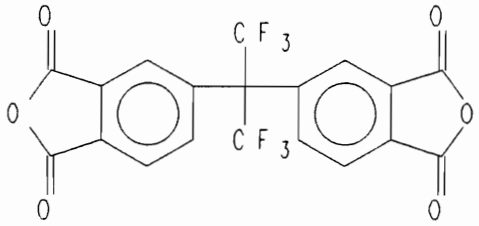

Purification procedure: High purity white free flowing powder 6FDA was kindly donated from the supplier and used after vacuum drying to impart unique thermal properties to polyimides.

3.3.4. 4,4'-Oxydiphthalic anhydride (ODPA)

Supplier: Occidental Chemical Corporation
Molecular formula: $C_{16}H_6O_7$
Molecular weight, g/mol: 310.22
Melting point, °C: 228
Vapor pressure, mmHg/°C: 1/200
Chemical structure:

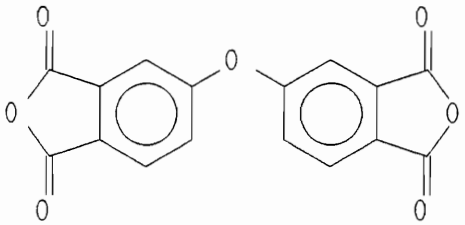

Purification procedure: ODPA was received as an slightly tan crystalline powder and used after vacuum drying without further purification.

3.3.5. Diphenylsulfone tetracarboxylicdianhydride (DSDA)

Supplier: Chriskev Chemical Co.
Molecular formula: $C_{16}H_6O_8S$
Molecular weight, g/mol: 358.28
Melting point, °C: greater than 260°C
Chemical structure:

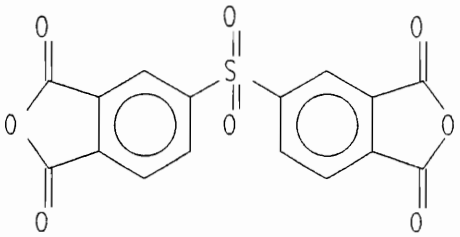

Purification procedure: High purity DSDA was received as an free flowing powder and used after vacuum drying prior to use without further purification. Since DSDA is very sensitive to moisture due to its high reactivity to the nucleophiles it was stored under rigorously dry conditions.

3.3.6. Phthalic anhydride (PA)

Supplier: Aldrich
Molecular formula: $C_8H_4O_3$
Molecular weight, g/mol: 148.12
Boiling point, °C/mmHg: 284/760
Melting point, °C: 131~134
Chemical structure:

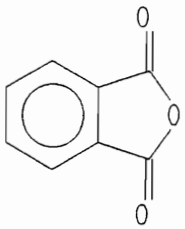

Purification procedure: The white, flaky PA was easily purified by a sublimation process at an oil bath setting of 130°C and was stored in the desiccator under nitrogen.

3.4. Synthesis of end group and molecular weight controlled poly(amic acid) homo - and copolymers

Poly(amic acid)s were synthesized in a four neck round bottomed flask equipped with a nitrogen inlet, thermocouple, a drying tube, and a overhead mechanical stirrer. The apparatus was flamed prior to use via a Bunsen burner to minimize any residual moisture. For all of the poly(amic acid) syntheses, the dianhydride was reacted with diamine by adding incrementally to the diamine solution. This monomer addition order is considered to be extremely important in the polyamic acid synthesis reaction because under these reaction conditions a small amount of dianhydride can be reacted with large excess amount of diamine throughout the reaction which may help minimize possible competing reactions such as hydrolysis of anhydride with any small amount of water which could still be present in the reaction system (30). When phthalic anhydride was used to control end groups and molecular weight of poly(amic acid)s, it was added to the stirring solution of diamine in NMP prior to the addition of the solid dianhydride. At the initial stages of poly(amic acid) synthesis, a cold water or

ice/sodium chloride bath was used to control the reaction temperature at room temperature (~25°C) or lower. The reaction was allowed to proceed for at least 8 hours. Three representative sample calculations for the monomer quantities and reaction procedures for the synthesis of poly(amic acid)s will be given. Typical examples for controlled end group and molecular weight poly(amic acid) homopolymers, for copolymers with varying ratios of different aromatic dianhydride monomers and finally for amine terminated BTDA containing polyamic acid for network formation studies will be provided in the next section.

3.4.1. Number average molecular weights in step polymerizations

Number average molecular weight and end groups of condensation polymers can be controlled via the Carothers equation (205) which relates the extent of reaction and the average functionality to the number average degree of polymerization. That is,

$$\langle Xn \rangle = \frac{N_0}{\frac{1}{2}\,(2\,N_0 - N_0\,p\,f_{av})} = \frac{2}{2 - p\,f_{av}} \qquad \text{Eq. 3 - 1}$$

$$= \frac{2}{2 - f_{av}} \quad (\text{when } p = 1) \qquad \text{Eq. 3 - 2}$$

These are the Carothers equations where <Xn> is the number average degree of polymerization of the reaction mixture, p is the extent of reaction and f_{av} is the average number of functional groups per monomer molecule. <Xn>, the average number of monomer residues in an average polymer molecule, is not necessarily equal to the degree of polymerization <DPn> which is defined as the number average of repeat units in an average polymer molecule. In the context of AA-BB type polymerization, <Xn> is twice number of <DPn> since each repeat unit contains two monomer residues.

Practical polymerization reactions are allowed to proceed to nearly completion ($p \cong 1$) and thus the molecular weight of condensation polymers is controlled by changing the number average functionality, f_{av}. That is,

$$f_{av} = \frac{\text{number of useful equivalents of functional groups}}{\text{number of moles of monomers}}$$

$$= \frac{\Sigma N_i f_i}{\Sigma N_i} \qquad \text{Eq. 3 -3}$$

Where N_i is the number of moles of species i and f_i is the number of functional groups of species i. The definition of Eq.3-3 holds strictly when functional groups of opposite kinds are present in equal concentrations since the excess reactant of the opposite functional groups does not enter

the polymerization in the absence of side reactions. In the case of polymerization which forms AB links and in which $n_A < n_B$, where n_i is the number of equivalents of functional groups of species i. In this case f_{av} is given by

$$f_{av} = \frac{2\ n_A}{\Sigma\ N_i} = \frac{2\ n_A}{N_A + N_B} \qquad \text{Eq. 3 - 4}$$

The average number of functional groups, f_{av}, is usually controlled by either upsetting stoichiometry of difunctional monomers or adding monofunctional monomer as an end capper to control molecular weight and end groups.

If the difunctional monomer B is used as an excess component, then B functional end groups are achieved. In this case f_{av} is given by

$$f_{av} = \frac{2\ n_A}{N_A + N_B} = \frac{4\ N_A}{N_A + N_B} = \frac{4\ N_A/N_B}{N_A/N_B + 1} \qquad \text{Eq. 3 - 5}$$

The quantity, $\frac{N_A}{N_B}$, is defined as a stoichiometric imbalance, r (less than 1), then

$$f_{av} = \frac{4\ r}{r + 1} \qquad \text{Eq. 3 - 6}$$

From Eq. 2 and Eq. 6

$$\langle Xn \rangle = \frac{1 + r}{1 - r} \qquad \text{Eq. 3 - 7}$$

On the other hand, if N_B' moles of monofunctional B monomer is used to control molecular weight,

$$f_{av} = \frac{\text{number of useful equivalents of functional groups}}{\text{number of moles of monomers}}$$

$$= \frac{\text{number of useful equivalents of A functional groups}}{\text{number of moles of monomers}} +$$

$$\frac{\text{number of useful equivalents of B functional groups}}{\text{number of moles of monomers}}$$

$$= \frac{2\ N_A}{N_A + N_B + N_B'} + \frac{2\ N_A}{N_A + N_B + N_B'}$$

$$= \frac{4\ N_A}{N_A + N_B + N_B'} = \frac{4\ r}{r + 1} \qquad \text{Eq. 3 - 8}$$

Where r is redefined stoichiometric imbalance by

$$r = \frac{N_A}{N_B + N_B'} \qquad (2N_A \leq 2N_B + N_B') \qquad \text{Eq. 3 - 9}$$

In Eq. 3 - 9 one point needs to be kept in mind, which is the constraint on the relationship between N_A, N_B, and N_B'. When the average number of functional groups (f_{av}) is defined in developing Carothers equation, the concept of useful equivalents was introduced since an excess of

opposite groups(in this instance the B functional group) will not be able to react. Thus, the constraint is $2N_A < 2N_B + N_{B'}$. Under this constraint r is always less than 1 since $2N_B + N_{B'} < 2N_B + 2N_{B'}$. Using Eq. 3 - 8 and Eq. 3 - 2 the number average degree of polymerization, <Xn>, has the same form as Eq. 3 - 7 with redefined stoichiometric imbalance by Eq. 3 - 9.

3.4.2. Sample calculation for the the synthesis of end-capped homopolyamic acid

The composition of the polymerization recipe for the synthesis of 4,4' - ODA/ODPA polyamic acid whose number average molecular weight of its corresponding polyimide is 40K may be calculated very easily as follows:

If we designate the aromatic dianhydride, phthalic anhydride and the diamine as AA, A and BB respectively, the structure of the phthalic anhydride endcapped polyamic acid would be $A(BBAA)_nBBA$ of which

$$<Mn> = (200 + 310 - 36)n + 200 + 148 \times 2 = 40000 \quad \text{Eq. 3-10}$$

In this calculation the values of 200, 310, 36, and 148 are molecular weight of 4,4'-ODA, ODPA, two moles of H_2O, and phthalic anhydride respectively. Eq. 3 - 10 yields n = 83.34, which means for every two moles of A monomer 83.34

moles of dianhydride and (83.34 + 1) moles of diamine are required. The recipe for the synthesis of 40K 4,4'-ODA/ODPA polyimide for a total batch size of 60 grams is shown in Table 3.1. The same results as above could be obtained using Carothers equation. Determination of a suitable polymerization recipe using the Carothers equation is shown in the section 3.4.1.

Table 3.1. Recipe for the synthesis of 40K 4,4' - ODA/ODPA polyimide

	moles	moles*	scaled moles**	MW	grams
4,4'-ODA	84.34	1	0.1175	200.24	23.5282
ODPA	83.34	0.98814	0.1161	310.22	36.0165
PA	2	0.02371	0.0027856	148.12	0.4126

* normalized moles based on 4,4' - ODA

** scaled moles for a batch size of 60 grams

3.4.3. Synthesis of end group and molecular weight controlled 4,4' - ODA/ODPA poly(amic acid)

End group and molecular weight controlled 4,4' - ODA/ODPA poly(amic acid) was synthesized using monomer quantities shown in Table 3.1. Thus 23.5282g of 4,4' - ODA was dissolved in 420g of dry NMP in a 1000ml four neck round bottom flask equipped with a mechanical stirrer, nitrogen inlet and a drying tube. After the diamine was completely

dissolved 0.2071g of phthalic anhydride was added to the stirring solution of the diamine and was allowed to react with the diamine for several minutes. Next, 36.0165g of ODPA was added incrementally to the diamine solution so that previous addition of the diamine had been dissolved before more dianhydride was added and a Teflon coated weighing dish was washed with 66g of dry NMP. After finishing the dianhydride addition the reaction was allowed to proceed for 12 more hours at room temperature under nitrogen atmosphere. After completion of the reaction, 54g of the azeotroping agent, CHP, was added and well agitated by a mechanical stirrer. The polyamic acid solution was then composed of 10%(w/w) solids, 81 %NMP, and 9%(w/w) CHP.

3.4.4. Sample calculation for the synthesis of copolyamic acids

In this section Carothers equation will be utilized to calculate the composition of the polymerization recipe for the synthesis of the end group and molecular weight controlled 4,4' - DDS/6FDA(15 wt.%), s-BPDA(85 wt. %) polyimide (40K). Once again if we designate the diamine monomer, the dianhydride monomers, and phthalic anhydride as BB, AA, and A, then the sequence of the phthalic anhydride end capped polyamic acid would be **A(BBAA)$_n$BBA** (Structure 1) of which

$$\langle Xn \rangle = 2\langle DPn \rangle + 1 = 2n + 1 \qquad \text{Eq. 3 - 11}$$

First, <Xn> were obtained using the desired molecular weight and considering the desired polymer sequence (Structure 1) as follows:

<DPn> =

$$\frac{\text{desired number average molecular weight - molecular weight}}{\text{molecular weight of repeat unit}}$$

$$= \frac{40000 - 248 - 2 \times 148}{248 + 0.105(444) + 0.895(294) - 36} = 75.6 \qquad \text{Eq. 3 - 12}$$

$$\langle Xn \rangle = 2 \langle DPn \rangle + 1 = 152.2 \qquad \text{Eq. 3 - 13}$$

In this calculation the values of 248, 148, 444, 294, and 36 are molecular weight of 4,4'-DDS, phthalic anhydride, 6FDA, s - BPDA, and two mole of H_2O respectively.
From Eq. 3 - 7, $\langle Xn \rangle = \frac{1 + r}{1 - r}$, with <Xn> = 152.2, r = 0.9869.
Now let's rewrite Eq. 3 - 9 for the system where A (anhydride) functional groups are excess component.

$$r = \frac{N_B}{N_A + N_A'} \quad (2N_B \leq 2N_A + N_A') \qquad \text{Eq. 3 - 14}$$

Eq. 3 - 14 has three independent variables for a given r value with the constraint. Now, if we let N_B = 1 the equation has still two independent variables, which means there are many solutions of the equation for a given r

value. However, there is an important constraint on the relationship between N_A and N_B. This constraint can be easily found by examining the desired polymer sequence (Structure 1) where number of BB molecules is one unit larger than that of AA molecules. Thus,

$$\frac{N_A}{N_B} = \frac{<DPn>}{<DPn> + 1} = \frac{75.6}{75.6 + 1} = 0.9869 \qquad \text{Eq. 3 - 15}$$

It is noteworthy to realize that the value of $\frac{N_A}{N_B}$ (=0.9869) is stoichiometric imbalance for the synthesis of amine terminated polyimide whose <Xn> = 152.2 (from Eq. 3 - 13) because

$$\frac{N_A}{N_B} = \frac{<DPn>}{<DPn> + 1} = \frac{2<DPn>}{2(DPn + 1)} = \frac{<Xn> - 1}{<Xn> + 1} = r.$$

Now, let N_B = 1. Then, N_A = 0.9869. From Eq. 3 - 14 with r = 0.9869, N_A =0.9869 and N_B = 1, the solution for N_A = 0.0263.

Next the quantities of weight percent of dianhydride compositions were converted to moles by dividing molecular weights and normalized by multiplying an appropriate number: moles of 6FDA : moles of s-BPDA

$$= \frac{15}{444.24} : \frac{85}{294.22} = 0.105 : 0.895.$$

Thus, the required number of moles of dianhydrides for every one mole of diamine is 0.105 x 0.9869 (= 0.1036245) moles of 6FDA and 0.895 x 0.9869 (= 0.883276) moles of s - BPDA. The recipe for the synthesis of 40K 4,4' - DDS/6FDA(15 wt. %), s - BPDA(85 wt. %) polyimide for a total batch size of 9 grams is shown in Table 3.2.

Table 3.2. Recipe for the synthesis of 40K 4,4' - DDS/6FDA(15 wt. %), s - BPDA(85 wt. %) polyimide

	4,4' - DDS	6FDA	s - BPDA	PA
molecular wt.	248.30	444.24	294.22	148.12
weight %	------	15	85	------
moles	------	0.105	0.895	------
normalized moles*	1.0	0.1036245	0.883276	0.0263
scaled moles**	0.016	0.001658	0.014132	0.0004208
wt. in gram	3.9728	0.7365	4.1579	0.0623

* moles required for every one mole of diamine

** scaled moles for a batch size of 9 grams

3.4.5. Synthesis of copolyamic acids

Various copolyamic acids were synthesized from the reaction of aromatic diamines and aromatic dianhydrides. For example, 4,4' - DDS/6FDA, s-BPDA polyamic acid whose number average of corresponding polyimide is 40K and whose aromatic dianhydride composition is composed of 15 wt. % 6FDA and 85

wt. % s-BPDA was synthesized using monomer quantities shown in Table 3.2. The synthetic procedure is very similar described in the section 3.4.3. Thus, 3.9728g of 4,4' - DDS was dissolved in 50 ml dry NMP in a 150ml four neck round bottom flask equipped with a mechanical stirrer, nitrogen inlet, and a drying tube. After the diamine was completely dissolved, 0.0623g of phthalic anhydride was added to the stirring solution of the diamine and was allowed to react with the diamine for several minutes. Next, the dry mixed powders composed of 0.7365g of 6FDA and 4.1579g of s-BPDA were added incrementally to the diamine solution. The previous addition of the diamine was allowed to dissolve before more dianhydride was added and the Teflon coated weighing dish was washed with 22 ml of NMP. For this particular system where one of the most unreactive monomers, 4,4'-DDS, is involved no significant heat of reaction was detected upon the addition of the mixture of dianhydrides, thus the amic acid synthesis reaction was run at room temperature for 12 hours under nitrogen atmosphere. After reaction was completed, 8ml of the azeotroping agent, ODCB, was added to strip off water generated in the subsequent imidization process. The polyamic acid solution was then solution imidized at an elevated temperature.

3.4.6. Synthesis of amine terminated BIS-A/BTDA polyamic acids

Low molecular weight amine terminated polyamic acids were synthesized for a model network formation study. The synthetic procedure is straightforward and very similar to that described in section 3.4.3 except that phthalic anhydride is not used. Thus, the calculation of compositions for the synthetic recipe for the synthesis of amine terminated BTDA/BIS-A polyimide with number average molecular weight of 5K will be shown.

The first step of calculation of compositions for the synthetic recipe is determination of <Xn>. Since the number average molecular weight of 5K is relatively small, it is important to consider the molecular weight of end groups in the calculation of the <Xn>, as we usually do. If we designate the aromatic dianhydride and diamine as AA and BB respectively. The structure of the amine terminated polyamic acid would be $BB(AABB)_n$ of which

$$<Xn> = 2n + 1,\ n = <DP_n> \qquad \text{Eq. 3-16}$$

$$\text{and}\quad <Mn> = (322 + 226 - 36)n + 226 \qquad \text{Eq. 3-17}$$

where the values of 322, 226, and 36 are molecular weights of BTDA,BIS-A, and two moles of H_2O respectively. The solution of Eq. 3 - 17 is n = <DPn> = 9.3. From these equations Eq. 3-16 and 3-17 with <Mn> = 5000, <Xn> = 19.6. From Eq. 3-7 with <Xn> = 19.6 stoichiometric imbalance r =

0.9029. Using our fundamental equation, $r = N_A/N_B$, N_A = 0.9029 and N_B = 1. The quantities for the synthesis of amine terminated BIS-A/BTDA polyamic acid (<Mn> of polyimide=5K) are shown in Table 3.3.

Table 3.3. Recipe for the synthesis of amine terminated BIS-A/BTDA polyamic acid (<Mn> of polyimide=5K)

	mw.	moles	scaled moles*	wt. in gram
BIS-A	226.32	1	0.04	9.0528
BTDA	322.23	0.9029	0.036116	11.6377

* scaled moles for a batch size of 20g.

3.5. Transformation of poly(amic acid)s into polyimides via solution imidization processes

Poly(amic acid)s were transformed into polyimides by utilizing well established thermal solution imidization techniques employed in this research. This procedure was found to be useful for synthesizing soluble fully imidized homo and copolymers.

The solution imidization was carried out in a four neck round bottomed flask equipped with thermocouple, a mechanical stirrer, a inverse Dean-Stark trap, a nitrogen gas inlet, drying tube, and condenser. The reaction temperature was precisely controlled ($\pm$1°C) via thermocouple using a temperature controllable hotplate. The amic acid solution (10% solid contents, NMP/azeotroping agent = 9/1)

was introduced into the reaction flask immersed in a preheated oil bath of which temperature is 20°C higher than reaction temperature and desired reaction temperature was obtained within 5 minutes. When ODCB was used as an azeotroping agent, the inverse Dean-Stark trap was filled with freshly distilled ODCB. Within two hours after the imidization reaction was started, a well-separated water phase was observed in the Dean-Stark trap. The poly(amic acid) solution was allowed to be imidized at constant reaction temperatures from 140 to 180C for at least 24 hours under a nitrogen purge. For imidization kinetics and mechanism investigations, reaction samples were taken into sample vials using disposable pipets at defined time intervals, then quenched using a dry ice - acetone bath, and stored in the refrigerator for future characterization. When polyimide powder was required the polyimide was recovered by precipitating the polyimide solution into large excess(~15 fold excess) amount of stirring methanol, filtering, rinsing with methanol, and drying in a vacuum oven for about 24 hours. For 6FDA containing polyimides methanol/water mixture, for example, 50/50 mixture, was a better precipitating non-solvent than methanol itself.

3.6. Preparation of a model imide

The model compound was prepared from the reaction of aniline and oxydiphthalic anhydride. 4.7263g (0.05075moles) of distilled aniline was added in 110ml of dry NMP. Next, 7.7555g (0.025moles) of oxydiphthalic anhydride was added into the aniline/NMP solution and allowed to react for about two hours at room temperature. After two hour reaction, 15ml of o-dichlorobenzene was added in the reaction mixture and the reaction mixture was heated at 180°C for 5 hours. As imidization proceeded the solution precipitated. White crystalline material (MP=297°C) was obtained after filtering the reaction mixture, washing with NMP and vacuum drying at 180°C overnight.

3.7. Preparation of polyimide/polybenzimidazole polymer blends

All of the polymer blends for the FTIR and thermal investigations were prepared by solution mixing of polybenzimidazole (PBI) in dimethyl acetamide (DMAc) and polyimides in DMAc or N-methyl pyrrolidone (NMP), each at a concentration of 3 to 8 weight percent. All of the polyimides, except 6FDA/4,4'-ODA polyimide, that have been investigated in this research were dissolved in DMAc because the 6FDA/4,4'-ODA polyimide solution in DMAc was a little bit turbid the polyimide was dissolved in NMP. For FTIR

investigations one drop of the dilute blend solutions was evenly spread on the sodium chloride salt plate, and then dried at 80°C for 2 days, at 188°C for 5 days, at 230°C for 10 hours and at 310°C for 2 hours under vacuum. Complete removal of solvent was confirmed by FTIR spectroscopy. For thermal analyses, blends were also prepared by casting of the relatively concentrated solutions (~8%) on the glass plates the films were dried under two different drying conditions as follows:

Drying condition 1: dried at 88°C under vacuum for a day, further dried at 190°C under vacuum for 5 days, washed with hot water (85°C) for 3 days and finally dried at 190°C under vacuum for 2 days.

Drying condition 2: dried at 88°C under vacuum for a day, further dried at 190°C under vacuum for 2 days and finally dried at 310°C under vacuum for 10 hours.

3.8. Characterization of a model imide, polyimides and blends

3.8.1. Potentiometric titration of carboxylic acid groups

Potentiometric titrations were successfully utilized to determine degree of imidization. Titrations of carboxylic acid functional groups of poly(amic acid) or partially imidized poly(amic acid) were performed using a MCI GT-05(COSA Instruments Corporation) automatic potentiometric titrator. Tetramethyl ammonium hydroxide in methanol

solution (~0.025N) whose exact concentration was determined by back-titration with potassium hydrogen phthalate was used as titrant. Samples for the titration were prepared by diluting 10%(w/w) polymer solution with 60 ml of dry NMP to require more than 4 ml of the titrant.

3.8.1.1. Blank titration

Blank volume could be obtained from a blank titration on the exact volume of the blank solvent, i. e. in this research 60 ml of NMP. In order to perform a blank titration it was necessary to obtain a value of the potential (mV) at an end point, which is characterized by a consistent value of the potential for a given system. As can be expected, however, end points need not to have strictly constant potential values for a given system since very small amount of titrant can cause big potential change near an equivalence point. Once a value of potential at an end point for a given system is determined, a blank titration was performed until potential reached the input value of the predetermined potential at an end point. Then the blank volume was determined by the volume of titrant required. Namely, the blank volume can be defined as follows: blank volume is the volume of titrant required for the value of the potential of the sample being titrated to be the predetermined value of potential at an end point for a given

system. There are at least two reasons why blank titration is performed as foregoing method: 1) at an end point the value of the potential is consistent for a given system and 2) blank titration usually does not show a distinct inflection point.

For polyamic acid (or partially imidized polyamic acid)/NMP systems in this research, end points had the values of potential of -440~380 mV therefore -410 mV was considered as a potential value at an end point for polyamic acid/imide systems. For the blank solvent, NMP, the potential was ~-415 mV. Thus, for the polyamic acid(or partially imidized polyamic acid)/NMP systems zero blank volume was considered. This assumption is reasonable by considering the fact that the value of the potential of the blank NMP decreases (more negative value) as titration is proceeded.

3.8.1.2. Derivation of the equation for the determination of degree of imidization by the titration method

The equation for the determination of the residual amount of carboxylic acid functional groups (% amic acid) could be easily derived from the fundamental titration equation. If we define several important variables as follows:

%AA = percent of residual amic acid

N = normal concentration of the titrant

V = volume of titrant consumed at the end point in ml

M_{ru} = molecular weight of a repeat unit of polymer

W = net weight of polymer sample in g

Then, the fundamental titration equation is given by $N_t = N_s$ where Nt = Number of equivalents of titrant and Ns = Number of equivalents of sample. Thus,

$$N\frac{V}{1000} = \frac{W\frac{\%AA}{100}}{\frac{M_{ru}}{2}} \qquad \text{Eq. 3-18}$$

Since every repeat unit has two equivalent acid functional moieties, half weight of the repeat unit was used in the denominator of Eq. 3-18. There is another important consideration in the developing the equation for the determination of residual amic acid content. As imidization proceeds the condensation product, water, is continuously generated and as a result molecular weight of the repeat unit decreases as a function of reaction time. Thus,

$$\frac{M_{ru}}{2} = \frac{M_{ru}(0)}{2} - 18\left(1 - \frac{\%AA}{100}\right) \qquad \text{Eq. 3-19}$$

Where 18 = molecular weight of H_2O (in g/mol)

$M_{ru}(0)$ = molecular weight of repeat unit of polyamic acid

Substituting Eq. 3-19 into Eq. 3-18 and after rearranging, we have

$$\%AA = \frac{\frac{M_{ru}(0)}{2} - 18}{\frac{10W}{NV} - 0.18} \qquad \text{Eq. 3-20}$$

3.8.2. Fourier Transform Infrared Spectroscopy(FTIR)

FTIR was used for the purpose of both conducting mechanistic investigations during solution imidization process and studying polyimide/polybenzimidazole blends. Nicolet MX-1 and Nicolet FX-800 instruments were used for obtaining spectra. Nicolet FX-800 was exclusively utilized for the study of the mechanism of solution imidization process. For the imidization mechanism study 2048 scans were collected and the anti-symmetric imide peak ($1720cm^{-1}$) was analyzed by taking the second derivative of the spectra.

3.8.3. Nuclear magnetic resonance spectroscopy (NMR)

NMR spectroscopy was used to obtain information on the microstructure of polyamic acid and to conduct mechanistic investigations of the solution imidization process. A Varian Unity 400 spectrometer operating at 399.952 MHz for ^1H was used to obtain the spectra. Samples analyzed could be powders, 10% polymer solution in NMP (90%)/azeotroping agent (10%) and 10% swellable polymer gel in NMP (90%)/azeotroping

agent (10%). Samples were dissolved in deuterated solvents such as chloroform-d1, acetone-d6, and dimethyl sulfoxide-d6 and all proton chemical shifts were referenced to internal tetramethyl silane (TMS). In the case of the 10% swellable polyimide gel (some of the BTDA containing polyimide), the gel was swelled by adding dry NMP to make final solid contents of 1 to 2% and then the lock solvent, dimethyl sulfoxide-d_6, was added.

Typical conditions for ^1H spectra included the acquisition of 64 scans using a sweep width of 6500 Hz, a pulse width of 3.9 msec, an acquisition time of 3.74 sec and a recycle delay of 1.0 sec. Typical conditions for the acquisition of ^{13}C spectra at 100.577 MHz included ^1H Waltz decoupling, a sweep width of 25000 Hz, an acquisition time of 1.2 sec, a pulse width of 6 μsec, and a recycle delay of 1.0 sec. The two dimensional ^1H-^1H COSY spectra were recorded using the phase sensitive COSY-90 software standard with the Varian unity. The sweep width in both dimensions was 619.8 Hz. The acquisition time in the f_2 dimension was 0.207 sec. Thirty-two transients were collected for each of the 64 incremental delays in the f_1 dimension with a recycle delay between transients of 0.8 sec. After zero filling once in the f_1 dimension the resulting data matrix was 256 x 256. The Gaussian function was applied in each dimension prior to Fourier Transform.

3.8.4. Mass spectrometry

Mass spectroscopy was performed on a VG 7070 E-HF spectrometer (VG Analytical, Manchester, UK) via a direct probe inlet. The magnetic field was scanned at a rate of 5 seconds per mass decade from m/z value of 1000 to 100. Source temperature was 200°C. Electron energy was 70 eV and the probe was heated to 450°C at 5°C/minute.

3.8.5. Intrinsic viscosity measurements

Intrinsic viscosities were measured for a various polyimide homo- and copolymers to obtain information on the relative molecular weights. Intrinsic viscosity measurements were also utilized to characterize 4,4'-ODA/ODPA polyamic acid and it's partially imidized material by solution imidization process at the intermediate stages. Cannon-Ubbelohde dilution viscometers with a proper capillary size were used to determine intrinsic viscosity. For all of the samples except partially imidized 4,4'-ODA/ODPA poyl(amic acid), polyimide powder was dissolved in NMP and for 4,4'-ODA/ODPA polyimide system for imidization mechanism study 10%(w/w) polymer solutions were dissolved in a 0.1M LiBr in dry NMP solution. All viscosity measurements were performed at 25°C in a temperature controlled water bath. The intrinsic viscosity values were determined by using flow

time data at four different concentrations and data were linearly extrapolated to the zero concentration.

3.8.6. Thermal characterization

3.8.6.1. Differential Scanning Calorimetry (DSC)

DSC was used to determine glass transition temperatures (T_gs) of various polyimides and polyimide-polybenzimidazole blends with a Perkin-Elmer DSC-4 or a DuPont 912 DSC with a DuPont 2100 thermal Analyst. DSC scans were run under a nitrogen atmosphere at 10°C/min heating rate. Accurate glass transition temperatures of polyimide homo- and copolymers were obtained from second scans after heating and cooling. Rapid cooling was used for amorphous polyimide samples to obtain clear glass transition temperature. DSC scans were run from 50°C to 400 (or 450°C) upto the fourth scan to measure the glass transition temperatures of the polybenzimidazole polyimide blend samples. To investigate the phase stability of the miscible blends, the blends were annealed for several minutes above the glass transition temperature of the blend and quenched-cooled to 50°C.

3.8.6.2. Thermogravimetric Analysis (TGA)

TGA was performed on either a Perkin-Elmer TMS-2 instrument or a DuPont 951 Thermogravimetric Analyzer on samples on either film or powder form in order to assess relative thermal stabilities of polyimide homo- and copolymers. Scans were run at the heating rate of 10°C/min in either air or nitrogen atmosphere.

3.8.6.3. Thermal Mechanical Analysis (TMA)

Penetration TMA experiments were performed on a Perkin-Elmer TMS-2 instrument on samples in film form of which thickness were about 1~2 mm to obtain glass transition temperatures of various polyimide samples. The sample was placed on the platform of a quartz sample tube and the deformation of the sample was measured under nonoscillatory load as a function of controlled temperature. TMA scans were run under a nitrogen atmosphere at 10°C/min.

CHAPTER 4

RESULTS AND DISCUSSION

4.1. Kinetic investigations of solution imidization processes

4.1.1. Introduction

Much work regarding kinetic investigations of imidization processes has been done on the conventional bulk thermal imidization processes. However, kinetics of the thermal imidization processes, particularly the solid phase thermal imidization processes, were reported to be very complicated (79,149-152). Since both the acid and amide functional groups belong to the same molecule, the first order kinetic equation has been almost exclusively used to treat imidization kinetic data (1,2,52,84,91,110,206). However the rate law of imidization is not well-established. For example, Laius et al. (143) reported that the reaction order of the thermal imidization processes varies from 2.2 to 3.2. Lavrov et al. (144) also observed two-step second order kinetics for the imidization of model amic acids in solution. It was also observed that carboxylic acids accelerate ring formation in the solid phase (171). Furthermore kinetics of solid phase imidizations have been known to be very complex physico-chemical processes (52), being affected by many factors such as degree of residual solvent (79,162), film thickness (79), molecular mobility

(94,143,164), physical state of polyamic acid (170), conformation of macrochains (169) and even the degree of imidization (97). Detailed discussion of these complicated features of thermal imidization processes were presented in CHAPTER 2, Section 2.1.5. Due to the complicated kinetic features of the solid phase thermal imidization processes, kinetic parameters obtained under certain bulk imidization conditions may not be compared to those obtained under other bulk imidization conditions and thus, those parameters may not be reliable. Some of the complications encountered in the conventional bulk thermal imidization processes are expected to be eliminated under solution imidization conditions. Thus, better information on the imidization kinetics could be achieved.

The objectives of this kinetic study were, therefore, to establish the rate law of imidization processes, to obtain reliable kinetic parameters imploying solution imidization technique and thus to reliably assess the effects of bridging groups (eg. such as X and Y in Figure 4.1.1) in both diamine and dianhydride components on the kinetics of solution imidization processes.

In these kinetic studies two basic assumptions were made to simplify the rate law. One is that the equal reactivity assumption for various amic acid groups in different chemical environments holds and the other is that

side reactions such as hydrolytic and unimolecular degradation of polyamic acids (58,63,64) have no practical effects on the kinetics of the imidization processes. To fulfil the equal reactivity assumption, monomers were deliberately selected. All of the monomers shown in Figure 4.1.1 are nonconjugated structures.

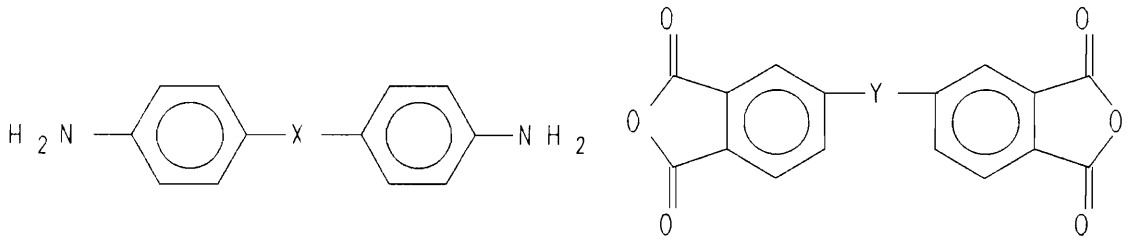

X = SO_2 (4,4'-DDS) and O (4,4'-ODA)

Y = SO_2 (DSDA), O (ODPA) and $C(CF_3)_2$ (6FDA)

Figure 4.1.1. Diamine and dianhydride monomers.

Due to the nonconjugated nature of the monomers the reactivities of the amic acid groups in the polyamic acids are expected to remain practically constant in the different chemical environments. The second assumption, whose validity is dependent upon the degree of side reactions, seems to be valid because the side reactions would occur to small extent as reported elsewhere (156,157). In this research phthalic anhydride end-capped polyamic acids whose number average molecular weights were controlled to 40K via the Carothers equation were used for the kinetic investigations. Polyamic

acid solutions composed of 10% solids, 81% NMP and 9% (wt./wt.) CHP were utilized for all of the kinetic investigations except concentration dependence experiments to establish the rate law of the imidization processes.

4.1.2. Degree of imidization by potentiometric titrations

The content of the residual acid groups of partially imidized poly(amic acid)s was required to follow imidization kinetics. FTIR spectroscopy has been proved to be a useful technique for the determination of the degree of imidization (1,2,79-82,97,111). However, when FTIR is used as a probe to follow imidization reactions, the observed quantities need to be normalized to obtain the degree of imidization. Therefore the rate constant is dependent upon the accuracy of the normalization factor, whereas for titration methods rate constants could be obtained from directly measured quantities of the amount of remaining acid groups. Thus, in this research non-aqueous potentiometric titrations were used to obtain the degree of imidization as a function of reaction time. And a weak base tetramethyl ammonium hydroxide was used to avoid the possible hydrolytic degradation of amide bonds during measurements.

A representative titration curve is shown in Figure 4.1.2 for the partially imidized 4,4'-ODA/ODPA polyamic acid for 80 minutes at 140°C. Figure 4.1.2 shows a clear

inflection point at the potential value of ca. -410mV. The inflection point near the potential value of -410mV is clearly the desired end point since the slope changes abruptly. In general, the degree of steepness of the slope near the equivalence point is dependent upon acidity and basicity of the system to be titrated with a steeper slope observed for strong acid/strong base titration (207). All of the titration plots of the partially imidized polyamic acid/imide showed clear end points at constant potential values for given systems.

Once an equivalence point and thus the volume of titrant consumed at an end point (an equivalent point) are determined the amount of residual amic acid (%AA) could be obtained using Eq. 3-20.

$$\%AA = \frac{\frac{M_{ru}(0)}{2} - 18}{\frac{10W}{NV} - 0.18} \qquad \text{Eq. 3-20}$$

For example, %AA of polyamic acid/imide whose titration plot is shown in Figure 4.1.2 was obtained by substituting appropriate values into Eq. 3-20 as follows;

$M_{ru}(0) = 200.2 + 310.2 = 510.4$

$10W = 0.7444$ (weight of 10 % polymer solution in g)

$N = 0.0241$ (normal concentration of titrant, equivalents/l)

V = 5.865 (ml) (volume of titrant consumed at an end point)

$$\text{Thus, \%AA} = \frac{\frac{510.4}{2} - 18}{\frac{0.7444}{0.0241 \times 5.865} - 0.18} = 46.6\ \%$$

Even though the amount of residual amic acid content (%AA) can be directly measured by non-aqueous potentiometric titration measurements small errors in the obtained values of residual amic acid contents resulting from some experimental errors in the concentrations of samples and those of titrants could be corrected by assuming that % AA of initial (unreacted) polyamic acid is 100%. The raw data such as sample size, volume of the titrant consumed at an end point, the values of potential at the end points and calculated % AA for various polyimide systems are given in the APPENDIX 1 (Tables 7.1 ~ 7.14). And the plots of reaction time (in minutes) vs. the amount of unreacted acid functional groups (%AA) for various polyimide systems are also shown in Figures 4.1.3 ~ 4.1.7.

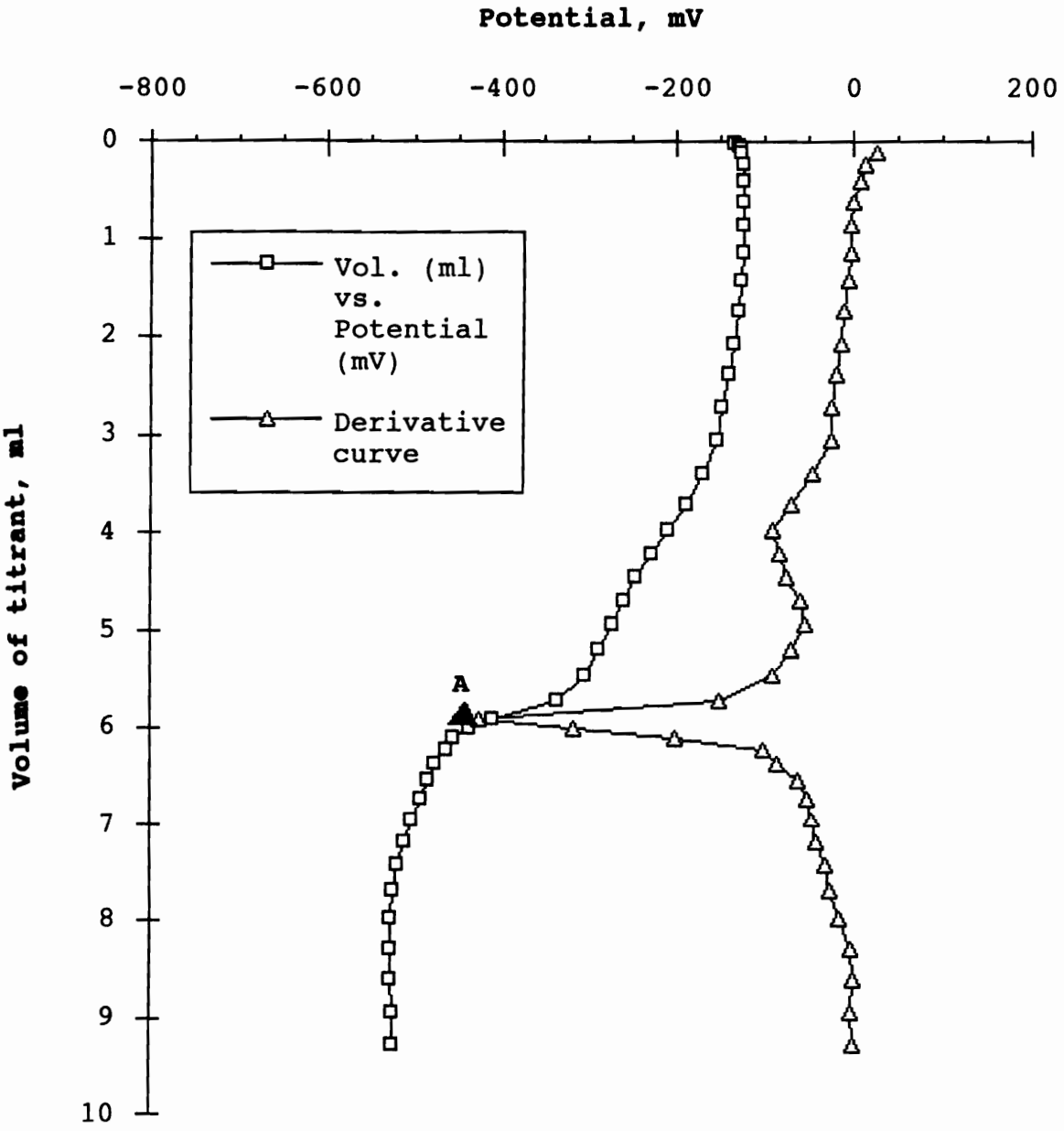

Figure 4.1.2. A typical titration plot for a 4,4'-ODA/ODPA polyimide system.

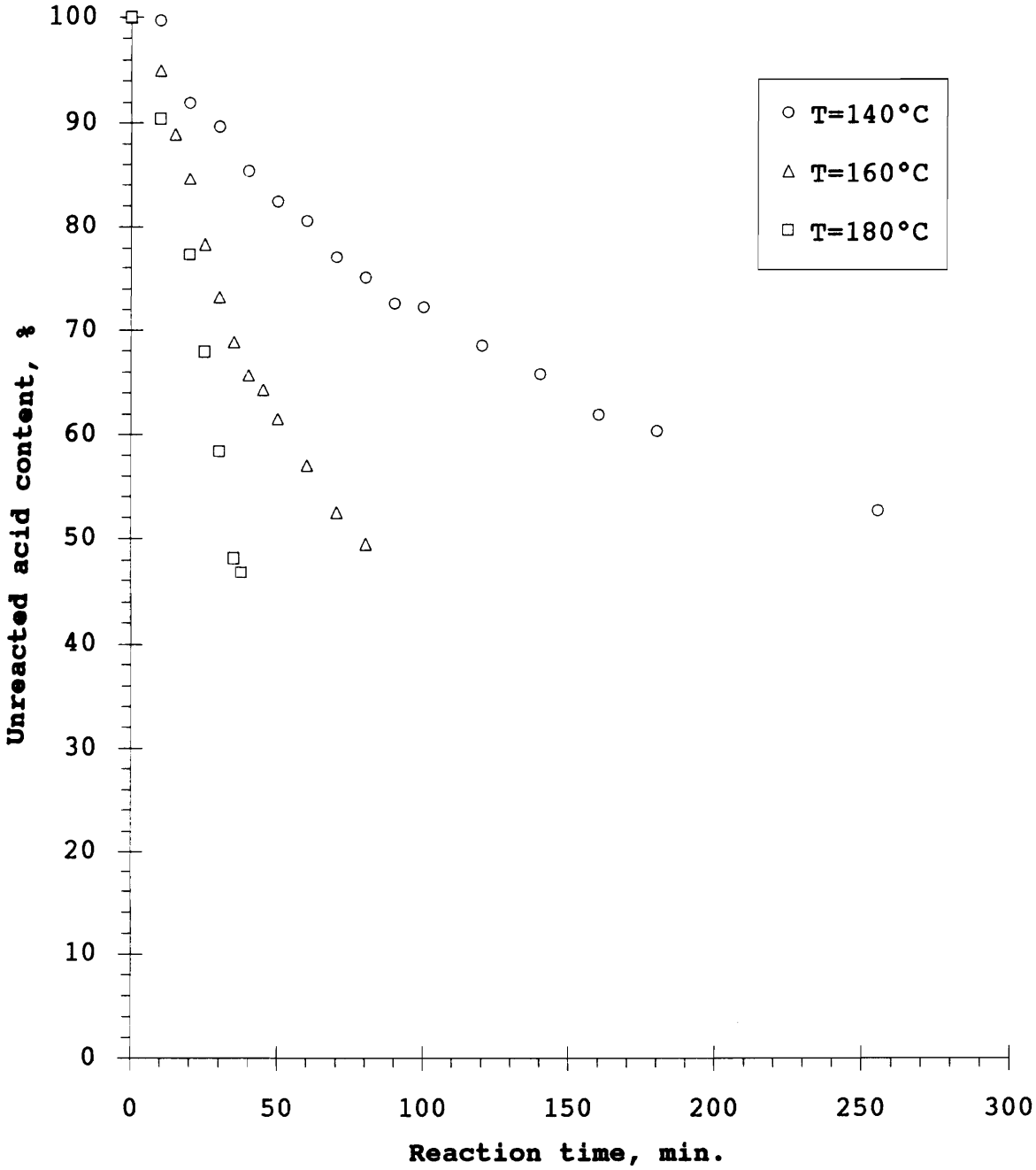

Figure 4.1.3. A plot of the amount of unreacted amic acid (%) vs. reaction time for 4,4'-DDS/DSDA polyimide system.

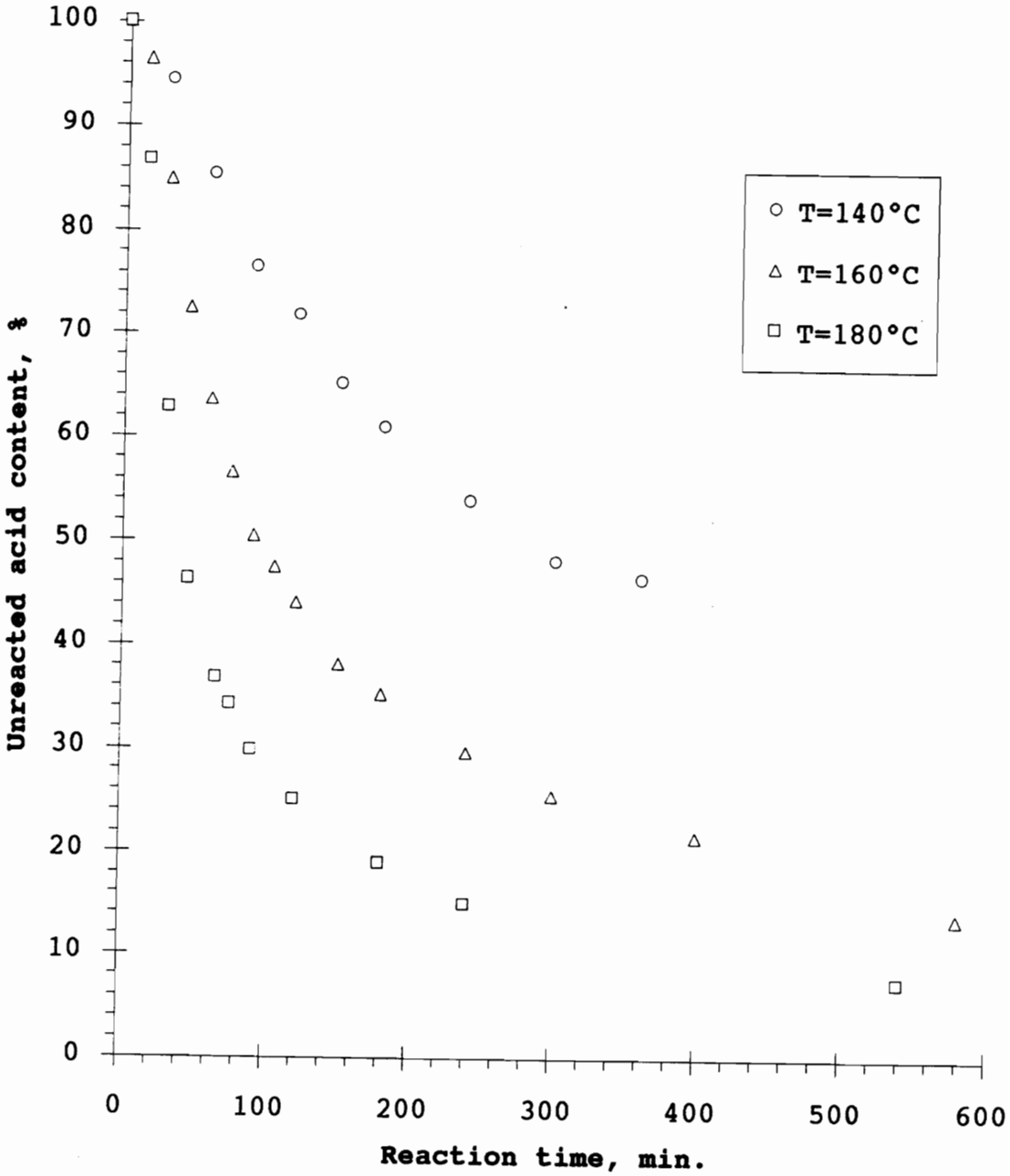

Figure 4.1.4. A plot of the amount of unreacted amic acid (%) vs. reaction time for 4,4'-DDS/ODPA polyimide system.

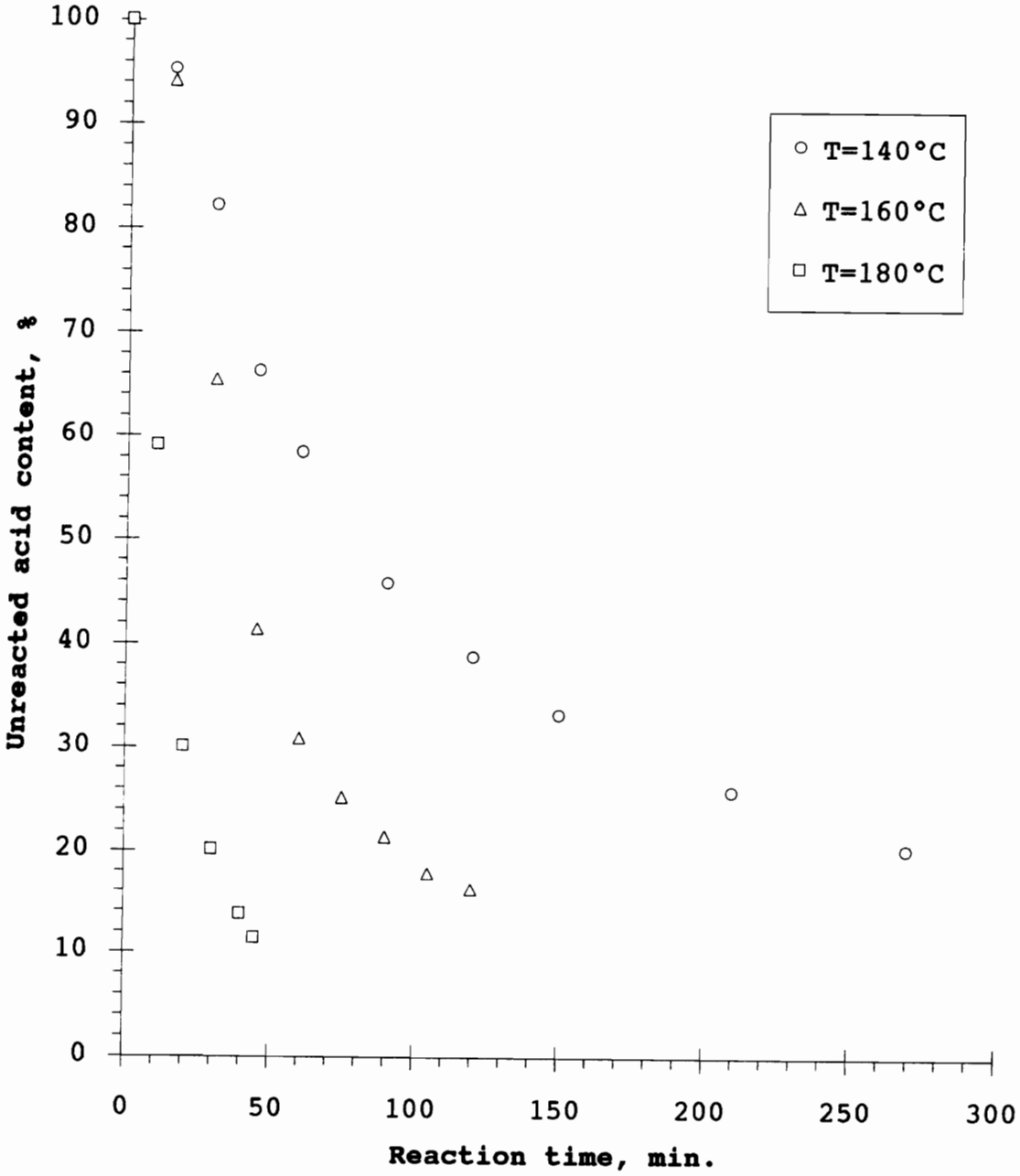

Figure 4.1.5. A plot of the amount of unreacted amic acid (%) vs. reaction time for 4,4'-ODA/DSDA polyimide system.

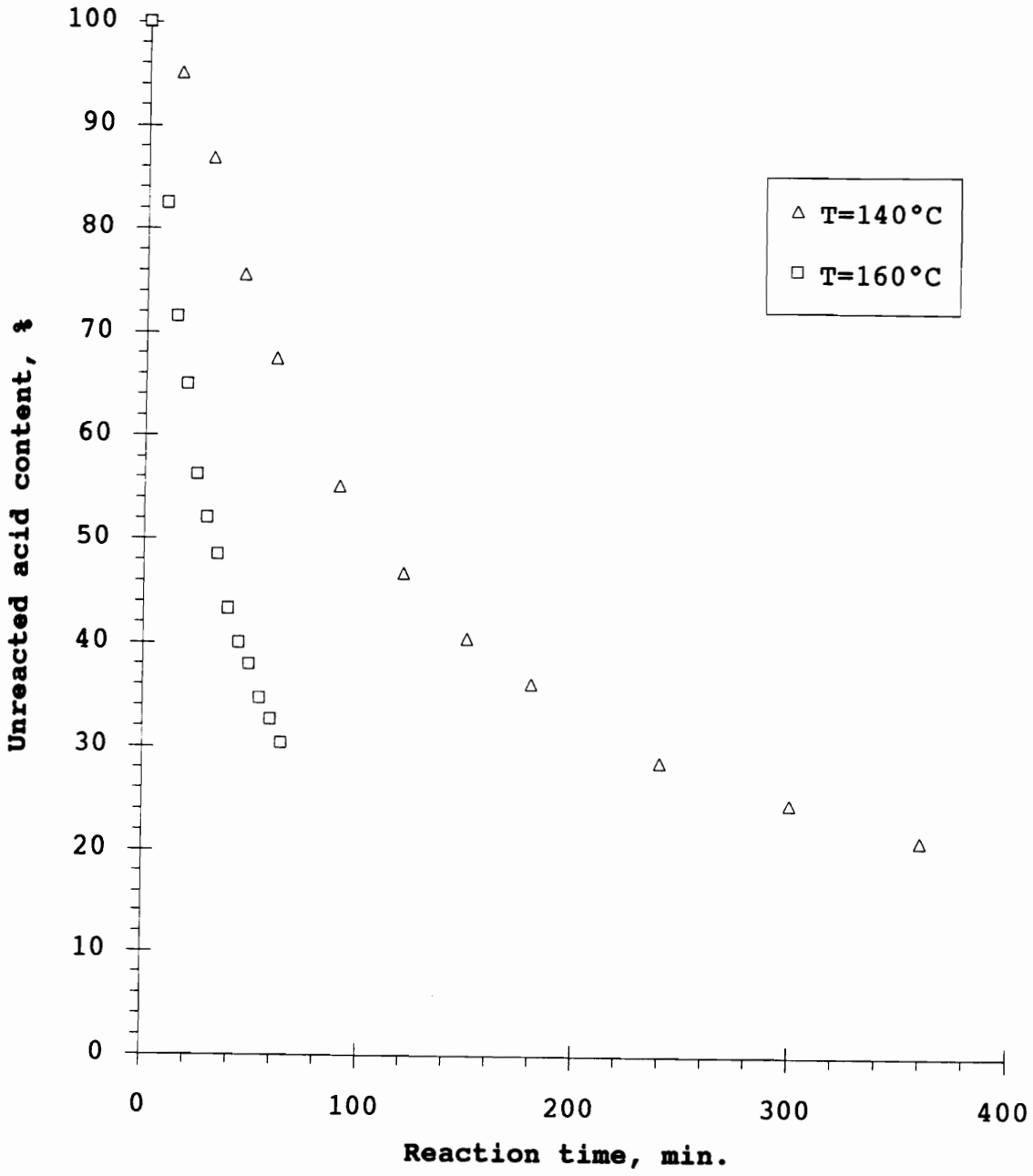

Figure 4.1.6. A plot of the amount of unreacted amic acid (%) vs. reaction time for 4,4'-ODA/6FDA polyimide system

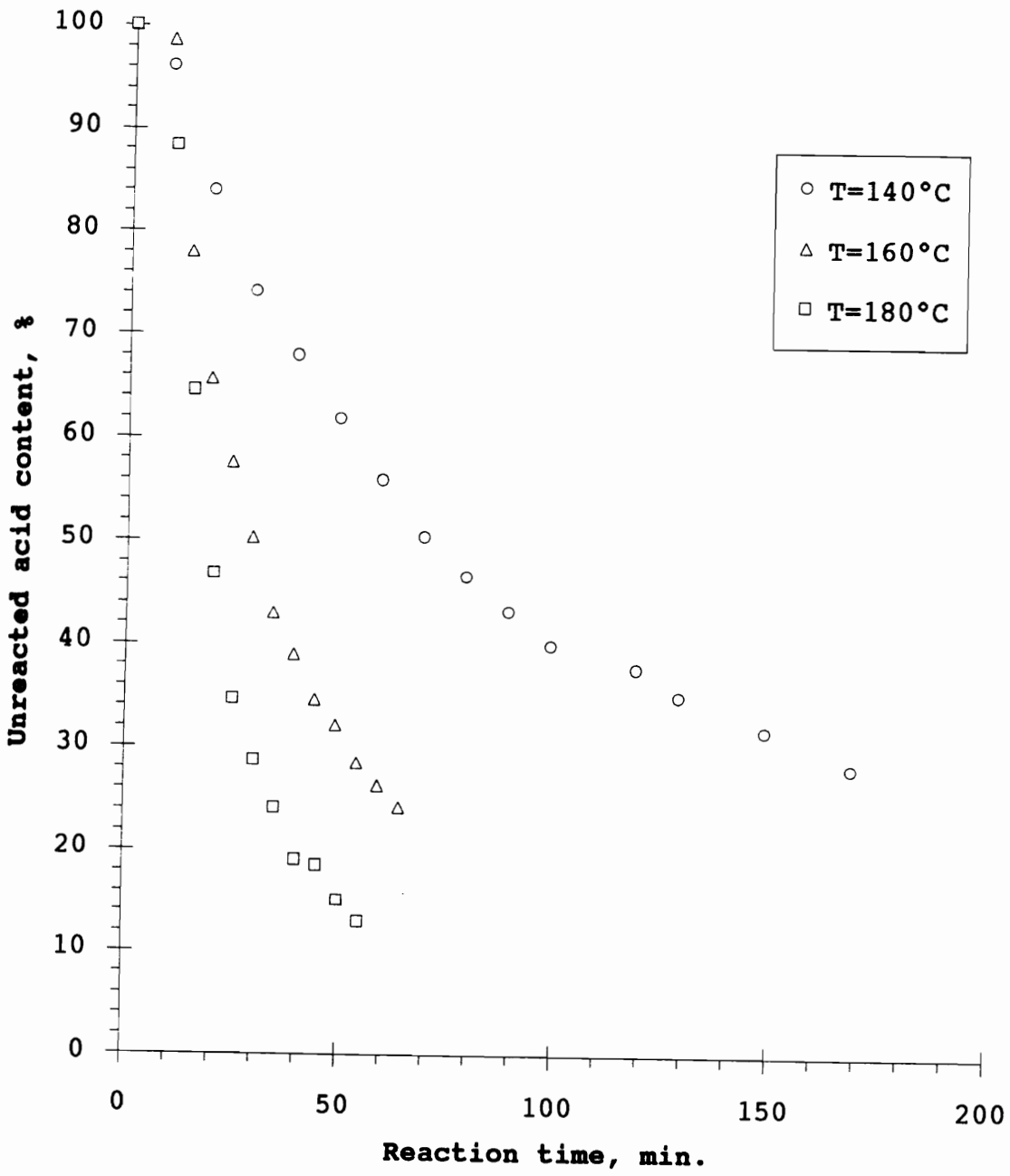

Figure 4.1.7. A plot of the amount of unreacted amic acid (%) vs. reaction time for 4,4'-ODA/ODPA polyimide system.

4.1.3. Determination of the reaction order of solution imidization processes

Since both acid and amide functional groups belong to the same molecule many kinetic data have been analyzed using the first order kinetic equation (1,2,52,84,91,110,206):

$$\ln (1-p) = -kt \qquad \text{Eq. 4.1}$$

where p is degree of imidization, k is a rate constant and t is reaction time.

The first order kinetic plots of -ln(1-p) vs. reaction time for 4,4'-DDS/DSDA, 4,4'-DDS/ODPA, 4,4'-ODA/DSDA, 4,4'-ODA/6FDA and 4,4'-ODA/ODPA polyimide systems are shown in the APPENDIX 2 (Figures 7.1 ~ 7.5). And derived kinetic parameters based upon first order kinetics are also shown in the APPENDIX 2 (Table 7.15). Those kinetic plots show that the kinetics of imidization could be described by the first order kinetics up to relatively high conversions as compared to those for the more conventional solid phase imidization processes. However deviations from first order kinetics at relatively high conversions were also observed in those Figures 7.1~7.5. As discussed earlier in CHAPTER 2 such deviations were observed at early imidization stages (eg. 30~40% conversion) (158) in the solid phase bulk thermal imidization processes. These complicated behaviors have been

interpreted in terms of decreased molecular mobility (94,143,164), kinetic nonequivalence (169) and effects of solvents (79,97,162). In the solution imidization processes, however, there is no increased Tg effect since polymers are in solution and no changes in solvent effects since polar solvent, NMP, is in excess throughout. And kinetically non-equivalent conformations are also expected to exchange rapidly in solution at elevated temperatures. Therefore deviations from first order kinetics at 50~70% conversions in our experimental results (Figures 7.1 ~ 5 in the APPENDIX 2) could be due to other reasons and might give a clue to the rate law of the solution imidization processes. The determination of reaction order from bulk imidization kinetic data might be very difficult because 1) as mentioned early imidization rates are strongly dependent upon many external variables and imidization kinetics show stepwise characteristics at low conversions (30 ~ 40%) and 2) It is also impossible to determine the reaction order by analyzing kinetic data obtained at low conversions because data for the second order reaction are also well fitted to the first order kinetic equation at low conversion (208). The pertinent figure in that reference is reproduced in Figure 4.1.8.

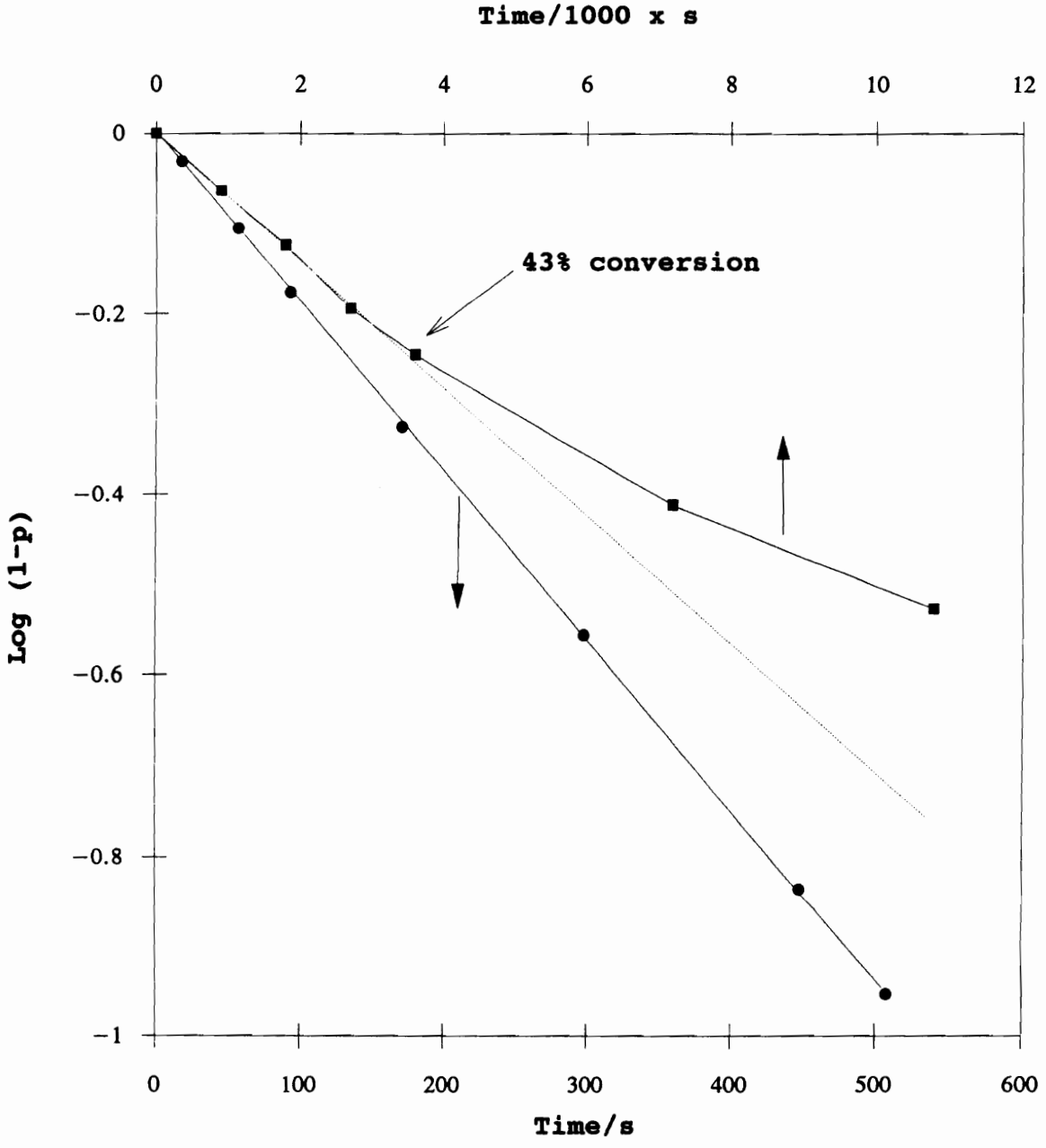

Figure 4.1.8. Kinetic data for first order and for second order reactions plotted as if both were first order. First order (circle); second order (square).

Since second order kinetic data are also fitted to the first order kinetics at low conversions, analysis of kinetic results of imidization of polyamic acid at low conversions cannot provide clear conclusions as to the reaction order. Thus, kinetic parameters obtained from thermal solid phase imidization process assuming first order kinetics are not reliable.

Based upon the observed deviations of our kinetic data from the first order kinetic equation and the earlier work by Laius et al.(143) and Lavrov et al.(144), concentration dependence experiments were performed to determine the reaction order of the thermal imidization processes. Solution imidization of the 4,4'-ODA/ODPA polyamic acids, at sufficiently different initial concentrations, 5, 10 and 15 solids wt. %, were conducted at the imidization temperature of 160°C. As shown in the Figure 4.1.9 the rate of imidization is strongly dependent upon initial concentration of the polyamic acid solution. If the imidization reaction follows first order kinetics there must be no concentration dependence on the reaction rate. Using the Noyes equation (209) second order kinetics were obtained. A detailed procedure for the determination of reaction order from our kinetic data (Figure 4.1.9) is given in the APPENDIX 3. We further investigated the effects of acid on the imidization kinetics. Figure 4.1.10 shows the effects of small amount of

acid, p-toluene sulfonic acid, on the imidization of 10% solution of 4,4'-ODA/ODPA polyamic acid solutions at 130°C. Acid catalysis of the imidizations was clearly observed. Thus, the imidization processes are characterized by acid catalyzed second order reactions. These experiments appear to be the first demonstration that second order kinetics in solution imidization processes are followed up to high conversions (ca. 90%).

Thus, the imidization reaction follows auto acid catalyzed second order kinetics. And the rate law of solution imidization processes is given by

$$-\frac{dN}{dt} = kN^2 \qquad \text{Eq. 4.2}$$

where N is the number of acid functional groups at time t and k is a second order rate constant. The solution of Eq. 4.2 can be easily obtained. That is,

$$\frac{1}{N} - \frac{1}{N_0} = kt \qquad \text{Eq. 4.3}$$

where N_0 is the number of initial acid functional groups at t = 0. From Eq. 4.3 with $N = N_0(1-p)$,

$$\frac{1}{1-p} = N_0kt + 1 \qquad \text{Eq. 4.4}$$

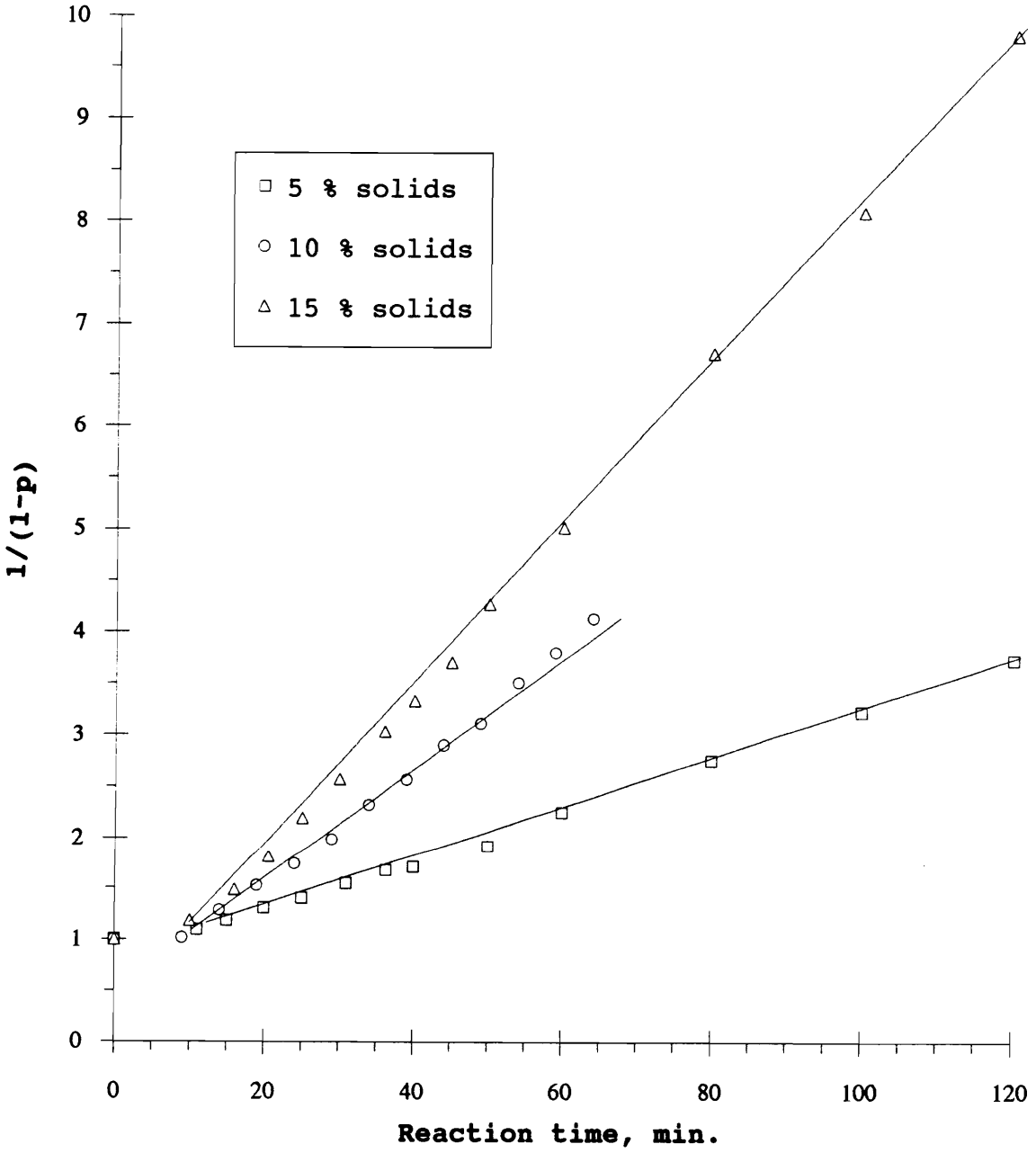

Figure 4.1.9. Demonstration of the concentration dependence of the rate of imidization for the 4,4'-ODA/ODPA polyimide system (reaction temperature = 160°C).

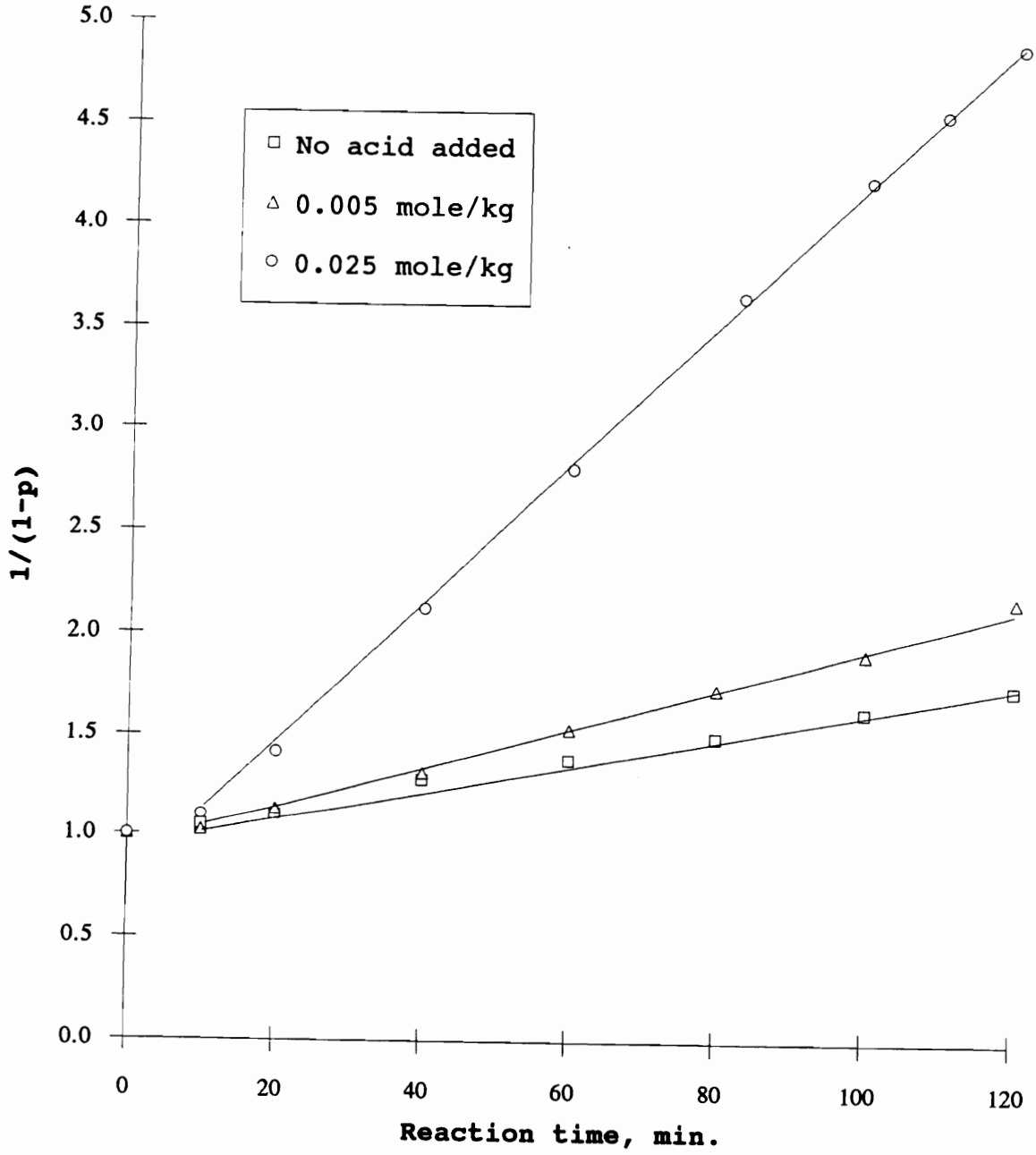

Figure 4.1.10. Acid catalysis of imidization of 4,4'-ODA/ODPA polyamic acids at 130°C, 10% solids.

4.1.4. Effects of bridging groups on the reactivity

Second order kinetic plots of reaction time vs. $\frac{1}{1-p}$, respectively, for 4,4'-DDS/DSDA, 4,4'-DDS/ODPA, 4,4'-ODA/DSDA, 4,4'-ODA/6FDA and 4,4'-ODA/ODPA are shown in the Figures 4.1.11 ~ 15. All of the kinetic data were well fitted to the second order kinetic equation up to high conversion throughout imidization processes except 4,4'-DDS/DSDA and 4,4'-ODA/DSDA polyimide systems. Due to rigid characteristics of the DSDA monomer, those two polymer systems precipitated during the imidization procedures. Rate constants could be obtained from the slope of the second order kinetic plots of reaction time vs. $\frac{1}{1-p}$. One representative example for the calculation of a rate constant will be given for 4,4'-DDS/DSDA polyimide system at the imidization temperature of 140°C. Since the slope is, in fact, equal to N_0k (see Eq. 4.4) the value of N_0 is needed to get the second order rate constant k. For 10% (w/w) 4,4'-DDS/DSDA polyimide system,

$$N_0 = 0.1 \times \frac{2}{\text{molecular weight of repeat unit}} = 0.1 \times \frac{2}{606.58}$$

$$\cong 3.3 \times 10^{-4} \text{ (mol/g)}.$$

With this N_0 value and the slope of Figure 4.11, 39 x 10^{-4} /min., k was 12 (g mol^{-1} min^{-1}).

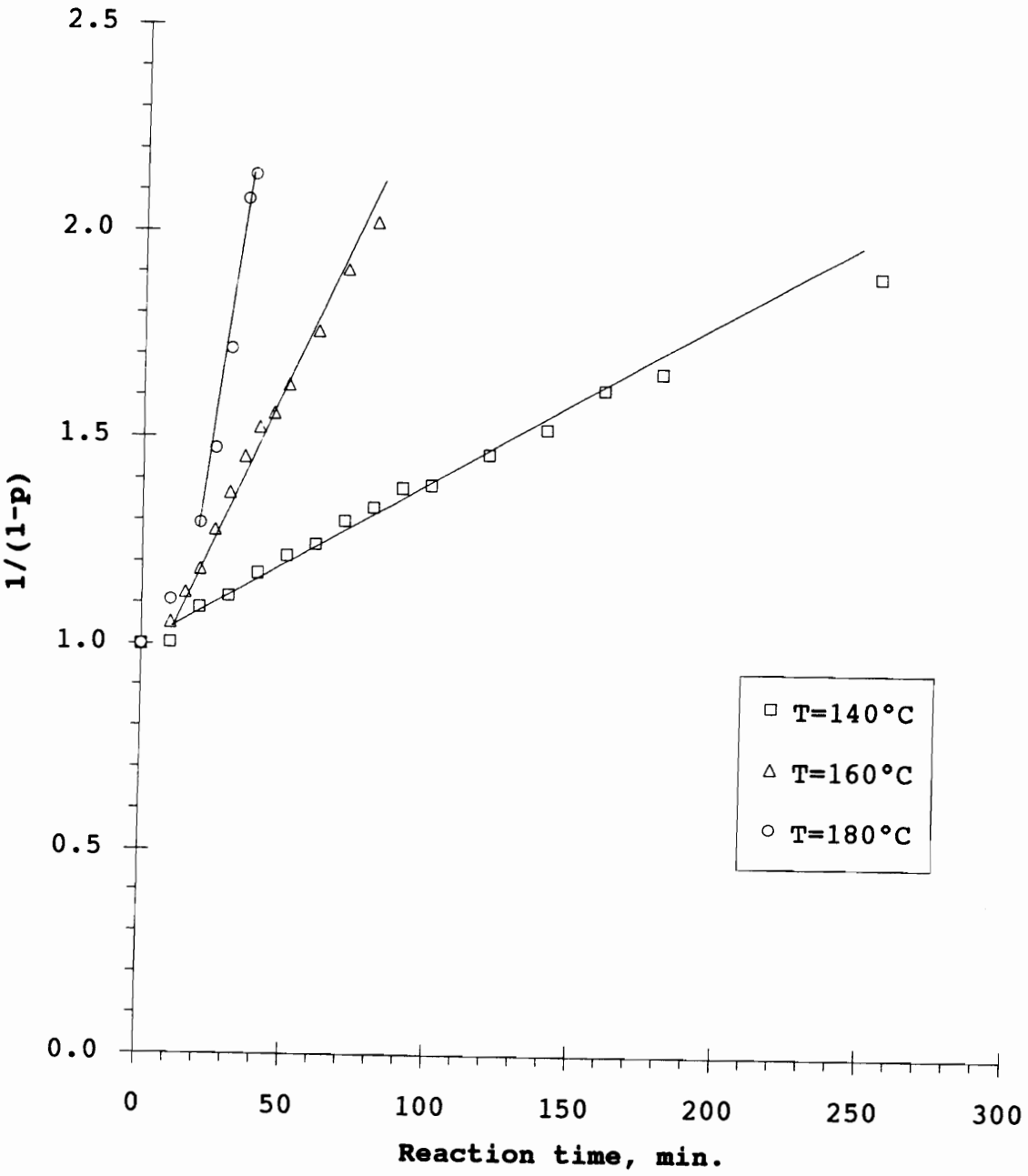

Figure 4.1.11. A second order kinetic plot of $\frac{1}{1-p}$ vs. reaction time for 4,4'-DDS/DSDA polyimide system.

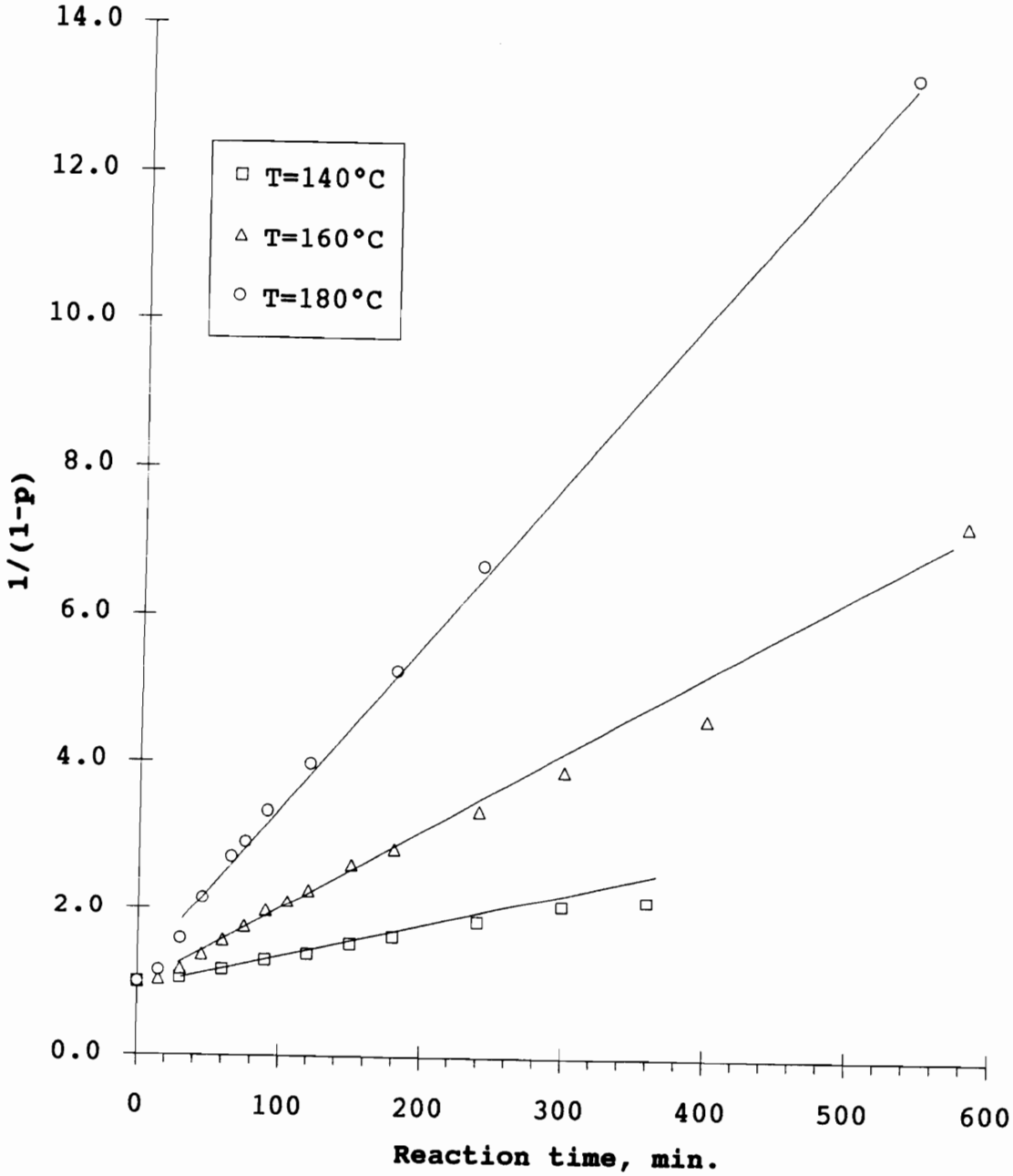

Figure 4.1.12. A second order kinetic plot of $\frac{1}{1-p}$ vs. reaction time for 4,4'-DDS/ODPA polyimide system.

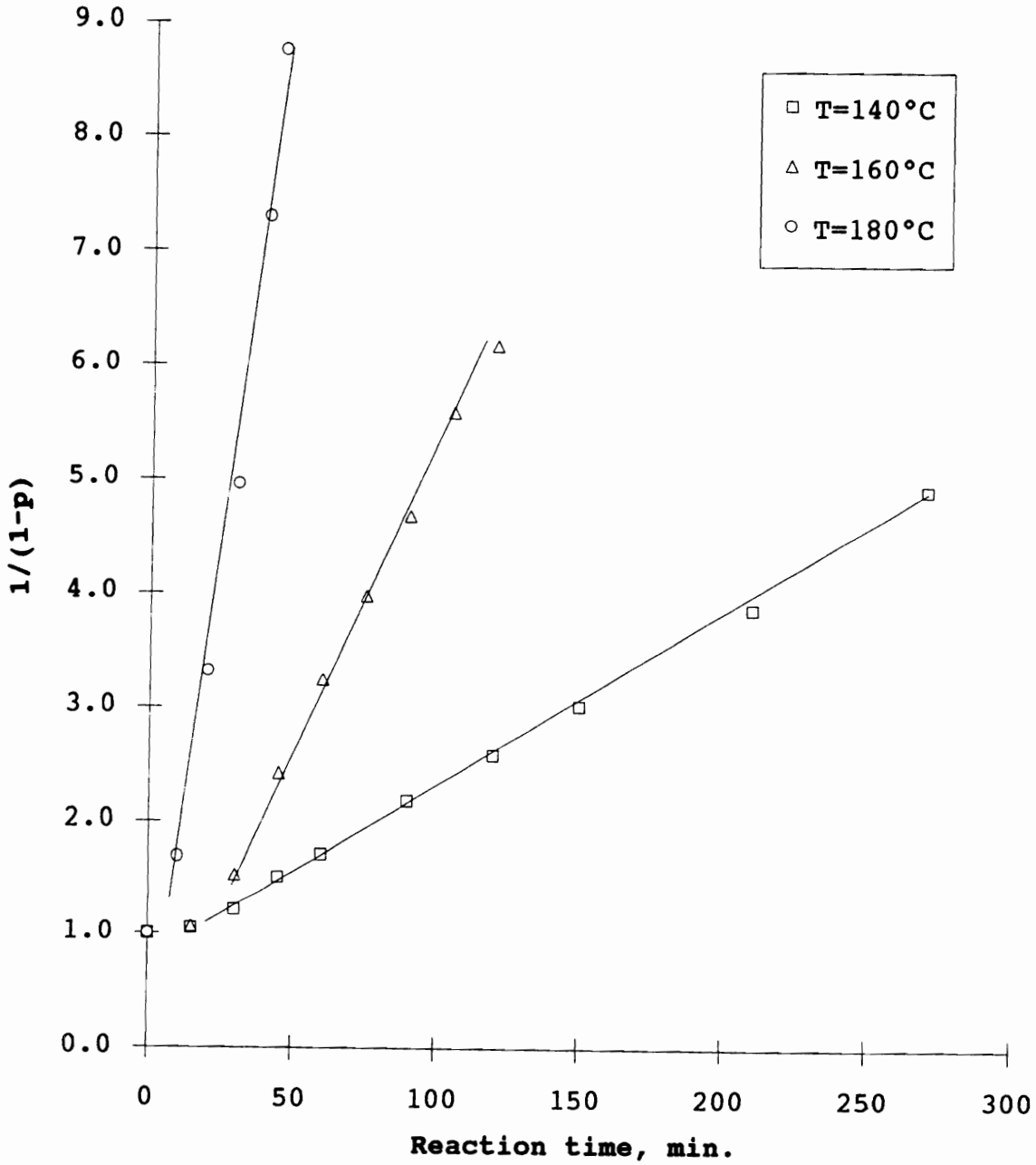

Figure 4.1.13. A second order kinetic plot of $\frac{1}{1-p}$ vs. reaction time for 4,4'-ODA/DSDA polyimide system.

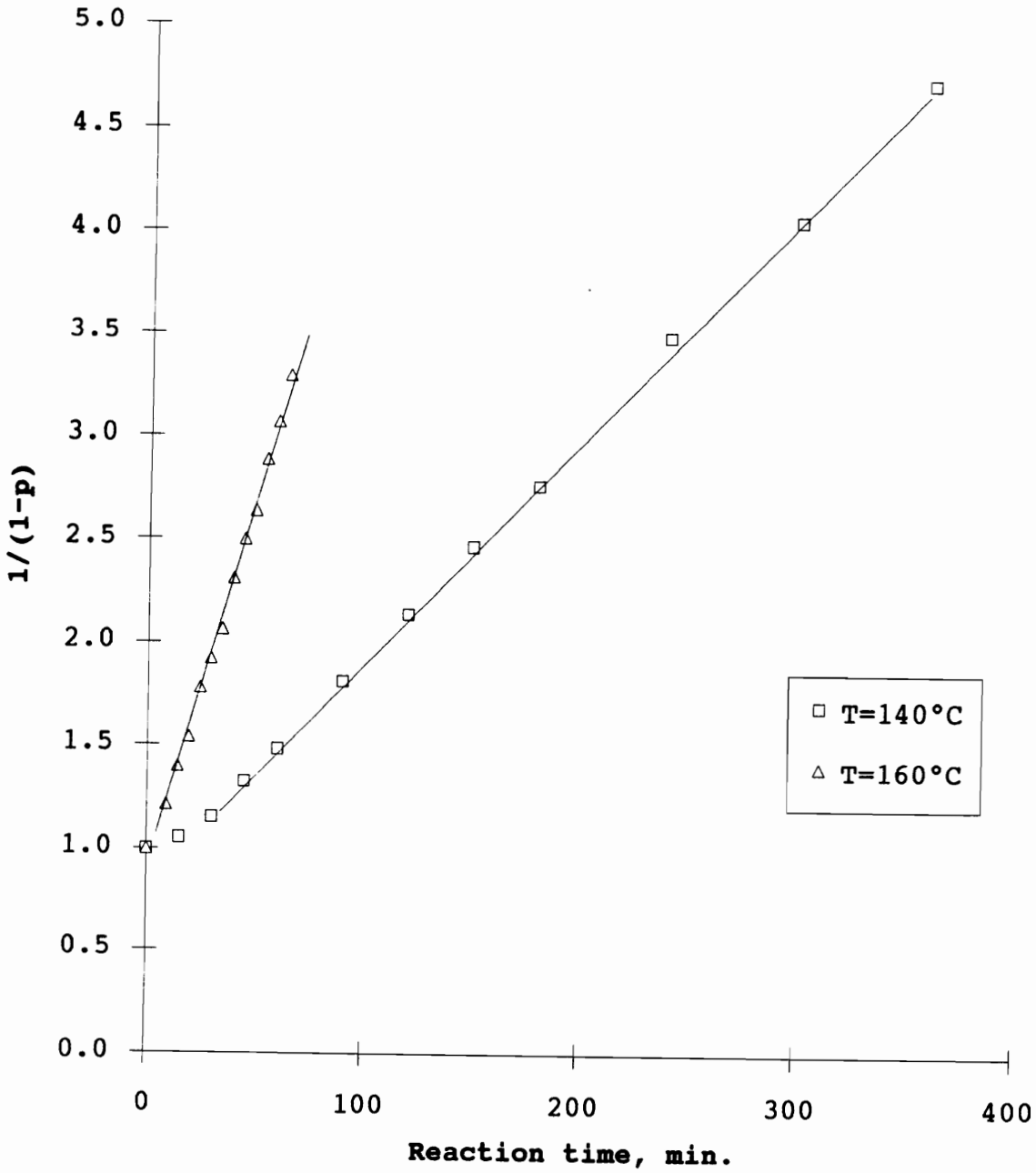

Figure 4.1.14. A second order kinetic plot of $\frac{1}{1-p}$ vs. reaction time for 4,4'-ODA/6FDA polyimide system.

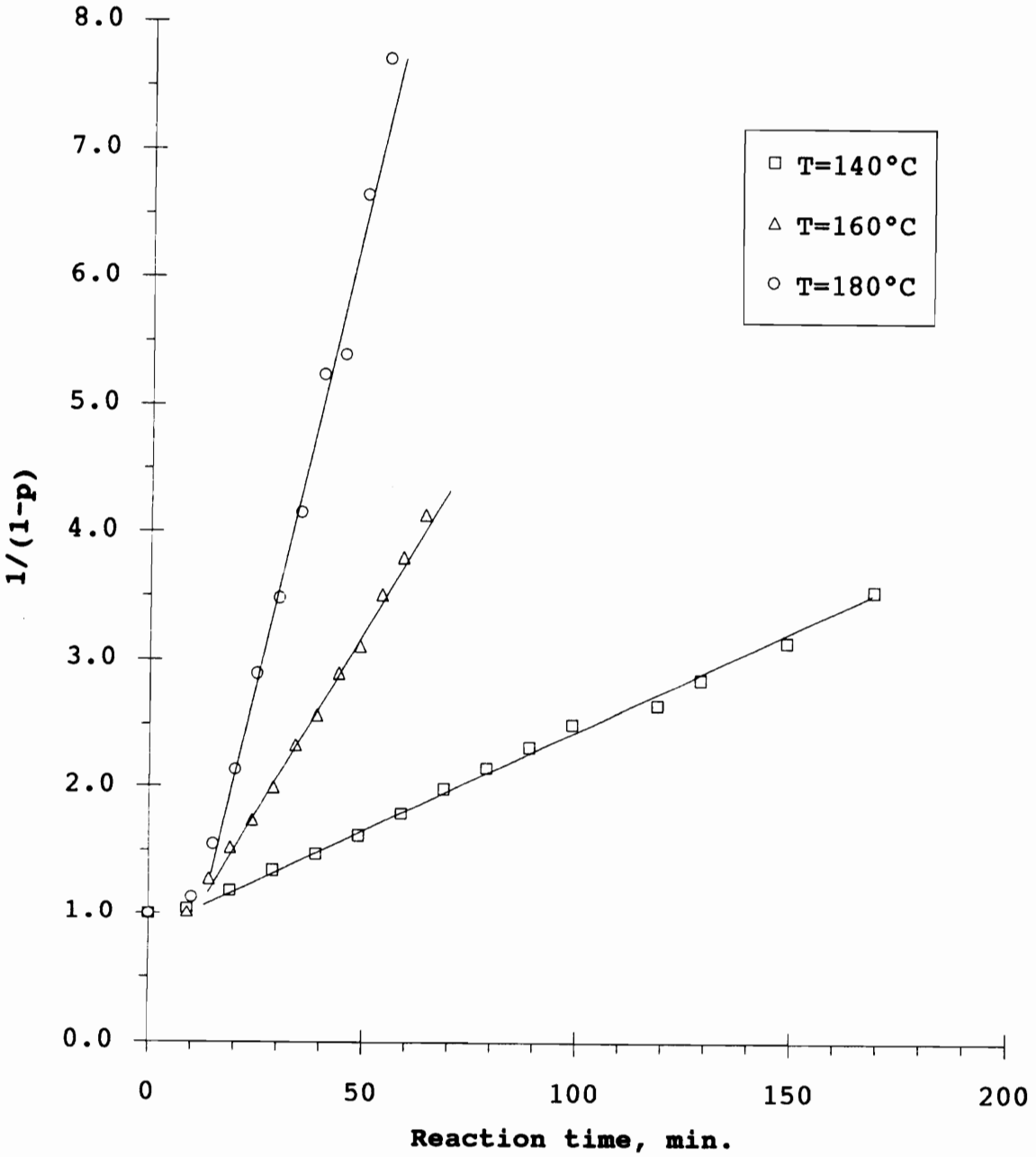

Figure 4.1.15. A second order kinetic plot of $\frac{1}{1-p}$ vs. reaction time for 4,4'-ODA/ODPA polyimide system.

The temperature dependence of the rate constants could be expressed by the Arrhenius relation (Eq. 4.5) which employs frequency factor (A) and activation energy (Ea) or the absolute rate theory relation (Eq. 4.6) which employs two adjustable parameters, activation enthalpy (ΔH^*) and activation entropy (ΔS^*).

$$k = A \exp(-\frac{Ea}{RT}) \qquad \text{Eq. 4.5}$$

$$k = \kappa \frac{RT}{Lh} \exp(\frac{\Delta S^*}{R}) \exp(-\frac{\Delta H^*}{RT}) \qquad \text{Eq. 4.6}$$

In the Eq. 4.6 κ is a transmission coefficient which is usually taken as unity, L is the Avogadro constant and h is the Plank constant. Based upon these two equations (Eq. 4.5 and Eq. 4.6) and rate constants, kinetic parameters were obtained. The Arrhenius plot and the derived kinetic parameters are shown in the Figure 4.1.16 and Table 4.1, respectively. The kinetic results in Table 4.1 demonstrate that the rate of imidization reaction is influenced by the heteroatom bridging groups in the both diamine and dianhydride components. In the temperature range examined reactivity order for the imidization is 4,4'-ODA/DSDA$\geq$4,4'-ODA/ODPA$\cong$4,4'-ODA/6FDA>>4,4'-DDS/DSDA$\geq$4,4'-DDS/ODPA polyimide system. Obviously an electron donating group (-O-) in the diamine component accelerates the rate of imidization

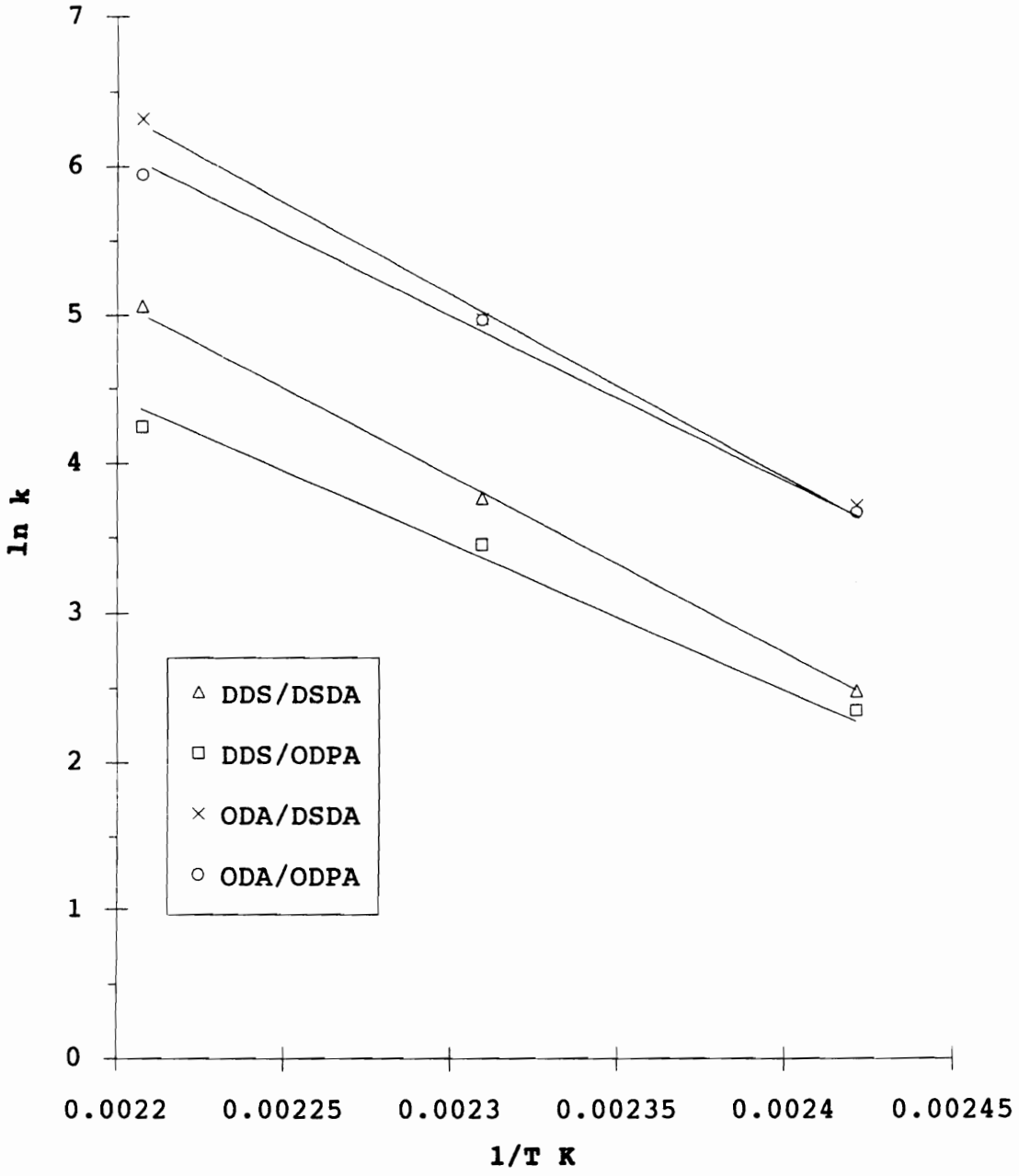

Figure 4.1.16. Arrhenius plot of second order kinetic data for polyimide systems.

Table 4. 1. Kinetic parameters derived from second order kinetics for various polyimide systems.

Polyimide	k, g/mol min					ΔH^*	ΔS^*
systems	140°C	160°C	180°C	Ea (KJ/mol)	ln(A min)	(KJ/mol)	(J/mol K)
4,4'-DDS/DSDA	12±1	43±1	160±20	100 ± 3	31.6	97 ± 3	-27.5
4,4'-DDS/ODPA	11±1	32±1	70±3	74 ± 5	23.9	70 ± 5	-91.9
4,4'-ODA/DSDA	41±1	144±3	560±40	101 ± 5	33.2	97 ± 5	-14.6
4,4'-ODA/ODPA	39±1	144±3	380±20	89 ± 5	29.5	85 ± 5	-45.0
4,4'-ODA/6FDA	35±1	120±2					

Where k is a rate constant, Ea is an activation energy, A is Arrhenius frequency factor, ΔH^* (KJ/mol) is the activation enthalpy and ΔS^* is the activation entropy.

significantly due to direct electronic effects on the amide nitrogen atom. The rates of imidization for the 4,4'-ODA/ODPA polyimide system containing an electron donating group in the dianhydride component were observed to be comparable to those of the 4,4'-ODA/DSDA polyimide system containing a strong electron withdrawing group in the dianhydride component at low temperatures, 140 and 160°C. Moreover, the rates of imidization for the 4,4'-DDS/ODPA polyimide were also comparable to those of the 4,4'-DDS/DSDA polyimide system at low temperatures. In addition, polyimide systems containing DSDA showed slightly increased imidization rates at 180°C. Furthermore, 4,4'-ODA/6FDA polyimide system containing electron withdrawing group in the dianhyride component showed a slightly decreased rate of imidization compared to those of 4,4'-ODA/DSDA and 4,4'-ODA/ODPA polyimide systems. Thus, the effects of the bridging groups of dianhydride components on the reactivity were relatively small. One may speculate on this behavior as follows; Figure 4.1.17 shows one of the repeat units in the polyamic acid. A bridge group X in the diamine component can exert a direct electronic effect on the amide nitrogen atom which is in the para position with respect to X via resonance. On the other hand, the Y group in the dianhydride component may exert electronic effects on both the amide nitrogen and acid carbonyl groups. For example, if Y is an

electron donating group such as oxygen it will decrease the electrophilicity of the para-acid carbonyl group (A in Figure 4.1.17) via resonance. At the same time the oxygen atom would increase the electron density of the para-amide carbonyl group (B in Figure 4.1.17). Thus, the nucleophilicity of the amide nitrogen (B in Figure 4.1.17) would be increased. But the Y group would exert more electronic effects on the para acid carbonyl groups than on the para-amide nitrogen groups. As a result, electron donating groups in the dianhydride components is expected to decrease the rate of imidization. Although the electronic effects may not be as significant as those of diamine components.

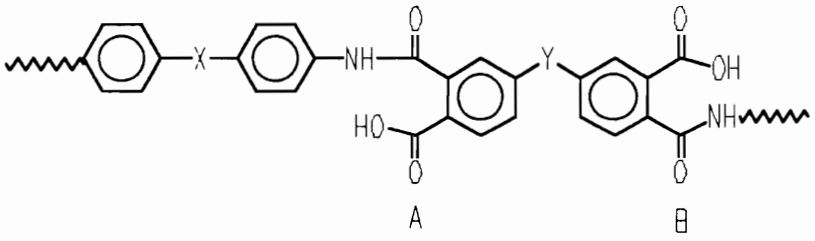

Figure 4.1.17. A representative repeat of a polyamic acid.

For intramolecular reactions it was suggested that optimum orientations of reactive functional groups are required to allow adequate interactions between those functional groups (175,107 210,211). Due to this reason it was considered that chain stiffness also plays an important

role in the intramolecular reactions. If this argument is true the rigid DSDA component might have tendency to reduce the rate of imidization. In this case, the stiffness of the dianhydride components would have a more significant influence on the reactivity than that of diamine components because both acid groups and amide groups exist in dianhydride portions.

The activation parameters shown in the Table 4.1 may not be explained in a simple fashion, but the slowest reaction rate for 4,4'-DDS/ODPA polyimide system might be primarily due to a relatively large negative activation entropy. However, it is important to note that the numerical values of pre-exponential factors such as the activation entropy (ΔS^*) and Arrhenius frequency factor (A) vary with the choice of concentration units, except for first order reactions (212).

4.1.5. A proposed imidization mechanism for the solution imidization processes

Kinetic data which were obtained could be summarized as follows:

1) the imidization processes were characterized by the acid catalyzed second order kinetics.

2) the rate of imidization was directly affected by the electronic effects of diamine components.

Based upon the obtained kinetic data, we propose a reasonable imidization mechanism shown in Figure 4.1.18. In fact, mechanisms for the imidization reactions involving a prior dissociation of carboxylic acid functional groups may not be excluded. In this case, however, information on proton transfer steps is needed. The reaction mechanism shown in Figure 4.1.18 is characterized by a bimolecular, concerted mechanistic feature. Based upon the effects of diamine components on the reactivity, the first step should be a rate determining step (r. d. s.). The reaction mechanism generates second order kinetics and is also consistent with the acid catalysis.

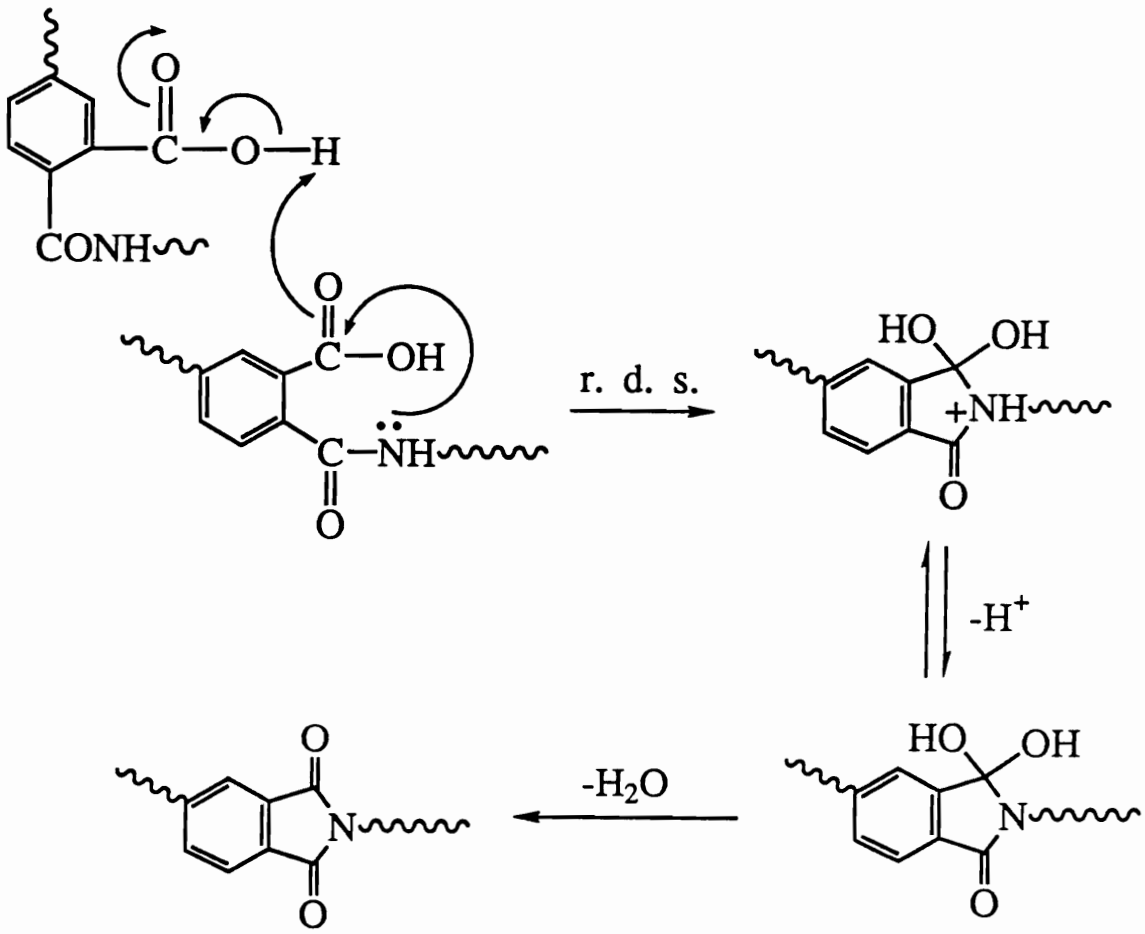

Figure 4.1.18. A possible reaction mechanism for the solution imidization process.

4.1.6. Summary of the kinetic study of the solution imidization processes

Solution imidization processes were followed successfully by a direct titration method. When the generally accepted and thus widely utilized first order kinetics for imidization reaction was applied to kinetic data obtained from solution imidization of various polyimide systems the kinetic data deviated from the first order kinetics at the high degrees of imidization. However, those kinetic data were well fitted to second order kinetics throughout the imidization processes for all of the polyimide systems investigated. Furthermore, the second order kinetic nature of the solution imidization processes were generated by performing imidization reactions as a function of three different initial concentrations of the polyamic acid solutions. The imidization reactions were further demonstrated to be acid catalyzed. Heteroatom functional groups in the diamine and dianhydride components influenced the imidization kinetics: 1) the rate of imidization was directly influenced by the electronic effects of heteroatoms in the diamine components. Thus, an electron donating group caused large increase in the rate of imidization. 2) the effects of the bridging groups in the anhydride components on the reactivity were not as simply interpreted and the electronic effects appeared to be relatively minor.

4.2. NMR characterization of polyamic acids

4.2.1. Acid and amide signal assignments

^{1}H-NMR spectra of the polyamic acids shows two peaks downfield, one at around 13 ppm due to the acid and the other at around 10.5 ppm due to the amide functional groups. Even in the literature (88,213) the acid and amide proton signal assignments have apparently been incorrect, perhaps because the acid proton signal shifts upfield in the presence of a small amount of residual water, and thus only one peak at around 10.5 ppm is observed. In this section deuterium exchange experiments were conducted in order to unambiguously assign the acid and amide protons.

Figure 4.2.1 shows the ^{1}H-NMR spectra of the polyamic acid/imide from the reaction of 4,4'-ODA/ODPA. After the imidization was completed, the two signals at 13 and 10.4 ppm completely disappeared (Figure 4.2.1-e). When one drop of D_2O was added, a broad signal at 13 ppm completely disappeared. On the other hand, the signal at 10.4 ppm was still present, but the intensity of the signal decreased significantly. When several drops of D_2O were added the proton signals at 10.4 almost disappeared (Figure 4.2.1-c). These experiments showed different extents of exchange between the protons of the carboxylic acid functional groups and deuterium atoms of D_2O. From these experiments the signal at 13 ppm which showed more extent of exchange is

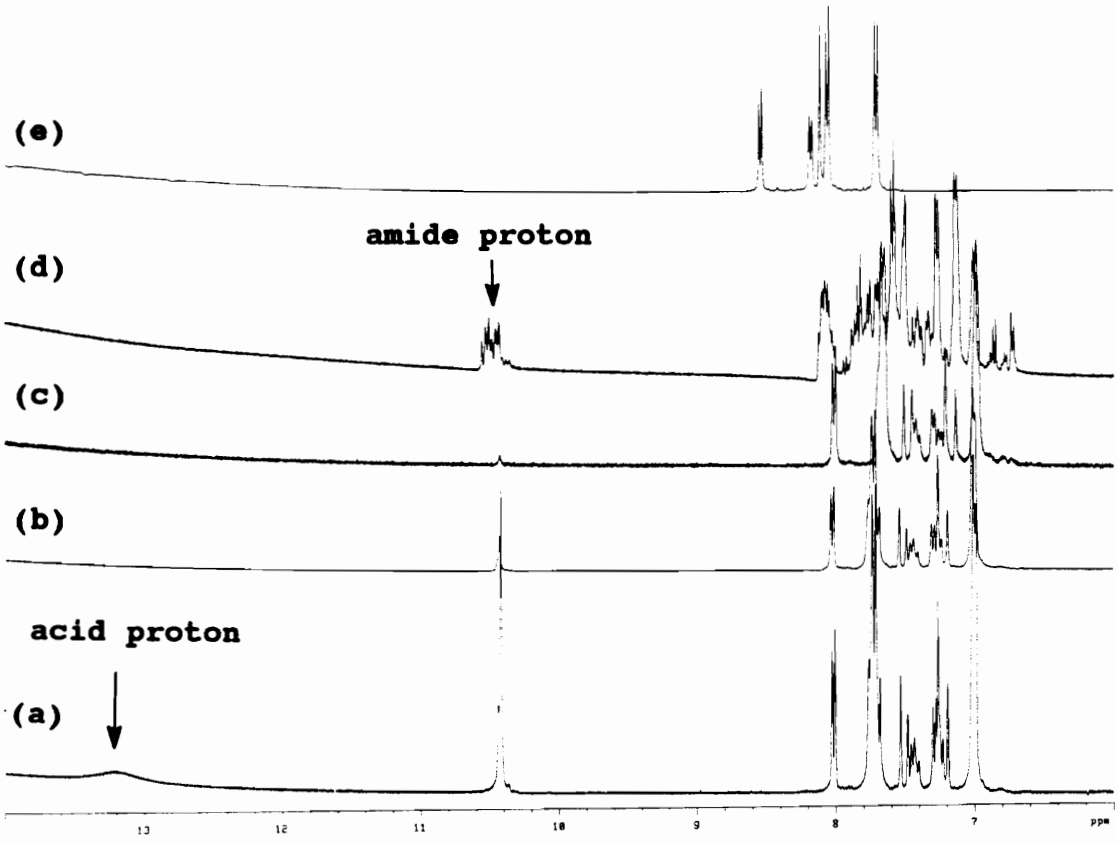

Figure 4.2.1. ^{1}H-NMR spectra of the polyamic acid from the reaction of 4,4'-ODA/ODPA: (a) unreacted polyamic acid; (b) after one drop of D_2O addition into polyamic acid; (c) after several drops of D_2O addition into polyamic acid; (d) partially imidized polyamic acid; (e) completely imidized polymer.

assigned to the acid proton and the signal at 10.4 ppm which showed less extent of exchange is considered to be the amide proton.

4.2.2. Isomeric compositions of the polyamic acid precursors

Since the amine functional groups can react with the anhydride functional groups by two different pathways, there are three isomeric structures in a polyamic acid when a triad containing two dianhydride and one diamine portion, is considered. The various microstructures of the polyamic acid synthesized from the reaction of 4,4'-ODA and ODPA in NMP at room temperature were characterized by NMR spectroscopy. ^{1}H-NMR spectra and the contour plot of 1H-1H COSY spectra of 4,4'-ODA/ODPA polyamic acid (theoretical <Mn> = 40K) are shown in Figure 4.2.1. Using additivity and connectivity information obtained from the 1H-1H COSY spectra (Figure 4.2.1) it was possible to assign the very complicated proton spectra of 4,4'-ODA/ODPA polyamic acid. Figure 4.2.2 shows the ^{1}H-^{1}H COSY spectra of the 4,4'-ODA/ODPA polyamic acid and Figure 4.2.3 shows ^{1}H-NMR spectra with assigned chemical structures. From the signal intensity information of the ^{1}H-NMR spectra of the polyamic acid (Figure 4.2.1) the microstructure of the polyamic acid could be obtained.

The several quantities regarding the microstructure compositions were defined as follows:

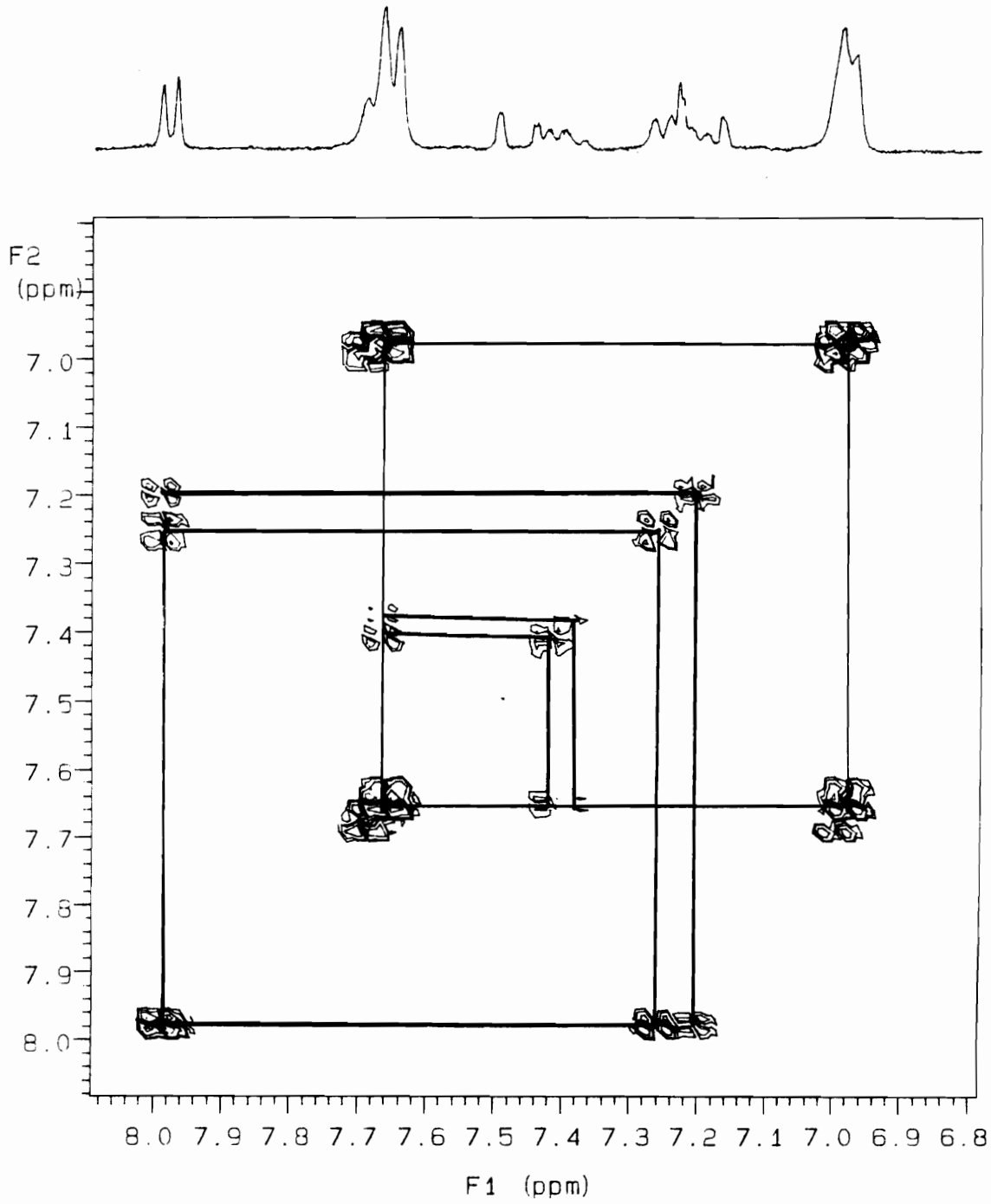

Figure 4.2.2. ^{1}H-NMR spectra and contour plot of ^{1}H-^{1}H COSY spectra of 4,4'-ODA/ODPA polyamic acid.

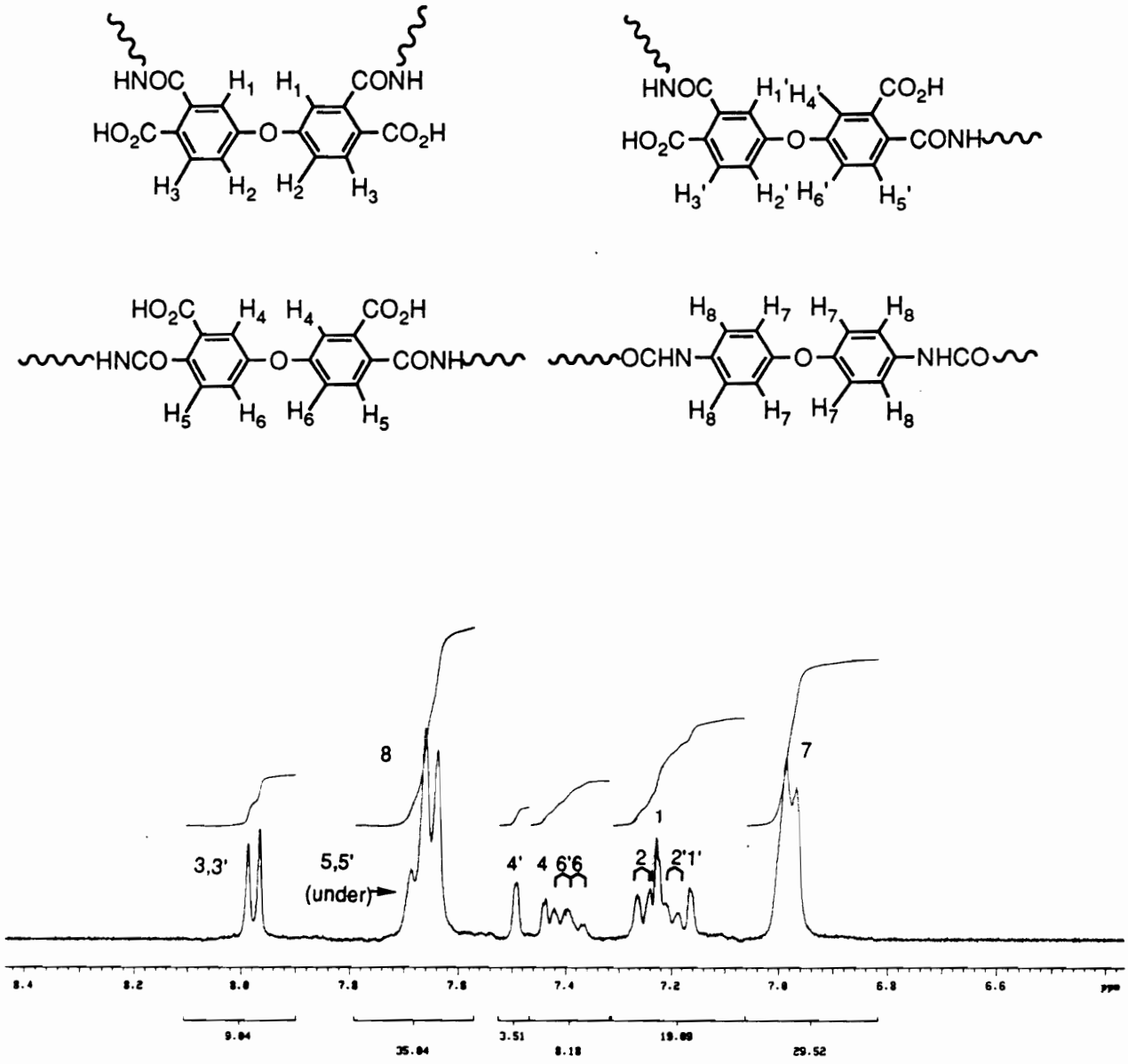

Figure 4.2.3. ^{1}H-NMR spectra of 4,4'-ODA/ODPA polyamic acid

p(mm) = x; composition of meta-meta linkages

2p(mp) = y; observed composition of meta-para linkages

p(pp) = z; composition of para-para linkages

Where p is the probability and x, y and z are variables.Then, we have following relationships:

$$x + y + z = 1 \qquad \text{Eq. 4.7}$$

$$I_3 + I_{3'} = \frac{I_t}{14}(2x + y) = 9.0 \qquad \text{Eq. 4.8}$$

$$I_5 + I_{5'} = \frac{I_t}{14}(2z + y) = \frac{I_t}{14}(2 - 2x - y)$$

$$= 35.0 - 29.5 = 5.5 \qquad \text{Eq. 4.9}$$

$$I_{4'} = \frac{I_t}{14} y = 3.5 \qquad \text{Eq. 4.10}$$

$$I_4 + I_{6'} + I_6 = \frac{I_t}{14}(2z + y + 2z)$$

$$= \frac{I_t}{14}(4 - 4x - 3y) = 8.2 \qquad \text{Eq. 4.11}$$

$$I_2 + I_1 + I_{2'} + I_{1'} = \frac{I_t}{14}(2x + 2x + y + y)$$

$$= \frac{I_t}{14}(4x + 2y) = 19.1 \qquad \text{Eq. 4.12}$$

Where I_t's are integrals of H_i's and I_t is total aromatic integral (104.3).

Eq. 4.10 gave a value of 0.47 for y and by substituting this value into eq's 4.2 ~ 6 values of x were obtained as 0.37, 0.40, 0.37 and 0.41 respectively. Internal consistency in the calculation of x values were observed with some experimental errors which confirmed the correct decoding of the ^{1}H-NMR spectra of a polyamic acid. The average of these values was 0.39. Substitution of the values x and y into Eq. 4.7 gave a value of 0.14 for z. Therefore the polyamic acid prepared from 4,4'-ODA and ODPA in NMP at room temperature was composed of 0.39 meta-meta isomer {p(mm)}, 0.47 meta-para isomer {2p(mp)} and 0.14 para-para isomer {p(pp)}. The microstructure information was also obtained from ^{13}C-NMR spectra of 4,4'-ODA/ODPA polyamic acid. ^{1}H decoupled ^{13}C-NMR spectra of 4,4-ODA/ODPA polyamic acid in the quaternary carbon (carbon atoms which are attached to ether oxygen atom) region is shown in Figure 4.2.4. The assignment of ^{13}C-NMR signals was performed utilizing additivity informations obtained from known spectra of ODPA containing polyamic acid (214). Figure 4.2.4 gave microstructure compositions of 0.38 for meta-meta linkages {p(mm)}, 0.47 for meta-para linkages {p(mp)} and 0.15 for para-para linkages {p(pp)}. The compositions of isomeric ratios of 4,4'-ODA/ODPA polyamic acid obtained from the signal intensity of ^{1}H decoupled 13C-NMR spectra were similar to

those obtained from 1H-NMR spectra, which further confirmed our correct decoding of ^{1}H-NMR spectra (Figure 4.2.2).

From the higher order microstructure information, lower order information could be obtained using the following relationships:

$$p(m) = p(mm) + p(mp) \qquad \text{Eq. 4.13}$$

$$p(p) = p(pm) + p(pp) \qquad \text{Eq. 4.14}$$

$$p(mp) = p(pm);\ \text{reversibility rule} \qquad \text{Eq. 4.15}$$

When the microstructure compositions obtained from ^{13}C-NMR spectra were used the above equations gave 0.61 for the concentration of meta linkage {p(m)} and 0.39 for that of para linkage {p(p)}. Applying a zero-th order Markovian distribution for the reaction of 4,4'-ODA and ODPA, the following relationships can be utilized:

$$p(mm) = \{p(m)\}^2 \qquad \text{Eq. 4.16}$$

$$p(mp) = p(m)p(p) \qquad \text{Eq. 4.17}$$

$$p(pp) = \{p(p)\}^2 \qquad \text{Eq. 4.18}$$

The microstructure compositions were independently obtained from equations, Eq. 4.16 ~ 4.18. Thus, the amount of meta linkages {p(m)} was 0.61, and that of para linkage was 0.39. These obtained values were same as those calculated from

equations Eq. 4.7 ~ 4.9, which implies that reactivity of anhydride groups of ODPA with amine groups of 4,4'-ODA is independent of whether neighboring groups are reacted or not. The high abundance of meta linkages also implies that the meta carbonyl groups with respect to the ether oxygen atom are more electrophilic than para-carbonyl groups with respect to the ether oxygen atom under the reaction conditions.

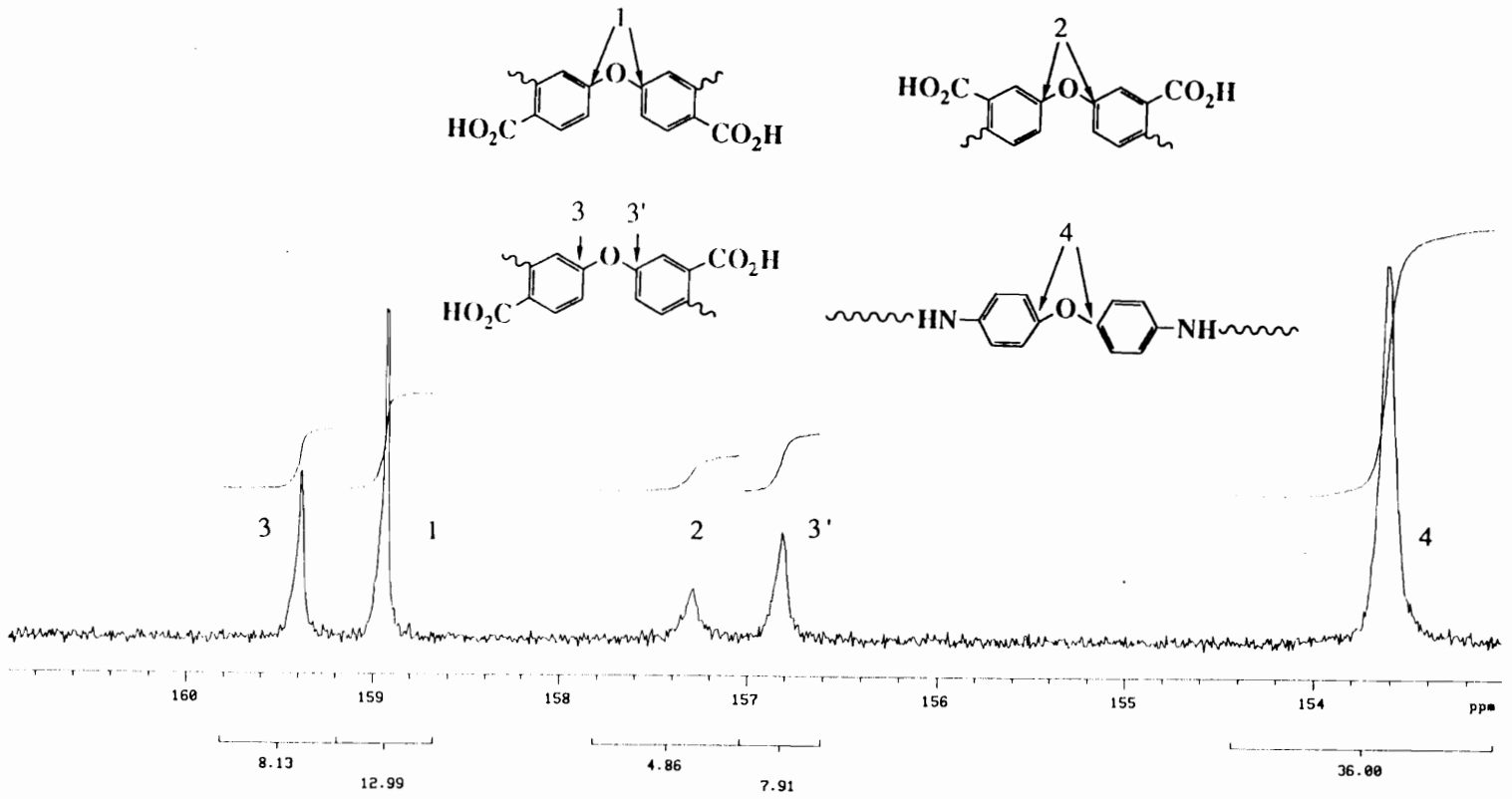

Figure 4.2.4. ^{13}C-NMR spectra of 4,4'-ODA/ODPA polyamic acid synthesized at room temperature in NMP.

4.3. Side reactions in the imidization processes

4.3.1. Background

Possibilities of curing reactions other than cycloimidization have been reported by many investigators (114,117,121-124,133-141,162,216). For example, a decrease in molecular weight was observed during thermal imidization processes (114). Anhydride formation determined by FTIR spectroscopy during polyamic acid cure provided further evidence for degradation of the polyamic acid precursor (117,162,216).

Other side reactions proposed in the bulk thermal imidization processes are branching and cross-link formation (121-124,133-141). Cross-linking reactions have long been thought to occur during bulk thermal imidization processes since many fully imidized polyimides display insolubility and infusibility. Sacher (122) specculated that initial imidization proceeds through intermolecular imidization (expressed as "transimidization") rather than cyclization by considering ring strain involved during imide ring formation, delocalization of amide nitrogen lone pair electrons and steric hindrance of acid carbonyl groups. Recently Snyder et al. (123,124) reported FTIR spectroscopic data which he interpreted as intermolecular imide link formation (Figure 4.3.1). These conclusions were reached by analyzing imide carbonyl stretching region of the infrared

spectra (1717 ~ 1735 cm^{-1}) as a function of "curing" conditions.

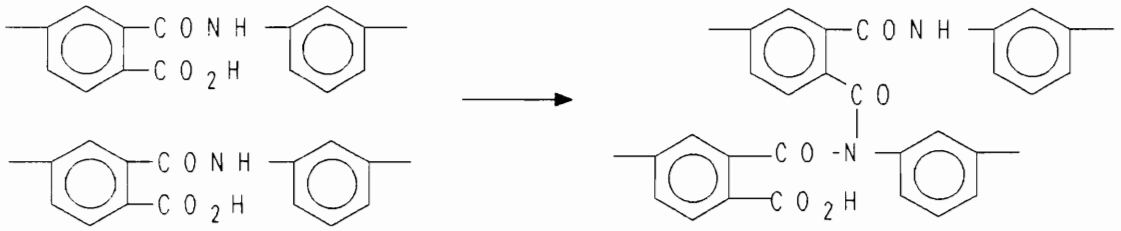

Figure 4.3.1. Intermolecular imide link formation during the imidization of polyamic.

Besides this intermolecular imidization reaction, cross-link reactions through recombination of free radicals generated by decarboxylation of unreacted amic acid groups and terminal anhydride groups at high temperature were also reported (139).

These side reactions, if they occur under our solution imidization conditions, would obviously have significant effects on the properties of polyimides such as molecular weight, solution properties and mechanical and thermal properties of polymers. In order to produce novel polyimides, detailed information and better understanding of imidization processes are necessary. Section 4.3.2 provides studies of the polyamic acid degradation during thermal solution imidization processes. Section 4.3.3 details studies of the proposed intermolecular imide link formation.

In the final section 4.3.4, the imine formation reaction that we propose will be demonstrated.

4.3.2. Degradation of polyamic acid structure structures

4.3.2.1. NMR studies of the solution imidization processes

Figure 4.3.2 shows ^{1}H-NMR spectra of 4,4'-ODA/ODPA polyamic acid/imides at intermediate stages. As imidization proceeded the characteristic amic acid peaks originally present decreased in intensity and new peaks developed. Especially in the 6.6-6.9 ppm region, upfield shifted small peaks developed at very beginning of imidization stages, increased in intensity as imidization proceeded and then almost completely disappeared when imidization was completed.

From the ^{1}H-^{1}H COSY spectra of partially "cured" 4,4'-ODA/ODPA polyimide shown in Figure 4.3.3 the ^{1}H-^{1}H connectivity between 6.67ppm and 6.85 ppm peaks is observed. Using this connectivity and upfield shifted nature of these peaks, it was possible to assign these to protons to terminal amino aromatic moieties:

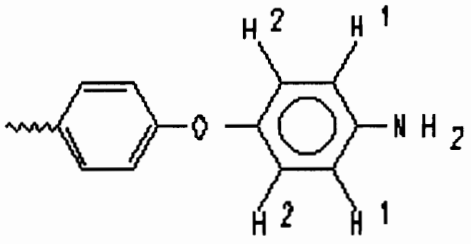

d_{H1} = 6.67 ppm, d_{H2} = 6.85 ppm, $J_{1,2}$ = 8.0H_z

This result is clear and direct evidence of degradation of amide bonds in the polymer backbone during the imidization processes. Since it was reported that polyamic acids are in equilibrium with decomposed amine and anhydride terminated polymer fractions (61), the degradation is considered to be due to hydrolysis of amide bonds and unimolecular decomposition of the polymer backbone. It may not be easy to resolve those different effects.

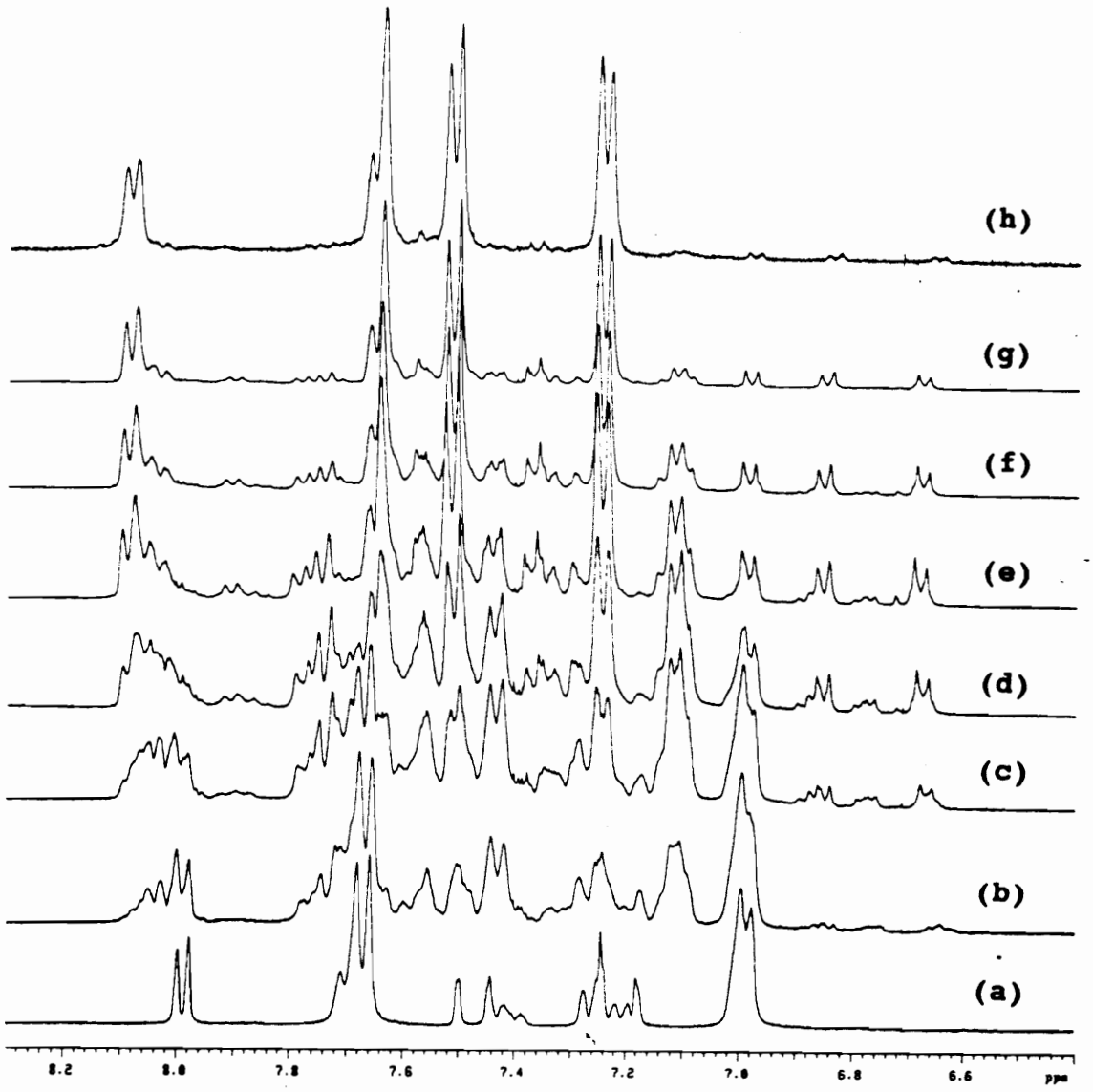

Figure 4.3.2. ^{1}H-NMR spectra of 4,4'-ODA/ODPA polyamic acid/imide at different imidization stages imidized at 150°C: (a) 0 hr (polyamic acid); (b) 0.33hr; (c) 0.5 hr; (d) 0.88 hr; (e) 1.33 hr; (f) 2hr; (g) 4hr; (h) 21 hr reaction.

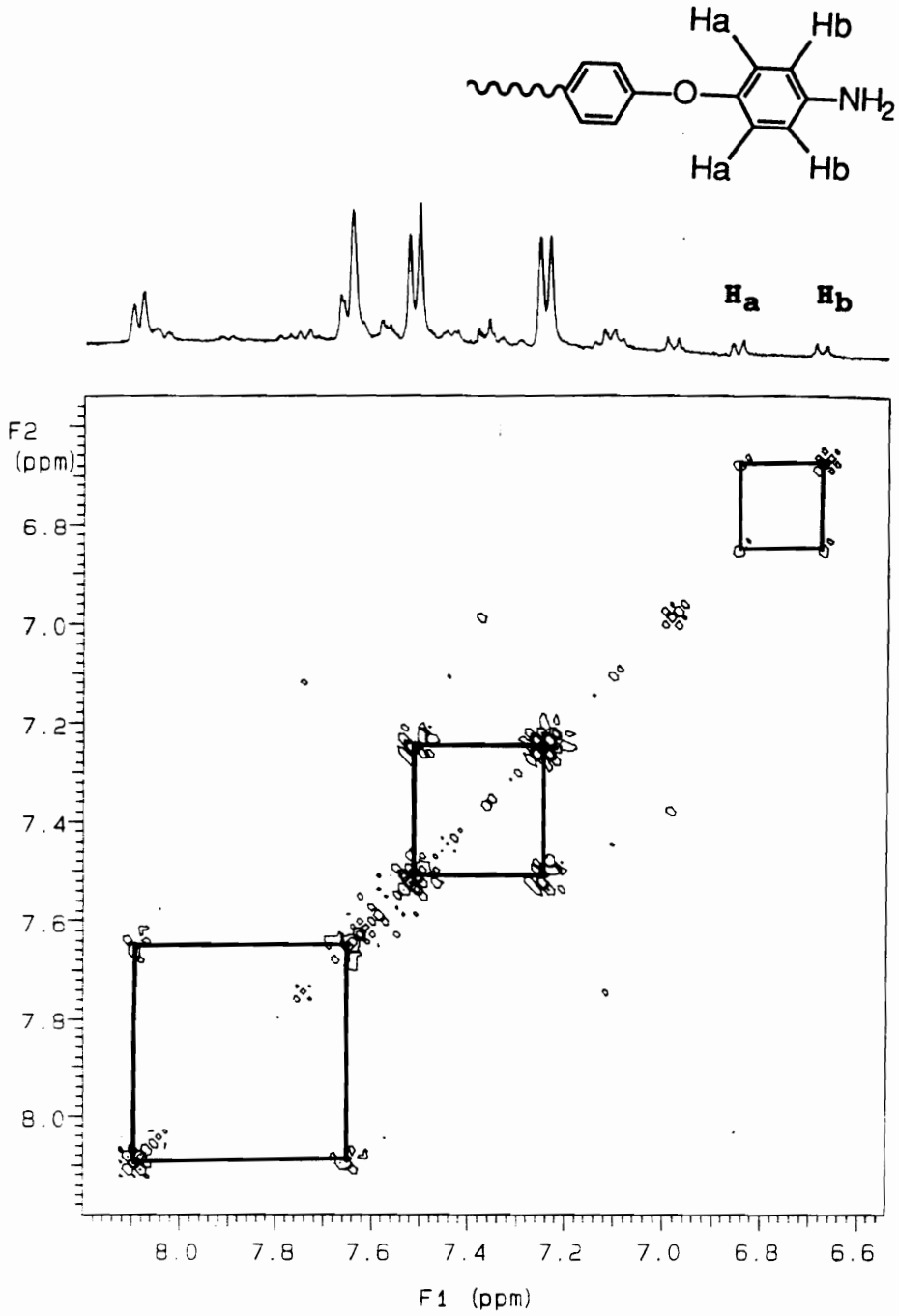

Figure 4.3.3. ^{1}H-^{1}H COSY spectra of partially imidized 4,4'-ODA/ODPA polyimide (3hrs., at 150°C).

4.3.2.2. Molecular weight (intrinsic viscosity) change during the solution imidization processes

Molecular weight aspects of solution imidization processes were studied by combined proton NMR spectroscopy and solution viscosity measurements. All of the intrinsic measurements were performed in anhydrous 0.1M LiBr in NMP solution at 25°C to minimize polyelectrolyte effects (12,67,215,216) which might occur for dilute polyamic acid solutions. Since polyimides with high degree of imidization (above ca. 98 % degree of imidization) showed thermoreversible gelation phenomena polyimide samples taken at defined time intervals were diluted with dry 0.1 M LiBr/NMP solution after quenching using dryice/acetone bath in order to prevent physical gelation. The gelation phenomena were a strong function of molecular weight (which was also a function of imidization time), aging temperature, polymer concentration and aging time.

Figures 4.3.4 ~ 4.3.6 show intrinsic viscosity data as a function of reaction time at 140, 150 and 180°C respectively. A dramatic decrease in intrinsic viscosity at the very initial stages of imidization process was observed. Further imidization gave rise to increase in viscosity. A noticeable temperature effect on the solution viscosity was also observed. At relatively low imidization temperatures (140 and 150°C) intrinsic viscosity increased very slowly

and even degraded products, amines and anhydrides (or diacids) did not react completely. As can be realized in Figure 4.3.1-(h) where a sample imidized for 21 hours still showed signals due to terminal amino aromatic moieties at 6.67 and 6.85 ppm even though their intensities were small. The presence of those signals is an indication of incomplete "relinking" of degraded products at 150°C. At high imidization temperature (180°C), however, intrinsic viscosity rapidly increased to reasonably high values and then gradually increased to the limiting value.

Figure 4.3.7 shows ^{1}H-NMR spectra of polyamic acid/imide which was imidized at 180°C as a function of imidization time. Since completely imidized 4,4'-ODA/ODPA polyimide was insoluble in DMSO (dimethyl sulfoxide) dry NMP was added to dissolve the polyimide for NMR characterization. When polyimide samples were diluted with dry NMP, aromatic protons in the range of from 7.5 to 7.6 ppm were well resolved and even a chemical shift change was also observed as shown in Figure 4.3.6-(h). Complete imidization, in terms of "relinking" of the partially degraded products and further cyclization of the reproduced amic acid, was possible at 180°C. Thus, Figure 4.3.6-(h) shows complete disappearance of 6.67 and 6.85 ppm signals of the end groups and is entirely consistent with a complete "relinking" reaction. The implication of these findings is

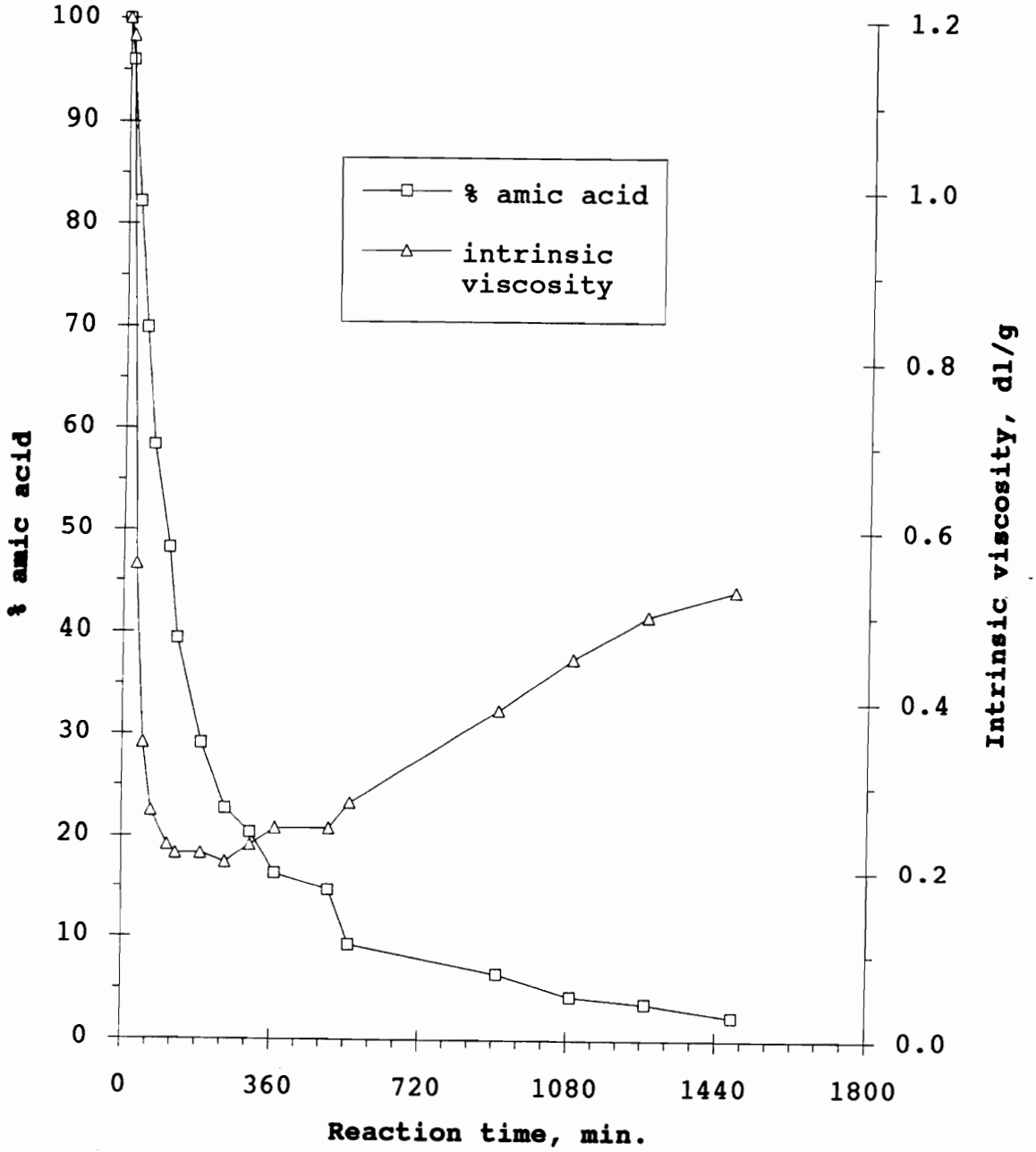

Figure 4.3.4. Remaining amic acid content and intrinsic viscosity as a function of reaction time at 140°C.

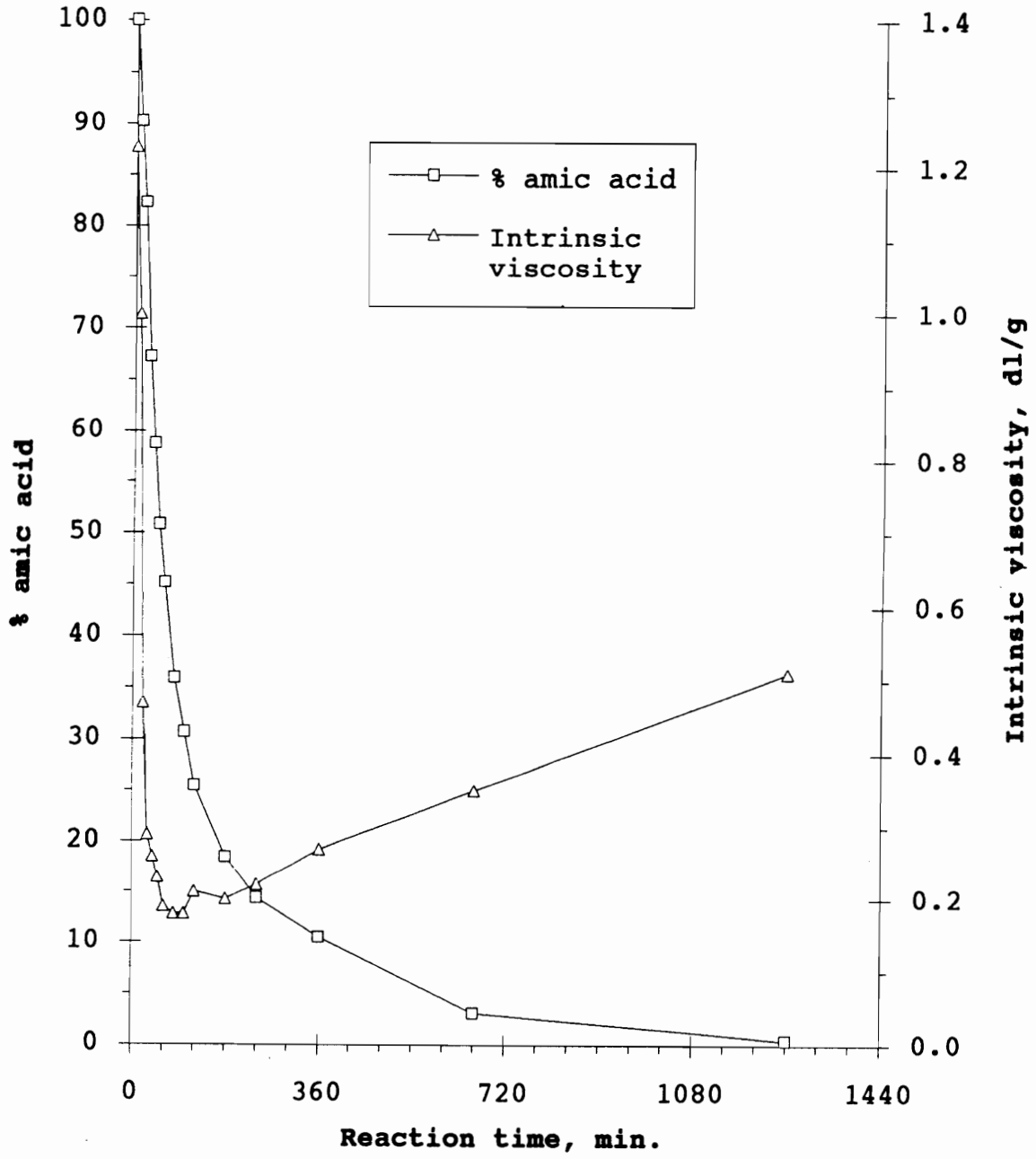

Figure 4.3.5. Remaining amic acid content and intrinsic viscosity as a function of reaction time at 150°C.

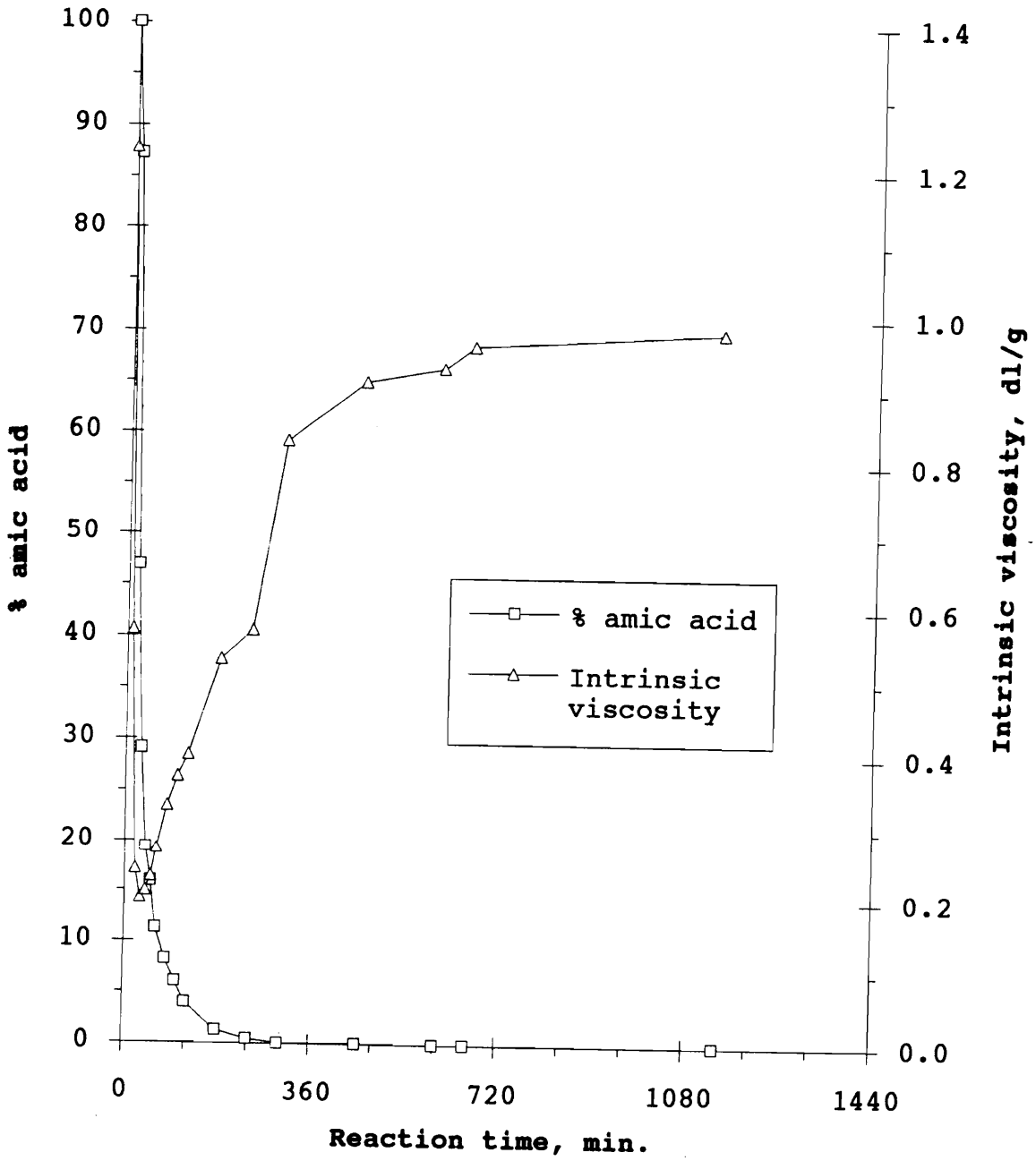

Figure 4.3.6. Remaining amic acid content and intrinsic viscosity as a function of reaction time at 180°C.

significant for the high performance polyimide synthesis since it demonstrates that proper imidization conditions are required to ensure complete recombination of the broken chains and their subsequent cycloimidization. Implicitly, this also necessary to achieve successful molecular weight control and to maximize thermal and hydrolytic stability.

Integration of the aromatic protons of the NH_2 containing aromatic end groups at 6.67 ppm could be utilized to determine number average molecular weight of polyamic acid/imide at intermediate imidization stages if the degree of polymerization was not too large by using the following equation:

$$\langle Mn \rangle = \frac{Nr}{Ne/2} M = \frac{Nr}{(N0 + Na + Nb)/2} M = \frac{Nr}{N0 + 2Nb/2} M \qquad \text{Eq. 4.19}$$

Where N_r = number of repeat units, N_e = number of end groups, N_0 = number of end groups of initial polyamic acid before degradation, N_a = number of anhydride groups and/or their degraded product diacid functional groups formed by degradation of amide bonds, N_b = number of NH_2 groups, M = molecular weight of repeat units (510-36p, p is degree of imidization).

Since the initial molecular weight of polyamic acid was high enough and it was not determined experimentally, the exact <Mn>'s of partially imidized polyamic acid could not be

obtained. However, we can use the quantity of $\frac{N_r}{(N_a + N_b)/2}$ as a direct measure of degradation of amide bonds and number average molecular weight of polyamic acid/imide at intermediate stages. The quantity of $\frac{N_r}{(N_a + N_b)/2}$ was calculated from the ratio of the integrals for the total aromatic protons as compared to the integrals of terminal aromatic ortho protons with respect to the NH_2 (6.67 ppm) in accord with the following equation:

$$\frac{N_r}{(N_a + N_b)/2} = \frac{N_r}{2N_b/2} = \frac{N_r}{N_b} = \frac{\text{Total aromatic integral}/14}{\text{6.67 ppm integral}/2} \qquad \text{Eq. 4.20}$$

The values of $\frac{N_r}{N_b}$ obtained from ^{1}H-NMR spectra utilizing Eq. 4.20, Figure 4.3.8 and 4.3.9, also showed similar trends as intrinsic viscosities shown in Figure 4.3.5 and 4.3.6. Those observed behaviors well correlate with ^{1}H-NMR spectra shown in Figure 4.3.2 and Figure 4.3.7. The relatively low intrinsic viscosities for the polyimides which were almost completely imidized at 140°C and 150°C were a function of the incomplete "relinking" reaction of the degraded products, NH_2 groups and diacid (or anhydride) groups.

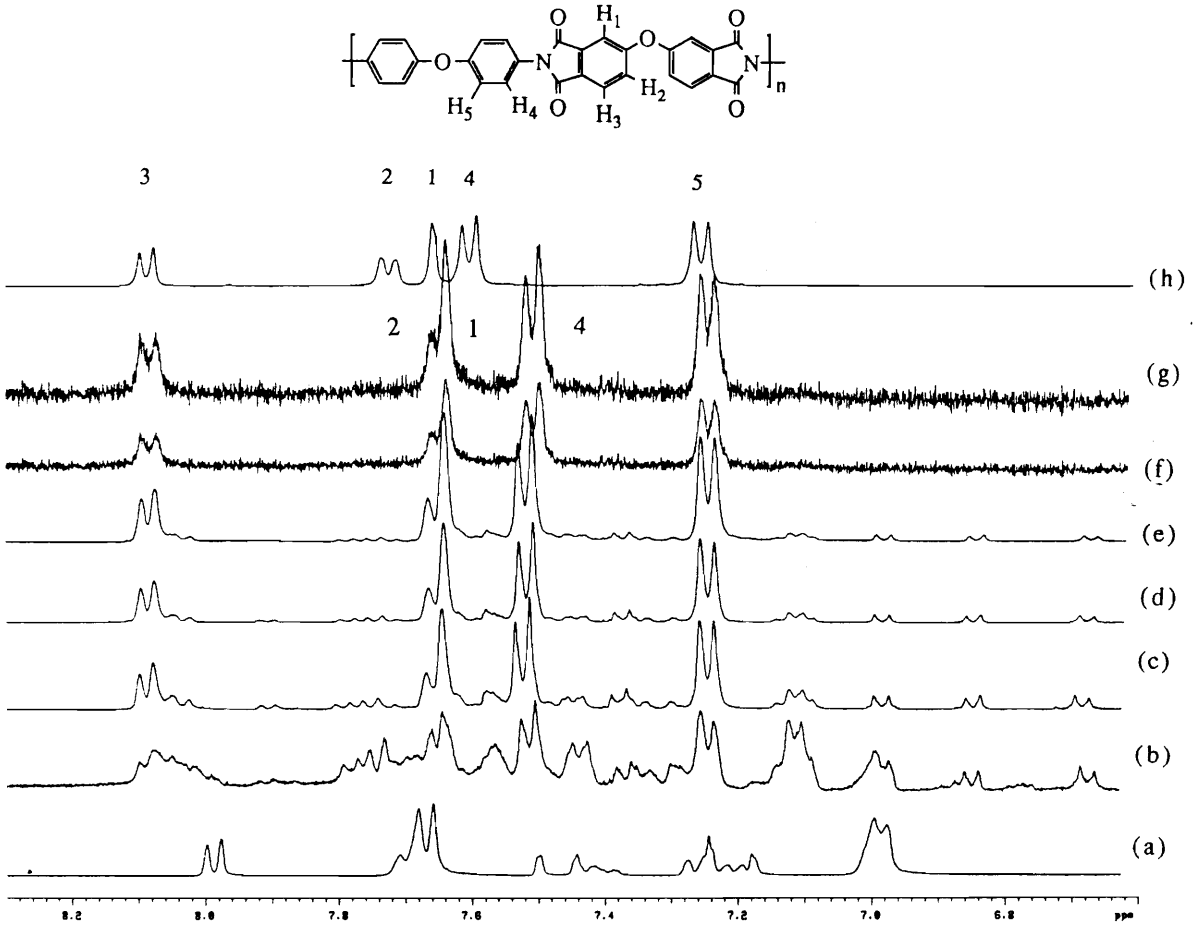

Figure 4.3.7. ^{1}H-NMR spectra of 4,4'-ODA/ODPA polyamic acid/imide at different imidization stages imidized at 180°C: (a) 0 hr (polyamic acid); (b) 0.33hr; (c) 0.66 hr; (d) 1 hr; (e) 1.66 hr; (f) 3 hr; (g) 11 hr reaction; (h) 11 hr reaction (diluted with dry NMP).

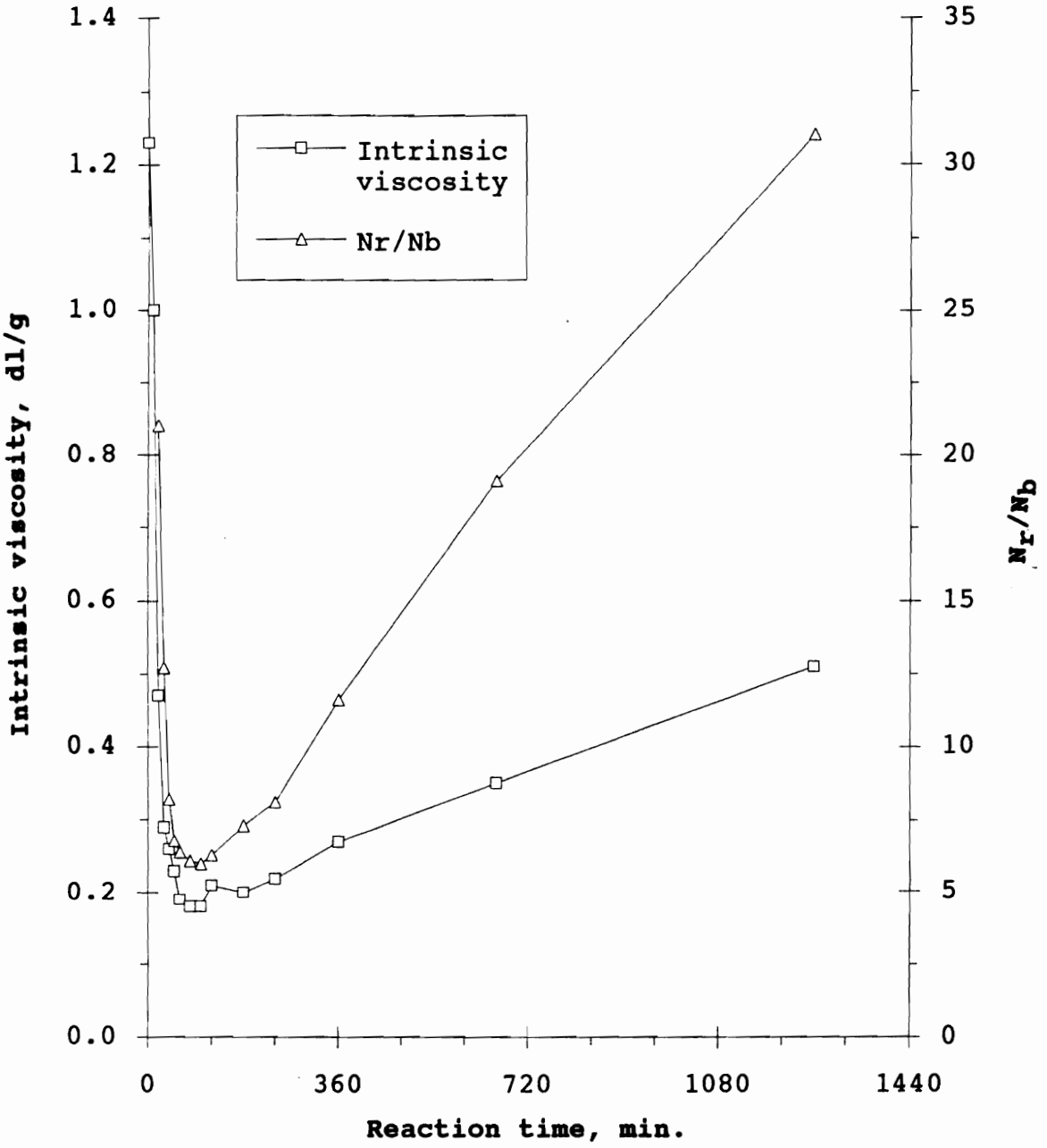

Figure 4.3.8. Intrinsic viscosity and Nr/Nb defined by Eq. 4.20 vs. reaction time at 150°C.

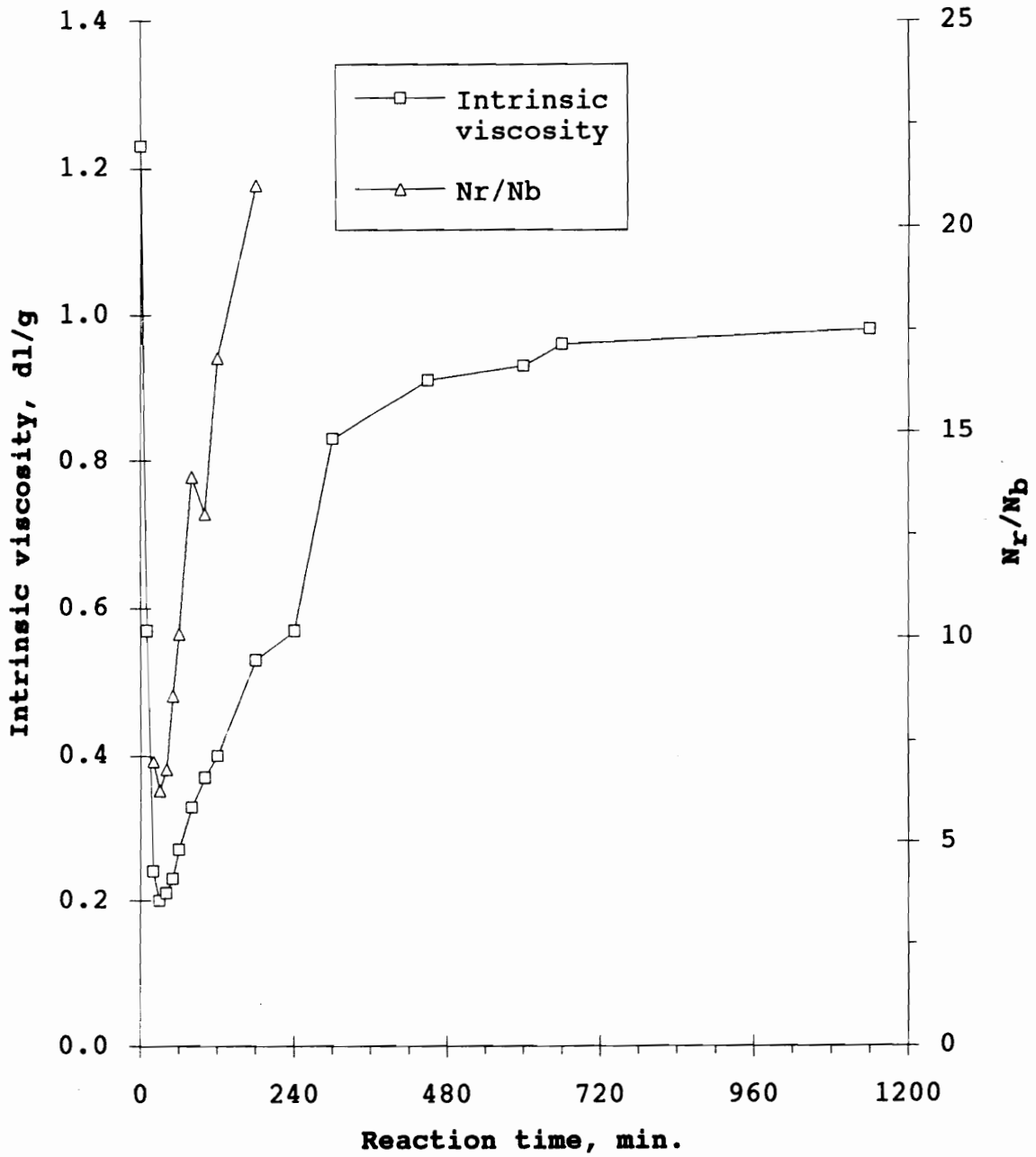

Figure 4.3.9. Intrinsic viscosity and Nr/Nb defined by Eq. 4.20 vs. reaction time at 180°C.

4.3.3. Possible intermolecular imide link formation

Snyder et al. (124) utilized FTIR spectroscopy to study the species actually formed during thermal imidization of poly(pyromellitic dianhydride oxydianiline). They investigated asymmetric imide carbonyl modes of the FTIR spectra of polyimides as a function of curing conditions to demonstrate the formation of intermolecular imide links (Figure 4.3.1). Polyimides are characterized by a pair of characteristic imide carbonyl bands; one higher frequency and less intense symmetric mode at 1780 and the other lower frequency and more intense asymmetric carbonyl mode around 1720 cm^{-1} (Figure 4.3.10) (217).

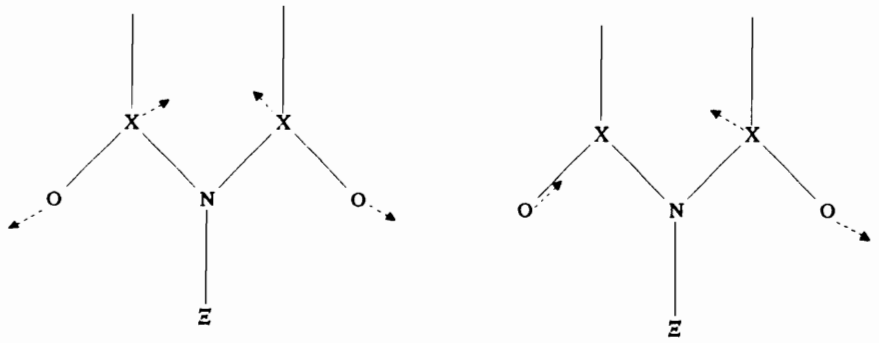

Figure 4.3.10. Symmetric and anti-symmetric vibrations of the imide moiety (217).

Actually, the broad band around anti-symmetric imide carbonyl region is a composite of various overlapping contributions from intramolecular imide carbonyl links, unreacted amic acid carbonyl groups, and intermolecular

imide links, if they were formed. It was observed that second derivatives of the anti-symmetric imide carbonyl modes of polyimides cured under different imidization conditions were functions of curing conditions, which in fact was utilized as evidence of intermolecular imide link formations. They considered that the net contribution of intermolecular imide links can be resolved from other effects such as dipole-dipole intermolecular interactions or other vibrational effects by performing FTIR studies of polyimides as a function of curing conditions (124). However, it has been well known that the FTIR patterns of carbonyl modes are much more complex due to dipole-dipole interaction of C=O groups (128), hydrogen bonding effects, and the participation of υ(C=O) in Fermi resonance with overtone of any vibration or the constituent frequency of the same symmetry (129-132).

Figure 4.3.11 shows the transmittance spectrum of polyimide powder (the polyimide powder was mixed with KBr and a KBr pellet was prepared) from the reaction of 4,4'-ODA and ODPA. 4,4'-ODA/ODPA polyimide was synthesized by employing the solution imidization technique at 10% solid content (NMP/ODCB=9/1) at 180°C for 24 hours. The polyimide was recovered by precipitating the polyimide solution into a large excess amount of stirring methanol, rinsing with methanol, and drying in a vacuum oven for 24 hours at 180°C.

The second derivative shown in the Figure 4.3.11 indicates that the anti-symmetric peak is composed of at least two peaks, one near 1733.4 cm-1 and the other near 1716.3 cm^{-1}. The multiplicity of the carbonyl absorption might be due to Fermi resonance. Kardash et al. (132) observed a well resolved splitting of the anti-symmetric carbonyl stretch for substituted N-phenyl phthalimides, for example, one at 1736 cm-1 and the other at 1717 cm-1 for N-phenylphthalimide even in the FTIR spectra itself. These frequencies are exactly the same as those of the 4,4'-ODA/ODPA polyimide powder. They proposed that the character of the absorption of N-phenylphthalimides was determined by the participation of υ(C=O) in Fermi resonance with 2υ(Ph-CO).

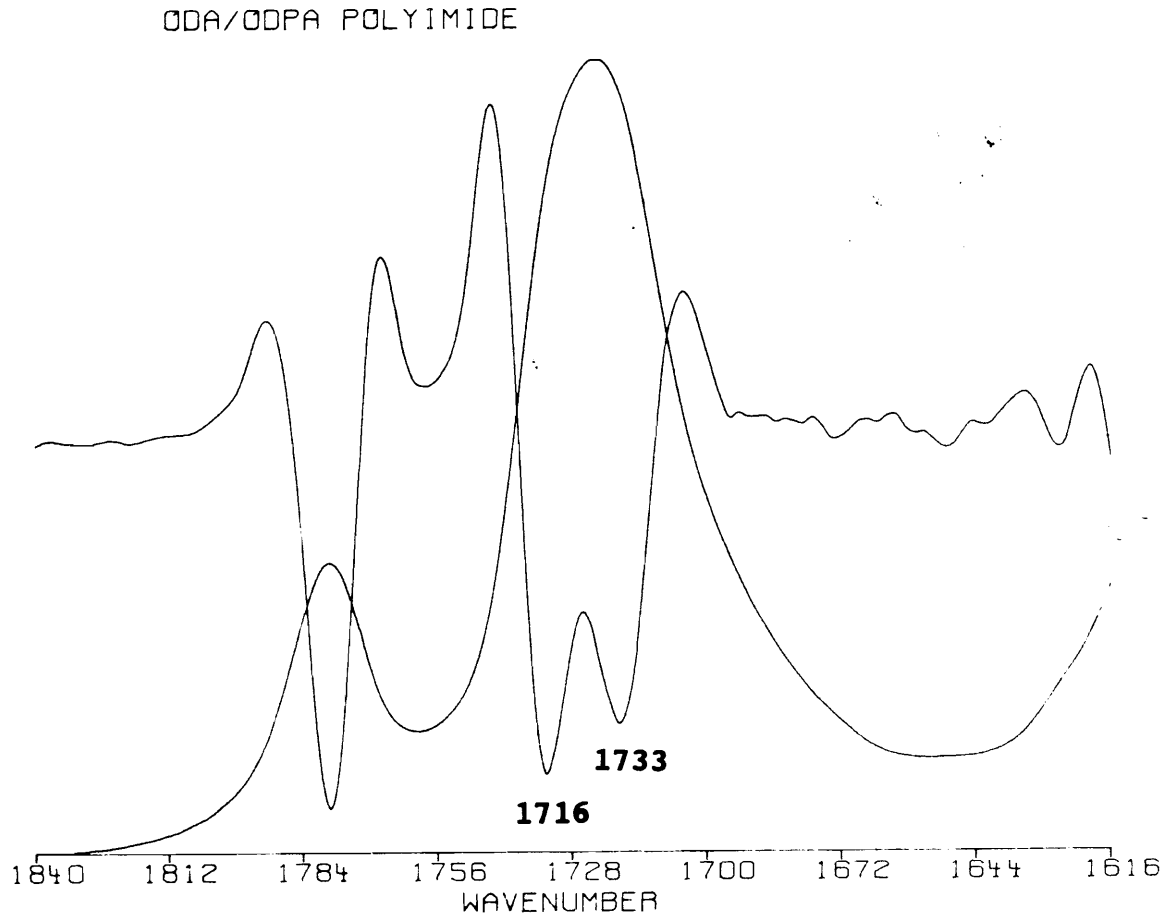

Figure 4.3.11. Carbonyl region of the infrared spectrum of 4,4'-ODA/ODPA polyimide powder (KBr) in transmittance. The top spectrum is a second derivative trace.

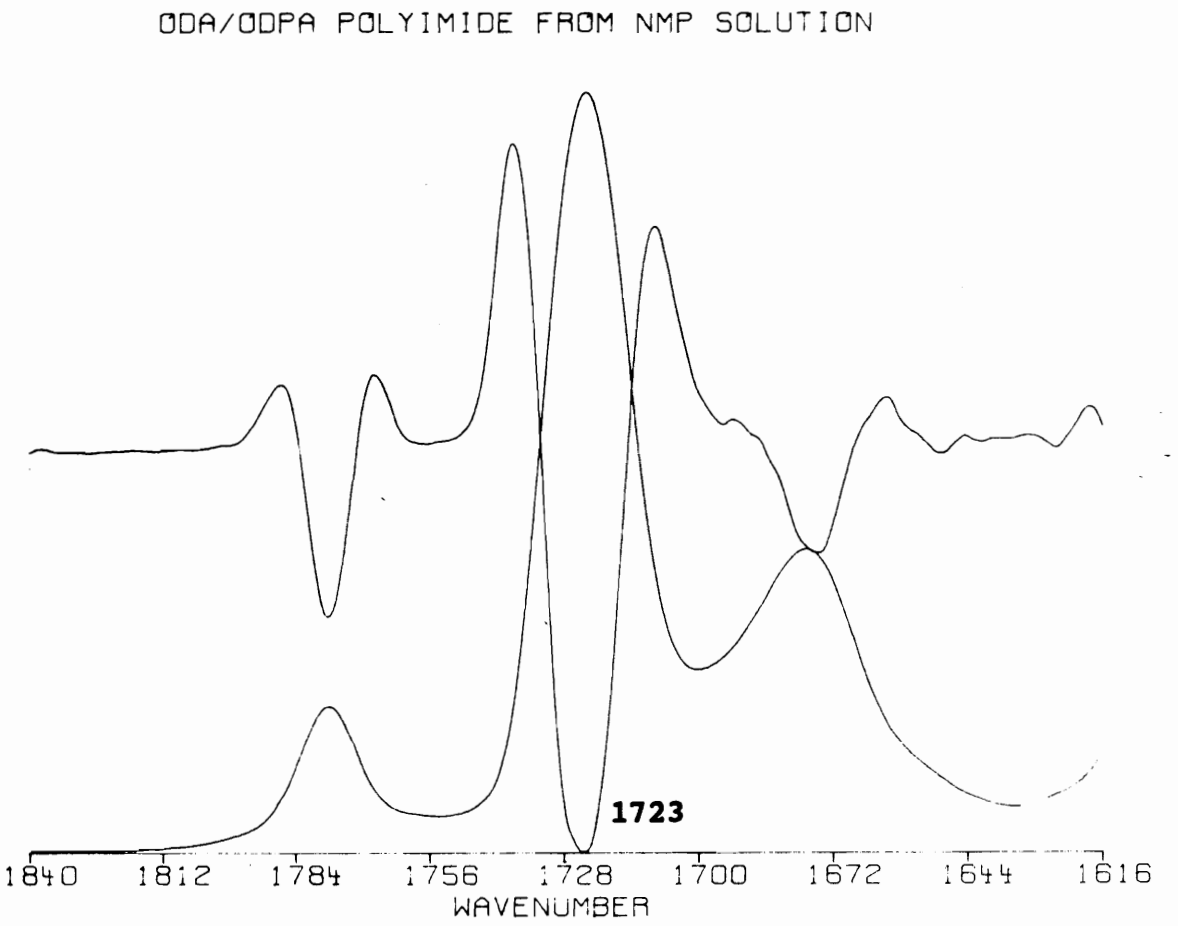

Figure 4.3.12. Carbonyl region of the transmittance infrared spectrum of 4,4'-ODA/ODPA polyimide film on the NaCl salt plat. The spectrum was obtained after 12 hour drying at room temperature under vacuum. The top spectrum is a second derivative trace.

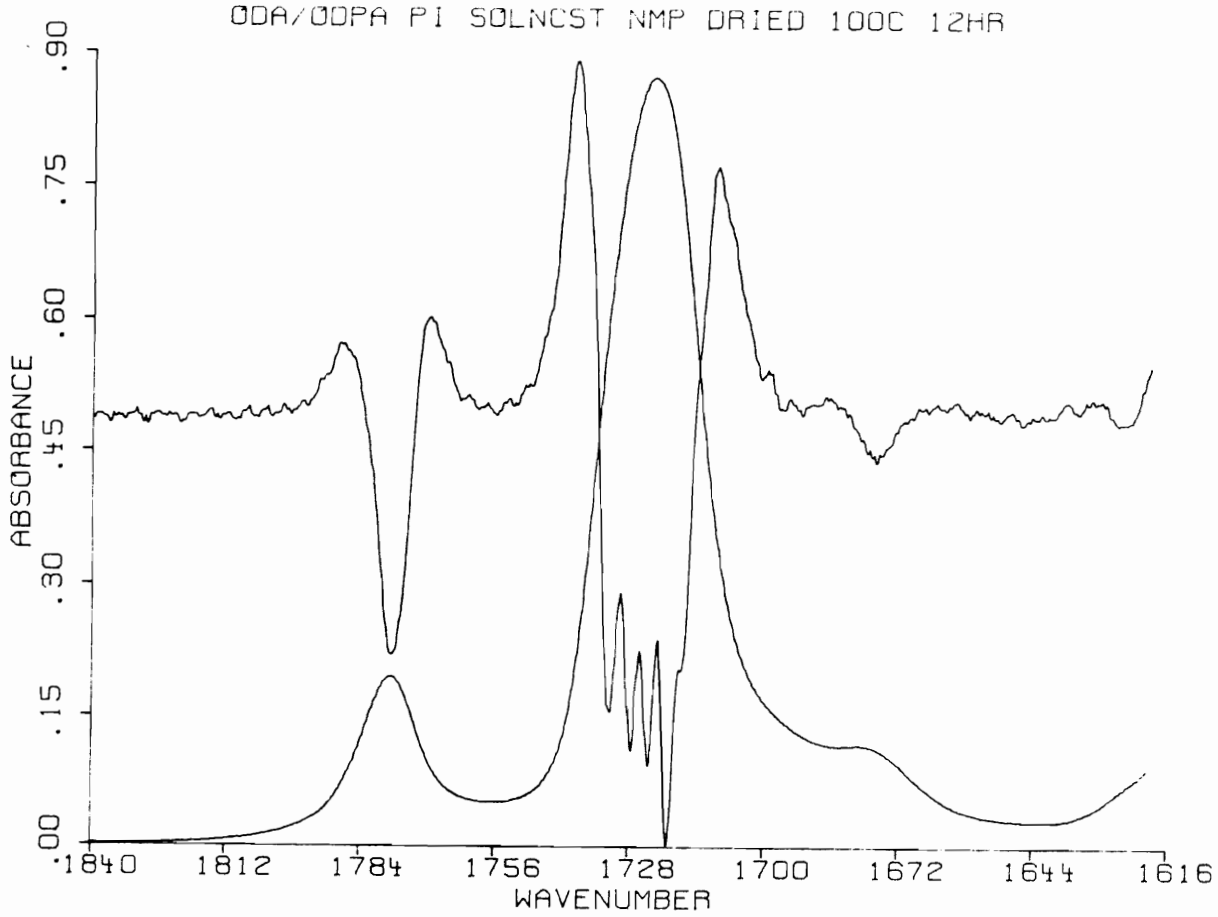

Figure 4.3.13. Carbonyl region of the transmittance infrared spectrum of 4,4'-ODA/ODPA polyimide film on the NaCl salt plat. The sample was dried under vacuum as follows: for 12 hours at room temperature and for 12 hours at 100°C. The top spectrum is a second derivative trace.

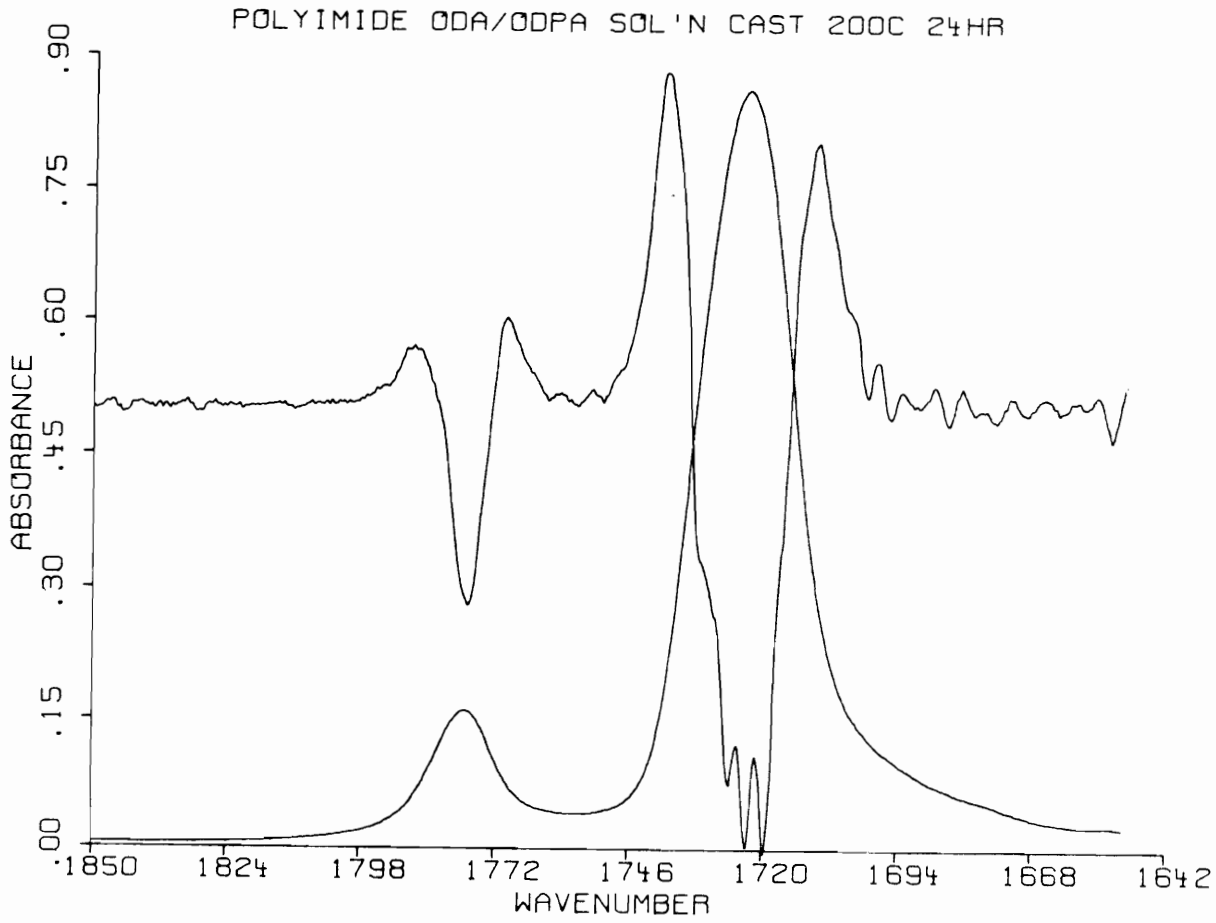

Figure 4.3.14. Carbonyl region of the transmittance infrared spectrum of 4,4'-ODA/ODPA polyimide film on the NaCl salt plat. The sample was dried under vacuum as follows: for 12 hours at room temperature, for 12 hours at 100°C and for 24 hours at 200°C. The top spectrum is a second derivative trace.

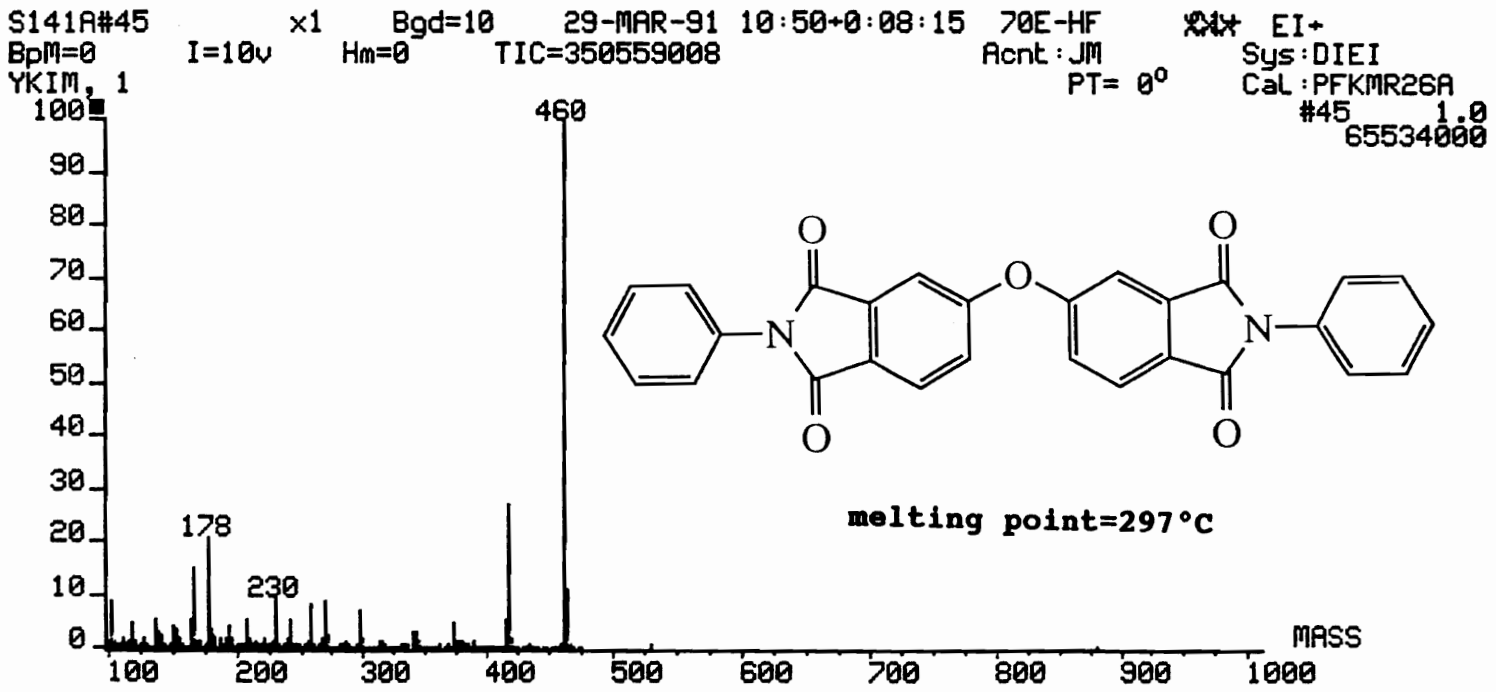

Figure 4.3.15. Mass spectrum of the model imide synthesized from the reaction of ODPA and aniline.

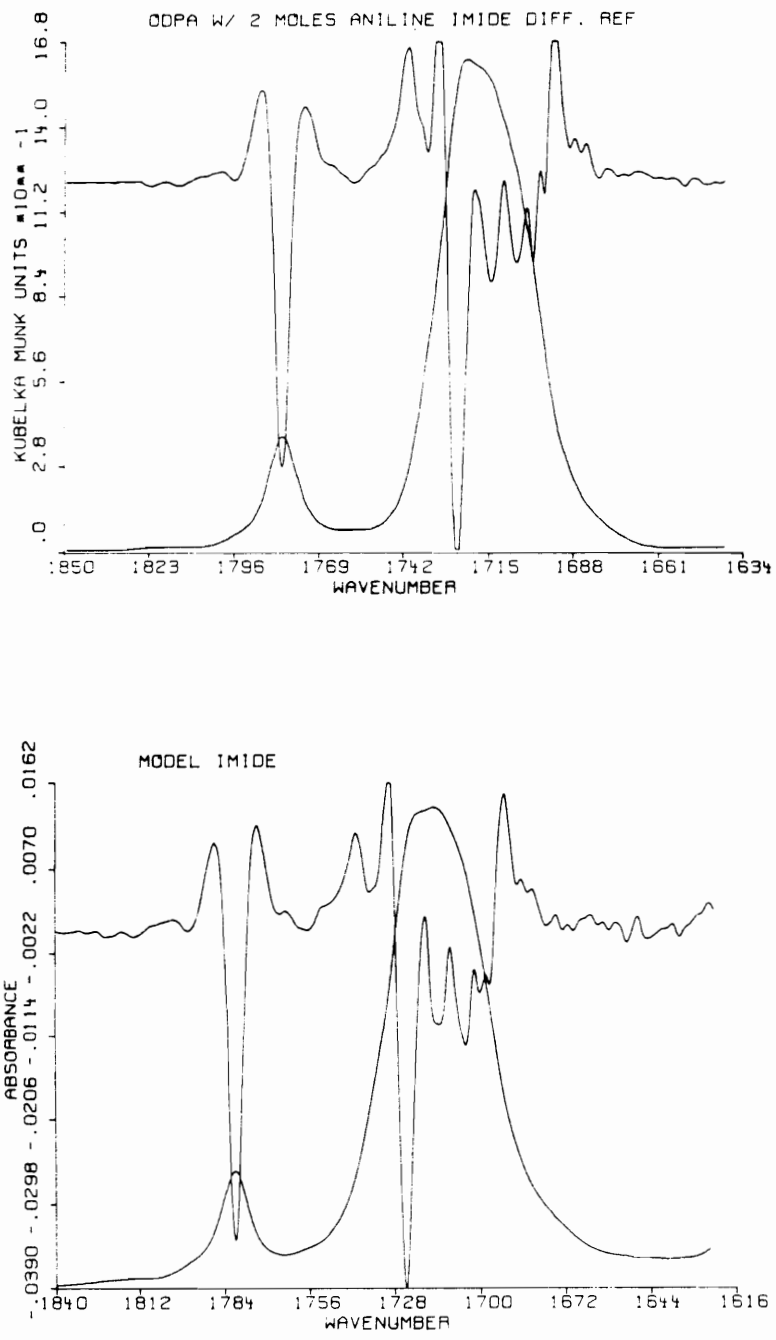

Figure 4.3.16. Carbonyl region of the infrared spectra of the model imide from the reaction of aniline and ODPA. The bottom spectrum was obtained in transmission and the top spectrum was obtained in diffuse reflectance.

In the Figure 4.3.12 transmittance FTIR spectrum of the same polyimide is shown. The polyimide powder was dissolved in NMP and the dilute polyimide solution was evenly spread on the NaCl salt plate. The sample was dried at room temperature for 12 hours under vacuum. The FTIR spectra (Figure 4.3.12) showed NMP carbonyl stretch centered at 1680 cm^{-1}. FTIR spectra of the same polyimide dried under different conditions are shown Figure 4.3.13 and 4.3.14 (See figure captions for drying conditions). As indicated from the NMP carbonyl stretch, the amount of NMP in these samples are different. The changes in the second derivatives of asymmetric carbonyl modes centered at 1720 cm^{-1} were noted in Figures 4.3.12~14. Especially, the sample dried at room temperature for 12 hours showed one peak in the second derivative trace. This is not surprising since the polar solvent NMP could interact with carbonyl groups of imide rings (H-bonding). The previously referenced work (132) demonstrated that the intensity of the doublet of the asymmetric carbonyl mode (1717 and 1736 cm^{-1}) were significantly reflected by the nature of the solvents where the model imides were dissolved. Thus, the intensity of the 1736 cm^{-1} peak of N-phenyphthalimide almost disappeared in m-cresol which is capable of forming hydrogen bonds with imide carbonyl groups. The effects of polar solvents on the carbonyl doublets in other compounds such as ethylene

carbonate were also reported (129). For example, the carbonyl doublet of ethylene carbonate due to Fermi resonance appear at 1867 and 1758 cm^{-1} in vapor state. In methylene iodide, those two peaks appear at 1805 and 1774 cm^{-1} (129). We do not believe that any structural change occurred during the drying conditions. Thus, the observed spectral changes are due to differece in the amount of residual NMP. Thus, the observed complex behavior of the asymmetric carbonyl mode of the polyimide centered at 1720 cm^{-1} is due to, at least in part, Fermi resonance. And also FTIR spectrum of the polyimide powder sample differs from those of solvent cast films. These spectral changes suggest that the physical states of the polyimides, bulk or dispersed state in KBr, also strongly influence the splitting of the anti-symmetric carbonyl band.

The model imide was prepared from the reaction of ODPA (1 mol.) and aniline (2.03 mol.) as described in Section 3.6. The colorless, crystalline model compound was obtained and it showed a sharp melting point of 297°C. The mass spectra shown in the Figure 4.3.15 clearly shows the molecular ion (molecular weight of model imide=460.45). This pure model compound was further characterized by FTIR spectroscopy. The powder of the model imide was mixed with KBr and spectra obtained in diffuse reflectance (top spectrum) and in transmittance (bottom spectrum) are shown

in the Figure 4.3.16. No spectral difference between the diffuse reflectance and transmittance spectra was observed, however, some difference of the spectral features between the polyimide (Figure 4.3.11~4) and model imide (Figure 4.3.16) was observed. This spectral difference might be, in part, due to crystallinity difference between amorphous polyimide and crystalline model compound. From these FTIR studies of polyimide and the model imide we found that anti-symmetric imide carbonyl bands of the cyclized imide bands (no cross-links) around 1720 cm^{-1} were observed to be composed of multiple peaks probably due to Fermi resonance and splitting patterns were also functions of the amount of NMP, physical state of polyimide (bulk or dispersed) and crystallinity (model compound). The amount of NMP, changes in physical state and crystallinity may have influence on the degree of hydrogen bond, intermolecular dipole-dipole interactions and crystal field splitting, which in turn may influence the splitting pattern of the anti-symmetric carbonyl mode. These experimental results suggested that the splitting pattern of anti-symmetric carbonyl mode was so complicated that FTIR investigations of the anti-symmetric imide carbonyl stretch are not a reliable methodology for the identification of any actually formed species during imidization processes. If FTIR investigations of imide carbonyl modes is to be used for the purpose of identifying

side products, a detailed study of the effects of the residual solvent and physical states on the FTIR spectra should first be conducted.

As shown in Figure 4.3.7 (g), ^{1}H-NMR spectra of the 4,4'-ODA/ODPA polyimide was very well-defined thus, no evidence for the intermolecular the imidization reaction can be found. The fact that the proposed intermolecular imide link formation does not occur under our solution imidization conditions can be further supported since many soluble polyimides with controlled molecular weights have been prepared by the solution imidization techniques.

4.3.4. Ketimine formation during solution imidization processes

Imine formation reaction between a carbonyl group and a primary amine is one of the classical reactions of organic chemistry and the imine formation reaction has been utilized for the synthesis of semicrystalline polyarylene ethers (218) and polyarylene sulfides (219) via amorphous ketimine precursors. For benzophenone tetracarboxylic dianhydride (BTDA) containing polyimide systems, there is a strong possibility of ketimine formation reaction, however, which has not yet been studied in necessary detail in polyimide chemistry. In this section studies of ketimine formation during solution imidization of BTDA/BIS-A polyamic acids will be presented.

Under certain imidization conditions, gelation due to ketimine formation was observed during imidization of BTDA containing polyamic acids. However, the formed gels were easily hydrolyzed at room temperature by addition of catalytic amount of aqueous hydrochloric acid, which is one of the characteristic features of ketimine compounds. Direct evidence of the ketimine formation reaction was obtained from ^{1}H-NMR spectroscopy. Figure 4.3.17 and 4.3.18 show the ^{1}H-NMR spectra from the imidization of amine terminated 3.5K BIS-A/BTDA polyamic acid as a function of reaction time. The imidization of the amine terminated polyamic acid (10% solids) was carried out at 130°C in NMP(9)/toluene(1)

solution. Using the Dean-Stark trap containing dry toluene, the azeotroping agent, toluene, was continuously refluxed during the imidization reaction. The two peaks at 6.53 ppm and 6.89 ppm in the bottom spectrum (Figure 4.18-A) are due to the aminophenyl end groups, providing existence of amine terminated end groups. After 8 hour reaction, spectrum B was obtained. At this stage, no solution viscosity change was noted. For next 40 minutes the azeotroping agent toluene was stripped off from the reaction flask and within 40 minutes the polymer solution formed gel. For the ^{1}H-NMR characterization, the polyimide gel was diluted with a large excess amount of dry NMP to swell the gel and DMSO-d_6 was added, then the final concentrations were less than 1 %. The formed gel was found to be easily hydrolyzed within a few minutes by addition of aqueous hydrochloric acid and it was also found to be hydrolyzed at room temperature without added acids. After addition of small amount of water, hydrolysis was allowed to proceed for three days. After three days, a significant solution viscosity drop was noted and the peaks at 6.8 ppm and 7.5 ppm almost disappeared. After hydrolysis spectrum-D was obtained. Thus, the peaks at 6.8 ppm and 7.5 ppm are assigned to ketimine containing aromatic protons as shown in Figure 4.18.

Table 4.2 shows the results of gelation study of amine terminated BTDA/BIS-A polyimide systems. As shown in Table

4.2, it was found that extremely dry reaction conditions and low reaction temperatures favored imine formation reactions. The fact that gelation was observed only for the high molecular weight 80K system when imidized at 180°C suggests that ketimine formation reaction during imidization processes is a non-quantitative reaction. Thus, even a small extent of ketimine reaction caused gelation for large macromolecules (80K). The requirement of the extremely dry reaction conditions for the imine formation reaction was a quite natural result since the imine functional group is hydrolytically unstable and the removal of water drives the reaction to the direction of the imine formation. The temperature dependence of the imine formation reaction is not clearly understood at this point, but one plausible explanation is acid catalysis of the imine formation reaction. It is known that ketimine formation is favored at an intermediate pH (3~5) because acid has effects on both nucleophilicity of amine functional groups and electrophilicity of carbonyl groups (220,221). From our earlier studies of imidization kinetics it is obvious that the rate of imidization at 180°C is significantly different from that conducted at 130°C. Thus, at 180°C the imidization was so fast that acidity of the medium was not appropriate for ketimine formation; however, at low temperature (130°C)

perhaps the optimum pH of the system was achieved due to the relatively slow imidization rate.

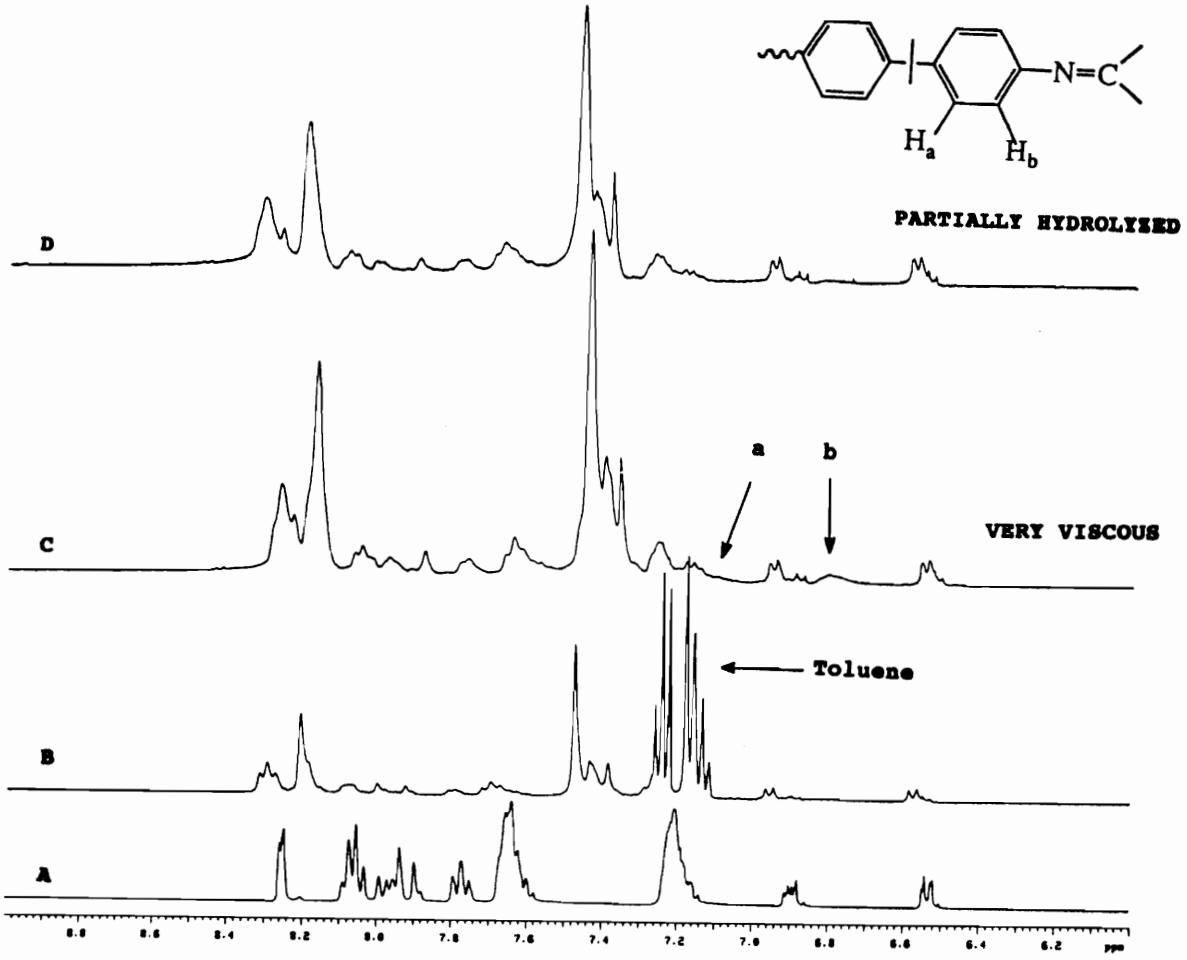

Figure 4.3.17. ^{1}H-NMR spectra from the imidization of amine terminated 3.5K BIS-A/BTDA polyamic acid at 130°C; (A) polyamic acid; (B) 8 hour imidization; (C) 8.67 hour imidization; (D) Polymer sample whose 1H-NMR spectra is shown in (C) was hydrolyzed for 3 days without acid catalysis.

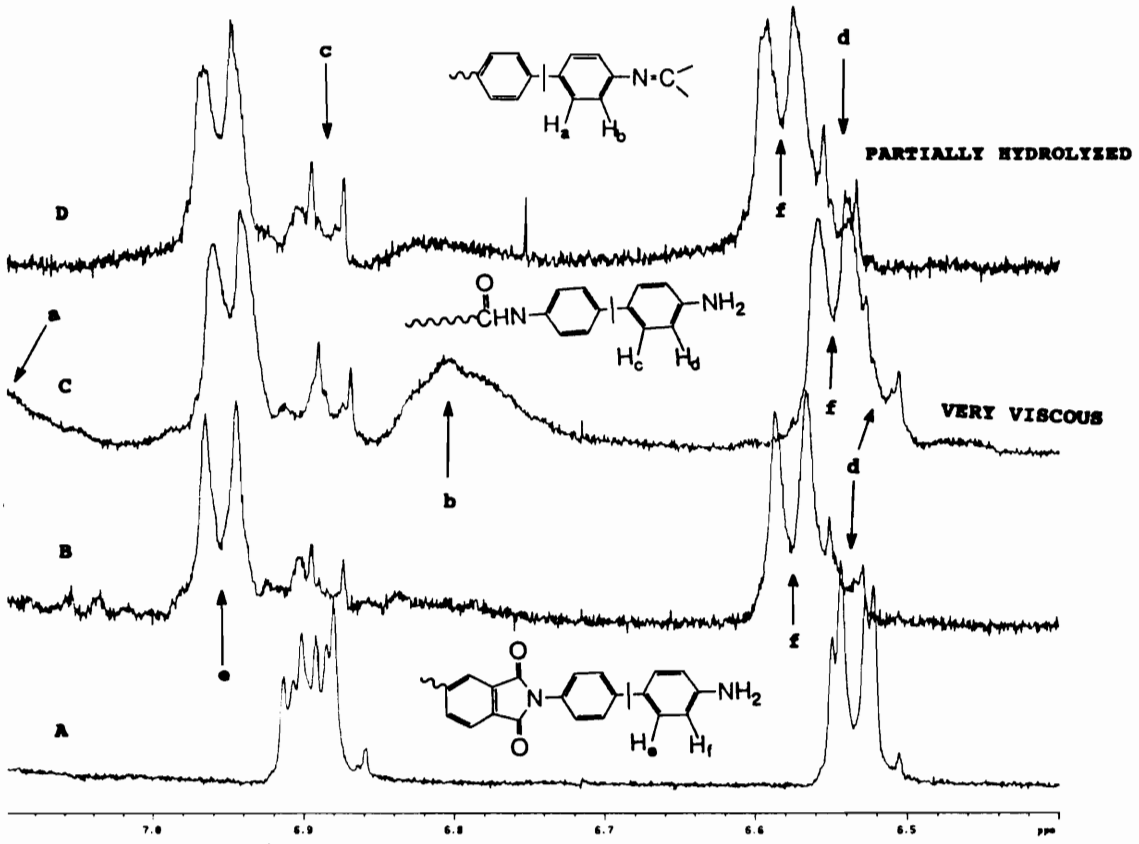

Figure 4.3.18. Expended ^{1}H-NMR spectra of the ^{1}H-NMR spectra shown in Figure 4.3.17 in the range of 6.4 to 7.1 ppm.

Table 4.2. Gelation behavior of amine terminated BTDA/BIS-A polyimides.

End groups	<Mn>**	Rxn. Temp., °C	Solvents***	Gelation$
Amines	80K	180	NMP(9)/ODCB(1)	Yes
Amines	10K	180	NMP(9)/CHP(1)	No
Amines	5K	180	NMP(9)/ODCB(1)	No
Amines	5K	130	NMP(9)/Tol(1)	Yes
Amines*	3.5K	130	NMP(8.5)/Tol(1.5)	Yes
Anhydrides	5K	180	NMP(9)/ODCB(1)	No

* After 8 hour imidization, toluene was stripped off from the reaction flask

** theoretical number average molecular weight via Carothers equation.

*** NMP=N-methyl pyrrolidone
ODCB=o-dichlorobenzene
CHP=N-cyclohexyl pyrrolidone
Tol=toluene.

$ Yes; gelation occurred within 24 hour reaction
No; gelation did not occur within 24 hour reaction

4.4. Synthesis of soluble, high glass transition temperature polyimides with controlled molecular weights and end groups

The polyimide homo- and copolymers were synthesized by the well-established two-step, one-pot solution imidization procedure involving the generation of soluble polyamic acid prepolymers and the subsequent dehydroimidization of the polyamic acid prepolymers. Thus, polyamic acids were first synthesized by reacting aromatic diamines with aromatic dianhydrides in the dipolar aprotic solvent NMP. And then the polyamic acids were subsequently heated to form the corresponding polyimides with evolution of water. In the second step azeotroping agents were used to remove water effectively. In this study some efforts were made to synthesize soluble homo- and copolyimides with controlled molecular weight and end groups.

4.4.1. Characterization of homopolyimides

A series of controlled molecular weight homopolymers was synthesized using various diamine, dianhydrides and phthalic anhydride. The molecular weights of soluble polyimides were determined by measuring intrinsic viscosities. The intrinsic viscosity, glass transition temperatures of homopolyimides are shown in the Table 4.3. As shown in the Table 4.3 BTDA/4,4'-DDS and BTDA/4,4'-ODA systems precipitated during imidization procedures. In

direct contrast, BTDA produced a soluble polyimide with 3,3'-DDS. The flexible dianhydride ODPA also formed soluble polyimides with various aromatic diamines. Thus, ODPA/4,4'-ODA and ODPA/4,4'-DDS polyimides led to soluble materials. ODPA/4,4'-ODA polyimide was completely soluble in both NMP and DMAc, but ODPA/4,4'-DDS polyimide formed slightly turbid solution in DMAC. Polymerization of 6FDA with many aromatic diamines produced soluble materials. Even with p-PDA (p-phenylene diamine) 6FDA produced a easily soluble polyimide. When s-BPDA (symmetric biphenylene dianhydride) which does not contain a flexible linkage was polymerized with 3,3'-DDS or m-PDA, the polyimides precipitated during the imidization procedures as shown in the bottom rows of the Table 4.3. From these observations the solubility trend was deduced as follows:

6FDA>ODPA>BTDA>s-BPDA and

3,3'-DDS>4,4'-ODA>4,4'-DDS

The glass transition temperature is the region where the polymer undergoes transition from a glassy state to a rubbery state. In this region there is a sharp change in physical properties such as the modulus, heat capacity and a thermal expansion coefficient. The ability of the polymer system to sustain a load also changes abruptly in the glass transition region. Therefore, the glass transition

temperature is one of the most important polymer parameters because it defines the upper service temperature limit for a structural application. The monomer structural variations in the polyimides had pronounced effects on the glass transition temperatures. As listed in the Table 4.3 more flexible meta linkage imparts a lower glass transition temperature. The effects of diamines and dianhydrides on the glass transition temperatures were significant. The glass transition temperatures increased in the following order:

4,4'-DDS>BIS-A>4,4'-ODA>3,3'-DDS and

6FDA>BTDA>ODPA

Table 4.3. Intrinsic viscosities and glass transition temperatures of BTDA, ODPA, 6FDA and s-BPDA based homopolyimides

Polyimide system	Theor. <Mn>	[η] 25°C, NMP	Tg (°C) by DSC
BTDA/3,3'-DDS	40K	0.36	267
BTDA/3,3'-DDS	12.5K	0.29	----
BTDA/4,4'-DDS	12.5K	precipitated during polymerization	
BTDA/4,4'-ODA	12.5K	precipitated during polymerization	
ODPA/BIS-A	40K	0.56	290
ODPA/3,3'-DDS	40K	0.43	248
ODPA/4,4'-DDS	15K	0.26	----
ODPA/4,4'-DDS	40K	0.39	305
ODPA/4,4'-ODA	20K	0.55	271
6FDA/BIS-A	40K	0.67	312
6FDA/4,4'-DDS	15K	0.30	----
6FDA/4,4'-DDS	40K	0.35	343
6FDA/4,4'-ODA	30K	0.55	309
6FDA/p-PDA	15K	0.45	----
6FDA/p-PDA	40K	0.56	342
s-BPDA/3,3'-DDS	40K	precipitated during polymerization	
s-BPDA/m-PDA	20K	precipitated during polymerization	

4.4.2. Characterization of copolyimides

BTDA/4,4'-DDS polyimide system precipitated during the polymerization procedure. However, the incorporation of ODPA in the copolymerization with BTDA and 4,4'-DDS generated soluble materials. The intrinsic viscosities and glass transition temperatures of the 6FDA, BTDA and ODPA based polyimides are shown in the Table 4.4. For the BTDA/ ODPA/4,4'-DDS polyimide system the glass transition temperatures increased with increasing the amount of BTDA component. This Tg trend was consistent with that obtained from homopolymerization.

Although the s-BPDA/3,3'-DDS system precipitated during the polymerization procedure (Table 4.3), the incorporation of 6FDA in the copolyimides eliminated the precipitation problem and thus made it possible to produce soluble copolyimides from the reaction of s-BPDA, 6FDA and 4,4'-DDS. Incorporation of 6FDA in polyimides has been used to lower dielectric constants and moisture absorption, but it has also led to polyimides which have high thermal expansion and which are solvent sensitive. s-BPDA was expected to impart some important properties to the polyimides such as solvent resistance, low thermal expansion coefficients and good thermo-oxidative stabilities. Due to these reasons the amount of s-BPDA was maximized versus 6FDA in the copolymerization with 4,4'-DDS or p-PDA. The copolyimide

based upon 80% s-BPDA/20% 6FDA/4,4'-DDS was soluble in NMP. The glass transition temperatures which were measured by the TMA penetration mode and intrinsic viscosities of 6FDA and s-BPDA based copolymers are displayed in the Table 4.5. One of the representative TMA measurements is also provided in the Figure 4.4.1. Glass transition temperatures of the s-BPDA/6FDA/4,4'-DDS copolyimides in this study ranged from 343 to 359°C with increasing the amount of s-BPDA component as shown in the Table 4.5. Symmetric biphenylene dianhydride (s-BPDA) was very effective in increasing Tg's of the 6FDA/s-BPDA/p-PDA copolyimide system. Copolymerization of p-PDA with 85/15 mole % ratio of 6FDA/s-BPDA produced a soluble, film forming material whose Tg was 20° higher than that of 6FDA/p-PDA homopolyimide. However, the copolymerization of 20% s-BPDA and 80 mole % 6FDA with p-PDA precipitated during the solution imidization.

Besides the high glass transition temperature requirement, the thermo-oxidative stability of polyimides is another important consideration for a structural application. In this study thermo-oxidative stability was measured by thermogravimetric analysis at a constant heating rate of 10°C per minute in a flowing air. Figures 4.4.2 and 4.4.3 show TGA thermograms of the s-BPDA/6FDA/4,4'-DDS and s-BPDA/6FDA/p-PDA copolyimides, respectively, to show the effect of s-BPDA incorporation on the thermo-oxidative

stabilities. The thermo-oxidative stabilty was a function of chemical composition: it increases with increasing s-BPDA content. The temperatures at which 5 and 10% wt. losses are observed are summarized in Table 4.6.

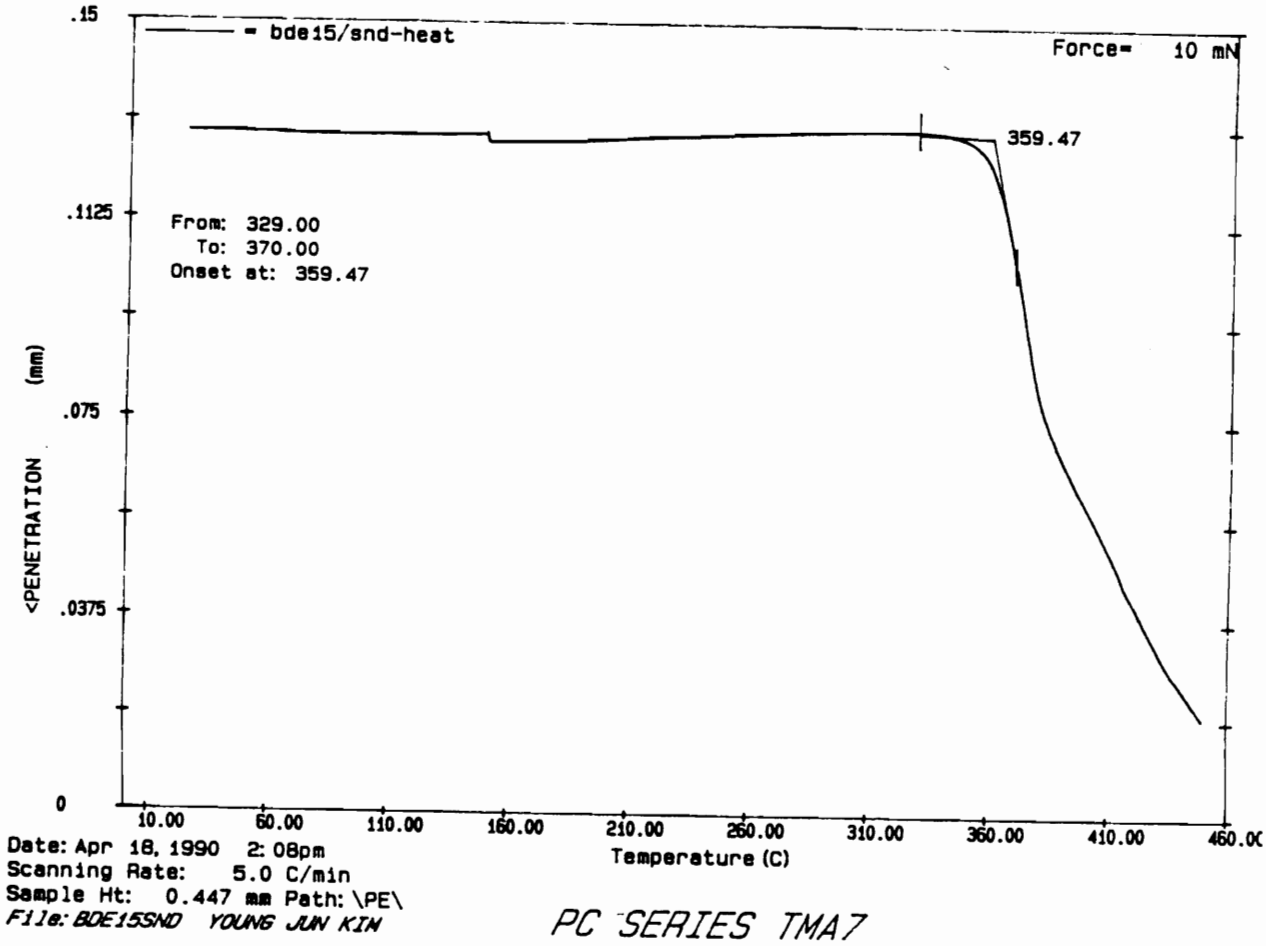

Figure 4.4.1. TMA thermogram of the polyimide from the copolymerization of 22/78 mole % 6FDA/s-BPDA with 4,4'-DDS for determination of the glass transition temperature.

Table 4.4. Intrinsic viscosities and glass transition temperatures of 6FDA, BTDA and ODPA based copolyimides

Polyimide system*			Theor.	[η]	Tg (°C)
ODPA	BTDA	Diamine	<Mn>	25°C, NMP	by DSC
75	25	4,4'-DDS	75K	0.71	311
25	75	4,4'-DDS	75K	0.87	322
75	25	4,4'-DDS	25K	0.44	307
ODPA	6FDA				
60	40	m-PDA	40K	0.40	293

*) By mole %

Table 4.5. Intrinsic viscosities and glass transition temperatures of 6FDA and s-BPDA based copolyimides

Polyimide system*			Theor.	[η]	Tg (°C)
6FDA	s-BPDA	Diamine	<Mn>	25°C, NMP	by TMA
100	0	4,4'-DDS	40K	0.35	343
72	28	4,4'-DDS	40K	0.30	348
22	78	4,4'-DDS	40K	0.36	359
90	10	4,4'-DDS	40K	0.30	365
20	80	3,3'-DDS	40K	0.52	290**
100	0	p-PDA	40K	0.56	342
85	15	p-PDA	40K	0.59	360
80	20	p-PDA	40K	precipitated during polymerization	

*) By mole %

**) Tg by DSC

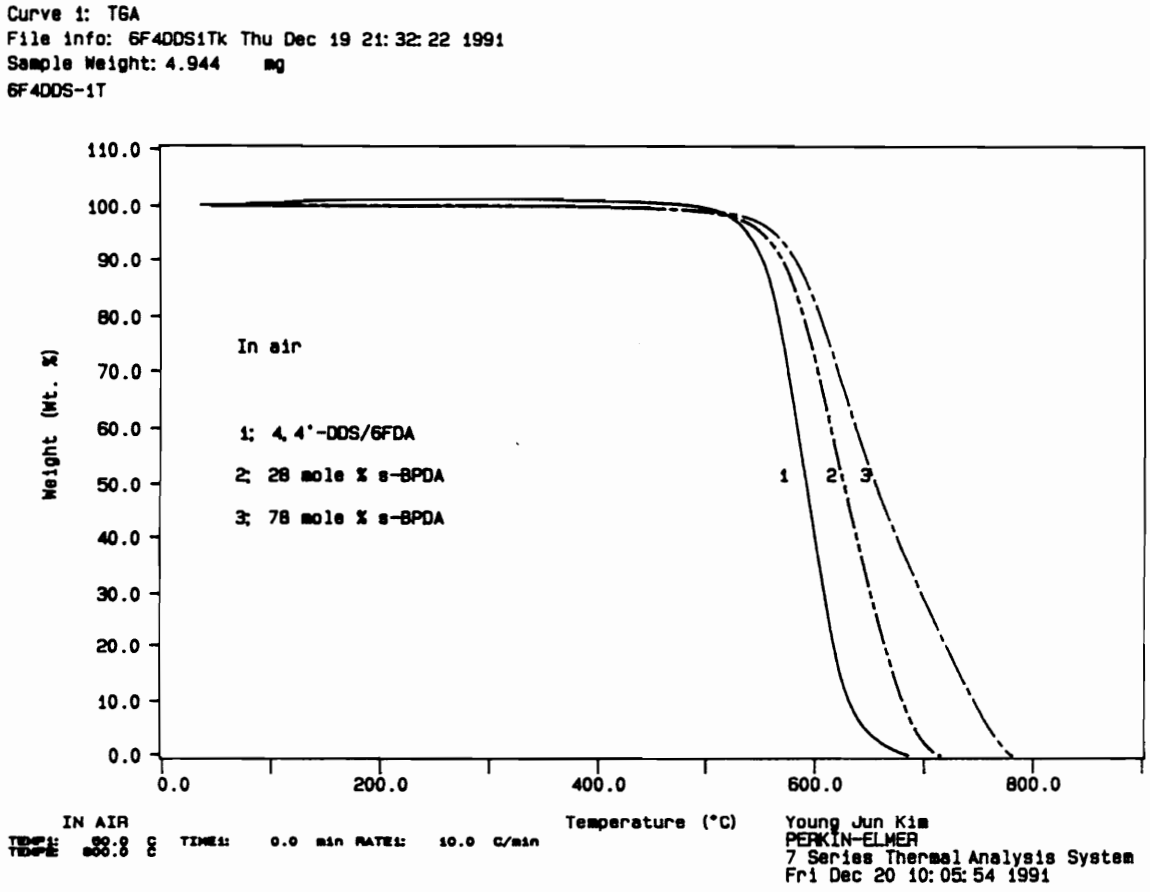

Figure 4.4.2. Thermogravimetric analysis of 4,4'-DDS/s-BPDA/6FDA based homo- and copolyimides (In air; 10°C/min.): (1) 4,4'-DDS/6FDA homopolyimide; (2) 4,4'-DDS/28 mole % s-BPDA/72 mole % 6FDA; (3) 4,4'-DDS/78 mole % s-BPDA/22 mole % 6FDA copolyimide.

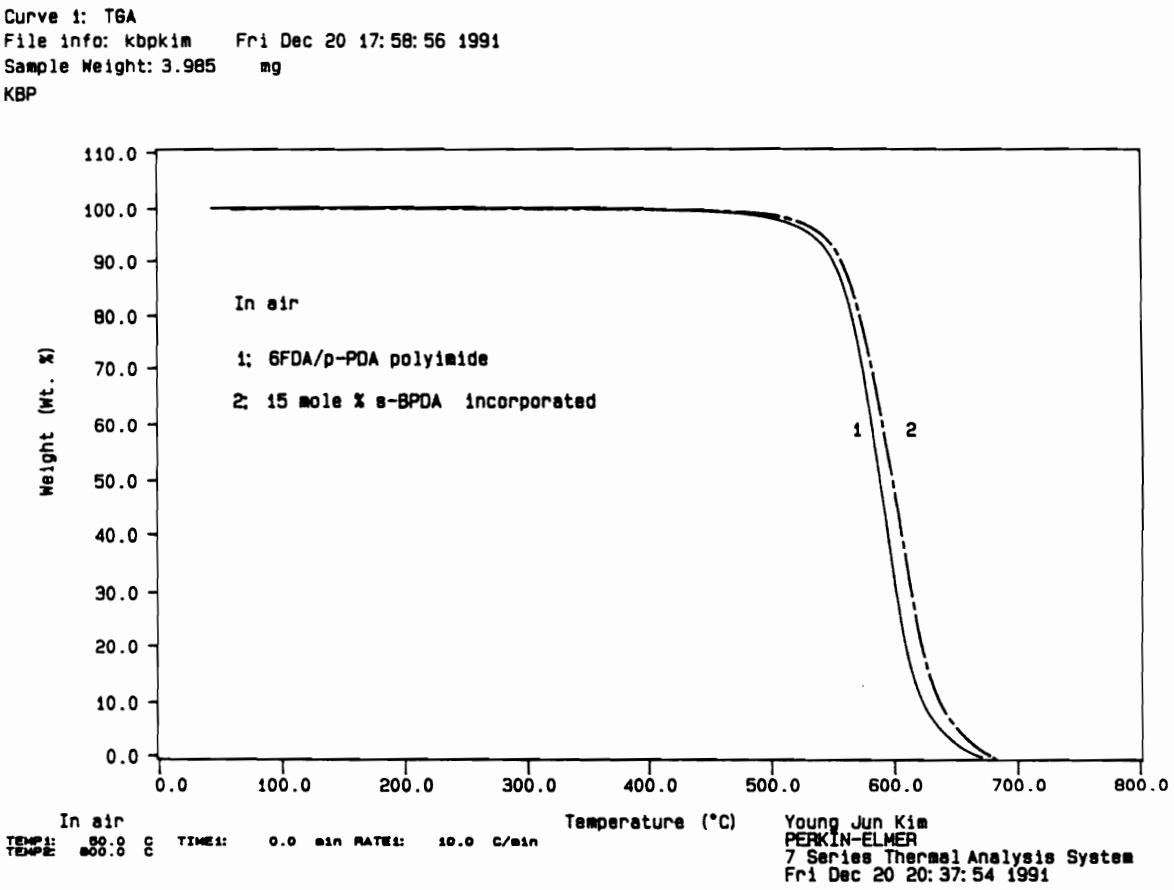

Figure 4.4.3. Thermogravimetric analysis of s-BPDA/6FDA/p-PDA based homo- and copolyimides (In air; 10°C/min.): (1) 6FDA/p-PDA homopolyimide; (2) 15 mole % s-BPDA/85 mole % 6FDA/p-PDA coplyimide.

Table 4.6. TGA decomposition temperatures of s-BPDA and 6FDA based homo- and copolyimides (5 and 10% weight loss in air, °C)

Polyimide system*			5% wt. loss	10% wt. loss
6FDA	s-BPDA	Diamine	°C	°C
100	0	4,4'-DDS	537	552
72	28	4,4'-DDS	551	570
22	78	4,4'-DDS	563	583
100	0	p-PDA	534	551
85	15	p-PDA	543	558

*) By mole %

4.5. Miscibility of blends of polyimides (PI's) with polybezimidazole (PBI)

4.5.1. Introduction

High performance miscible polymer blends based upon polyimides and polybenzimidazole have been reported (186-195). Blend miscibility was confirmed by the presence of single composition dependent Tg's lying between those of the constituent components, well defined tan δ relaxation peaks associated with the glass transitions and the formation of optically clear transparent films. Polymer mixtures usually have so little combinatorial entropy of mixing that very small positive heats of mixing suffice to bring about phase separation. Therefore miscibility in polymer blends is attributed to the existence of specific interactions between the blend compositions. To obtain evidence for the existence of specific interactions and to elucidate the nature of these interactions FTIR spectroscopy has been utilized (189,191).

This section describes polymer blends formed from PBI and phthalic anhydride end-capped polyimides. Various polyimides were used to investigate miscibility as a function of structural variations of the polyimide component. The polyimides and PBI that were used in this study are shown below:

3,3'-DDS/ODPA polyimide: [η]=0.43 dl/g at 25°C in NMP, Tg=248°C by DSC

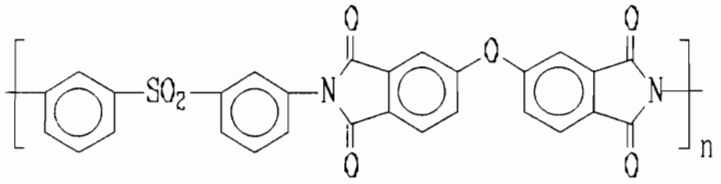

3,3'-DDS/BTDA polyimide: [η]=0.36 dl/g at 25°C in NMP, Tg=267°C by DSC

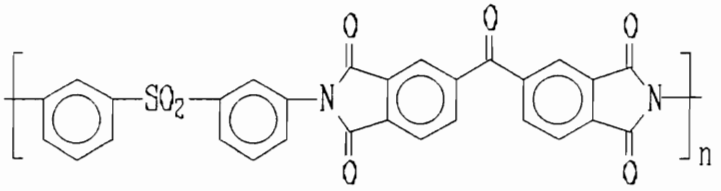

BIS-A/ODPA polyimide: [η]=0.56 dl/g at 25°C in NMP, Tg=293°C by DSC

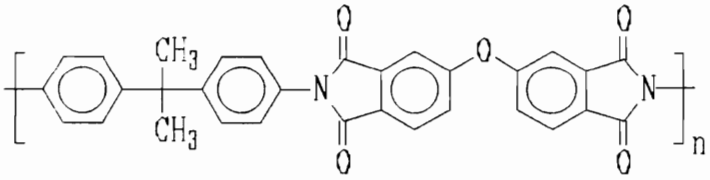

4,4'-DDS/6FDA polyimide: [η]=0.35 dl/g at 25°C in NMP, Tg=344°C by DSC

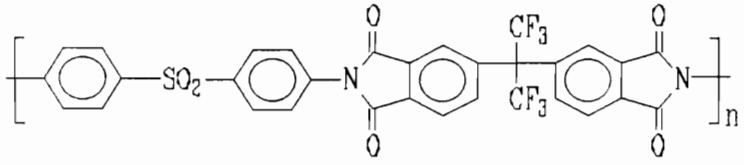

4,4'-ODA/6FDA polyimide: [η]=0.67 dl/g at 25°C in NMP, Tg=298°C by DSC

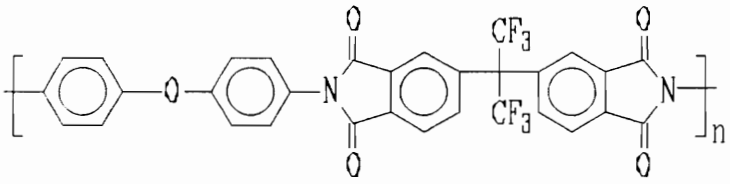

BIS-A/6FDA polyimide: [η]=0.67 dl/g at 25°C in NMP, Tg=312°C by DSC

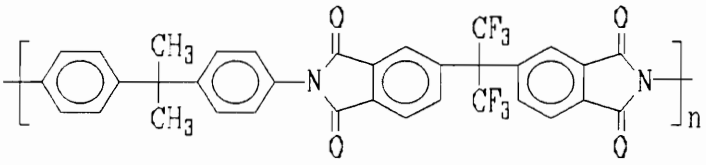

End-capped PBI (Hoechst Celenease): [η]=0.56 dl/g at 25°C in DMAc, Tg=425°C from a literature (187), Tg=405°C from DSC (Third heat, Tg was measured on the cast film from PBI/DMAC solution and a low Tg value was obtained due to residual solvent)

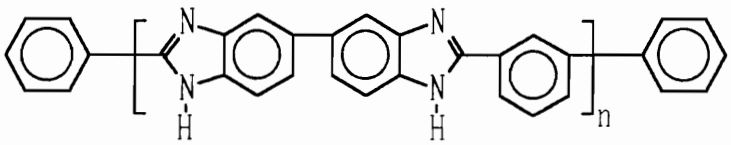

4.5.2. Effects of structural variations of the polyimide components on miscibility

All of the polymer blends for the thermal analyses were prepared by solution mixing of PBI in DMAc and polyimides in DMAc (or NMP) as described in detail in the experimental part. Since high boiling point, polar solvents are good compatibilizers for polymer blends it is important to remove solvents completely. MacKnight et al. (192) prepared PBI/polyimide blends by solution casting of blend solutions on the glass plates. Most of the solvent was removed far below glass transition temperatures of the blends (for example, 180°C) and then the residual solvent was removed by washing them with hot water for several days to avoid possible phase separation during sample preparation procedure. As shown in the Figure 4.5.1, however, it was observed that significant amount of residual solvent remained in the blends which were dried according to the above mentioned procedures. Indeed it is very difficult to remove the high boiling point, polar solvent in the blends below their glass transition temperatures. It was found that drying at the high temperature was more effective in removing the residual solvent than by washing with hot water (See Figure 4.5.1). In this study polymer blends were carefully dried below expected glass transition temperatures of the blends (in fact, below a binodal curve since a LCST

was reported for other PBI/polyimide blends) to avoid possible phase separations. The maximum drying temperature was 310±10°C.

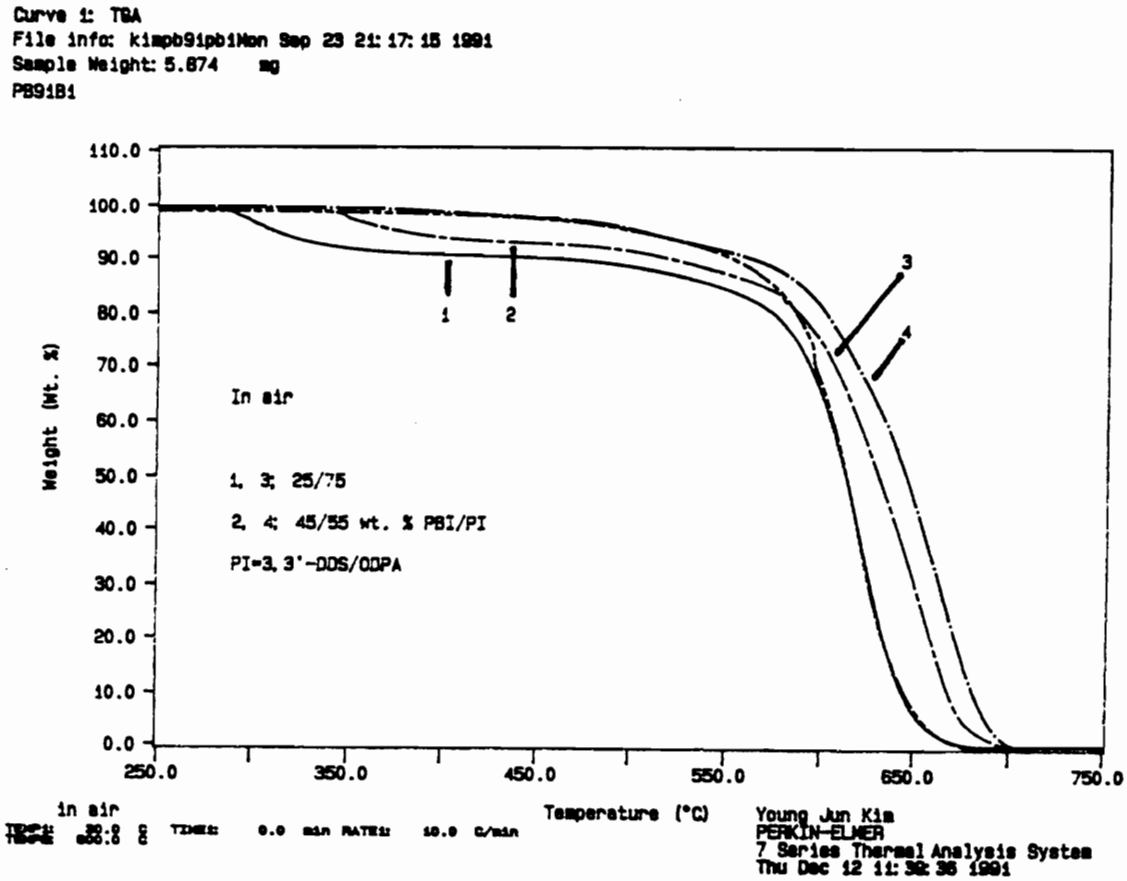

Figure 4.5.1. Thermogravimetric analysis of PBI/(3,3'-DDS/ODPA) blends; 1, 3; 25/75 and 2, 4; 45/55 wt. % PBI/PI blends. For 1 and 2 blends were dried at 88°C for a day, at 190°C for 5 days, washed with hot water (85°C) for 3 days and finally dried at 190°C for 2 days. For 3 and 4 blends were dried at 88°C for a day, at 190°C for 5 days and 310 ± 10°C for 10 hours.

Table 4.7. Glass transition temperatures (°C) of PBI/PI(3,3'-DDS/ODPA) blends

PBI wt %	1st heat	2nd heat	3rd heat	4th heat	Tg*
0		247**	247**	248**	247
25		271	274	283	282
45	282	297	302		314
63	308	325	337	340	346
82	323	335	348	350	384
82	323	357**	353**	359**	384

* Calculated Tg's by the Fox equation

** After the first heat samples were annealed at 400°C for 20 minutes.

Table 4.8. Glass transition temperatures (°C) of PBI/PI(3,3'-DDS/BTDA) blends

PBI wt %	1st heat	2nd heat	3rd heat	4th heat	Tg*
0	265	267	267	267	
20		292	291	293	293
40		326	326	326	321
60		342	352	364	352
60		363**			352
80	334	349	360	365	386
80		376**	380**		386

* Calculated Tg's by the Fox equation.

** After the first heat samples were annealed at 400°C for 20 minutes.

Tables 4.7~8 show glass transition temperatures of PBI/PI(3,3'-DDS/ODPA) and PBI/PI(3,3'-DDS/BTDA) polymer blends. All glass transition temperatures were measured by DSC at a heating rate of 10°C/minute from 50 to 400°C for the first three scans and from 50 to 450°C for the fourth scan. And, as otherwise stated, slow cooling at an ambient temperature was used. 3,3'-DDS/ODPA and 3,3'-DDS/BTDA were determined to be miscible with PBI for all blend compositions and the miscibility was retained, at least, up to 400°C. As shown in the Tables 4.7 and 4.8 all of the blends showed composition dependent single Tg's lying between those of the constituent components. Furthermore, optically clear, transparent films were also obtained from those blends, which was a first indication of miscibility in those blends. Blends that were annealed at 400°C for 20 minutes showed limiting values of glass transition temperatures. For the samples that were not annealed at 400°C, however, glass transition temperatures increased slightly with increasing number of scans due to the gradual removal of the residual solvent. PBI/PI(3,3'-DDS/ODPA), PBI/PI(3,3'-DDS/BTDA) blend compositions showed clearly defined glass transitions in a narrow transition range. Some of the representative DSC thermograms are shown in the Figure 4.5.2.

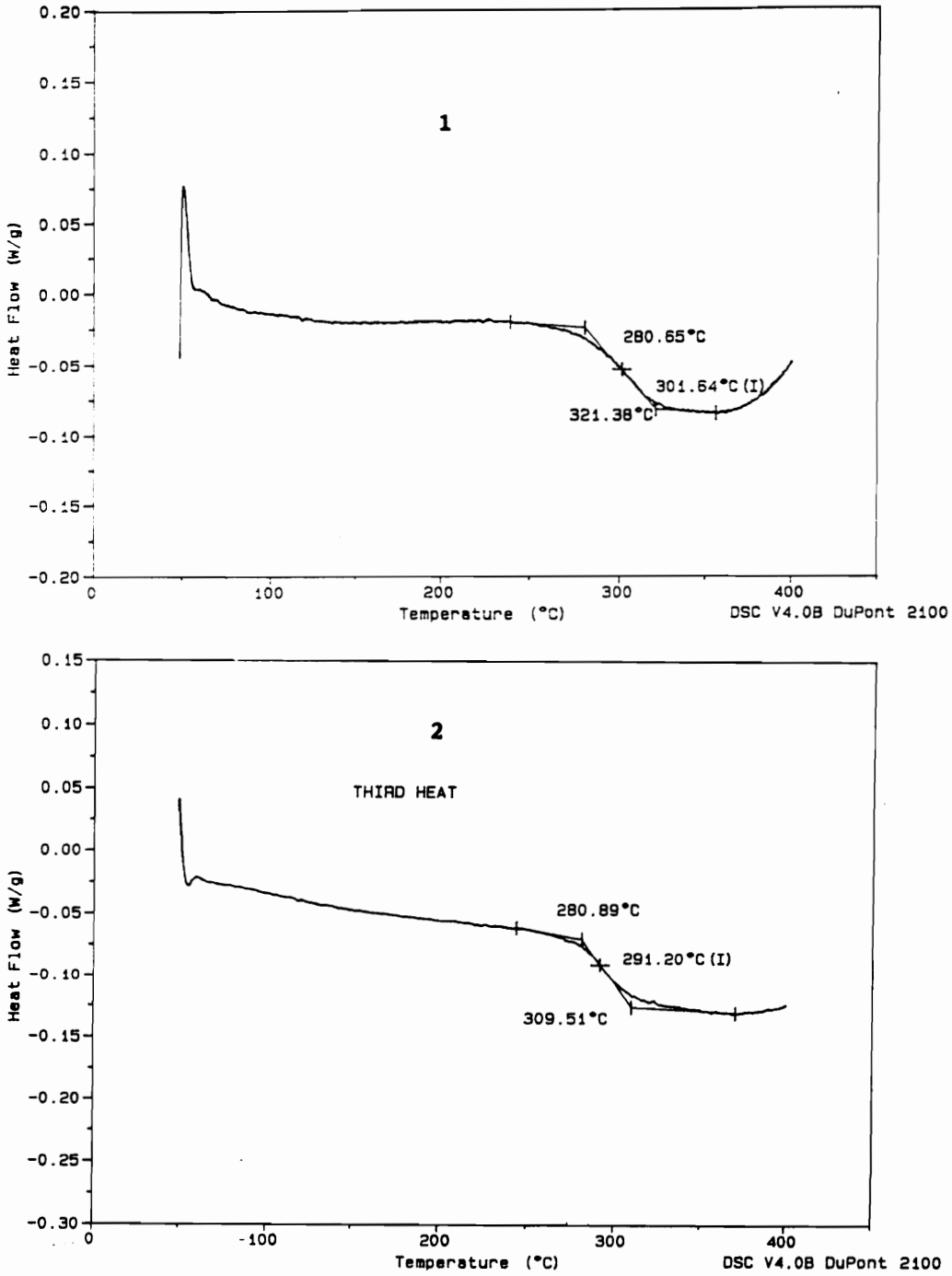

Figure 4.5.2. DSC thermograms of (1) third heat of PBI/(3,3'-DDS/ODPA) 45/55 wt%, (2) third heat of PBI/(3,3'-DDS/BTDA) 20/80 wt%.

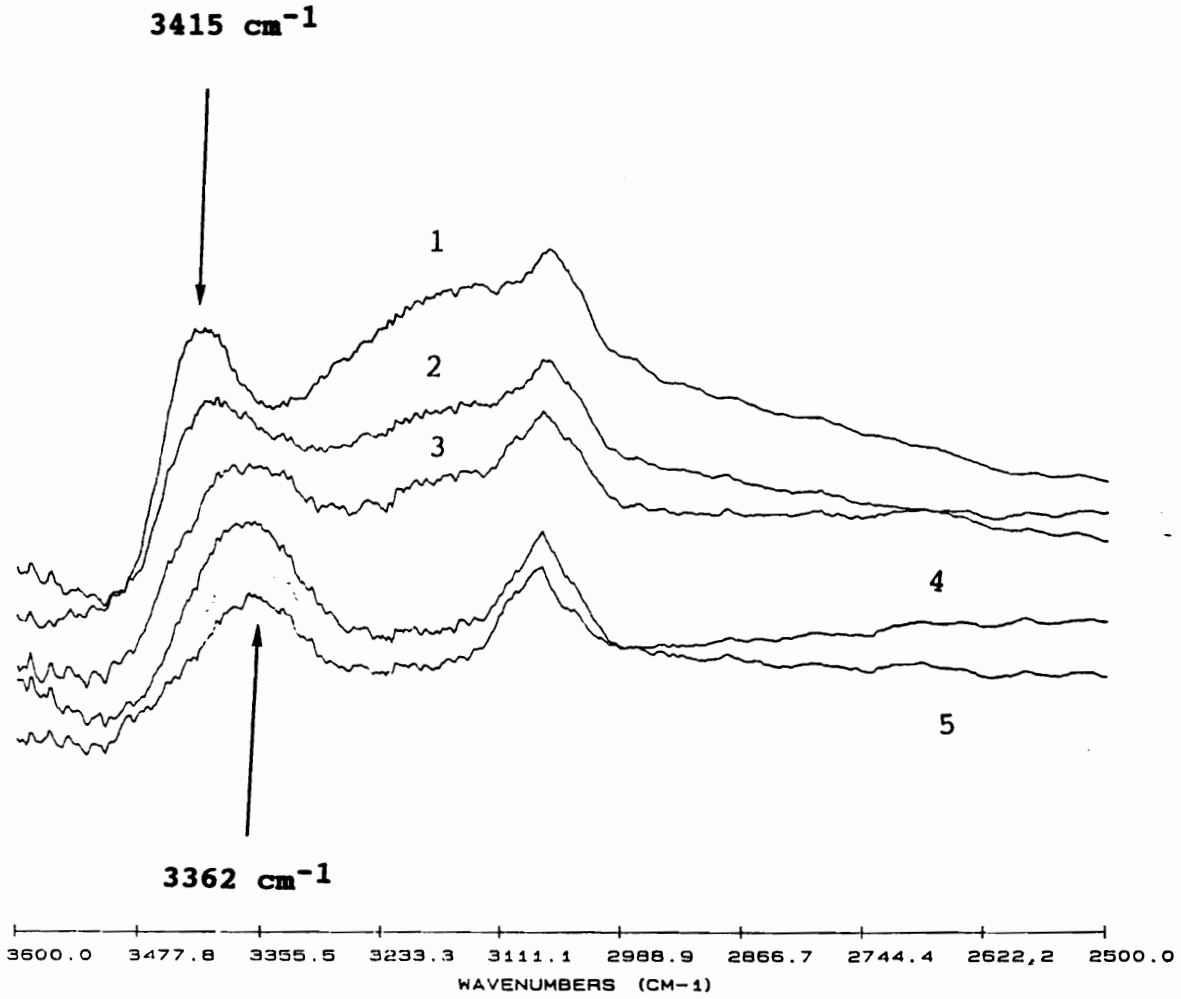

Figure 4.5.3. FTIR spectra of the N-H stretch region for (1) pure PBI, (2) 82/18 wt %, (3) 63/37 wt %, (4) 45/55 wt %, (5) 25/75 wt % PBI/(3,3'-DDS/ODPA) polymer blends.

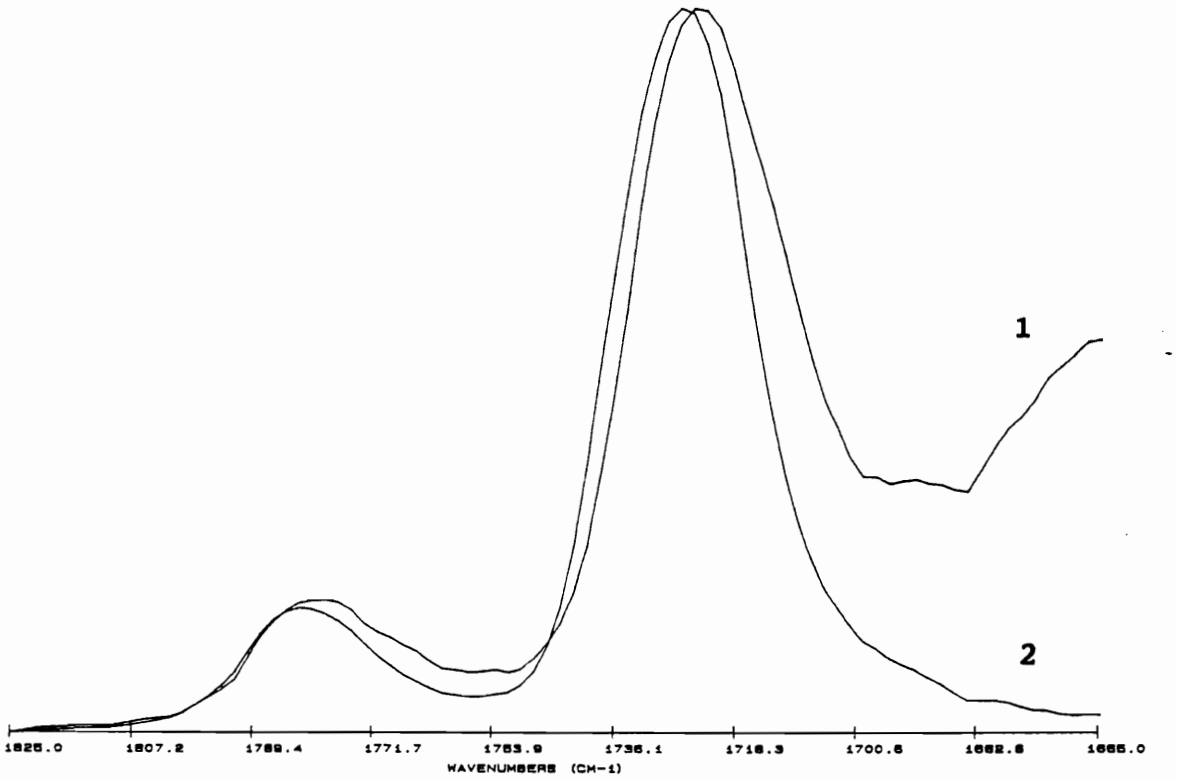

Figure 4.5.4. FTIR spectra of the imide carbonyl stretch region for (1) 82/18 wt % PBI/(3,3'-DDS/ODPA) blends, (2) pure 3,3'-DDS/ODPA polyimide.

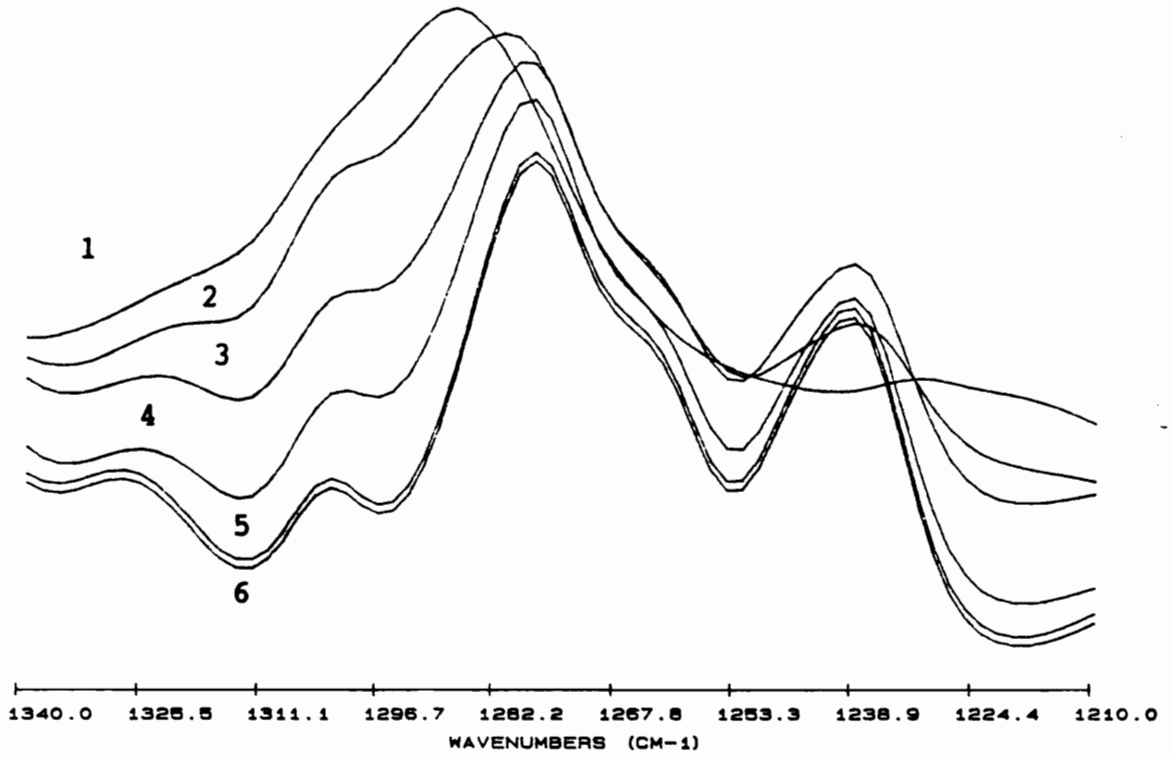

Figure 4.5.5. FTIR spectra of anti-symmetric sulfonyl mode and C-O(ether) stretch region for (1) pure PBI, (2) 82/18 wt %, (3) 63/37 wt %, (4) 45/55 wt %, (5) 25/75 wt % PBI/(3,3'-DDS/ODPA) polymer blends, (6) 3,3'-DDS/ODPA polyimide.

FTIR spectroscopy was further utilized to provide evidence for the specific interactions which cause miscibility in those blend systems. Following vibrational frequencies were used as analytical peaks: Characteristic imide peaks such as imide I (symmetric imide carbonyl mode, ca. 1778 cm^{-1}), imide II (anti-symmetric imide carbonyl mode, ca. 1720 cm^{-1}) and imide III (ca. 1370 cm^{-1}), other vibrational frequencies due to heteroatom functional groups (ether, carbonyl and sulfonyl groups) and characteristic PBI peaks such as N-H stretch (3415 cm^{-1}) and C-N(H) stretch (tentative assignment, ca. 1287 cm^{-1} for pure PBI). Figure 4.5.3 shows FTIR spectra of the imidazole NH stretch region of PBI/(3,3'DDS/ODPA) polyimide blends. The N-H stretch band of pure PBI centered at 3415 cm-1 shifted lower frequencies (3362 cm^{-1} for 25 PBI/75 PI wt. %) and also showed a band broadening with increasing polyimide content in the blends. In the Figure 4.5.4 imide carbonyl modes are shown. Whereas the N-H stretch mode showed big frequency shifts (maximum $\Delta\nu \cong 55$ cm^{-1}) with increasing the polyimide contents in the blends the carbonyl mode did not display a large frequency shift ($\Delta\nu \cong 3$ cm^{-1}). Nevertheless a significant band broadening was noted. Figure 4.5.5 shows anti-symmetric sulfonyl mode and C-O(ether) mode of PBI/(3,3'-DDS/ODPA) polyimide blends. The anti-symmetric sulfonyl mode (1272 cm^{-1} for the pure 3,3'-DDS/ODPA polyimide) and tentatively

assigned C-N(H) mode of polybenzimidazole (1286.7 cm^{-1} for pure PBI) were completely overlapped. The C-O stretch mode did not display large frequency shifts with increasing polyimide contents in the blends, too, however, significant band broadenings of those bands were also observed. These observations, large NH frequency shifts, small frequency shifts and significant band broadening of other functional groups, were quite general for other miscible PBI/polyimide blend systems such as PBI/(3,3'-DDS/BTDA) and PBI/PI(BIS-A/ODPA) blends.

Following Tables 4.9 and 4.10 show vibrational frequencies of PBI/PI(3,3'-DDS/ODPA) and PBI/PI(3,3'-DDS/BTDA) blends. In these Tables the asymmetric SO2 vibrational mode and the C-N(H) stretch are not given because those peaks were completely overlapped.

Table 4.9. Maximum frequencies (cm^{-1}) of the N-H stretch of polybenzimidazole, imide modes, C-O stretch and SO2 vibrational modes of PBI/(3,3'-DDS/ODPA) polyimide blends.

PBI wt %	N-H	Imide II	Imide II	Imide III	C-O	s-SO_2*
0		1783.7	1726.2	1368.7	1239.6	1160.6
25	3362	1782.2	1726.2	1368.1	1239.4	1159.9
45	3365	1782.2	1725.6	1367.6	1239.4	1159.4
63	3376	1781.4	1724.8	1367.2	1238.4	1158.5
82	3396	1780.4	1723.6	1366.8	1238.0	1158.3
100	3415					

* Symmetric SO_2 vibrational mode. This band was broad.

Table 4.10. Maximum frequencies (cm^{-1}) of the N-H stretch of polybenzimidazole, imide modes, C=O stretch and SO2 vibrational modes of PBI/(3,3'-DDS/BTDA) polyimide blends.

PBI wt %	N-H	Imide I	Imide II	Imide III	C=O	s-SO_2*
0		1782.3	1727.2	1371.6	1672.2	1159.2
20	3368	1781.6	1726.2	1370.6	1672.2	1158.4
40	3370	1781.4	1726.0	1369.8	1671.4	1157.4
60	3385	1781.4	1725.6	1368.9	1670.4	1156.6
80	3402	1781.1	1725.3	1368.4	1669.7	1156.4
100	3415					

* Symmetric SO_2 vibrational mode.

Table 4.11. Glass transition temperatures (°C)* of PBI/PI(BIS-A/ODPA) blends

PBI wt %	1st heat	2nd heat	3rd heat	4th heat	Tg**
0	289(283)$	290(283)	291	290	
25	319(321)	broad#	broad#	broad#	320
25@	317	324	324	324	320
50		346	341	346	351
75		355	358	361	386

* After first heat all samples except the 25 % PBI sample marked by @ were annealed at 400°C for 20 minutes.

** Calculated Tg's by the Fox equation.

$ The values in the parentheses were measured by Perkin-Elmer Thermal Analysis system.

Very broad transitions ranging from 270°C to 370°C.

@ The sample was scanned from 50°C to 350°C up to fourth heat at a heating rate of 10°C/minute without annealing at 400°C.

Glass transition temperatures of PBI/PI(BIS-A/ODPA) blends are provided in Table 4.11. Composition dependent Tg's were also detected over all composition range. One of the interesting features of this blend system was that the 25/75 wt. % PBI/PI blend showed very broad transitions ranging from 270 to370 °C once it was annealed at 400°C for 20 minutes (Figure 4.5.6). On the other hand the same blend composition (25/75 wt. %) which was heated up to 350°C showed well-defined glass transitions in a narrow transition range (Figure 4.5.7). The broadening of glass transition range for the annealed sample (25/75 wt. % PBI/PI) might be due to partial phase demixing during the annealing process, which in turn suggested the presence of a LCST (the lower critical solution temperature) whose existence was reported for the other PBI/polyimide blend systems.[2] The effect of heat treatment on the miscibility of
the 25/75 wt. % PBI/PI(BIS-A/ODPA) blend was further investigated. DSC measurements on the miscible blend of PBI and (BIS-A/ODPA) polyimide are shown in the Figure 4.5.8. After heat treatment at 420°C for 3 minutes phase separation occurred (Figure 4.5.8-2). The glass transition of the polyimide rich phase was observed at 282°C which corresponds to Tg of the pure polyimide (283°C). The glass transition temperature of the regenerated polyimide rich phase (282°C) suggested that complete phase separation during the

annealing process. However, glass transition of the minor component PBI rich phase (probably a pure PBI phase) was not detected for several reasons; low concentration of the PBI component, rigid characteristics of PBI macrochains and thermal degradation of polymers at high temperatures. DSC measurements on the same blend which was annealed at 380°C for 3 minutes is shown in the Figure 4.5.9. The glass transition of the miscible blend at 321°C disappeared completely and very weak second order transition (Tg=287°C) was observed. Because the entropic contribution to Gibbs free energy due to temperature increase is so small that thermal stability of miscibility in polymer blends is governed by the temperature dependence of degree of interactions between two polymeric components. It seems that the enthalpic interaction, the hydrogen bonding between imidazole N-H and electron rich heteroatom containing functional groups in the imide component, decreases as a temperature increases.

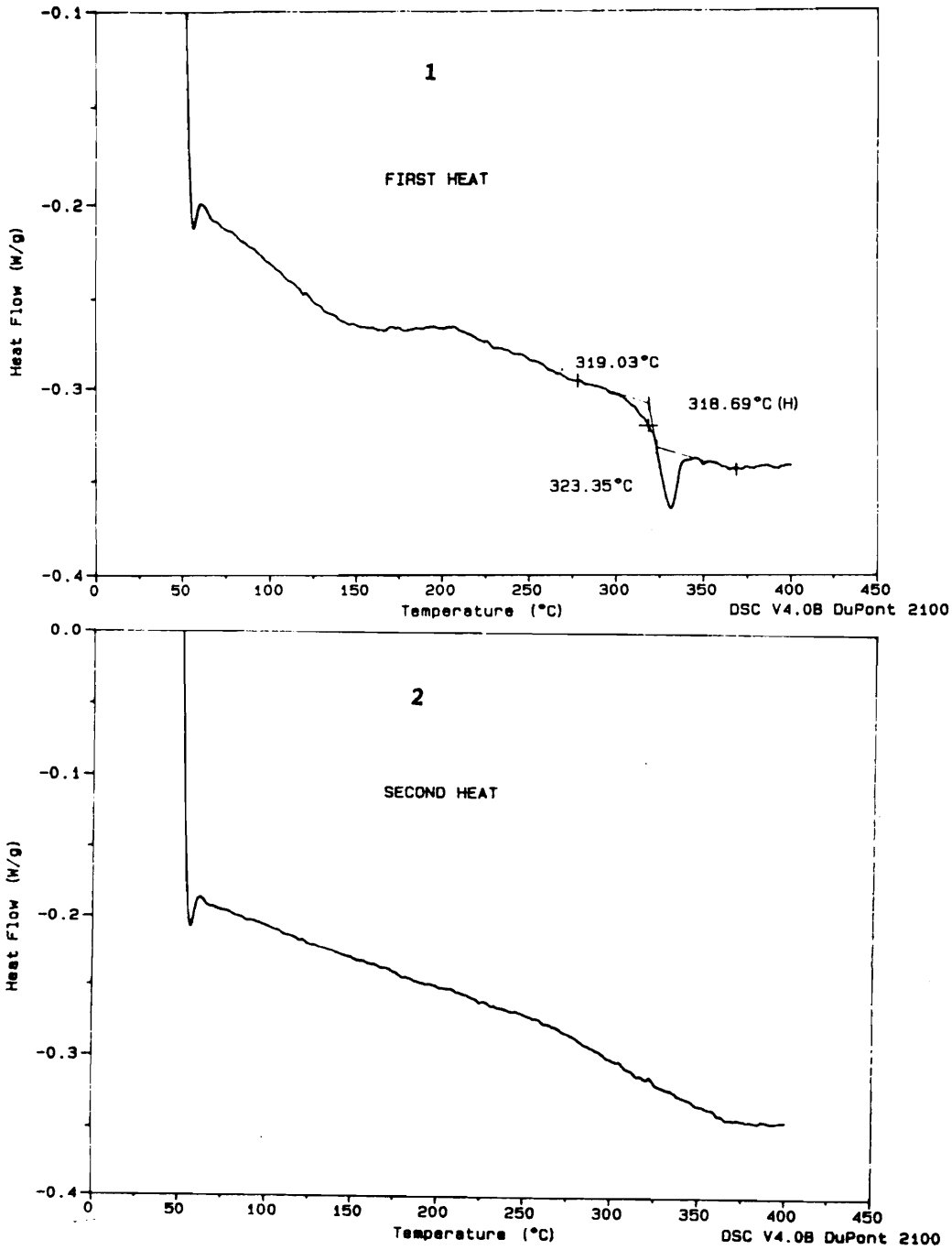

Figure 4.5.6. DSC thermograms of the 25/75 wt.% PBI/PI(BIS-A/ODPA) blend: For (1) the first heat; For (2) after annealing at 400°C for 20 minutes.

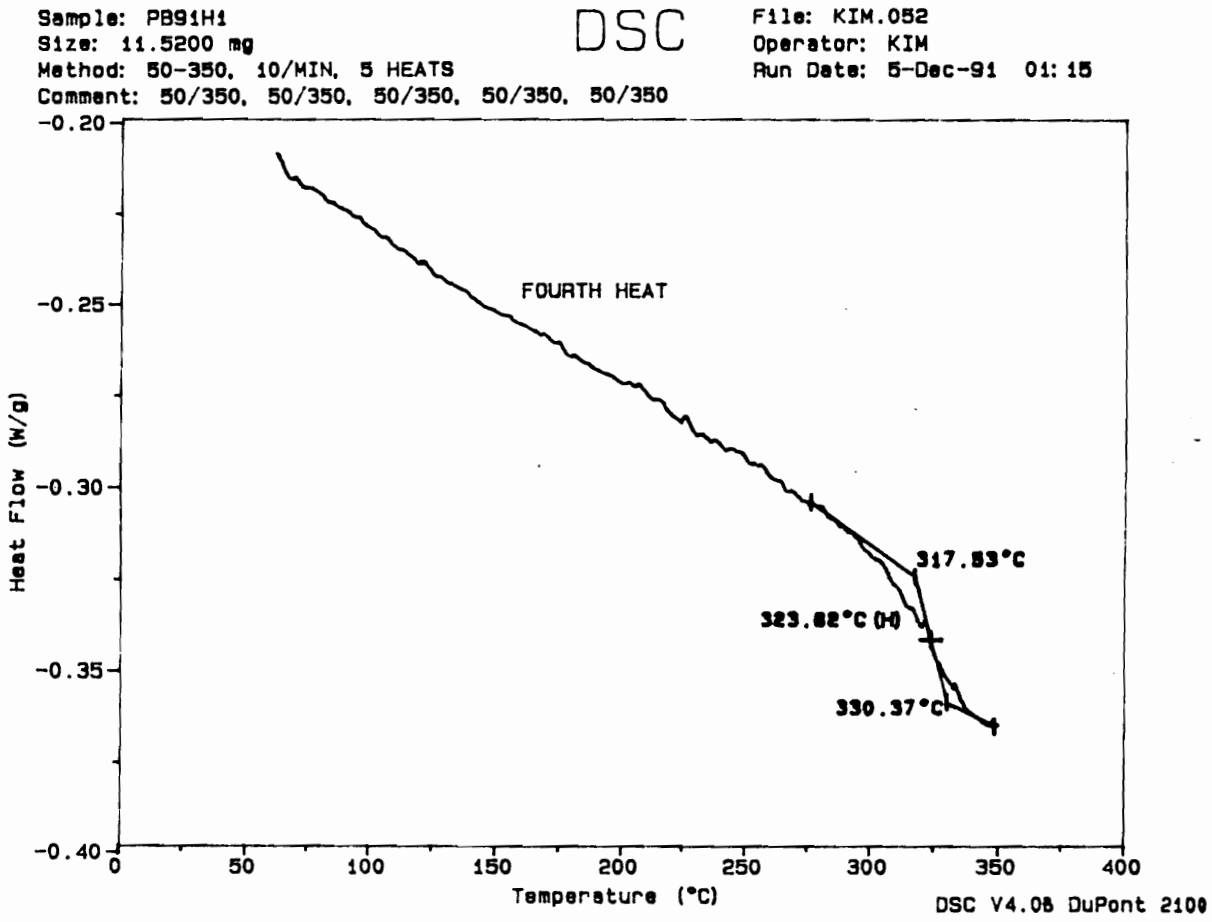

Figure 4.5.7. The fourth DSC scan of the miscible 25/75 wt. % PBI/(BIS-A/ODPA) polyimide blend: The sample was heated at 10°C/minute in a DSC from 50 to 350°C.

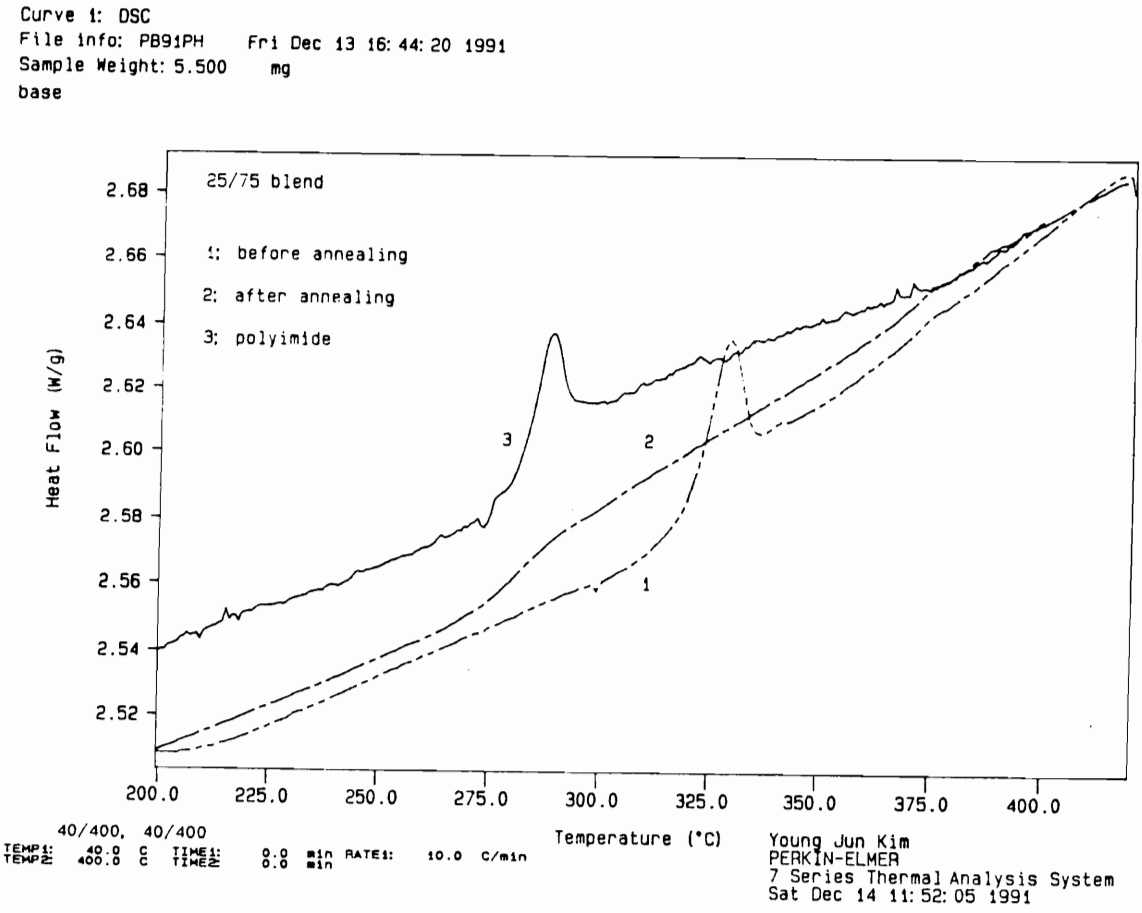

Figure 4.5.8. Effect of heat treatment on the miscibility of the 25/75 wt. % PBI/(BIS-A/ODPA) polyimide blend. The sample was first-scanned to 420°C and annealed at that templerature for 3 minutes and fast-cooled to 40°C: (1) before annealing; (2) after annealing; (3) pure (BIS-A/ODPA) polyimide

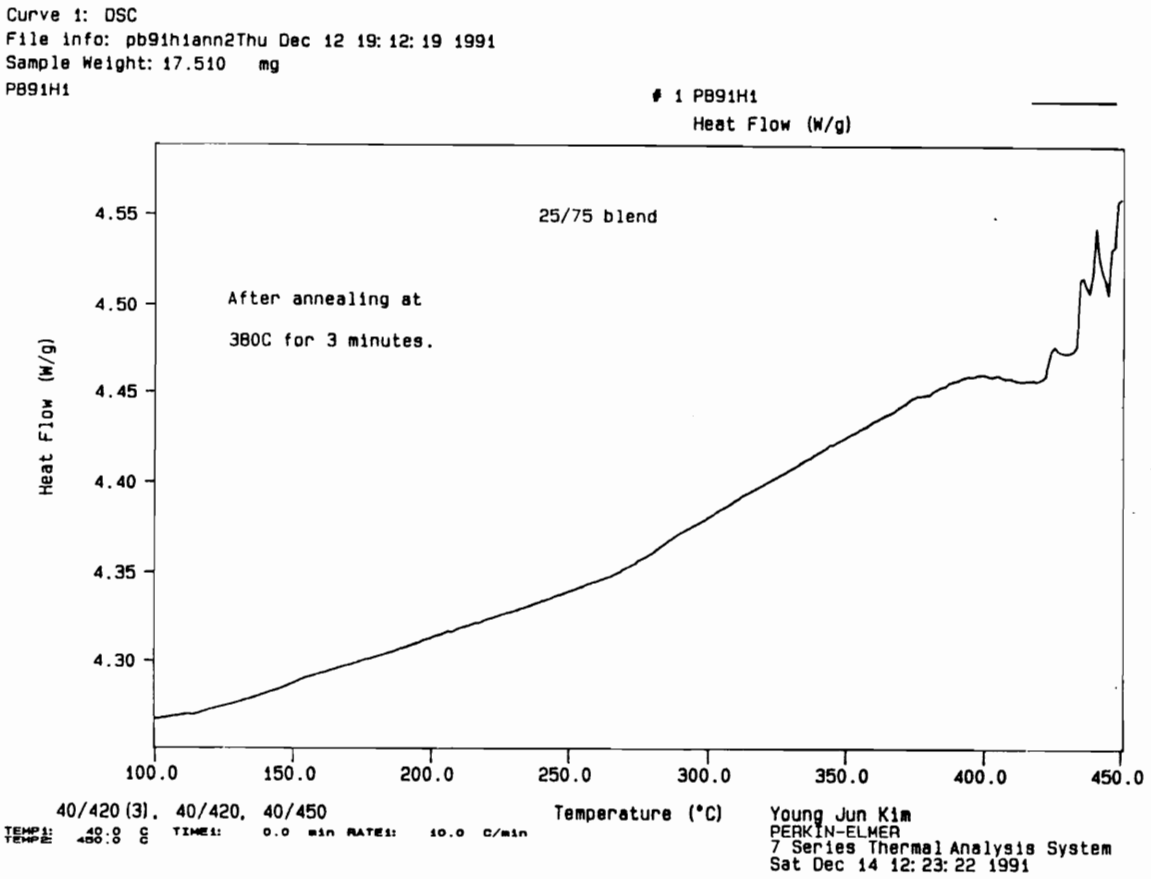

Figure 4.5.9. Effect of heat treatment on the miscibility of the 25/75 wt. % PBI/PI(BIS-A/ODPA) polyimide blend. The second scan after annealing the sample at 380°C for 3 minutes.

Evidence for the specific interactions between PBI and BIS-A/ODPA polyimide was also observed in the FTIR spectra. N-H stretch band displayed displacement to lower frequencies with increasing polyimide component in the blends, while other characteristic peaks were significantly broadened. Table 4.12 shows characteristic frequencies in the PBI/(BIS-A/ODPA) polyimide blends.

Table 4.12. Maximum frequencies (cm-1) of the N-H stretch of polybenzimidazole, imide modes, C-O stretch of PBI/(BIS-A/ODPA) polyimide blends.

PBI wt %	N-H	Imide I	Imide II	Imide III	C-O
0		1778.3	1724.8	1373.6	1238.4
25	3353.1	1777.9	1723.5	1375.0	1238.4
50	3356.2	1777.4	1716.8	1375.2	1238.3
75	3404.7	1775.9	1714.9	1376.0	1237.1
100	3415				

Three blend systems discussed so far showed miscibility over all composition range, however, immiscibility was also found for other PBI/polyimide systems when polar polyimide components were replaced by non-polar components. Tables 4.13 shows glass transition temperatures of PBI/(BIS-A/6FDA) polymer blends. The formation of optically opaque films were the first indication that this blend systems might be immiscible. Both 20/80 and 40/60 wt. % PBI/(BIS-A/6FDA) blends showed glass transitions at 310°C where the

corresponding pure polyimide showed a glass transition (Figure 4.10). However glass transition temperature of pure PBI was not detected either. These simple experiments clearly demonstrated that the interactions of imidazole moiety and imide groups are not sufficient enough for miscibility. Interestingly, 60/40 blend did not show any glass transition. And further FTIR spectra of this blend system did not show any evidence for interactions between PBI and polyimide groups (no N-H frequency shift).

Tables 4.14~4.15 show glass transition temperatures of PBI/PI(4,4'-DDS/6FDA) and PBI/PI(4,4'-ODA/6FDA) polymer blends. 25/75 blends showed glass transition temperatures of pure polyimides. FTIR spectra for these two blend systems, PBI/(4,4'-DDS/6FDA) and PBI/(4,4'-ODA/6FDA), showed no indication for the specific interactions between PBI and polyimide components. Representative FTIR spectra of the N-H stretch band of PBI in the PBI/(4,4'-ODA/6FDA) blends are shown in the Figure 4.5.11. Even though the FTIR spectra showed no indication for the specific interactions for these blend compositions thermal transition behaviors were more or less complex as shown in the Tables 4.14~15. Low PBI content blends (25 %) yielded glass transition temperatures which were identical with those of pure polyimides, however Tg of PBI was not detected by DSC (Figure 4.5.12). For the 50/50 blends of PBI/(4,4'-DDS/6FDA) and PBI/(4,4'-ODA/6FDA)

no transition was observed. Figure 4.5.13 shows DSC thermograms of the 50/50 wt. % PBI/(4,4'-DDS/6FDA) blend up to the fourth scan. And for the highest PBI content 75/25 blends very broad transitions ranging from 300 to 400°C were detected (Figure 4.5.14). These observations of no transition or very broad transitions suggested partial miscibility between PBI and polyimides in the high PBI content blends.

Table 4.13. Glass transition temperatures (°C)* of PBI/PI(BIS-A/6FDA) blends

PBI wt %	1st heat	2nd heat	3rd heat	4th heat	Tg**
0		312			
20	311	311	311	310	331
40	308	310	308	310	352
60	N. T.***	N. T.	N. T.	N. T.	375

* After the first heat all samples were annealed at 400°C for 20 minutes.

** Calculated Tg's by the Fox equation.

*** No transition was observed

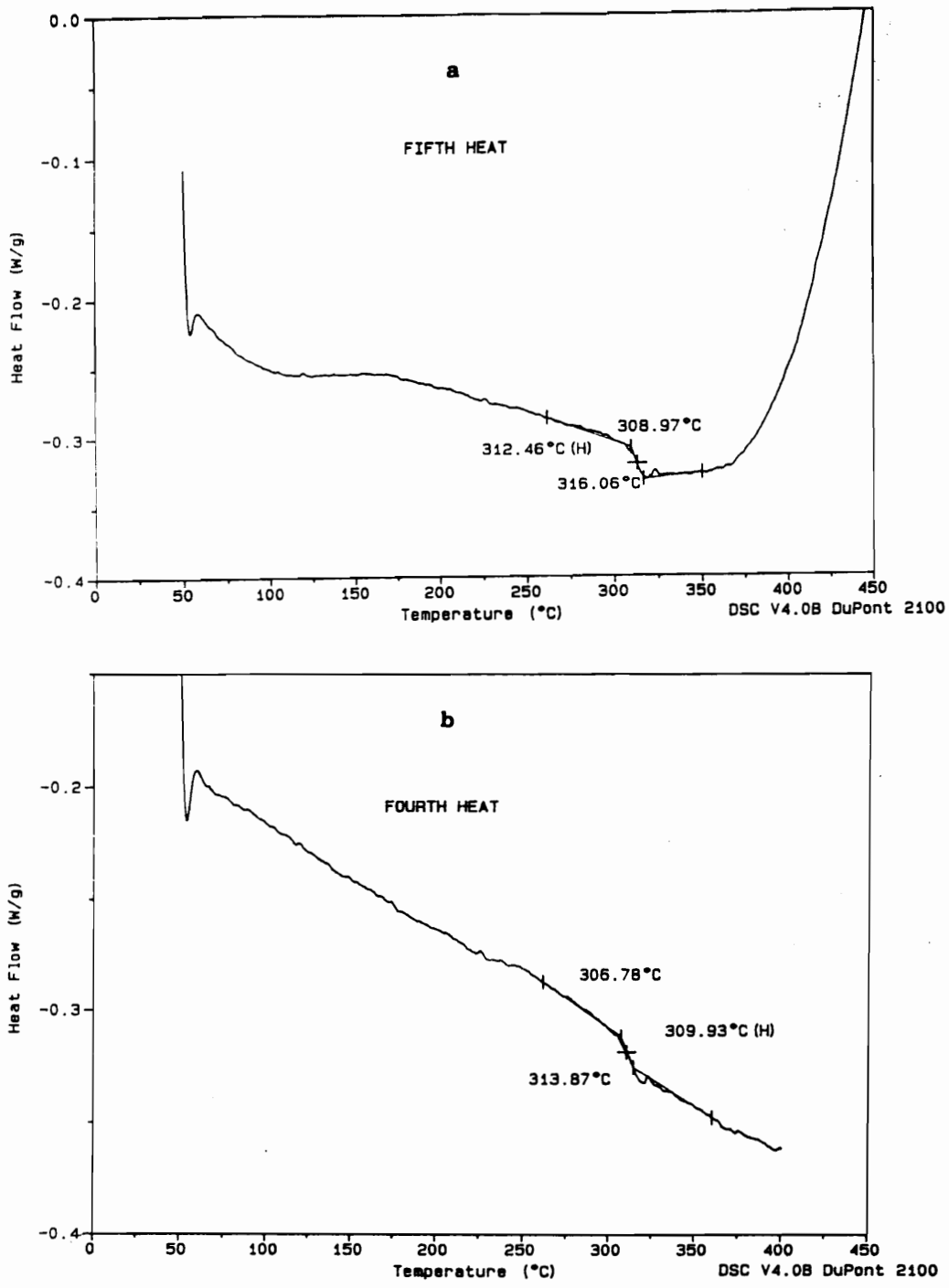

Figure 4.5.10. DSC thermograms of (a) 20/80 and (b) 40/60 wt. %. PBI/PI(BIS-A/6FDA) blends.

Table 4.14. Glass transition temperatures (°C)* of PBI/PI(4,4'-DDS/6FDA) blends

PBI wt %	1st heat	2nd heat	3rd heat	4th heat	Tg**
0	323	342	345	343	
25	331	341	341	342	362
50	329	N. T.***	N. T.	N. T.	382
50@	335	N. T.	N. T.	N. T.	382
75		broad#	broad	broad	403
75@		broad	broad	broad	403

* After first heat all samples except the 50/50 blend marked by @ were annealed at 400°C for 20 minutes.
** Calculated Tg's by the Fox equation.
*** No transition was observed.
# Very broad transitions ranging from 330°C to 400°C.
@ For the first three scans the samples were scanned from 50°C to 400°C and for the fourth scan the sample was heated from 50 to 450°C.

Table 4.15. Glass transition temperatures (°C)* of PBI/PI(4,4'-DDS/6FDA) blends

PBI wt %	1st heat	2nd heat	3rd heat	4th heat	Tg**
0	293	292	299	298	
25	301	302	302	302	325
50		N. T***.	N. T.	N. T.	355
75	311	broad#	broad	broad	388

* After the first heat all samples were annealed at 400°C for 20 minutes.
** Calculated Tg's by the Fox equation.
*** No transition was observed
# Very broad transitions ranging from 330 to 400°C

Figure 4.5.11. FTIR spectra of N-H stretch region for PBI/PI(4,4'-ODA/6FDA) blends: (1) 50/50; (2) 75/25 wt. % PBI/polyimide blend; (3) Pure PBI

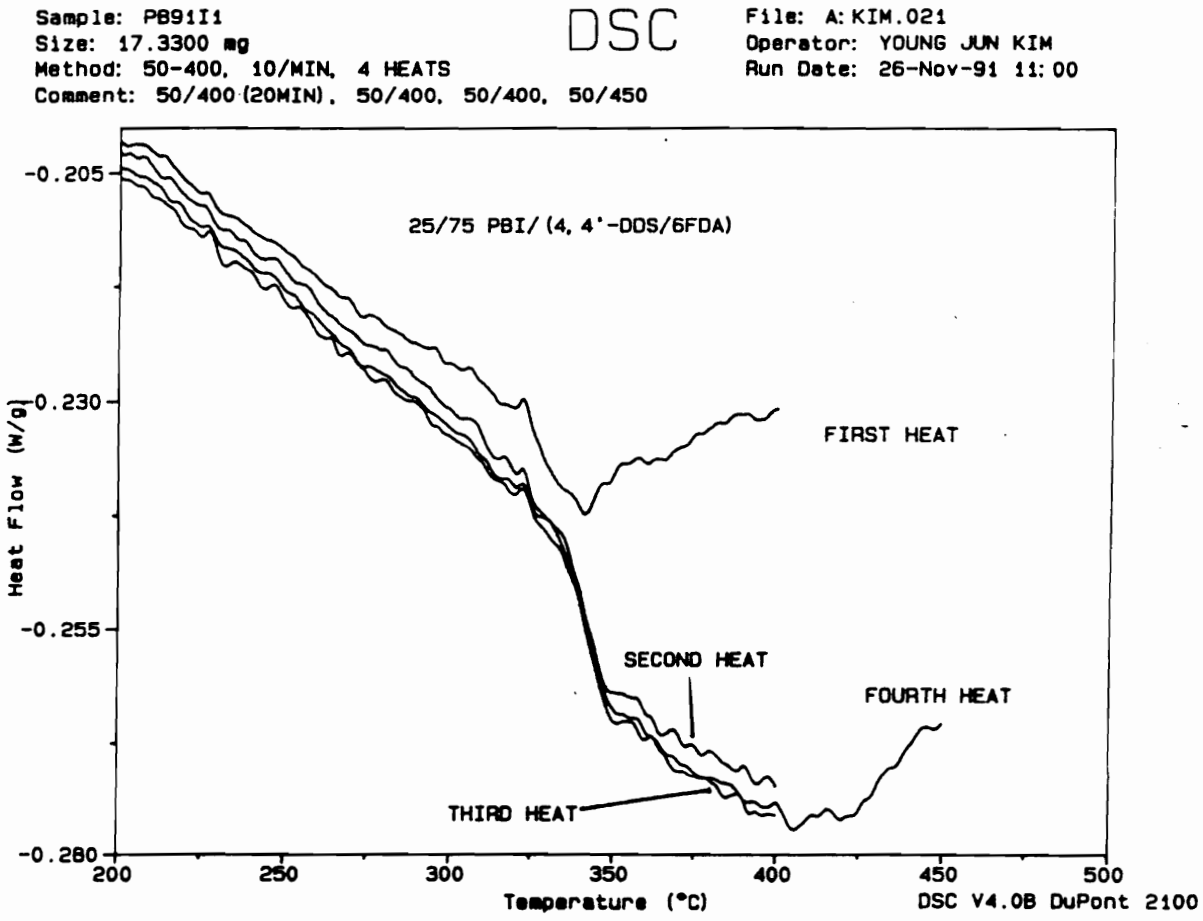

Figure 4.5.12. DSC measurements of the 25/75 wt. % PBI/PI(4,4'-DDS/6FDA) blend. The sample was hold at 400°C for 20 minutes after the first scan.

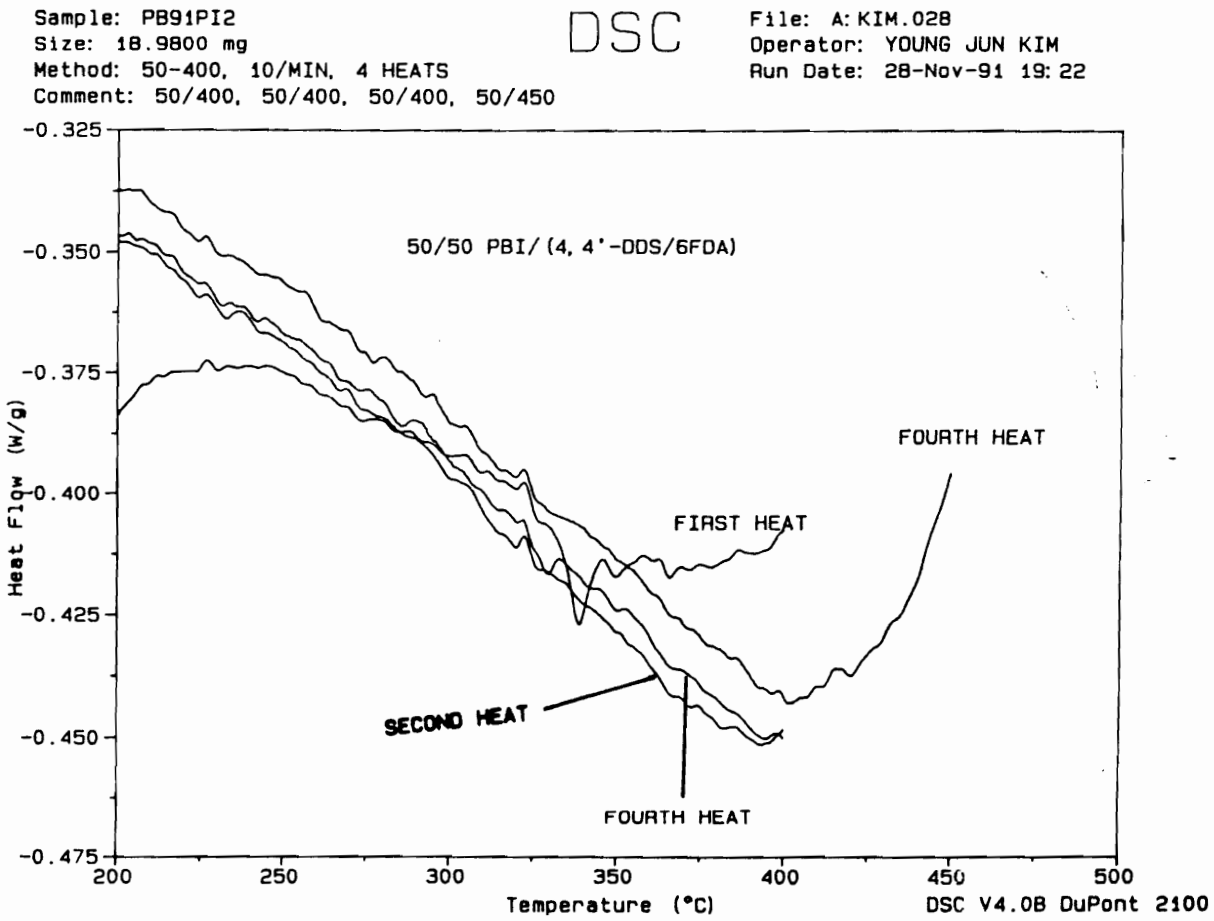

Figure 4.5.13. DSC thermograms of 50/50 PBI/PI(4,4'-DDS/6FDA) blend. The sample was not hold at 400°C for 20 minutes.

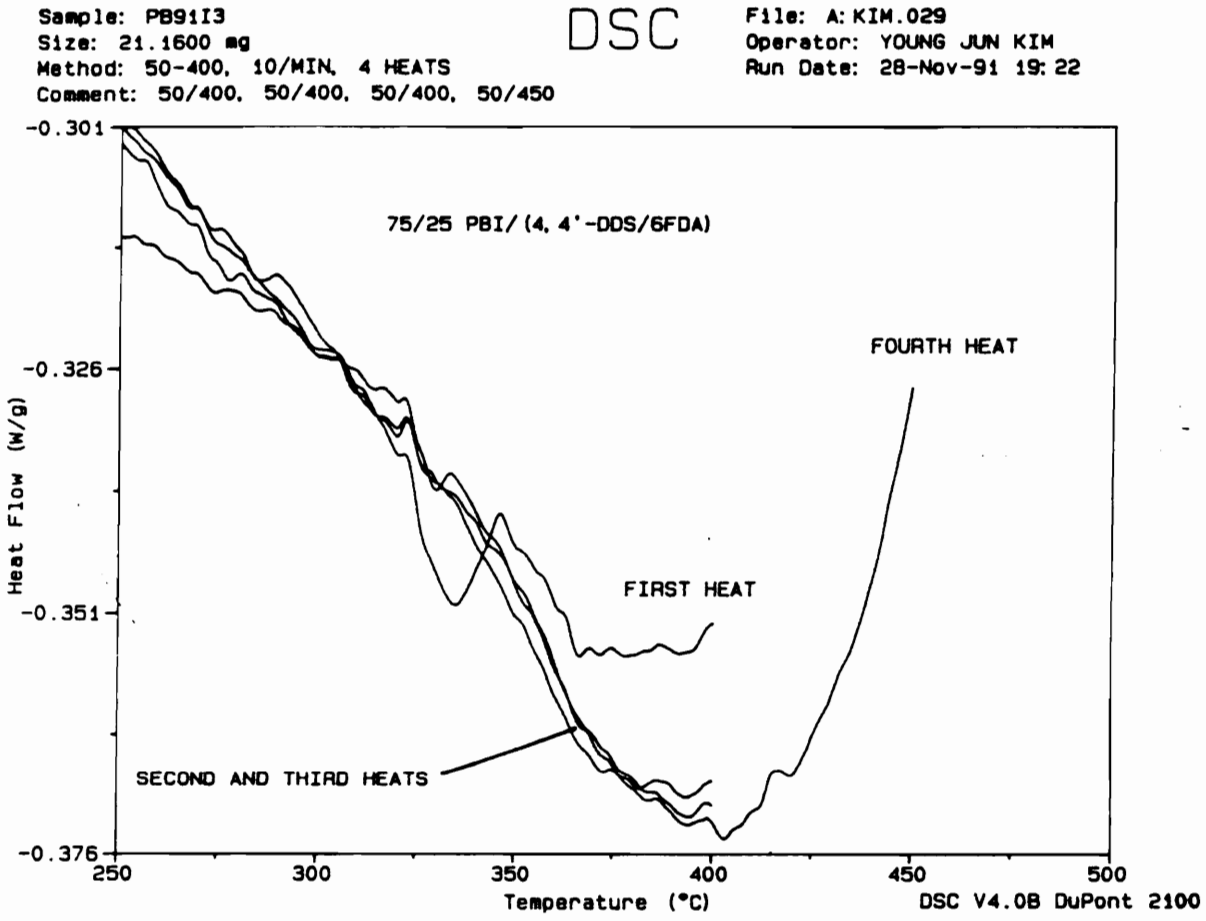

Figure 4.5.14. DSC thermograms of 75/25 PBI/PI(4,4'-DDS/6FDA) blend. The sample was not hold at 400°C for 20 minutes.

CHAPTER 5

CONCLUSIONS

Detailed fundamental kinetic and mechanistic studies of the formation of high performance fully cyclized polyimides were performed using spectroscopy, titrations and viscosity measurements. Second order kinetics were generated especially from the concentration dependence experiments and the imidization reaction was demonstrated to be acid catalyzed. While the solid phase bulk thermal imidization process has been known as a "physico-chemical process" and characterized by the two step kinetic process, solution imidization processes have been much less studied. This approaches appear to be the first demonstration that second order kinetics are followed up to high conversions (c.a. 90%). This one step solution imidization processes is ascribed to the complete removal of constraints, such as a Tg rise and the existence of "kinetically non-equivalent states" of amic acid groups, that have been used to explain the complex kinetic features of the solid phase imidization processes. Thus, a solution imidization process could be defined as a "chemical process" where kinetics are governed by chemical reactivities of amic acid groups. Heteroatom functional groups in the diamine and dianhydride components influenced the imidization kinetics. Thus, an electron

donating group in the diamine component accelerated the rate of imidization very significantly but, somewhat surprisingly the effects of dianhydride components on the rate of imidization were relatively small, as compared to those of diamine components.

Two dimensional ^{1}H-^{1}H Correlation Spectroscopy (^{1}H-^{1}H COSY) clearly demonstrated the partial degradation of amide bonds, hydrolysis and unimolecular decomposition, during NMP/CHP solution imidization of polyamic acids synthesized from oxydianiline and oxydiphthalic anhydride. At the very initial stages of the imidization process the molecular weight of the materials was observed to be dramatically decreased by just minor amounts of degradation. Subsequently, the molecular weight increased as the "recombination" of the broken chains proceeded upon further imidization. Nevertheless, complete recombination and cycloimidization, as evidenced by well-defined ^{1}H-NMR spectra, were possible under proper imidization conditions. The implication of these findings is significant for the high performance polyimide synthesis since it demonstrates that proper imidization conditions are required to ensure complete recombination of the broken chains and their subsequent cycloimidization. Implicitly, this also necessary to achieve a successful molecular weight control and to maximize thermal and hydrolytic stability.

A proposed intermolecular imide link formation reaction which has been suggested by others was also investigated with polyimide derived from oxydianiline and oxydiphthalic anhydride and a model imide from the reaction of oxydiphthalic anhydride and aniline. Both this model imide and the polyimide were characterized by FTIR spectroscopy. Second derivative traces of the asymmetric carbonyl mode centered at ~1720 cm^{-1} of the FTIR spectra for both the model imide and polyimide were observed to be very complex and were significantly changed by small difference in the amount of the residual solvent (NMP). The complex behavior of the second derivative traces was interpreted in view point of, at least in part, the participation of overtone of the same symmetry in Fermi resonance with the asymmetric carbonyl mode. The change of the second derivative traces of the asymmetric carbonyl modes as a function of reaction conditions had been considered to be due to formation of other species not due to other vibrational effects. Thus, it had been suggested to be evidence for intermolecular imide link formation. As the very complex behavior of the second derivative traces suggests, the FTIR investigations of the asymmetric carbonyl mode is not a reliable methodology for identifying the actual species formed during imidization processes. Further, well-defined ^{1}H-NMR spectra and measurable expected intrinsic viscosity values of the

ODA/ODPA polyimide suggested that the proposed intermolecular imide formation reaction does not occur under solution imidization conditions.

Imidization of polyamic acids derived from ketone containing BTDA and BIS-A was also investigated utilizing ^{1}H-NMR spectroscopy since there is a possibility of imine formation reaction. ^{1}H-NMR spectroscopy provided direct evidence for the imine linkage formation. Under certain imidization conditions gelation due to imine formation was observed during imidization of BTDA/BIS-A polyamic acids. Extremely dry reaction conditions and relatively low reaction temperatures, eg, 130°C, favored imine formation reactions. The requirement of the extremely dry reaction condition for the imine formation reaction was a quite natural result since the imine functional group is hydrolytically unstable and the removal of water drives the reaction in the direction of the imine formation. The temperature dependence of the imine formation reaction is not clearly understood at this point, but one plausible explanation is acid catalysis of the imine formation reaction. As expected, the formed gel was easily hydrolyzed by addition of catalytic amount of aqueous hydrochloric acid.

A variety of soluble homo- and copolyimides with controlled molecular weight and end groups have been

synthesized by the two step, one pot imidization procedure involving the initial generation of soluble polyamic acid prepolymers and the subsequent dehydroimidization of the polyamic acid prepolymers. Phthalic anhydride was used to control molecular weight and to generate non-reactive end groups, which have been considered to be critical for the polyimides to be inert to radical formations at high temperatures. Variations of the diamine and dianhydride monomers produced significant changes in the solubility, glass transition temperature, and thermo-oxidative stabilities. Incorporation of symmetric biphenylene dianhydride (s-BPDA) was found to increase glass transition temperatures and thermo-oxidative stabilities of copolyimides. For example, copolymerization of p-PDA with 85/15 mole % ratio of 6FDA/s-BPDA produced a soluble copolyimide. The Tg of the copolyimide was 20°C higher than that of 6FDA/p-PDA homopolyimide. Moreover copolymerization of 4,4'-DDS with a 22/78 mole % ratio of 6FDA/s-BPDA produced a soluble copolyimide whose 5 % wt. loss temperature determined by TGA analysis was 30°C higher than that of 6FDA/4,4'-DDS homopolyimide.

To investigate miscibility as a function of structural variations of the polyimide component, various polyimides (PI's) were solution blended with polybenzimidazole (PBI). The miscibility of the PBI/PI blends was found to improve

with increasing polarity of the polyimide component. Thus, 3,3'-DDS/BTDA, 3,3'-DDS/ODPA, BIS-A/ODPA polyimide systems were found to be miscible with PBI as determined by the single, composition dependent Tg's lying between those of the constituent components. FTIR spectroscopy was further utilized to provide evidence for the specific interactions which cause miscibility in the PBI/PI blends. For the miscible blends, large lower imidazole N-H frequency shifts in the blend compositions (maximum $\Delta n \cong 55$ cm-1) were observed. The blend system based upon BIS-A/ODPA polyimide and PBI showed a lower critical solution temperature (LCST), which suggested that the hydrogen bonding interaction between imidazole N-H and electron rich heteroatom containing functional groups in the imide component was critical for the observed miscibility and that this enthalpic effect decreases as temperature increases. When the polar polyimide components were replaced by non-polar components miscibility was significantly reduced. Thus, miscibility was not obtained for polyimides based upon 6FDA such as 4,4'-DDS/6FDA, 4,4'-ODA/6FDA and BIS-A/6FDA polyimide systems.

CHAPTER 6

SUGGESTED FUTURE STUDIES

During the course of this multidisciplinary research many kinetic and mechanistic aspects of the polyimide formation, the relationship of polyimide structure to properties and miscibility with polybenzimidazole have been exploited. However, many fundamental aspects deserve further investigation.

Even though the main research area in this dissertation was centered around cyclization of polyamic acid, the first stage polyamic acid synthetic step is also as important as the imidization step. The area of interest includes the elucidation of polyamic acid molecular weight equilibration as a function of time and temperature, perhaps utilizing gel permeation chromatography (GPC), light scattering, and solution viscosity measurements. Investigations of polyamic acid microstructure compositions as a function of reaction temperature, solvent, and monomer structural variations would also be of interest.

In this research auto-catalyzed second order kinetic feature for the solution imidization process was demonstrated. However, it is highly probable that during the conventional solid phase imidization processes kinetics might change from initial second order to later first order

because carboxylic acid groups may not effectively catalyze the imidization reaction in a true solvent free solid phase. This could be demonstrated by performing kinetic study of completely solvent free polyamic acid at different initial concentrations in inert matrix resins. The second order kinetic feature of imidization processes suggested that correct kinetic parameters can not be obtained from solid phase imidization kinetic data because the concentration of polyamic acid (solid content) changes constantly throughout imidization processes. Thus, the solution imidization technique is highly recommended to obtain correct kinetic parameters for various monomers. If conjugated diamines and dianhydrides are used, the equal reactivity assumption may not hold for the imidization reaction and various amic acid groups in different chemical environments may have different reactivity. For these situations, ^{13}C-NMR spectroscopy could be the best method to follow imidization reactions.

Since the imidization process is indeed a dynamic process where chain scission and recombination of the broken chains occur throughout the imidization process, molecular weight and molecular weight distribution change constantly, too. Fortunately, however, the "mending" of the broken chains seems to be a stochastic process. Thus, the final molecular weight distribution of fully imidized polyimide would be exactly same as that of the corresponding polyamic

acid. However, these aspects merit further investigations since information which could be obtained from these experiments would further aid in the synthesis of well-defined controlled molecular weight polyimides.

Some polyimide solutions such as 4,4'-ODA/ODPA polyimide in NMP showed thermoreversible gelation behavior. The gelation behavior was observed to be a strong function of molecular weight, solution concentration, and temperature dependence. Differential scanning calorimetry, X-ray scattering and scanning electron microscopy might be utilized to elucidate the gelation mechanism that account for the gelation of polyimide solutions.

When polar polyimide components, in the solution cast PBI/PI blends, were replaced by non-polar components such as 6FDA/4,4'-DDS, 6FDA/4,4'-ODA, and 6FDA/BIS-A polyimides, miscibility with PBI was not obtained. This does not necessarily mean that those blend systems are immiscible because the details of the mixing process determine the morphology of the resulting blend. Thus, considerable care must be exercised in the preparation stage to assure that a physical equilibrium has been achieved. Solution cast preparation method offers possibilities for misleading results if a closed-loop, two-phase region in the ternary-phase diagram exists. Therefore, these important factors should be taken into account in the processing protocols and

investigation of the samples prepared by a precipitation method is needed to confirm the observed immiscibility.

APPENDIX: Work sheets for kinetic investigations, kinetic plots and tables of kinetic parameters

APPENDIX 1. Work sheets for kinetic investigations

Work sheets for kinetic investigations of various polyimide systems are shown in the following tables where

t, min.= reaction time in minute

t, hr = reaction time in hour

S.S.= weight of 10 % (w/w) polymer solution in gram

V = volume of titrant at an equivalence point in ml

- E = negative value of potential at an equivalence point in mV

%AA = % of unreacted amic acid functional groups

%AA' = normalized %AA with respect to unreacted polyamic acid

p = degree of imidization = $1 - \frac{\%AA}{100}$, $\ln(1 - p) = \ln\frac{\%AA}{100}$

N = normal concentration of the titrant

Table 7.1. A work-sheet for 4,4'-DDS/DSDA polyimide system at imidization temperature of 140°C, (N = 0.0239).

t, min.	S.S., g	V, ml	-E, mV	%AA	%AA'	-ln(1-p)	1/(1-p)
0	0.5301	7.61	413	104.1	100.0	0.000	1.000
10	0.5793	8.29	420	103.8	99.7	0.003	1.003
20	0.5268	6.98	361	95.7	91.9	0.085	1.088
30	0.5264	6.81	377	93.3	89.6	0.110	1.116
40	0.5855	7.23	353	88.9	85.3	0.159	1.172
50	0.5956	7.11	349	85.8	82.3	0.194	1.214
60	0.6080	7.11	359	83.8	80.5	0.217	1.242
70	0.6115	6.85	343	80.2	77.0	0.261	1.299
80	0.5098	5.57	360	78.2	75.0	0.287	1.333
90	0.5880	6.23	337	75.6	72.6	0.321	1.378
100	0.6912	7.28	365	75.1	72.2	0.326	1.386
120	0.6711	6.72	356	71.3	68.5	0.379	1.460
140	0.5880	5.66	363	68.4	65.7	0.420	1.522
160	0.7597	6.90	343	64.4	61.8	0.481	1.617
180	0.5341	4.73	361	62.8	60.3	0.506	1.659
255	0.5833	4.54	362	54.9	52.7	0.641	1.899

Table 7.2. A work-sheet for 4,4'-DDS/DSDA polyimide system at imidization temperature of 160°C, (N = 0.0208).

t, min.	S.S., g	V, ml	-E, mV	%AA	%AA'	-ln(1-p)	1/(1-p)
0	0.6492	10.77	400	104.9	100.0	0.000	1.000
10	0.5361	8.48	342	99.6	95.0	0.052	1.053
15	0.5837	8.67	361	93.3	88.9	0.118	1.125
20	0.5478	7.77	370	88.8	84.6	0.167	1.182
25	0.5148	6.78	351	82.2	78.3	0.244	1.277
30	0.6948	8.58	344	76.8	73.2	0.312	1.366
35	0.6071	7.07	341	72.2	68.9	0.373	1.452
40	0.6757	7.52	334	68.9	65.6	0.421	1.523
45	0.6629	7.23	362	67.4	64.2	0.443	1.557
50	0.5985	6.26	360	64.5	61.5	0.486	1.626
60	0.6024	5.85	358	59.7	56.9	0.563	1.756
70	0.7486	6.72	343	55.0	52.4	0.645	1.907
80	0.7950	6.73	346	51.9	49.4	0.704	2.023

Table 7.3. A work-sheet for 4,4'-DDS/DSDA polyimide system at imidization temperature of 180°C, (N = 0.0208).

t, min	S.S., g	V, ml	-E, mV	%AA	%AA'	-ln(1-p)	1/(1-p)
0	0.6492	10.77	400	104.9	100.0	0.000	1.000
10	0.6285	9.49	339	94.8	90.4	0.101	1.106
20	0.6589	8.57	344	81.1	77.3	0.257	1.293
25	0.6632	7.63	337	71.3	67.9	0.387	1.472
30	0.6653	6.62	363	61.3	58.4	0.538	1.712
35	0.8329	6.88	350	50.5	48.1	0.731	2.077
37.5	0.9154	7.35	359	49.1	46.8	0.759	2.136

Table 7.4. A work-sheet for 4,4'-DDS/ODPA polyimide system at imidization temperature of 140°C, (N = 0.026).

t, min	S.S., g	V, ml	-E, mV	%AA	%AA'	-ln(1-p)	1/(1-p)
0	0.5424	7.45	438	99.6	100.0	0.000	1.000
30	0.5014	6.53	436	94.1	94.5	0.057	1.058
60	0.5405	6.40	429	85.1	85.4	0.158	1.171
90	0.5150	5.50	403	76.3	76.5	0.267	1.306
120	0.5300	5.33	419	71.6	71.9	0.330	1.391
150	0.5480	5.02	410	65.0	65.2	0.427	1.533
180	0.6360	5.47	407	60.8	61.0	0.494	1.638
240	0.6952	5.31	401	53.8	54.0	0.617	1.853
300	0.8250	5.65	394	48.0	48.2	0.730	2.075
360	0.3985	2.64	421	46.4	46.6	0.764	2.146

Table 7.5. A work-sheet for 4,4'-DDS/ODPA polyimide system at imidization temperature of 160 °C, (N = 0.026).

t, min	S.S., g	V, ml	-E, mV	%AA	%AA'	-ln(1-p)	1/(1-p)
0	0.5424	7.45	438	99.6	100.0	0.000	1.000
15	0.6152	8.16	424	96.0	96.4	0.037	1.037
30	0.5750	6.77	412	84.6	84.9	0.163	1.178
45	0.5680	5.76	414	72.2	72.5	0.322	1.379
60	0.5059	4.52	411	63.4	63.6	0.453	1.572
75	0.4360	3.48	431	56.4	56.6	0.570	1.768
90	0.5508	3.94	416	50.3	50.5	0.684	1.981
105	0.5634	3.80	415	47.3	47.5	0.745	2.107
120	0.4820	3.03	416	43.9	44.1	0.818	2.267
150	0.6387	3.50	401	38.0	38.1	0.965	2.625
180	0.6543	3.30	405	35.1	35.2	1.044	2.840
240	0.6625	2.83	398	29.6	29.7	1.214	3.367
300	0.7707	2.84	389	25.4	25.5	1.365	3.914
400	0.5753	1.80	394	21.5	21.6	1.531	4.623
580	0.7030	1.40	386	13.7	13.7	1.987	7.294

Table 7.6. A work-sheet for 4,4'-DDS/ODPA polyimide system at imidization temperature of 180°C, (N = 0.026).

t, min.	S.S., g	V, ml	-E, mV	%AA	%AA'	-ln(1-p)	1/(1-p)
0	0.5424	7.45	438	99.6	100.0	0.000	1.000
15	0.5146	6.19	445	86.5	86.8	0.141	1.152
30	0.6140	5.43	418	62.6	62.8	0.465	1.592
45	0.6240	4.11	403	46.2	46.4	0.769	2.157
65	0.5688	3.00	403	36.7	36.8	1.000	2.718
75	0.6196	3.04	401	34.1	34.3	1.071	2.919
90	0.6340	2.72	402	29.8	29.9	1.208	3.346
120	0.6510	2.36	402	25.0	25.1	1.383	3.986
180	0.5970	1.65	400	19.0	19.0	1.659	5.253
240	0.7107	1.54	383	14.9	15.0	1.900	6.685
540	0.8612	0.94	370	7.5	7.5	2.589	13.317

Table 7.7. A work-sheet for 4,4'-ODA/DSDA polyimide system at imidization temperature of 140°C, (N = 0.026).

t, min.	S.S., g	V, ml	-E, mV	%AA	%AA'	-ln(1-p)	1/(1-p)
0	0.6123	8.51	416	101.0	100.0	0.000	1.000
15	0.6125	8.14	425	96.3	95.3	0.048	1.049
30	0.6732	7.78	461	82.9	82.1	0.197	1.218
45	0.8090	7.62	393	66.9	66.3	0.411	1.509
60	0.7282	6.08	390	59.0	58.4	0.537	1.711
90	0.7762	5.12	373	46.3	45.8	0.781	2.183
120	0.8116	4.56	404	39.2	38.8	0.948	2.579
150	0.9374	4.52	405	33.5	33.2	1.102	3.011
210	0.9985	3.77	409	26.1	25.8	1.353	3.869
270	1.4633	4.36	384	20.5	20.3	1.593	4.919

Table 7.8. A work-sheet for 4,4'-ODA/DSDA polyimide system at imidization temperature of 160°C, (N = 0.026).

t, min.	S.S., g	V, ml	-E, mV	%AA	%AA'	-ln(1-p)	1/(1-p)
0	0.6123	8.51		101.0	100.0	0.000	1.000
15	0.7395	9.71	441	95.0	94.1	0.061	1.063
30	0.7425	6.91	384	66.1	65.4	0.424	1.529
45	0.8095	4.83	393	41.7	41.3	0.884	2.420
60	0.8392	3.77	389	31.2	30.9	1.176	3.241
75	0.9225	3.39	409	25.4	25.2	1.379	3.971
90	0.9420	2.95	415	21.6	21.4	1.542	4.675
105	1.2460	3.27	397	18.0	17.9	1.722	5.595
120	1.1244	2.68	417	16.4	16.2	1.820	6.173

Table 7.9. A work-sheet for 4,4'-ODA/DSDA polyimide system at imidization temperature of 180°C, (N = 0.026).

t, min.	S.S., g	V, ml	-E, mV	%AA	%AA'	-ln(1-p)	1/(1-p)
0	0.6123	8.51		101.0	100.0	0.000	1.000
10	0.9229	7.98	360	59.7	59.1	0.525	1.691
20	0.7820	3.43	413	30.4	30.1	1.200	3.321
30	1.2035	3.56	398	20.4	20.2	1.601	4.958
40	1.2570	2.54	420	13.8	13.7	1.988	7.300
45	1.6245	2.74	413	11.5	11.4	2.170	8.761

Table 7.10. A work-sheet for 4,4'-ODA/6FDA polyimide system at imidization temperature of 140°C, (N = 0.0257).

t, min	S.S., g	V, ml	-E, mV	%AA	%AA'	-ln(1-p)	1/(1-p)
0	0.6847	8.32	439	100.6	100.0	0.000	1.000
15	0.7506	8.69	431	95.6	95.1	0.051	1.052
30	0.6970	7.41	446	87.4	86.8	0.141	1.152
45	0.7540	7.02	424	76.0	75.6	0.280	1.323
60	0.7848	6.55	404	67.9	67.5	0.393	1.482
90	0.9208	6.33	417	55.5	55.1	0.595	1.813
120	1.0091	5.91	425	47.1	46.8	0.759	2.137
150	0.9557	4.87	428	40.8	40.5	0.903	2.467
180	0.8888	4.05	445	36.4	36.2	1.016	2.762
240	1.0530	3.82	426	28.9	28.7	1.249	3.486
300	1.0050	3.14	438	24.8	24.7	1.400	4.054
360	1.1459	3.08	444	21.3	21.2	1.552	4.722

Table 7.11. A work-sheet for 4,4'-ODA/6FDA polyimide system at imidization temperature of 160°C, (N = 0.0221).

t, min.	S.S., g	V, ml	-E, mV	%AA	%AA'	-ln(1-p)	1/(1-p)
0	0.4573	6.71	407	104.7	100.0	0.000	1.000
9	0.5468	6.68	385	86.3	82.5	0.193	1.213
14	0.4876	5.20	400	74.9	71.5	0.335	1.399
19	0.4679	4.55	402	68.0	65.0	0.431	1.539
24	0.4577	3.87	400	58.9	56.2	0.576	1.779
29	0.4429	3.48	407	54.5	52.1	0.652	1.920
34	0.4067	2.98	411	50.8	48.5	0.724	2.062
39	0.3837	2.52	403	45.3	43.3	0.837	2.310
44	0.4786	2.91	407	41.9	40.0	0.915	2.498
49	0.5192	3.00	416	39.7	37.9	0.970	2.637
54	0.5682	3.00	405	36.3	34.7	1.059	2.882
59	0.5716	2.85	400	34.2	32.6	1.120	3.065
64	0.6782	3.15	401	31.8	30.4	1.192	3.292

Table 7.12. A work-sheet for 4,4'-ODA/ODPA polyimide system at imidization temperature of 140°C, (N = 0.0241).

t, min.	S.S., g	V, ml	-E, mV	%AA	%AA'	-ln(1-p)	1/(1-p)
0	0.4740	7.72	408	100.1	100.0	0.000	1.000
9	0.4797	7.53	413	96.3	96.1	0.039	1.040
19	0.4479	6.20	407	84.1	84.0	0.175	1.191
29	0.5263	6.47	407	74.2	74.1	0.299	1.349
39	0.5544	6.28	412	68.1	68.0	0.386	1.471
49	0.4926	5.10	406	61.9	61.9	0.480	1.616
59	0.6150	5.78	414	56.0	55.9	0.581	1.788
69	0.6541	5.57	414	50.5	50.4	0.685	1.983
79	0.7444	5.87	410	46.6	46.6	0.765	2.148
89	0.8388	6.16	403	43.3	43.3	0.838	2.312
99	0.9937	6.76	400	40.0	40.0	0.916	2.500
119	0.7974	5.13	407	37.8	37.8	0.974	2.648
129	1.0493	6.28	394	35.1	35.1	1.047	2.850
149	0.8054	4.38	399	31.9	31.8	1.145	3.143
169	1.2363	5.99	399	28.3	28.2	1.265	3.543

Table 7.13. A work-sheet for 4,4'-ODA/ODPA polyimide system at imidization temperature of 160°C, (N = 0.0241).

t, min.	S.S., g	V, ml	-E, mV	%AA	%AA'	-ln(1-p)	1/(1-p)
0	0.5062	8.05	415	97.5	100.0	0.000	1.000
9	0.3864	6.06	433	96.2	98.6	0.014	1.014
14	0.5784	7.28	398	76.1	78.0	0.249	1.282
19	0.6323	6.75	390	64.0	65.6	0.422	1.524
24	0.5863	5.53	411	56.1	57.6	0.552	1.737
29	0.5273	4.36	417	49.0	50.2	0.689	1.991
34	0.6778	4.82	414	41.9	43.0	0.844	2.326
39	0.6350	4.10	421	38.0	39.0	0.943	2.567
44	0.5975	3.43	412	33.7	34.5	1.063	2.896
49	0.5407	2.90	418	31.4	32.2	1.135	3.110
54	0.7680	3.66	412	27.8	28.5	1.255	3.508
59	0.7768	3.42	405	25.7	26.3	1.335	3.800
64	1.0050	4.08	402	23.6	24.2	1.418	4.131

Table 7.14. A work-sheet for 4,4'-ODA/ODPA polyimide system at imidization temperature of 180°C, (N = 0.0241).

t, min.	S.S., g	V, ml	-E, mV	%AA	%AA'	-ln(1-p)	1/(1-p)
0	0.4315	7.13	427	101.7	100.0	0.000	1.000
10	0.4679	6.89	428	89.9	88.4	0.124	1.132
15	0.4413	4.83	418	65.6	64.5	0.438	1.550
20	0.5117	4.11	426	47.5	46.7	0.760	2.139
25	0.4696	2.82	436	35.2	34.6	1.061	2.891
30	0.4486	2.24	452	29.2	28.7	1.248	3.482
35	0.4893	2.06	452	24.5	24.1	1.422	4.146
40	0.5952	1.99	437	19.4	19.1	1.655	5.235
45	0.4250	1.38	451	18.9	18.6	1.684	5.388
50	0.6890	1.83	446	15.3	15.1	1.893	6.638
55	0.9059	2.07	443	13.2	13.0	2.042	7.708

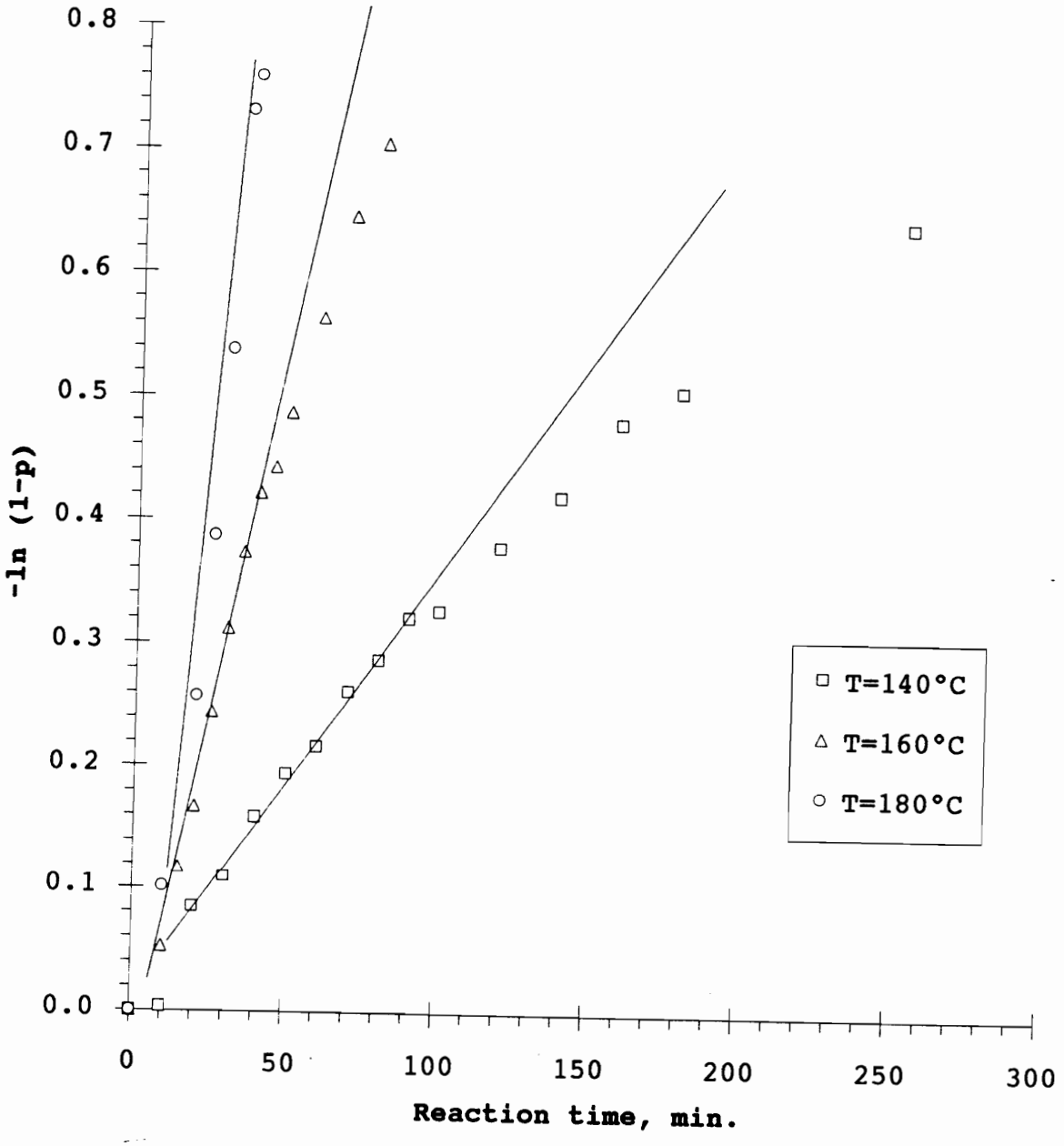

Figure 7.1. A first order kinetic plot of -ln(1-p) vs. reaction time for 4,4'-DDS/DSDA polyimide system.

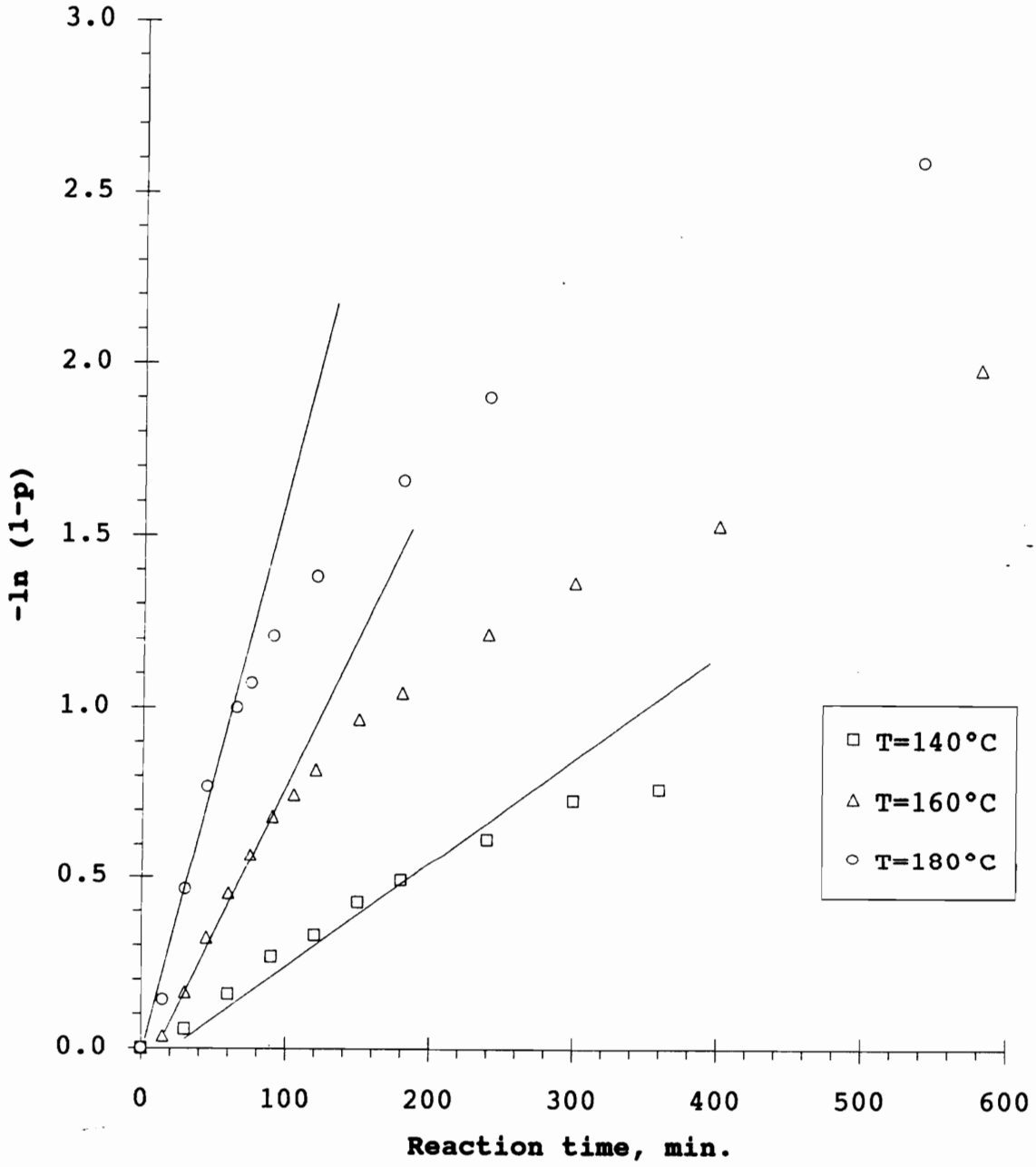

Figure 7.2. A first order kinetic plot of -ln(1-p) vs. reaction time for 4,4'-DDS/ODPA polyimide system.

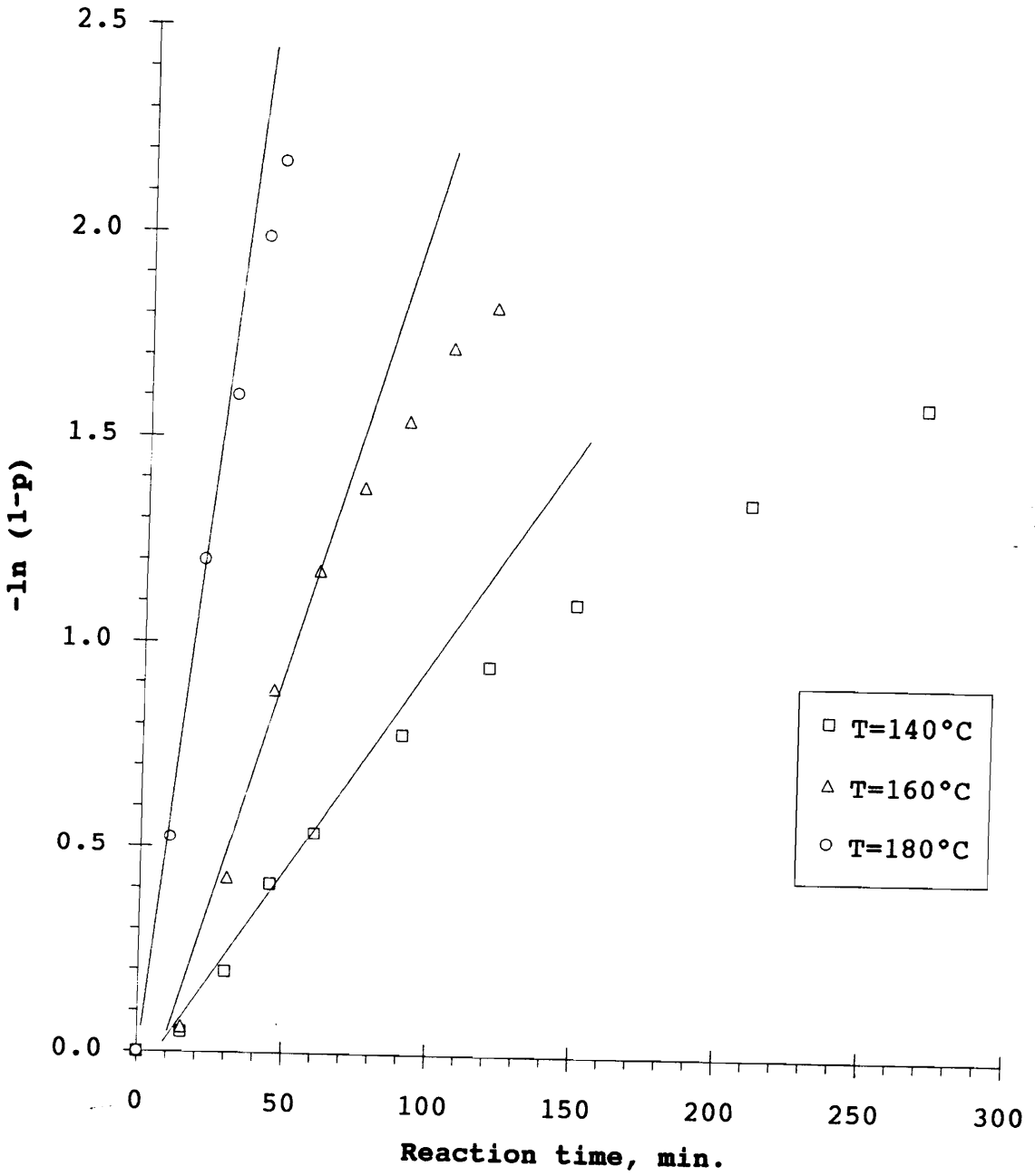

Figure 7.3. A first order kinetic plot of -ln(1-p) vs. reaction time for 4,4'-ODA/DSDA polyimide system.

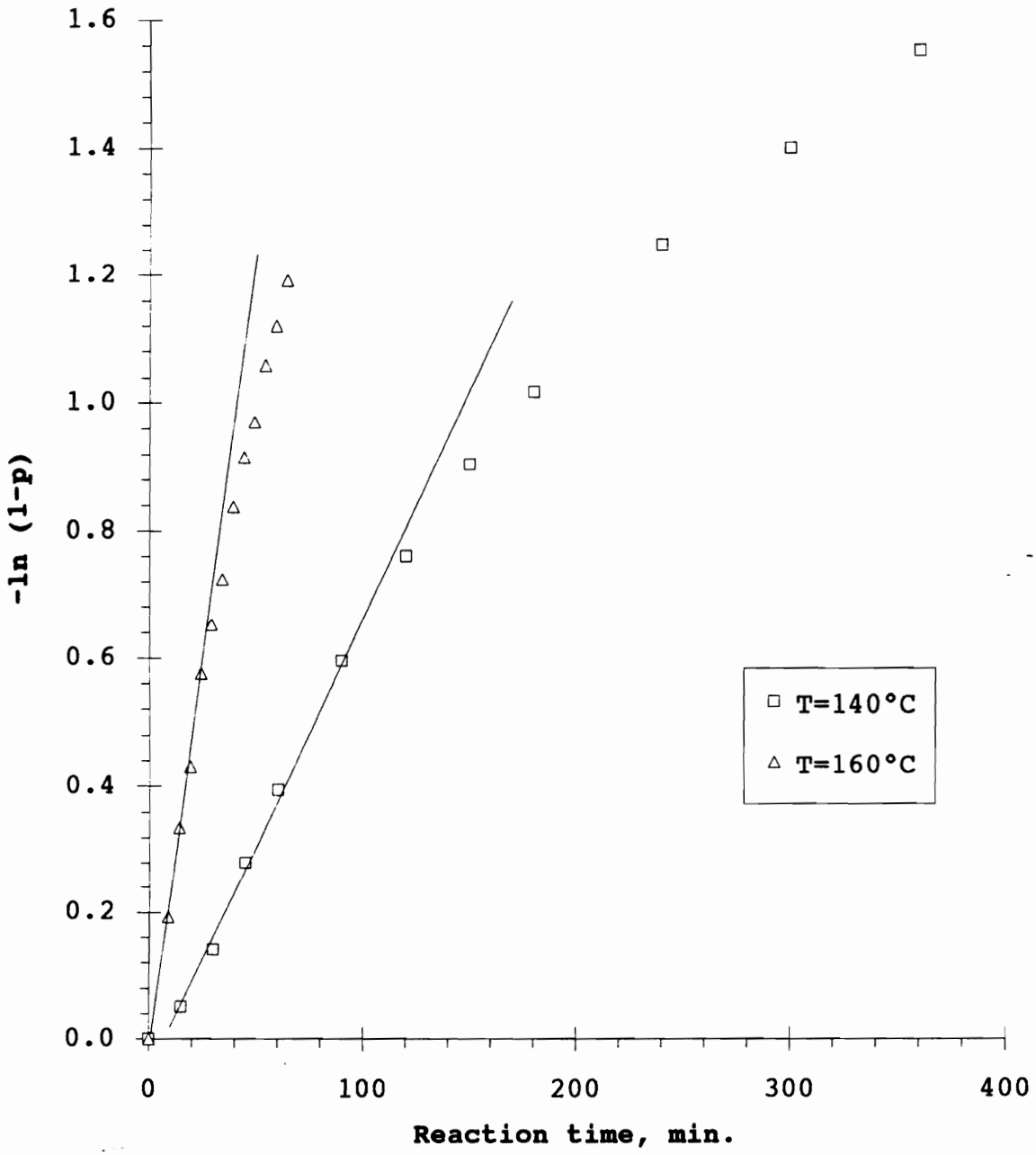

Figure 7.4. A kinetic plot of -ln(1-p) vs. reaction time for 4,4'-ODA/6FDA polyimide system.

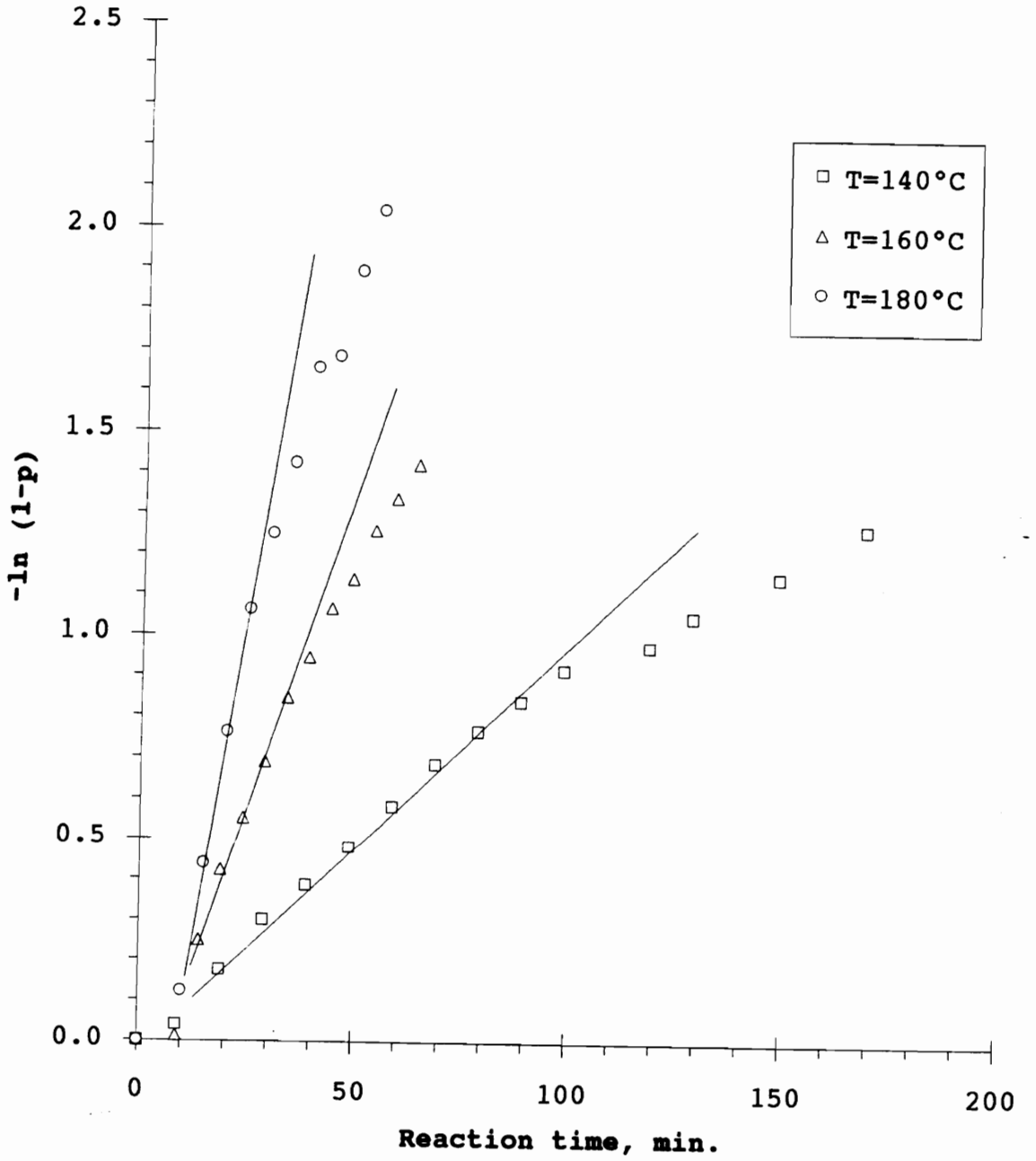

Figure 7.5. A first order kinetic plot of -ln(1-p) vs. reaction time for 4,4'-ODA/ODPA polyimide system.

Table 7.15. Kinetic parameters derived from first order kinetics for various polyimide systems.

Polyimide system	Rate constants , k $min.^{-1}$ 140°C	160°C	180°C	Ea (KJ/mol)	ln (A min)	ΔH^* (KJ/mol)	ΔS^* (KJ/mol°K)
4,4'-DDS/DSDA	3.5±0.1	13±0.5	32±2	86±6	20±1.7	83±6.0	-130±14
4,4'-DDS/ODPA	3.1±0.2	9.1±0.4	21±0.5	75±3	16±0.8	71±3.0	-160±7
4,4'-ODA/DSDA	11±0.8	26±1.5	56±3.7	62±0.3	14±0.1	59±0.2	-180±0.3
4,4'-ODA/ODPA	9.6±0.3	27±1.1	61±0.6	72±2.5	16±0.7	71±2.6	-140±1.8
4,4'-ODA/6FDA	7.5±0.1	22±0.9					

Where k is a rate constant, Ea is an activation energy, A is Arrhenius frequency factor, ΔH^* is the activation enthalpy and ΔS^* is the activation entropy.

APPENDIX 3. Determination of the reaction order in solution imidization processes

The rate expression for the cycloimidization of amic acid to imide is of the form

$$\frac{-dN}{dt} = kN^n = k(N_0 - x)^n \qquad \text{Eq. 1.3.1}$$

where N is the number of acid functional groups, N_0 is the initial number of acid functional groups, x is the number of imide functional groups, k is a rate constant and n is a reaction order.

For the above rate expression (Eq. 1.3.1) reaction order is given by Eq. 1.3.2

$$n = 1 + \frac{\log t'_{1/2} - \log t_{1/2}}{\log N_0 - \log N'_0} \qquad \text{Eq. 1.3.2}$$

where N_0 and N'_0 are number of initial acid functional groups per unit volume and $t_{1/2}$ and $t'_{1/2}$ are the half-life periods, the times required for one-half of given reactants to be consumed when the number of initial acid functional groups are N_0 and N'_0, respectively. With this equation the order of reaction can be calculated directly from data on two runs at sufficiently different initial concentrations.

Tables 7.16 and 7.17 show titration data and calculated kinetic data from those data. Second order kinetic plots of

$\frac{1}{1-p}$ against time for concentration dependence experiments of solution imidization are shown in the Figure 7.6. Data points in Figure 7.6 followed second order kinetics once reaction temperatures reached to the desired reaction temperature (160°C). For the preset preaction temperature to be reached an induction preiod (ca. 10 minutes) was required. Thus, the first data points were not used. Using data points that follow second order kinetics following regression lines were obtained:

For 15 % solids, $\frac{1}{1-p} = 0.080\ t + 0.22$ Eq. 1.3.3

For 5 % solids, $\frac{1}{1-p} = 0.024\ t + 0.79$ Eq. 1.3.4

Using these two equations half-life periods at different concentrations can be obtained. First let's calculate the half-period for the run on the 15 % solids. After 10 minute reaction % AA is 84.5 % (See Table 1.3.1) therefore at t = $t_{1/2}$ + 10, %AA = $\frac{84.5}{2}$ = 42 (p = 0.58). From Eq. 1.3.3 with p = 0.58, t = 27. Thus, $t_{1/2}$ = 27 - 10 = 17. For the imidization on the 5 % solids after 11 minute reaction % AA is 91.4 % (See Table 1.3.2). At t = t'1/2 + 11, %AA = $\frac{92.8}{2}$ = 46 (p = 0.54). From Eq. 1.3.4 with p = 0.54, $t'_{1/2}$ = 46.7. Now, let the number of acid functional groups of partially imidized 15 % solid content polyamic acid at %AA = 84.5 be C_0 then, that of partially imidized 5 % solid content

polyamic acid at %AA = 91.4 is $\frac{91.4}{3} \times \frac{1}{84.5} C_0 = 0.36C_0$. From Noyes equation (Eq. 1.3.1) with $N_0 = C_0$, $t_{1/2} = 17$, $N'_0 = 0.36C_0$ and $t'_{1/2} = 46.7$.

$$n = 1 + \frac{\log 46.7 - \log 17.0}{\log C_0 - \log 0.36C_0} = 1.99 \cong 2$$

Table 7.16. A work-sheet for imidization of 15 % solid 4,4'-ODA/ODPA polyamic acid at imidization temperature of 160 °C, (N = 0.0262).

t, min.	S.S.	V, ml	-E, mV	%AA	%AA'	-ln(1-p)	1/(1-p)
0	0.6445	14.37	403	99.3	100.0	0.000	1.000
10	0.9037	17.20	373	83.8	84.5	0.169	1.184
16	0.5098	7.84	427	67.0	67.4	0.394	1.483
20.5	0.6199	7.89	437	54.9	55.3	0.592	1.808
25	0.5244	5.54	452	45.2	45.6	0.786	2.195
30	0.624	5.65	435	38.6	38.9	0.944	2.571
36	0.7655	5.91	429	32.7	33.0	1.109	3.032
40	0.7203	5.07	453	29.8	30.0	1.202	3.328
45	0.8168	5.18	426	26.8	27.0	1.310	3.705
50	1.0835	5.98	454	23.2	23.4	1.452	4.271
60	1.1449	5.39	462	19.8	19.9	1.612	5.015
80	1.4777	5.22	426	14.8	14.9	1.904	6.715
100	1.5052	4.42	440	12.3	12.4	2.090	8.084
120	2.3454	5.69	404	10.1	10.2	2.283	9.807

Table 7.17. A work-sheet for imidization of 5 % solid 4,4'-ODA/ODPA polyamic acid at imidization temperature of 160°C, (N = 0.0262).

t, min.	S.S.	V, ml	-E, mV	%AA	%AA'	-ln(1-p)	1/(1-p)
0	1.0354	7.85	452	101.5	100.0	0.000	1.000
11	1.1725	8.18	428	92.8	91.4	0.090	1.094
15	1.1954	7.75	423	85.8	84.6	0.167	1.182
20	1.3194	7.80	440	77.8	76.7	0.265	1.304
25	1.4682	8.10	425	72.3	71.3	0.338	1.403
31	1.6447	8.27	433	65.5	64.6	0.437	1.548
36.33	1.7888	8.33	399	60.5	59.7	0.517	1.676
40	1.8760	8.57	476	59.3	58.4	0.537	1.712
50	1.9153	7.83	457	52.8	52.1	0.653	1.920
60	2.1157	7.41	424	45.0	44.4	0.813	2.254
80	2.4544	7.07	405	36.8	36.2	1.015	2.760
100	2.7911	6.90	455	31.4	31.0	1.172	3.227
120	3.2981	7.07	398	27.2	26.8	1.318	3.734

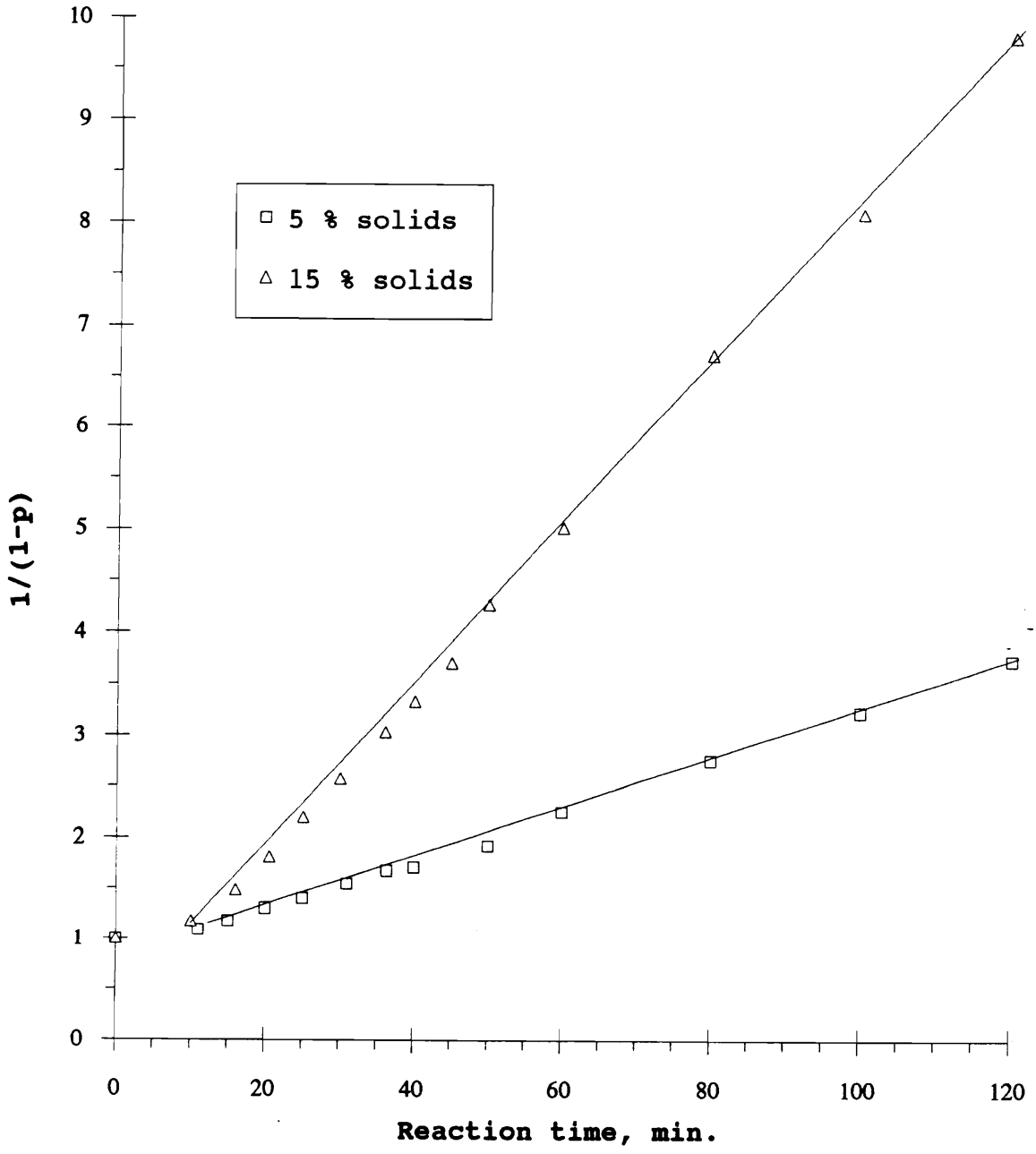

Figure 7.6. A second order kinetic plot of 1/(1-p) against reaction time for the imidization of 4,4'-ODA/ODPA based polyamic acid at two different initial solid concentrations at imidization temperature of 160°C. See Table 7.16 and 7.17.

APPENDIX 4. Effects of acid (p-toluene sulfonic acid) on the rate of imidization

Table 7.18. A work-sheet for acid catalysis experiments of imidization of 4,4'-ODA/ODPA polyamic acid; No acid was used, reaction temperature = 130°C, 10% solids (NMP/CHP = 9/1).

t, min.	S.S., g	V, ml	-E, mV	%AA	%AA'	-ln(1-p)	1/(1-p)
0	0.7548	11.25	435	98.8	100.0	0.000	1.000
10	0.8248	12.06	446	96.8	98.0	0.021	1.021
10	1.0619	15.13	409	94.1	95.3	0.049	1.050
20	0.6987	9.51	430	89.6	90.7	0.098	1.103
40	0.5703	6.73	533	77.0	78.0	0.249	1.283
60	0.8213	9.01	431	71.3	72.2	0.326	1.385
80	0.8878	9.06	448	66.0	66.8	0.403	1.496
100	0.8106	7.63	433	60.7	61.5	0.487	1.627
120	0.7846	6.92	453	56.7	57.4	0.555	1.742

Table 7.19. A work-sheet for acid catalysis experiments of imidization of 4,4'-ODA/ODPA polyamic acid; 0.005 mole p-toluene sulfonic acid/Kg polymer solution, reaction temperature = 130°C, 10% solids (NMP/CHP = 9/1), N=0.026.

t, min.	S.S., g	V, ml	-E, mV	%AA	%AA'	-ln(1-p)	1/(1-p)
0	0.6225	9.29	421	98.9	100.0	0.000	1.000
10	1.0809	15.78	382	96.6	97.7	0.024	1.024
20	0.9321	12.36	390	87.2	88.1	0.127	1.135
40	0.9977	11.51	456	75.2	76.0	0.275	1.316
60	0.9527	9.49	393	64.4	65.1	0.430	1.537
80	0.7699	6.82	421	57.0	57.6	0.552	1.736
100	0.8340	6.73	459	51.7	52.3	0.649	1.914
120	1.0518	7.50	437	45.5	46.0	0.777	2.175

Table 7.20. A work-sheet for acid catalysis experiments of imidization of 4,4'-ODA/ODPA polyamic acid; 0.025 mole p-toluene sulfonic acid/Kg polymer solution, reaction temperature = 130°C, 10% solids (NMP/CHP = 9/1), N=0.026.

t, min.	S.S., g	V, ml	-E, mV	%AA	%AA'	-ln(1-p)	1/(1-p)
0	0.6210	9.25	405	98.8	100.0	0.000	1.000
10	0.8567	11.65	419	89.5	90.6	0.098	1.103
20	0.517	5.73	451	69.7	70.6	0.348	1.417
40	0.8709	6.36	429	46.6	47.2	0.751	2.120
60	0.8409	4.68	439	35.2	35.7	1.030	2.801
83	0.9840	4.23	445	27.1	27.4	1.294	3.649
100	1.1129	4.15	450	23.4	23.7	1.439	4.218
110	1.4586	5.06	442	21.7	22.0	1.514	4.545
120	1.3144	4.26	439	20.3	20.5	1.584	4.873

REFERENCES

1. K. L. Mittal, ed., "Polyimides: Synthesis, Chracterization and Applications", Vol. 1 & 2, Plenum, N. Y., 1984.

2. C. J. Feger, M. M. Khojasteh and J. E. McGrath, Ed. "Polyimides: Materials, Chemistry and Characterization," Elsevier Science Publishers B, V., Amsterdam, 1989.

3. D. Wilson, H. D. Stenzenberger and P. M. Hergenrother, Ed., Polyimides, Blackie & Son Ltd., Glasgow and London, 1990.

4. P. J. Cavana and W. F. Winters, PMR-15 Polyimide/Graphite Fiber Composite Fan Blade, NAS CR 135113, Feb. 1976.

5. W. M. Edwards and M. Robinson, US Pat. 2,710,853, 1955.

6. J. H. Lupinski and R. S. Moore Ed., "Polymeric Materials for Electronics Packaging and Interconnection," ACS Symposium Series 407, American Chemical Society, Washington, DC, 1989.

7. A. M. Wilson, Thin Solid Films 83, 145, 1981.

8. A. J. P. Theuwissen and G. J. Declerck, IEEE Electron. Devices Lett. 10, 308, 1982.

9. W. S. Ruska, Microelectronic Processing (McGraw-Hill, New York, 1987), pp. 290~291.

10. R. J. Jensen, J. P. Cummings, and H. Vora, IEEE Trans. Components, Hybrids, and Manufacturing Technology 7, 384, 1984.

11. C. J. Denton, D. R. Day, D. F. Priore, S. D. Senturia, E. S. Anolick, and D. Scheider, J. Electronic Mater. 14, 119, 1985.

12. G. M. Bower and L. W. Frost, J. Polym. Sci. A, 1, 3135, 1963.

13. S. R. Sandler and W. Karo, 'Polymer Synthesis', Academic Press, New York, p216, 1974.

14. C. E. Sroog, A. L. Endrey, S. V. Abramo, C. E. Berr, W. M. Edwards, and K. L. Olivier, J. Polym. Sci. A, 3, 1373, 1965.

15. E. Lavin, A. H. Markhart, and V. O. Skuter (to Monsanto), U. S. Pat. 3,260,691, July 12, 1962.

16. P. Delvigs, Li-Chen Nsu, and T. T. Serafini, J. Polym. Sci. B, 8, 1970.

17. W. J. Farrisey, J. S. Rose, P. S. Carlton, A. C. S. Polym. Prepr. 9, 1581, 1968.

18. R. A. Meyers, J. Polym. Sci. A, 1, 2757, 1969.

19. W. M. Edwards and I. M. Robinson (to E. I. DuPont), U. S. Pat. 2,876,609, 1959.

20. W. M. Edwards and I. M. Robinson (to E. I. DuPont), U. S. Pat. 3,179,614, 1965.

21. W. M. Edwards and I. M. Robinson (to E. I. DuPont), U. S. Pat. 3,179,634, 1965.

22. L. W. Frost and G. M. Bower, U. S. Pat. 3,179,635, 1965.

23. A. L. Endrey, U. S. Pat. 3,179,630, 1965.

24. S. V. Vinorgadova, Ya. S. Wygodskii, V. D. Vorob'ev, N. A. Churochkina, L. I. Chudina, T. N. Spirina, and V. V. Korshak, Polym. Sci. U. S. S. R., 16, 584, 1974.

25. A. N. Pravednikov, I. Ye. Kardash, N. P. Glukhoyedov, and A. Ya. Ardashnikov, Polym. Sci. USSR, 15, 399, 1973.

26. A. Ya. Ardashnikov, I. Ye. Kardash, and A. N. Pravednikov, Polym. Sci. USSR, 13, 2092, 1971.

27. P. P. Nechayev, Ya. S. Vygodskii, G. Ye. Zaikov, and S. V. Vinogradova, Polm. Sci. U. S. S. R., 18, 1903, 1976.

28. Y. V. Kamzolkina, G. Teiyes, P. P. Nechayev, Z. V. Gerashchenko, Y. S. Vygodskii, and G. Y. Zaikov, Vysokomol. Soyed., A18, 2764, 1976.

29. E. L. Johnson, J. Appl. Polym. Sci. 15, 2825, 1971.

30. R. A. Dine-Hart and W. W. Wright, J. Appl. Polym. Sci., 11, 609, 1967.

31. W. Volksen and P. M. Cotts, in 'Polyimides' Vol. 1 (Ed. K. L. Mittal), Plenum Press, p163, 1984.

32. L. E. Frost and I. Kesse, J. Appl. Polymer Sci., 8, 1039, 1964.

33. V. M. Svetlichnyi, K. K. Kalnin'sh, V. V. Kudryavtsev, and M.M. Koton, Dokl. Akad. Nauk SSSR (Engl. Transl.), 237, 693, 1977.

34. M. M. Koton, Polym. Sci. USSR, A, 13, 1513, 1971.

35. M. M. Koton et al., Polym. Sci. USSR, A, 16, 2411, 1974.

36. V. A. Zubkov, M. M. Koton, V. V. Kudryavtsev, and V. M. Svetlichnyi, Zh. Org. Khim. (engl. Transl.), 17, 1501, 1982.

37. V. D. Moiseev, N. G. Avetisyan, A. G. Chernova, and A. A. Atrushkevich, Plast, Massy. (engl. Transl.), 3, 6, 1971.

38. P. J. Lillford and D. P. N. Satchell, J. Chem. Soc. B360, 1967.

39. V. A. Solomin et al., Dokl. Chem. (engl. Transl.), 236, 139, 1977.

40. S. V. Vinogradova et al., Polym. Sci. U. S. S. R., A21, 1166, 1979.

41. V. I. Kolegov et al., Polym. Sci. U. S. S. R., A19, 2146, 1977.

42. M. M. Koton, V. M. Svetlichny, V. V. Kudriavtsev, V. E. Smirnova, T. A. Ustinov and Yu. A. Moskvichev, Vysokomol., Soedin., A22, 1058, 1980.

43. B. A. Zhubanov, V. A. Solomin, P. E. Messerle, N. G. Avetisian and V. D. Moiseev, Vysokomol. Soedin., A19, 2500, 1977.

44. Ya. S. Vygodsky, M. N. Spirina, P. P. Nechev, L. I. Chudinova, C. E. Zaikov, V. V. Korshak and S. V. Vinogradova, Vysokomol. Soedin., A19, 1516, 1977.

45. B. A. Zhubanov, P. E. Messerle and V. A. Solomin, Vysokomol. Soedin., B17, 560, 1975.

46. B. F. Malichenko and A. E. Borodin, Vysokomol. Soedin., B21, 356, 1979.

47. W. Wrasidlo, P. M. Hergenrother, and H. H. Levine, Polym. Prepr., 5, 141, 1964.

48. M. H. Loucheux and A. Bandert, J. Polym. Sci. 48, 405, 1960.

49. M. Idelson and E. R. Blout, J. Am. Chem. Soc., 79, 3948, 1957.

50. P. J. Lillford and D. P. N. satchell, J. Chem. Soc. B, 360, 1967.

51. R. L. Kaas, J. Polym. Sci. A, 19, 2255, 1981.

52. M. I. Bessonov, M. M. Koton, V. V. Kudryavtsev, and L. A. Laius, "Polyimides: thermally Stable Polymers," 2nd edn, Plenum, New York, pp 14-56, 1987.

53. M. M. Koton, V. V. Kudriavtsev and V. M. Svetlichny, in K. L. Mittal, ed., "Polyimides: Synthesis, Chracterization and Applications", Vol. 1 & 2, Plenum, N. Y., 1984.

54. V. M. Svetlichnyi, V. V. Kudryavtsev, N. A. Adrova, and M. M. Koton, Zh. Org. Khim. (Engl. Trans.) 10, 1907, 1974.

55. L. P. Hammett, Physical Organic Chemistry, McGraw-Hill, New York, 1970.

56. Ya. S. Vygodskii, T. N. Spirina, P. P. Nechayev, L. I. Chudina, G. Ye. Zaikov, V. V. Korshak, and S. V. Vinogradova, Vysokomol. soyed. A19, 1516, 1977.

57. N. G. Bel'nikevich, V. M.Denisov, L. N. Korzahavin and S. Ya. Frankel, Vysokomol. Soedin. A, 23, 1268, 1981.

58. Y. V. Kamzolkina, G. Teiyes, P. P. Nechayev, Z. V. Gerashchenko, Y. S. Vygodskii, and G. Y. Zaikov, Vyskomol. soyed. A, 18, 2764, 1976.

59. J. I. Jones, F. W. Ochynski, and F. A. Rackley, Chem. Ind., 1686, 1962.

60. W. T. Whang and S. C. Wu, J. Polym. Sci. A, 26, 2749, 1988.

61. M. L. Bender, Y. L. Chow, and Chloupek, J. Am. Chem. Soc., 80, 5380, 1958.

62. C. E. Sroog, J. Polym. Sci. Macromolecular Rev., 11, 161, 1976.

63. W. Volksen and P. M. Cotts, in 'Polyimides' Vol. 1 (Ed. K. L. Mittal), Plenum Press, p163, 1984.

64. C. C. Walker, J. Polym. Sci. A, 26, 1649, 1988.

65. T. Miwa and S. Numata, Polymer, 30, 893, 1989.

66. J. A. Kreuz, J. Polym. Sci. A, 28, 3787, 1990.

67. P. M. Cotts in "Polyimides: Synthesis, Chracterization and Applications", Vol. 1, K. L. Mittal, ed., Plenum, N. Y., p223, 1984.

68. P. P. Nefedov, Polym. Sci. U.S.S.R., 23, 1055, 1981.

69. C. E. Sroog, in "Encyclopedia of Polymer Science and Technology", Vol. 11, (Ed. N. Bikales), Wiley, New York, pp. 247-272, 1969.

70. P. C. Cassidy and N.C. Fawcett, in "Encyclopedia of Chemical Technology", Vol. 18, (Ed. M. Grayson), Wiley, New York, pp. 704-719, 1982.

71. J. W. Verbicky, Jr., in "Encyclopedia of Polymer Science and Engineering", Vol. 12, (Eds. H. F. Mark, N. M. Bikales, C. G. Overberger and G. Menges), 2nd edn Wiley, New York, pp. 364-383, 1988.

72. P. R. Young and A. C. Chang, SAMPE Prep., 30, 889, 1985.

73. D. Kumar, J.Polym. Sci., Polym. Chem. Ed., 18, 1376, 1970.

74. Yu. N. Sazanov, L. V. Krasilnikova, and L. M. Shcherbakova, Eur. Polym. J., 11, 801, 1975.

75. S. D. Bruck, Polymer, 6, 49, 1965.

76. A. N. Krasovskii, N. P. Antonov, M. M. Koton, K. K. Kalmin'sh, and V. V. Kudryavtsev, Vysokomol. Soed., A21, 945, 1979.

77. D. Kumar, J. Polym. Sci., Polym. Chem. Ed., 18, 1375, 1980.

78. A. I. Baise, J. Appl. Polm. Sci., 32, 4043, 1986.

79. R. Ginsberg and J. R. Susko, in "Polyimides: Synthesis, Characterization, and Applications," Vol. 1, K. L. Mittal, ed., Plenum, New York, p237, 1984.

80. G. A. Pasteur, H. E. Baier, and F. Vratny, in Thermal Analysis, B. Miller, Ed., Wiley-Heyden, Chichester, p. 1155, 1982.

81. M. Kramer, L. Wojciechowski, and P. Painter, Soc. of Plastics Engineers ANTEC Technical Papers, Los Angeles, pp. 273-294, 1984.

82. M. M. Koton, T. K. Meleshmo, V. V. Kudryavtsev, P. P. Nechayev, Ye. V. Kamzolkina, and N. N. Bogorad, Polym. Sci. U. S. S. R., 24, 791, 1982.

83. N. N. Barashkov, L. I. Semenova, and R. N. Nukukhametov, Polym. Sci. U. S. S. R., 25, 1264, 1983.

84. E. Pyun, R. J. Mathisen, and C. S. P. Sung, Macromolecules, 22, 1174, 1989.

85. M. Hasegawa, H. Arai, I. Mita, and R. Yokota, Polym. J., 22, 875, 1990.

86. V. M. Denisov, V. M. Svetlichnyi, V. A. Gindin, V. A. Zubkov, A. I. Kol'tsov, M. M. Koton, and V. V. Kudryavtsev, Polym. Sci. U. S. S. R., A21, 1644, 1979.

87. Marie-Florence Grenier-Loustalot and M. Barnaud, Makromol. Chem., Symp., 9, 9, 1987.

88. Marie-Florence Grenier-Loustalot, F. Joubert, and P. Grenier, J. Polym. Sci. Polym. Chem. Ed., 29, 1649, 1991.

89. S. G. Alekseyeva, S. V. Vinogradova, V. D. Vorob'yev, Ya. S. Vygodskii, V. V. Korshak, I. Ya. Slonim, T. N. Spirina, Ya. G. Urman, and L. I. Chudina, Polym. Sci. U. S. S. R., A21, 2434, 1979.

90. A. I. Kol'tsov, N. G. Bel'nikevich, V. M. Denisov, L. N. Korzhavin, N. V. Mikhailova, and V. N. Nikitin, Polym. Sci. U. S. S. R., A16, 2912, 1974.

91. N. J. Chu, J. W. Huang, C. H. Chang, Makromol. Chem., 190, 1799, 1989.

92. W. D. Weber and P. D. ACS PMSE Proc., 57, 341, 1987.

93. J. M. Sonnett, R. L. McCullough, A. J. Beeler, and T. P. Gannett, 4th International Conference on polyimides, Abstr., Session III-5, Ellenville, New York, Oct. 30~Nov. 1, 1991.

94. Shun-Ichi Numata, Koji Fujisaki, and N. Kinjo in "Polyimides: Synthesis, Characterization, and Applications," Vol. 1, K. L. Mittal, ed., Plenum, New York, p259, 1984.

95. H. H. Reimschuessel and L. G. Roldan, J. Polym. Sci., A2, 6, 559, 1968.

96. W. Wasidlo and J. M. Augl, J. Polym. Sci., A1, 7, 321, 1969.

97. J. A. Kruez, A. L. Endrey, F. P. Gay, and C. E. Sroog, J. Polym. Sci., A-1, 2607, 1966.

98. L. A. Laius, M. I. Bessonov, Ye. V. Kallistova, N. A. Adrova, and F. S. Florinskii, Polym. Sci. U. S. S. R., A9(10), 2470, 1967.

99. J. Hashem, H. A. Willis, and D. C. M. Squirrel, "Identification and Analysis of Plastics", pp. 328-329, Iliffe Books, London, 1972.

100. M. Navarre, in "Polyimides: Synthesis, Characterization, and Applications" Vol. 1, (Ed. K. Mittal), Plenum, New York, pp. 429-442, 1984.

101. C. A. Pryde, J. Polym.Sci., A27, 711, 1989.

102. R. W. Snyder, C. W. Sheen, and P. C. Painter, Polyimide Cure Kinetics, in Proc. of the Symposium on Polymeric Materials for Electronic Packaging and High Technology Applications, Honolulu,

Hawaii, Oct. 18~23, 1987, The Electronic Society, Vol. 88-17, 1988, pp. 71-78.

103. R. W. Snyder and C. W. Sheen, Appl. Spectrosc., 42, 655, 1988.

104. R. W. Snyder and C. W. Sheen, Appl. Spectrosc., 42, 296, 1988.

105. R. W. Snyder and C. W. Sheen, Computers Chem., 13, 61, 1988.

106. R. W. Snyder, C. W. Sheen, and P. C. Painter, Appl. Spectrosc., 42, 503, 1988.

107. R. W. Snyder, in C. J. Feger, M. M. Khojasteh and J. E. McGrath, Ed., "Polyimides: Materials, Chemistry, and Characterization," Elsevier Science Publishers B. V., Amsterdam, p. 363, 1989.

108. F. P. Gay and C. E. Berr, J. Polym. Sci., 6, 1935, 1968.

109. F. W. Harris, in D. Wilson, H.D. Stenzenberger, P. M. Hergenrother, Ed., "Polyimides," Chapman and Hall, New York, p. 1, 1990.

110. J. A. Kruez, A. L. Endrey, F. P. Gay, and C. E. Sroog, J. Polym. Sci., A-1, 2607, 1966.

111. V. M. Denisov, A. I. Kol'tsov, N. V. Mikhailova, V. N. Nikitin, M. I. Bessonov, N. A. Glukhov, and L. M. Shcherbakova, Polym. Sci. U. S. S. R., A18, 1780, 1976.

112. P. P. Nechayev, Ya. S. Vygodskii, G. Ye. Zaikov, and S. V. Vinogradova, Polm. Sci. U. S. S. R., 18, 1903, 1976.

113. Y. V. Kamzolkina, G. Teiyes, P. P. Nechyev, Z. V. Gerashchenko, Y. S. Vygodskii, and G. Y. Zaikov, Vysokomol. soyed., A18, 2764, 1976.

114. V. L. Bell, B. L. Stump, and H. Gager, J. Polym. Sci. polym. Chem. Ed., 14, 2275, 1976.

115. Y. V. Kamzolkina, P. P. Nechaev, V. S. Markin, Y. S. Vygodskii, T. V. Grigor'eva, and G. E. Zaikov, Dokl. AN SSSR, 219, 650, 1974.

116. P. R. Young, N. T. Wakelyn, and A. C. Chang, Preceedings of the Second International Conference on Polyimides, Ellenville, NY, Oct. 30~Nov. 1, p414, 1985.

117. P. R. Young and A. C. Chang, 30th SAMPE Symp. Prepr., 30, 889, 1986.

118. P. R. Young and A. C. Chang, 32nd SAMPE Symp. Prepr., 32, 1051, 1987.

119. P. R. Young and A. C. Chang, SAMPE J. March/April, 70, 1986.

120. P. R. Young, J. R. J. Davis, A. C. Chang and J. N. Richardson, J. Polym. Sci. Polym. Chem. Ed., 28, 3107, 1990.

121. P. Hermans and J. Streef, Die Makromolecular Chemie, 74, 133, 1964.

122. E. Sacher, J. Macromol. Sci. Phys., B 25, 405, 1986.

123. R. W. Snyder, B. Thomson, Y. Park, B. Bartges, D. Czerniaqski and P. Painter, Polym. Prepr., Am. Chem. Soc. Div. Polym. Chem., 29, 317, 1988.

124. R. W. Snyder, B. Thomson, B. Bartges, D. Czerniawski and P. C. Painter, Macromolecules, 22, 4166, 1989.

125. J. D. Summers, Ph. D. Thesis, VPI & SU, June 1988.

126. E. S. Moyer, Ph. D. Thesis, VPI & SU, Nov. 1989.

127. C. A. Arnold, Ph. D. Thesis, VPI & SU, Oct. 1989.

128. H. Ishida, S. T. Wellinghoff, E. Baer, and J. L. Koenig, Macromolecules, 13, 826, 1980.

129. L. J. Bellamy and R. L. Williams, Trans. Faraday Soc., 55, 14, 1959.

130. G. Allen, P. S. Ellington, and G. D. Meakins, J. Chem. Soc., 4, 1909, 1960.

131. C. N. R. Rako and R. Venktaraghavan, Spectrochim. Acta, 18, 273, 1962.

132. I. Ye. Kardash, D. Yu. Likhachev, M. B. Krotovich, N. V. Kozlova, I. L. Zhuraveva, Yu. S. Bogachev, and A. N. Pravednikov, Polym. Sci. U. S. S. R. A29, 1498, 1987.

133. S. Kuroda, K. Terauchi, K. Nogami, and I. Mita, Eur. Polm. J., 25, 1, 1989.

134. S. I. Kuroda and I. Mita, Eur. Polym. J., 25, 611, 1989.

135. R. A. Dine-Hart, D. B. V. Parker and W. W. Wright, Br. Polym. J., 3,222, 1971.

136. R. A. Dine-Hart, D. B. V. Parker and W. W. Wright, Br. Polym. J., 3,226, 1971.

137. R. A. Jewell and G. F. Sykes, "Chemistry and Properties of Crosslinked Polymers," S. S. Labana, Ed., Academic Press, New York, p. 97, 1977.

138. M. I. Tsapovetskii, L. A. Laius, Zhukova, L. A. Shibayev, N. G. Stepanov, M. I. Bessonov and M. M. Koton, Polym. Sci. U. S. S. R., 30, 295, 1988.

139. Yu. N. Sazanov and L. A. Shibayev, Thermochim. Acta, 15, 43, 1976.

140. M. M. Koton, et. al., in C. J. Feger, M. M. Khojasteh and J. E. McGrath, Ed., Polyimides: Materials, Chemistry and Characterization, Elsevier Science Publishers B. V., Amsterdam, p403, 1989.

141. M. M. Koton, S. Ya. Frenkel', Yu. N. Panov, L. S. Bolotnikova, V. M. Svetlichnyi, L. A. Shibayev, S. G. Kulichikhin, Ye. Ye. Krupnova, A. S. Reutov, and I. L. Ushakova, Polym. Sci. U. S. S. R., 30, 2600, 1988.

142. M. I. Bessonov, M. M. Koton, V. V. Kudryavtsev, and L. A. Laius, "Polyimides: Thermally Stable Polymers", 2nd Ed., Plenum, New York, p61, 1987.

143. L. A. Laius, M. I. Bessonov, Ye. V. Kallistova, N. A. Adrova and F. S. Florinskii, Polym. Sci. U. S. S. R., A9, 2470, 1967.

144. S. V. Lavrov, A. Ya. Arsashnikov, I. Ye. Kardash, and A. N. Pravednikov, Polym. Sci. U. S. S. R., 19, 1212, 1977.

145. G. Ordian, "Principles of Polymerization", 2nd. Ed., John Wiley & Sons, New York, 1981.

146. R. J. Mathisen, J. K. Yoo, C. S. P. Sung, Macromolecules, 20, 1414.

147. V. V. Korshak, Ya. G. Urman, S. G. Alekseeva, I. Ya Slonim, S. V. Vinogradova, Ya. S. Vygodskii, and Z. M. Nagiev, Makromol. Chem., Rapid Commun., 5, 695, 1984.

148. M. Hasegawa, H. Arai, I. Mita, and R. Yokota, Polym. J. 22, 875, 1990.

149. Ya. S. Vygodskii, T. N. Spirina, P. P. Nechayev, L. I. Chudina, G. Ya. Zaikov, V. V. Korshak, and S. V. Vinogradova, Polym. Sci. U. S. S. R., A19, 1738, 1977.

150. P. D. Frayer in "Polyimides: Synthesis, Characterization, and Applications," Vol. 1, K. L. Mittal, ed., Plenum, New York, p273, 1984.

151. L. A. Laius, M. I. Bessonov, and F. S. Florinskii, Polym. Sci. U. S. S. R., 13, 2257, 1971.

152. A. K. St. Clair and T. L. St. Clair, Polym. Prepr., 27, 406, 1986.

153. P. R. Young and A. C. Chang, SAMPE J., 22, 70, 1986.

154. C. Feger, SPE Conf. Proc., 45th Tech. Conf. 967, 1987.

155. S. V. Lavrov, I. Ye. Kardash, and A. N. Pravednikov, Polym. Sci. U. S. S. R., 10, 2727, 1977.

156. S. V. Serchenkova, M. V. Shablygin, T. V. Kravchenko, Z. G. Oprits, and G. I. Kudryavtsev, Vysokomol. Soedin., A20, 1137, 1987.

157. L. N. Korzhavin, L. A. Shibaev, S. V. Bronnikov, T. A. Antonov, Yu. N. Sazanov, and S. Ya. Frenkel', Vysokomol. Soedin, A22, 2027, 1980.

158. M. M. Koton, Vysokomol. Soedin., A21, 2496, 1976.

159. A. I. Baise, J. Appl. Polym. Sci., 32, 4043, 1986.

160. B. Thomson, Y. Park, P. C. Painter, and R. W. Snyder, Macromolecules, 22, 4159, 1989.

161. M. J. Brekner and C. Feger, J. Polym. Sci., Polym. Chem. Ed., 25, 2005,1987.

162. M. J. Brekner and C. Feger, J. Polym. Sci. A, 25, 2005, 1987.

163. M. J. Brekner and C. Feger, J. Polym. Sci., Polym. Chem. Ed., 25, 2479,1987.

164. V. V. Korshak, G. L. Berestneva, and Ya. B. Zimin, Dokl, Akad. Nauk (Engl. Transl.), 233, 598, 1977.

165. V. V. Korshak, G. L. Berestneva, I. P. Bragina, G. V. Eremina, and V. v. Krylova, Vysokomol. Soedin., A16, 1714, 1974.

166. J. D. Ferry, "Viscoelastic Properties of Polymers", 3rd Ed., John Wiley & Sons, Inc., 1980.

167. K. Horie and I. Mita, J. Polym. Sci., Polym. Chem. ed., 6, 2663, 1968.

168. I. Mita and K. Horie, J. Macromol. Sci. rev., Macromol. Chem., 91, 1987.

169. I. S. Milevskaya, N. V. Lukshina, and A. M. El'yashevich, Vysokomol. Soedin., A21, 1302, 1979.

170. L. A. Laius and M. I. Tsapovetskii, in "Polyimides: Synthesis and Characterization," Vol. 1 (Ed. K. Mittal), Plenum, New York, pp. 295-309, 1984.

171. S. V. Lavrov, O. B. Talankina, V. D. Vorob'ev, A. L. Izumnikov, I. E. Kardash, and A. N. Pravednikov, Polym. Sci. U. S. S. R., 22, 2069, 1980.

172. Z. V. Gerashchenko, Ya. S. Vygodskii, G. A. Slonimskii, A. A. Askadskii, V. S. Pankov, S. V. Vinogradova, V. G. Dashevskii, V. A. Klimova, and F. B. Sherman, Vysokomol. Soedin, 15, 1718, 1973.

173. A. I. Kol'tsov, N. G. Belnikevich, V. M. Denisov, L. N. Korzhavin, N. V. Michailova, and V. N. Nikitit, Vysokomol. Soedin., A16, 2506, 1974.

174. G. S. Kolesnikov, O. Ya. Fedotova, Hussein Hamid Mohhamed, Ali Al' Sufi, and S. F. Belevskii, Polym. Sci. U. S. S. R., 12, 370, 1970.

175. S. V. Lavrov, I. Ye. Kardash, and A. N. Pravednikov, Polym. Sci. U. S. S. R., A19, 2727, 1977.

176. E. P. Cizek, U. S. Patent 3,383,435, 1968 (assigned to General Electric Co.).

177. H. H. Irvin, U. S. Patent 3,010,936, 1961, (assigned to Borg-Warner Corp.).

178. G. L. Brode and J. V. Koleske, J. Macromol. Sci., Chem. 6(6), 1109, 1972.

179. O. Olabisi, L. M. Robeson, and M. T. Shaw, Polymer-Polymer Miscibility, Academic Press, Inc., New York, 1979.

180. W. J. MacKnight, F. E. Karasz, and J. R. Fried in D. R. Paul and S. Newman, eds., Polymer Blends, Vols. I and II, Academic Press, Inc., New York, 1978, Chaper 5.

181. D. R. Paul and J. W. Barlow, J. Macromol. Sci. Rev. Macromol. Chem. 18, 109, 1980.

182. R. Koningsveld, L. A. Kleintjens, and H. M. Schoffeleers, Pure Appl. Chem., 39, 1, 1974.

183. B. E. Sundquist and R. A. Oriani, J. Chem., Phys. 36, 2604, 1962.

184. Polymer Composites, 9, 443, Dec. 1988.

185. A. Buckley, D. E. Stuez, G. A. Serad, in "Encyclopedia of Polym. Sci. Eng.", H. Mark and N. Bikales, Eds., 11, John Wiley and Sons, New York, 572, 1988.

186. D. H. Chen, Y. P. Chen, C. A. Arnold, J. C. Hedrick, J. D. Graybeal and J. E. McGrath, 34th International SAMPE Symposium, 1247, 1989.

187. L. Leung, D. J. Williams, F. E. Krasz, and W. J. MacKnight, Polym. Bull., 16, 457, 1986.

188. G. Guerra, D. J. Williams, F. E. Krasz, and W. J. MacKnight, J. Polym. Sci. Part B: Polym. Phys., 26, 301, 1988.

189. G. Guerra, S. Choe, D. J. Williams, F. E. Krasz, and W. J. MacKnight, Macromolecules, 21, 231, 1988.

190. D. S. Lee and G. Quin, Polymer J., 21, 751, 1989.

191. P. Musto, F. E. Karasz and W. J. MacKnight, Macromolecules, 24, 4762, 1991.

192. S. Stankovic, G. Guerra, F. E. Karasz and William J. MacKnight, Polymer Communications, 29, 14, 1988.

193. K. Liang, G. Banhegyi, F. E. Karasz, and W. J. MacKnight, J. Polym. Sci: Part B, 29, 649, 1991.

194. M. Jaffe and M. Glick, 5th Quarter Technical Report, Polymer Blends, DARPA Order No. 6045, AFOSR Contract F49620-88-C-0014, August 1989.

195. J. Grobelny, D. M. Rice, F. E. Karasz, and W. J. MacKnight, Macromolecules, 23, 2139, 1990.

196. R. Yokota and R. Horiuchi, J. Polym. Sci., Polym. Letters, 26, 215, 1988.

197. D. Y. Yoon, M. Ree, W. Volksen, D. Hofer, L. Depero, and W. Parrish, Proceedings of the Third International Conference on Polyimides, sonsored by SPE, p1, 1988.

198. M. Ree, D. Y. Yoon and W. Volksen, Polym. Mat. Sci. Eng., 60, 179, 1989.

199. T. L. St. Clair, M. K. Gerber and C. R. Gautreaux, Polym. Mat. Sci. Eng., 60, 183, 1983.

200. N. J. Johnston, T. L. St. Clair, R. M. Baucom, and T. W. Towell, Soc. Adv. Mat. Proc. Eng., 34, 976, 1989.

201. T. Chung, R. H. Vora, and M. Jaffe, J. Polym. Sci., Polym. Chem. Ed., 29, 1207, 1991.

202. Ardashnikov, A. Ya., Kardash, I. Ye., Pravednikov, A. N., Vysokomol. Soyed., A13, 1863, 1971.

203. H. Ishida, S. T. Wellinghoff, E. Baer, and J. L. Koenig, Macromolecules, 13, 826, 1980.

204. D. D. Perrin, W. L. F. Armarego, and D. R. Perrin, "Purification of Laboratory Chemicals", Pergamon Press, N. Y., 1980.

205. A. Rudin, The Elements of Polymer Science and Engineering, Academic Press, Orlando, p168, 1982.

206. Ning-Jo Chu and Jian-Wen Huang, Polym. J., 22, 725, 1990.

207. D. C. Harris, Quantitative Chemical Analysis, W. H. Freeman and Company, New York, p372, 1980.

208. J. H. Espenson, Chemical Kinetics and Reaction Mechanism, McGraw-Hill Book Company, New York, p34, 1981.

209. J. W. Moore and R. G. Pearson, Kinetics and Mechanism (3rd Ed.), John Wiley & Sons, Inc., United Publishing & Promotion Co., Ltd., p60, 1984.

210. A. N. Pravednikov, I. Ye. Kardash, N. P. Glukhoyedov and A. Ya. Ardashnikov, Poym. Sci., U. S. S. R., 15, 399, 1973.

211. I. Ye. Kardash, A. Ya. Ardashnikov, V. S. Yakubovich, G. I. Braz, A. Ya. Yakubovich, and A. N. Pravednikov, Polym. Sci., U. S. S. R., 9(9), 2160, 1967.

212. J. H. Espenson, Chemical Kinetics and Reaction Mechanism, McGraw-Hill Book Company, New York, p120, 1981.

213. T. Matsuura, Y. Hasuda, S. Nishi and N. Yamada, Macromolecules, 24, 5001, 1991.

214. V. V. Korshak, Ya. G. Urman, S. G. Alekseeva, I. Ya. Slonim, S. V. Vinogradova, Ya. S. Vygodskii, Z. M. Nagiev, Makromol. Chem., Rapid Commun., 5, 695, 1984.

215. M. L. Wallach, J. Polym. Sci., A-2, 5, 653, 1967.

216. S. A. Swanson, P. M. Cotts, R. Siemens, S. H. Kim, Macromolecules, 24, 1352, 1991.

217. P. T. McKittrick and J. E. Katon, Applied Spectroscopy, 44, 812, 1990.

218. K. R. Lyon and J. E. McGrath, SAMPE, 36, 417, 1991.

219. K. R. Lyon, J. E. McGrath and J. F. Geibel, Polym. Materials Sci. and Engineering, Am., Chem. Soc. PMSE Div., 65, 249, 1991.

220. S. H. Pine, J. B. Hendrickson, D. J. Cram and G. S. Hammond, McGraw-Hill, Kogakusha, Ltd., Tokyo, p286, 1980.

221. T. H. Lowry and K. S. Richardson, "Mechanism and Theory in Organic Chemistry", second ed., p185, pp635-641, 1981.

222. P. M. Cotts, W. Volksen and S. Ferline, J. Polym. Sci., B, 30, 373, 1992.

VITA

Young Jun Kim was born in Masan, Korea on July 27, 1958 to Sue Tae Kim and Soon Bu Bae. He graduated from Masan High School in 1977. In the spring of the same year, he entered Seoul National University to begin his undergraduate studies. He received a bachelors degree in textile engineering in 1981. In February of 1984, he received his masters degree in chemistry from Korea Advanced Institute of Science and Technology (KAIST). In March, he joined Lucky Central Research Institute in Daejon, Korea where he worked on polymer chemistry until May, 1987. In the Fall of the same year he enrolled in the graduate program at Virginia Polytechnic Institute and State University in Blacksburg, Virginia to pursue his doctorate degree in chemistry with a major emphasis in polymer science. He received his doctorate degree in chemistry, specializing in polymer science in March, 1992.